THE EFFECT OF TURBO-CHARGING AND INTERCOOLINGON EMISSIONSGENERATION AND DURABILITY OF A DIESEL ENGINE

LOVELL DONALD EMSLIE

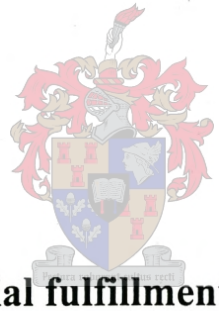

Thesis presented in partial fulfillment of the requirements for the degree of Master of Mechanical Engineering at the University of Stellenbosch

Dr AB Taylor
December 2001

DECLARATION

I, the undersigned, hereby declare that the work contained in this thesis is my own original work and that I have not previously in its entirety or in part submitted it at any university for a degree.

1 ABSTRACT

To reduce exhaust gas emissions in diesel engines and for engine upgrade purposes the major parameters and equipment that should be looked at are boost pressure, intake charge temperature, combustion chamber design and fuel injection equipment. Boost pressure is governed by the turbo-charger; with high-efficiency variable geometry turbo-chargers, effective control is possible to increase airflow rate at all operating conditions of the engine. Efficient air-to-air inter-cooling results in the engine being filled with a cooler air charge that will influence engine durability and heat rejection to the cooling system. The main objective of the investigation is to look at the influence of boost pressure and intake charge temperature on diesel combustion to better understand the processes where boost pressure is increased and intake charge temperature reduced to increase the brake mean effective pressure of the engine and reduce emissions generation.

By running an engine at different intake boost pressures and intake charge temperatures a 25-point matrix was formed at three different operating conditions. On completion of the engine testing, data processing and data evaluation, a number of important conclusions were made about the behaviour of the engine running under different conditions. This enabled the researcher to understand how boost pressure and intake charge temperature influence engine power output, fuel consumption, engine durability and exhaust gas emissions. The opinion is proved when, in most cases, the 75 test points were used to build multiple linear regression models to determine which engine parameters (dependent variables) have a significant effect on emissions generation and durability parameters.

From the data it is evident that boost pressure has a positive influence on most engine parameters, as an increase in boost pressure results in an increase in air mass flow through the engine. An increase in air mass flow reduces combustion chamber gas temperature as the result of an increase in excess air ratio during combustion.

A further result of the increase in excess air ratio is that less soot is formed during the first part of combustion and more soot and partly decomposed Hydrocarbon (HC) compounds are oxidised during the late combustion phase. Therefore, with an increase in boost pressure, Bosch smoke emissions reduce, but with a change in intake air temperature no difference in smoke concentration is seen except at the very low boost pressure and very high boost temperature test points where low air/fuel ratios exist and the slight increase in air-flow rate as a result of lower air inlet temperature has a big influence.

Nitric Oxide (NO) emissions, on the other hand, are more dependent on intake air temperature than on boost pressure, which was proved in the multiple regressions modelling performed on the test data. The flame zone and the post-flame zone temperature play the dominant role in NO formation. As explained in the results discussion on NO formation, intake air temperature influences the ignition mixture temperature and the subsequent flame zone temperature. A lower intake air condition results in longer ignition delay and increases the initial rate of combustion.

2 OPSOMMING

Die hoofparameters en toerusting wat in ag geneem moet word om uitlaatgasemissies in dieselenjins te verminder en om enjinkraguitset te verhoog, is inlaatdruk, inlaat lugtemperatuur, verbrandingskamerontwerp en brandstofinspuittoerusting. Inlaatdruk word beheer deur die turb-aanjaer. Met hoë effektiwiteit, veranderlike geometrie turbo-aanjaging, is effektiewe beheer moontlik om lugvloei-tempo deur die enjin te verhoog onder alle enjinwerkstoestande. Effektiewe lug-tot-lug tussenverkoeling laat die enjin met koeler inlaatlug vul, wat 'n uitwerking het op enjinlewensduur en hitte-verlies na die verkoelingsstelsel. Die hoofdoel van die navorsing is om die invloed van inlaatdruk en inlaat lugtemperatuur op dieselverbranding te ondersoek. Sodoende kry die navorser 'n beter begrip omtrent die prosesse waar inlaatdruk verhoog en inlaat lugtemperatuur verlaag word, om rem-gemiddelde effektiewe druk van die enjin te verhoog en uitlaatgas emissies te verlaag.

'n 25-punt matriks is opgestel deur die enjin by verskillende inlaatdrukke en inlaat lugtemperture te opereer, en by drie verskillende wringkragwerkstoestande. 'n Aantal belangrike gevolgtrekkings is gemaak omtrent enjinwerking onder verskillende werkstoestande na voltooiing van die enjintoetse, dataverwerking en data-evaluering. Sodoende het die navorser bepaal hoe inlaatdruk en inlaat lugtemperatuur kraglewering, brandstofverbruik, enjinlewensduur en uitlaatgasemissies beïnvloed. Om bogenoemde begrippe verder te ondersteun is 'n meervoudige, lineëre regressiemodel opgestel om te bepaal watter enjinparameters (afhanklike veranderlikes) 'n wesenlike effek op emissie-generasie en lewensduur het.

Van die data word afgelei dat inlaatdruk 'n positiewe effek op die meeste enjinparameters het, omdat hoër inlaatdruk die lugvloeitempo deur die enjin verhoog. Hoër lugmassavloei verminder verbrandingsgastemperatuur as gevolg van 'n hoër oortollige lugverhouding tydens verbranding.

'n Verdere gevolg van 'n hoër oortollige lugverhouding is dat minder roet gevorm word gedurende die eerste verbrandingsfase en meer roet en gedeeltelik verbrande koolwaterstofverbindings oksideer gedurende die finale verbrandingsfase. Dus, met 'n hoër inlaatdruk word Bosch rookemmissies verlaag. Geen wesenlike verandering in rookkonsentrasies word egter gesien met 'n verandering in inlaatlugtemperatuur nie, behalwe by baie lae inlaatdruk- en hoë inlaat lugtemperatuur-toetskondisies waar lae lug/brandstofverhoudings bestaan en 'n klein toename in lugmassavloei as gevolg van laer inlaat lugtempertuur'n groot invloed het.

Stikstofmonoksied (NO) emissies is meer afhanklik van inlaat lugtemperatuur as inlaatdruk. Dit is bewys in die meervoudige regressiemodel. Die vlamsone- en die na-vlamsone-temperatuur speel 'n groot rol in NO vorming. Inlaat lugtemperatuur beïnvloed die temperatuur van die onstekingsmengsel en die daaropvolgende vlamsone-temperatuur. 'n Laer inlaat lugtemperatuur veroorsaak 'n langer onstekingsvertraging en verhoog die aanvanklike verbrandingstempo.

ACKNOWLEDGEMENTS
The author wishes to record his sincere appreciation for the assistance given by:

Dr. A.B. Taylor, Senior Lecturer, Department of Mechanical Engineering, University of Stellenbosch, for his supervision and support during the course of the project.

Professor A.C. Hansen, Senior Lecturer, Department of Agricultural Engineering, University of Natal, for his support with the combustion analysis programme.

A.J. Bell, B.A. Vincent and D. Moran for their assistance in setting up test equipment and performing engine testing.

From *An Essay on Criticism*, by Alexander Pope

A little learning is a dangerous thing;
Drink deep, or taste not the Pierian spring:
There shallow draughts intoxicate the brain,
And drinking largely sobers us again.
Fired at first sight with what the Muse imparts,
In fearless youth we tempt the heights of arts,
While from the bounded level of our mind
Short views we take, nor see the lengths behind;
But more advanced, behold with strange surprise
New distant scenes of endless science rise!
So pleased at first the towering Alps we try,
Mount o'er the vales and seem to tread the sky,
The eternal snows appear already pass'd,
And the first clouds and mountains seem the last:
But, those attain'd, we tremble to survey
The growing labours of the lengthen'd way,
The increasing prospect tires our wandering eyes,
Hills peep over hills, and Alps on Alps arise!

3 TABLE OF CONTENTS

4 LIST OF TABLES

5 LIST OF FIGURES

6 INTRODUCTION

Diesel engines are the most efficient power plants among all known types of internal combustion engines. All over the world, heavy trucks, urban buses and industrial equipment are powered almost exclusively by diesel engines. In Europe, diesel-powered cars have become increasingly popular. The diesel engine is a major candidate to become the power plant of the future. Before that happens, however, further progress in diesel emission control is needed.

Internal combustion engines are significant contributors to air pollution, which has a damaging impact on our health and the environment, and is suspected to cause global climate changes. The environmental benefits of diesel engines such as low greenhouse gas emissions are mitigated by growing concern over emissions of nitrogen oxides and diesel particulates. Increasingly, tighter environmental regulations worldwide call for advanced emission controls and near-zero diesel emission levels in the years to come.

A sound understanding of the mechanism of combustion and information obtained through heat release analysis can be used to explain the effect of differences in engine design parameters on exhaust gas pollutants, fuel efficiency and aspects of engine durability. The effects of the different phases of combustion on exhaust gas emissions, engine performance and engine durability can be established, and engine design can be altered in such a way as to limit emissions and increase power output and engine life. In diesel emissions the main emphasis is on NO_X/Particulate emission trade-off and different particulate portions (carbon, lubricant oil and sulphates) (Heywood 1998).

To address some of the above issues it was decided to research the influence of boost pressure and intake charge temperature on diesel combustion. These influences on the combustion process will govern the formation of exhaust gas pollutants, combustion efficiency, engine durability and the overall fuel consumption of the engine. The outcome of the research should improve the understanding of the combustion process when boost pressure is increased and intake charge temperature is reduced to increase the brake mean effective pressure and fuel efficiency of the engine and to reduce emissions generation.

7 DIESEL COMBUSTION MECHANISM

For the onset of combustion, the compression ignition engine or diesel engine relies entirely on the fuel's ability to ignite spontaneously. To assist the onset of combustion in cold start or idle and low-load conditions, (especially at high engine speed) a glow plug is used. The glow plug assists the quicker onset of combustion and/or reduces exhaust gas emissions. The induced complete combustion at the above-mentioned engine operating conditions is of the highest importance to reduce unburned hydrocarbon and CO emissions.

The following engine parameters have a definite effect on engine behaviour:

- Engine combustion chamber design;
- Inlet port design and inlet and exhaust valve placement;
- Fuel injection pressure;
- Diesel injector design; and
- The fuel property itself.

The combustion chamber shape and inlet port design determine the air/fuel mixing process and the flow characteristics of the air, fuel and the later combustion gases (the combustion gases remaining in the chamber when most of the fuel is combusted) in the combustion chamber. The fuel injection equipment design and operation determine the rate of air/fuel mixing.

The fuel properties determine the fuel's ability to chemically prepare for combustion and the amount and rate of energy that can be released during the combustion process, and especially influence particulate matter exhaust gas emissions.

Diesel combustion can be divided into three phases:

- Starting with a short ignition delay;
- The initial stage of rapid combustion known as premixed combustion; and
- Diffusion combustion or mixing-controlled combustion (Heywood 1984).

Heywood (1984) also describes a fourth combustion phase which he calls the late combustion phase. This phase is not generally seen separate to mixing-controlled combustion, as the transition between the phases is not apparent.

7.1 IGNITION DELAY

Ignition delay can be defined as the time interval between start of injection and the start in combustion.

The start of injection is usually taken as the moment when the injector needle lifts off its seat. An injector needle-lift sensor is necessary to determine start of injection. If this apparatus is not available, an injector line pressure transducer or a clip-on transducer can be used.

The start of combustion is more difficult to determine precisely. It is best identified by the change in slope of the cylinder pressure data or the change in slope of the heat release rate, calculated from the pressure data. Another method that is widely used to determine the start of combustion - and the method used by the researcher - is to use the slope change on the rate of change in pressure data. The procedure will be described in detail in the combustion analysis section of this document.

Ignition delay is caused by different mechanisms which involve both physical and chemical processes. Due to the fact that the combustion chamber contents are in a heterogeneous state during the ignition delay, the physical and chemical delay periods run concurrently at different points (Taylor, 1989).

The physical delay period consists of the following processes:

1. Atomisation of the liquid fuel jet;
2. Heating of the fuel droplets;
3. Evaporation of the fuel droplets; and
4. Mixing of fuel vapour with air (Benson, et al, 1983 and Heywood, 1984).

During the chemical delay, the pre-combustion reactions reach completion. These reactions involve certain molecular chain-breaking or decomposition processes of the fuel, air and residual gas mixture, which yield various radicals, required to initiate

combustion (Saeed and Henein, 1983). These radicals (new chemical species called precursors) will at high enough concentrations lead to auto-ignition (Ferguson, 1986). When the pre-combustion processes are completed, the fuel is fully prepared but will not ignite unless a number of criteria are satisfied:

- The mixture ratio must be between the rich and lean limits for combustion; and
- The temperature must be above the spontaneous ignition temperature of the mixture.

The physical properties of a fuel have a dominant effect on the amount of fuel prepared during ignition delay, while the duration of ignition delay is determined largely by the fuel's chemical properties (Taylor, 1989).

The chemical ignition characteristics of the fuel affect the ignition delay. These properties of a fuel are very important in determining diesel engine operating characteristics such as fuel conversion efficiency, smoothness of operation, misfire, smoke, emissions, noise and ease of starting. The ignition quality of a fuel is defined by its cetane number, which is the fuel's ability to auto-ignite (Heywood, 1984).

Ignition delay has a significant effect on combustion and the formation of emissions, but to quantify such effects is not always that easy, as ignition delay depends not only on the chemical effects caused by the fuel, but also on the physical effects at the time of fuel injection.

The combination of chemical and physical effects influences ignition delay through various factors: (Heywood, 1984):

1. Good atomisation requires high fuel injection pressure, small injector hole diameter, optimum fuel viscosity and high cylinder pressure at the time of injection.
2. The rate of evaporation of the fuel droplets depends on the size of the droplets, their distribution and velocity, the pressure and temperature inside the chamber, and the volatility of the fuel.
3. The rate of air/fuel mixing is controlled largely by the injector and combustion chamber design. Certain engines are designed to amplify intake swirl levels and to increase the amount of squish and turbulence in the combustion chamber.

4. Injector design features such as the number and spatial arrangement of the injector holes determine the fuel spray pattern. The penetration of the spray depends on the size of the droplets, the injection pressure and the airflow characteristics.
5. Fuel volatility influences preparation rate by influencing evaporation rate.
6. Aromatic hydrocarbons have chemical bonds that are difficult to break and result in long ignition delay (Ferguson, 1986).
7. Increased air temperature caused by higher compression ratios will result in increased rate of fuel preparation and thus reduced ignition delay (Hardenberg, et al, 1993).

7.2 PREMIXED COMBUSTION

All the fuel that was physically and chemically prepared during ignition delay and satisfies all the criteria for ignition will burn during this phase of combustion. The duration of ignition delay determines the amount of mixture prepared, which controls the heat release rate and the amount of premixed combustion.

Auto-ignition occurs in the concentration band between the equivalence ratios of 1 and 1.5. Subsequent flame development, along mixture contours close to stoichiometric air/fuel mixture, occurs rapidly. This is thought to be due to spontaneous ignition of regions close to the first ignition site because of the rise in temperature associated with the strong pressure wave emanating from each ignition site, due to the local rapid chemical energy release. Spontaneous ignition at additional sites on the same spray, well separated from the original ignition location, can also occur. Turbulent mixing provides another flame-spreading mechanism, since there is no progressing flame front as in other premixed devices. From this point flame development is rapid, and as gas expansion occurs, the original injection spray plumes are deformed. These processes take place in each fuel spray in a closely comparable manner (Heywood, 1984).

Because the fuel and the oxidant are mixed on a molecular scale, premixed combustion rate is controlled by the rate of reaction alone. Premixed combustion will continue until all the mixture that has been prepared is consumed. It is thus evident that with extended ignition delays extremely high rates of heat release (ROHR) can occur. These high ROHR result in high rates of pressure rise that are responsible for the characteristic diesel knock (Taylor, 1989). The duration of the premixed combustion phase is short. These

factors make premixed combustion highly desirable, but unfortunately the associated rates of pressure rise result in excessive noise and engine stress (Taylor, 1987). It is also during premixed combustion that the endgas flame temperature reaches its maximum, which results in NO_X formation.

The burned gas within the flame-enveloped spray has only partially reacted and may be fuel rich. CO and CO_2 concentrations are high in these regions, but are oxidised later in the cycle as air is entrained into the spray region and additional energy is released (Heywood, 1984).

7.3 DIFFUSION COMBUSTION (MIXING-CONTROLLED COMBUSTION)

The fuel that is still in liquid phase during premixed combustion is not consumed during this phase but burned during diffusion combustion. In contrast to premixed combustion the pre-combustion reactions of diffusion combustion occur prior to the mixing of the fuel and air. As a result of the heat release during premixed combustion these pre-combustion reactions occur at a far higher temperature and pressure than those of premixed combustion. Combined with radicals already released, high pressure and temperature cause the ignition delay of diffusion combustion to be only a fraction of that of premixed combustion (Edwards, 1977).

The premixed flame completely surrounds the fuel droplets, and pre-combustion reactions of the evaporating fuel occur in the zone between the droplet and the flame. This pre-combustion zone does not contain adequate oxidising species and the reactions are pyrolitic (Taylor, 1987).

Pyrolysis refers to the reaction of fuel with insufficient or no oxidant. Pyrolitic reactions are usually endothermic and result in particulate emissions. The fuel evaporates from the droplets and undergoes pyrolitic pre-combustion reactions while flowing out of the combustion zone. The oxidant approaches the combustion zone from the outside and mixing occurs in the flame zone. The flame exists from the rich flammability limit on the inside to the lean limit on the outside of the fuel spray plume (Edwards, 1977).

Combustion cannot take place before evaporation and mixing have taken place, thus diffusion combustion is controlled by the rate of evaporation and mixing (Whitehouse and Way, 1984). For this reason diffusion combustion can be divided into two stages, the initial stage being controlled by the evaporation rate and the final stage being limited by the rate of mixing of the fuel and oxygen. It can be assumed that early in combustion, when oxygen is plentiful, combustion rate is controlled by evaporation rate. Later, when the temperature is higher and oxygen becomes scarce, combustion rate is controlled by the rate of mixing (Taylor, 1989).

Any factors affecting rates of evaporation and mixing will also affect diffusion combustion. Subsequently, in contrast with premixed combustion, diffusion combustion is controlled by the fuel's physical properties. These properties include fuel viscosity and volatility as well as injection pressure, as they influence fuel atomisation and evaporation. Swirl and fuel injection rate (increase in injection pressure) increase the air fuel-mixing rate within the fuel spray and therefore increase the heat release rate during the mixing-controlled combustion phase.

The duration of diffusion combustion affects efficiency if it is extended beyond 50^{o} crank angle (Taylor, 1987). As more fuel is burned later in the cycle, combustion temperatures will be lower, and therefore smoke formed in the early stages of combustion will be oxidised less effectively.

7.4 LATE COMBUSTION PHASE

Heat is released late into the expansion stroke for the following reason:
A small fraction of the fuel is not yet burned. A fraction of the fuel energy is present in soot and fuel-rich combustion product and can still be oxidised. The cylinder charge is non-uniform and mixing during this period promotes more complete combustion and less dissociated fuel gases (Heywood, 1984).

The kinetics of the final burnout processes become slower as the temperature in the combustion chamber decreases as the result of the expanding volume. It is during this phase that NO_X product formed during the premixed combustion phase will no longer be

able to decompose into nitrogen and oxygen, as the combustion chamber temperature has dropped below the decomposition temperature (Heywood, 1984).

Soot formed as the result of pyrolysis reactions during the diffusion combustion phase will "freeze" and will be emitted as particulate matter (PM) emissions. Below a certain temperature this combustion reaction will not occur as the combustion temperature drops as a result of the expansion process.

7.5 AIR MIXING MECHANISMS

7.5.1 Swirl

Swirl refers to the organised rotation of the air inlet charge about the cylinder axis and is created by bringing the intake flow into the cylinder with an initial angular momentum. During the engine cycle, some decay occurs due to friction, but a substantial amount of intake-generated swirl usually persists during the compression, combustion and expansion processes. In bowl-in-piston combustion chambers, the rotational motion set up during the intake stroke is substantially modified during compression. The bowl or cup serves to amplify the swirl during the intake process (Ferguson, 1986). Swirl is used in diesel engines to promote more rapid mixing between the induced air and the injected fuel (Heywood, 1984). Two general approaches are used to create swirl during the induction stroke:

- The flow is discharged into the cylinder tangentially toward the cylinder wall, where it is deflected sideways and downwards in a swirling motion.
- The swirl is largely generated in the inlet port. The flow is forced to rotate about the valve axis before it enters the cylinder.

Examples of the first type are directed port and reflective wall port, shown as A and B in figure 1, and the second type (helical ports) in C and D (Heywood, 1984).

With helical ports a higher flow discharge coefficient at equivalent levels of swirl is obtained, since the whole periphery of the valve open area can be utilised. A higher volumetric efficiency results. Also, helical ports are less sensitive to positional

displacements, such as can occur in casting, since the swirl generation depends mainly on the port geometry above the valve and not the position of the port relative to the cylinder axis.

Helical ports are capable of producing more swirl than directed ports at low valve lifts, but are inferior to directed ports at higher lifts. Either design creates swirl at the expense of volumetric efficiency, therefore high swirl ports are both helical and directed in design to supply good volumetric efficiency and swirl current (Ferguson, 1983).

Figure 1: Different types of swirl-generating inlet ports: (a) deflected wall; (b) directed; (c) Shallow ramp helical; (d) steep ramp helical. (Heywood, 1984: Fig 8.13)

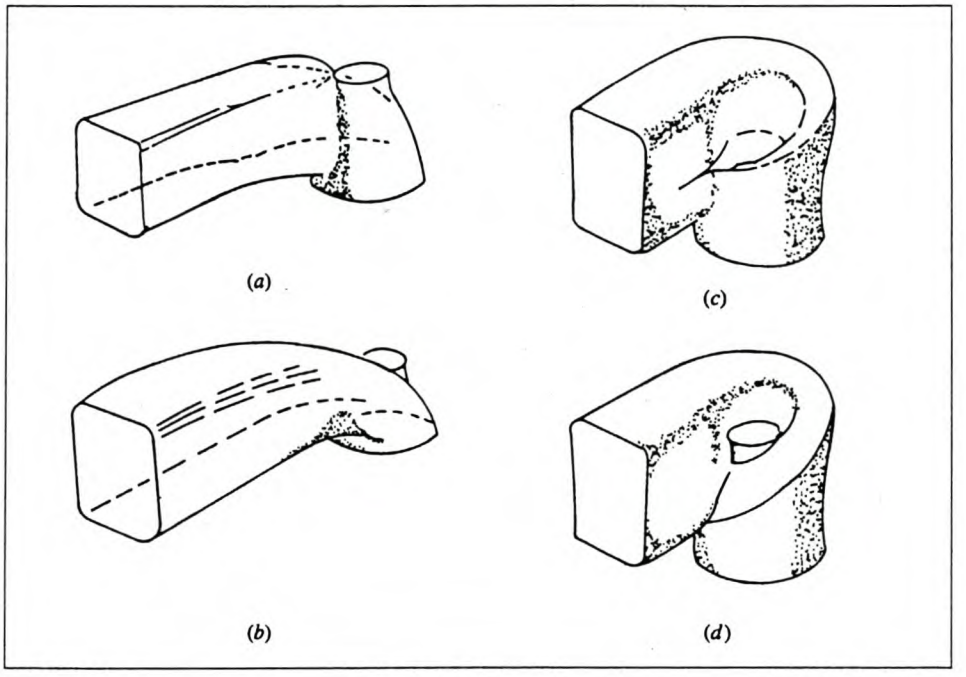

7.5.2 Squish

Squish is the radially inward or transverse gas motion that occurs towards the end of the compression stroke as parts of the piston and cylinder head approach one another closely (Heywood, 1984). Squish is most commonly associated with direct injection engines with bowl-in-piston combustion chamber design. The bowl or cup serves to establish squish.

The amount of squish is often defined by the percentage squish area – the percentage of the piston area that closely approaches the cylinder head (the shaded area on the piston indicated on Figure 2 expressed as a percentage of the total piston area, $\pi B^2/4$, (B: Bowl

Diameter). Squish generates gas motion as the result of an inflow of the combustion chamber content into the piston bowl when the squish area (of the piston) approaches the cylinder head.

Figure 2: Bowl-in-piston direct injection combustion chamber. (Heywood, 1984: Fig 8.19)

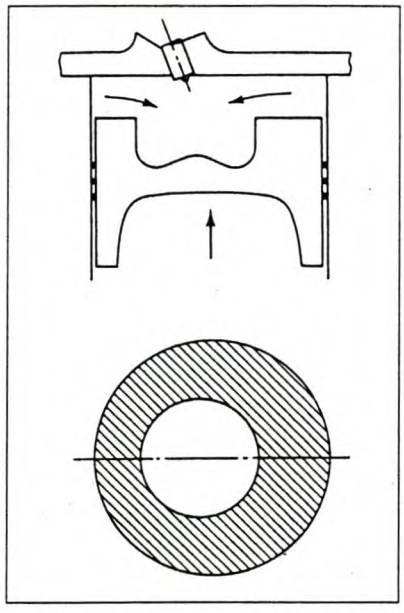

7.5.3 Turbulence

It has been generally accepted that the shear flow past the intake valve is the major source of turbulence in the engine and that this turbulence persists throughout the cycle. After intake valve closure (IVC), viscous shear stresses perform deformation work which increases the internal energy of the fluid at the expense of kinetic energy of the turbulent flow structure. Viscous dissipation therefore tends to reduce turbulence intensity during the cycle (Hansen, 1989). The piston bowl-bore diameter ratio and the piston crown-head clearance at Top Dead Centre (TDC) are factors which have a significant effect on the generation of turbulence. Production and dissipation of turbulence are governed by three main factors, excluding the initial generation of turbulence during the intake stroke (Hansen, 1989):

- Shear within the combustion chamber is created by angular velocity gradients caused by swirl deviating from solid body rotation. This shear process is a mechanism for generating and dissipating turbulence.
- Shear at the boundary layer adjoining the chamber walls has a similar mechanism of turbulence generation and dissipation.
- A third contributor is the result of compression. During compression, the turbulent kinetic energy is amplified due to the rapid distortion that the cylinder charge undergoes with rising cylinder pressure. Immediately after TDC there is a sharp rise in turbulence due to reversed squish. This mechanism for generating turbulence tends to decrease with increasing bowl-bore diameter ratio.

8 THE HEALTH EFFECTS OF DIESEL EXHAUST

Diesel engine emissions are highly complex mixtures. They consist of a wide range of organic and inorganic compounds distributed among the gaseous and particulate phases. Public health concern has arisen about these emissions for the following reasons (Nauss, 1999):

1. The particles in diesel emissions are very small (90% are less than 1μm by mass), making them readily respirable.
2. These particles have hundreds of chemicals adsorbed onto their surfaces, including many known or suspected mutagens and carcinogens.
3. The gaseous phase contains many irritants and toxic chemicals.
4. Oxides of nitrogen, which are ozone precursors, are among the combustion products in the gaseous phase.
5. The likelihood exists that humans be exposed to diesel emissions or their atmospheric transformation products in both ambient and occupational settings.

Diesel emissions have the potential to cause adverse health effects. These effects include cancer and other pulmonary and cardiovascular diseases. However, diesel engines are only one of many sources of ambient particulate matter and gaseous air pollutants. Therefore it is difficult to measure the exposures from various sources and to distinguish

the potential health risks attributable to exposure to diesel exhaust from those attributable to other air pollutants (Nauss, 1999).

9 DIESEL EMISSIONS FORMATION

Internal combustion engines contribute significantly to the urban air pollution problem. For this reason regulations limiting exhaust gas emissions emitted by spark ignition and compression ignition engines have become more and more stringent over the last decade.

Diesel engine exhaust contains oxides of nitrogen (nitric oxide, NO and small amounts of nitrogen dioxide NO_2), collectively known as NO_X, which is comparable to the concentration emitted by spark ignition (SI) engines. The hydrocarbon emission in the exhaust may also condense to form white smoke during starting and warm-up and during high speed, low load conditions. Particulate matter (PM) is also found in diesel engine exhaust and the concentration depends on the engine technology.

The composition of diesel exhaust varies considerably depending on engine type and operating conditions, fuel, lubricating oil, and whether an emissions control system is present. Diesel engine emissions have changed dramatically over the last 30 years because of improvements in engine technology, emissions controls and fuel formulation. Emissions of oxides of nitrogen and particulate matter from the diesel engines introduced in the late 1980s and early 1990s are significantly lower than those from older engines, as diesel engine technology was dominantly driven to reduce PM and NO_X emission.

In a diesel engine, since the fuel is injected just before combustion starts, the fuel distribution is non-uniform as a result of the fuel plume being injected into the combustion chamber. For this reason combustion is subdivided into small control volumes, which produce different combustion temperatures as a function of the oxygen/fuel ratio or fuel distribution and how the distribution changes due to mixing. Therefore lean oxygen/fuel ratios lead to increased NO_X formation, while at rich ratios a high soot formation is found. Due to the non-homogeneous conditions in diesel engines, both soot and NO_X occurs, however at different levels depending on engine load (Dürnholz, et al, 1992).

Figure 3 indicates how various parts of the fuel jet and the flame affect the formation of NO, unburned hydrocarbon and PM during premixed and mixing-controlled phases of combustion.

Nitric oxide forms in the high-temperature burned gas, but due to the non-uniform nature of diesel combustion, the formation rates are highest in the close to stoichiometric regions.

Soot forms in the rich unburned fuel-containing core of the fuel sprays within the flame region, where the fuel vapour is heated by mixing with hot burned gases. Soot then oxidises in the flame zone when in contact with oxygen, giving rise to the yellow luminous character of the flame.

Hydrocarbons and aldehydes originate in the regions where the flame quenches on the wall and where excessive dilution with air prevents the combustion process from either starting or proceeding to completion. Fuel that vaporises from the injector nozzle sac volume during the later stages of combustion is also a source of hydrocarbons.

Figure 3: Summary of pollutant formation mechanism in a direct injection diesel engine during "premixed" and "diffusion" combustion phase. (Heywood, 1984: Fig 11.13)

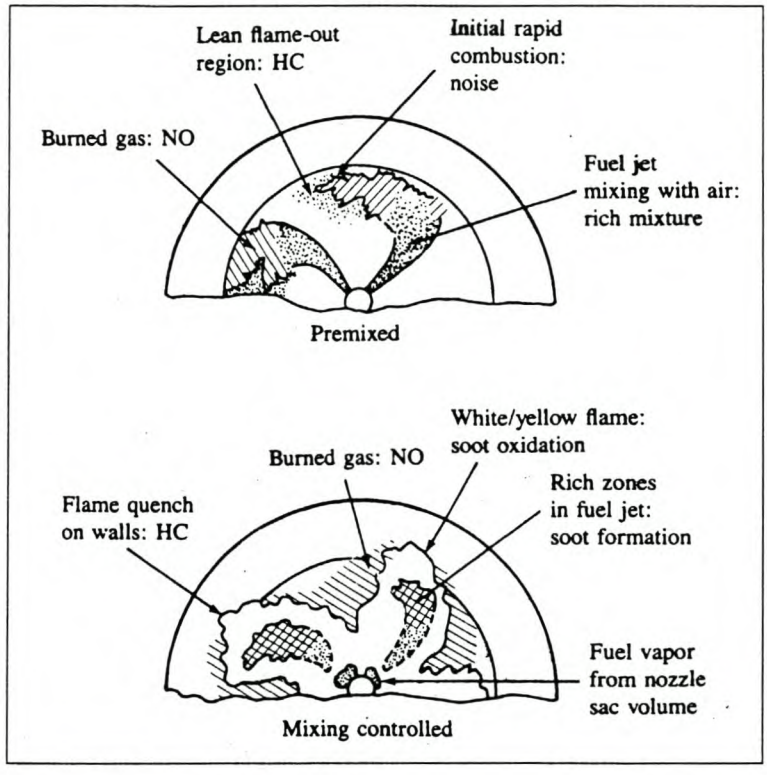

9.1 OXIDES OF NITROGEN (NO_X)

Nitric oxide (NO) and nitrogen dioxide (NO_2) are usually grouped together as NO_X emissions, but nitric oxide is the predominant oxide of nitrogen produced inside the combustion chamber of a diesel engine.

NO_X is formed during combustion as the result of the following mechanisms:

1. Thermal NO_X:

   Reactions during high temperature combustion processes in the vicinity of the flame zone generate both oxygen and nitrogen atoms and molecules by dissociation, which, according to the Zeldovich mechanism, subsequently result in nitric oxide (Herzog, et al, 1992). The local NO_X concentration reaches a peak at the point where the local burned gas equivalence ratio changes from rich to lean, or shortly after peak cylinder pressure has been reached. After the onset of combustion, the cylinder pressure and

temperature rise sharply (pre-mixed combustion phenomena) and result in increased fuel/air mixing, causing the local burned gas equivalence ratio to decrease and resulting in excess oxygen in the high temperature zone, a favourable environment for the formation of NO_X.

2. Oxygen NO_X:

   Chemical reaction in oxygen-poor layers of premixed combustion produces hydrocarbon radicals, which, together with nitrogen molecules form cyanides, from which nitric oxide originates from branch reactions (Herzog, et al, 1992).

3. Fuel NO_X:

   If fuel contains a significant amount of nitrogen, NO_X is formed from fuel-bound nitrogen during combustion at relatively low temperatures (Herzog, et al, 1992).

   During distillation, the fuel nitrogen is concentrated in the higher boiling fractions. In distillate fuels, the nitrogen can exist as amines and ring compounds, e.g. pyridine, quinoline and carbazoles. In the combustion chamber these compounds are likely to undergo some thermal decomposition prior to entering the combustion zone. The precursors to NO formation will therefore be low molecular weight nitrogen-containing compounds such as NH_3, HCN and CN. Detailed information on the kinetics of the NO formation from these compounds is limited. Oxidation of NO is usually rapid, occurring on a time scale comparable to that of the combustion reaction. The amount of fuel nitrogen converted to NO is sensitive to the fuel/air equivalence ratio. High NO yield is obtained from lean to stoichiometric mixtures and low yields are found for rich mixtures. The NO yield is only weakly dependent on temperature, in contrast to the strong temperature dependence of NO formed from atmospheric nitrogen (Heywood, 1984).

As the local burned gas equivalence (equivalence ratio is defined as the ratio of the actual fuel/air ratio to the stoichiometric fuel/air ratio) becomes leaner due to mixing with excess air, the NO_X concentration decreases, since formation becomes much slower as dilution occurs. There is a modest amount of NO decomposition.

Controlling NO_X requires the control of both the mixing and the combustion processes, with regard to local O_2/N_2 concentrations and local temperatures. This has an effect on

the rate of heat release, because as the rate of heat release increases, so NO_X increases (Rao, et al, 1993).

9.1.1 Nitric oxide (NO)

Nitric oxide is the predominant oxide of nitrogen produced inside the engine cylinder. The principle source of NO is the oxidation of atmospheric (molecular) nitrogen. However, if the fuel contains a significant amount of nitrogen, the oxidation of these components is an additional source of NO.

The mechanism of NO formulation has been studied extensively and it is generally accepted that during combustion of near stoichiometric fuel/air mixtures the principle reactions governing the formation of NO from molecular nitrogen are the following, which is known as the Zeldowich mechanism (Ferguson, 1986):

$$O + N_2 \rightarrow NO + N$$

$$N + O_2 \rightarrow NO + 0$$

$$N + OH \rightarrow NO + H$$

The critical time period for the formation of NO is when the burned gas temperature and pressure are at a maximum when the fuel/air mixture is close to stoichiometric air/fuel mixture, this being between the start of combustion and the occurrence of peak pressure. NO forms in both the flame front and the post-flame gases. The air/fuel mixture, which burns early in the combustion process, is the most critical to NO formation, as it is compressed to higher temperatures. Therefore NO formation in the post-flame gases almost always dominates any flame-front-produced NO. After peak pressure has occurred, burned gas temperature decreases as the cylinder gases expand. The combustion chamber temperature does not only decrease as the result of expansion, but also due to the mixing of high-temperature gas with air and cooler burned gas, which freeze the NO chemistry more rapidly than in a spark ignition engine, and result in much less decomposition of NO.

9.1.2 Nitrogen dioxide (NO_2)

Chemical equilibrium considerations indicate that for burned gases at typical flame temperature, the NO_2/NO ratio should be negligibly small, but not in the case of diesel engines, where they could constitute 10% to 30% of the total NO_X emissions. NO formed in the flame zone can be rapidly converted to NO_2 via reactions such as:

$$NO + HO_2 \rightarrow NO_2 + OH$$

Subsequently, conversion of this NO_2 to NO occurs via:

$$NO_2 + O \rightarrow NO + O_2,$$

unless the NO_2 in the flame is quenched by mixing with cooler fluid. This explanation is consistent with the highest NO_2/NO ratio occurring at light load, when the cooler region, which could quench the conversion of NO_2 back to NO is widespread (Heywood, 1984).

9.2 PARTICULATE EMISSIONS

Particulate matter basically consists of collections of primary particles (spherules) agglomerated into aggregates (hereafter called particles). The individual particles range in appearance from clusters of spherules to chains of spherules and can consist of up to 4000 spherules.

The spherules are combustion-generated soot particles, which vary in diameter between 10 and 80 nm, on which organic compounds have become absorbed.

These soot particles (Insoluble Fractions (INSOL)) and the organic compounds (Soluble Organic Fractions (SOF)) can be separated by using dichloromethane and a benzene-ethanol mixture. The SOF can further be divided into unburned fuel and oil-originated components by means of gas chromatography.

Table 1: Components of the soluble organic fraction. (Heywood, 1984: Table 11.9)

Fractions	Components of fractions	% mass of PM
Acidic	Aromatic or aliphatic Acidic function group Phenolic and carboxylic acids	3-5
Basic	Aromatic or aliphatic Basic function group Amines	<1-2
Paraffin	Aliphatics, normal and branched Numerous isomers from unburned fuel and lubricant	34-65
Aromatic	Unburned fuel, partial combustion and recombination of combustion products Lubricants	3-14
Oxyginated Hydrocarbons	Polar function group (No acidic or basic) Aldehydes, ketones or alcohols Aromatic phenols and quinones	7-15
Transitional	Aliphatic and aromatic Carbonyl fuction groups: ketones, aldehydes, esters and ethers	1-6
Insoluble	Aliphatics and aromatics Hydroxyl and carbonyl groups High molecular weight organic species Inorganic compounds Class fibers from filters	6-25

Sulphates (SO_4) can be separated from the INSOL by ultrasonic extraction, while the other substances in the INSOL can be treated as bound water and soot components (Kawatani, et al.).

9.2.1 Insoluble fractions (INSOL)

Soot is formed when fuel-rich mixtures are subjected to high temperatures, thus the temperature and equivalence ratio at a given time are critical as each parcel of fuel passes through the combustion process. The highest concentration of soot is found in the spray core region where the local equivalence ratio is at a maximum (In the extremely rich fuel vapour core, soot formation reaches a maximum) Soot concentrations rise rapidly soon after combustion starts.

Soot formation can be divided into two stages:

1. Particle formation

Fuel evaporates from the surface of the droplet and undergoes pre-combustion reactions in the absence of oxygen. These reactions are known as pyrolitic pre-combustion reactions and are responsible for PM emissions under certain conditions. The two types of molecules that are considered to be the most likely precursors for soot are various unsaturated hydrocarbons, particularly acetylene and its higher analogues, and the polycyclic aromatic hydrocarbons (PAH). The condensation reactions of gas-phase species such as these lead to the appearance of the first recognisable soot particles or nuclei. The nuclei are small, in the region of 2 ηm in diameter (Heywood, 1984).

2. Particle growth

The process by which the bulk of the solid-phase material is generated involves the attachment of gas phase species to the surface of the particles and their incorporation into the particulate phase. Particle growth includes surface growth, coagulation, and aggregation. To obtain surface growth, adsorption of species onto nuclei with the right hydrogen content or with higher hydrogen content, followed by dehydrogenation, or a combination of both processes is required to increase the volume (size) of the particle (Polyacetylenes and PAHs satisfy the requirement). Coagulation occurs simultaneously with surface growth, where particles collide and coalesce to increase the number of particle clusters or chains.

The soot formulation process continues until the oxidation process occurs due to mixing inside the combustion chamber, where soot or soot precursors are burned in the presence of oxygen. The process starts once fuel injection ceases and the rich cores mix to leaner equivalence ratios, and continue until the expansion process has cooled the gases considerably. The exhaust-emitted soot will depend on the balance of the formulation and the oxidation processes. A soot analysis show that almost all the soot formed is oxidised prior to exhaust (Heywood, 1984).

The soot particle undergoes a further mass addition process as the exhaust gases cool down and are diluted with air. Absorption into the soot particle surface and condensation

to form new particles of hydrocarbon species in the exhaust gases occur in the exhaust system and in the dilution tunnel, which simulates that which happens in the atmosphere.

Figure 4: Processes leading to net production of particulates. (Heywood, 1984: Fig 11.46)

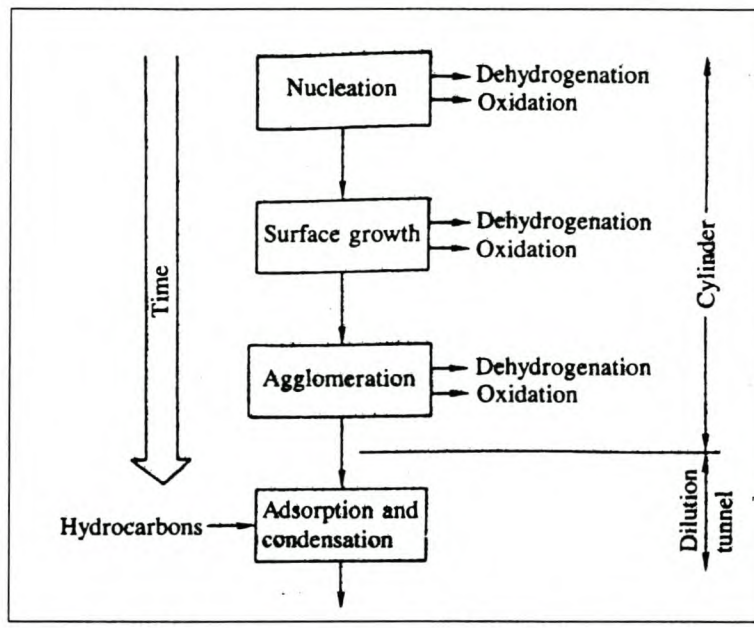

The main requirements of the fuel injection equipment (FIE) are to provide high fuel injection pressure and an optimised nozzle design to ensure a high rate of local air/fuel mixing of all the injected fuel. This results in a rapid entrainment of oxygen into the fuel spray, which suppresses the formation of soot (Greeves, et al, 1993).

9.2.2 Soluble organic fractions (SOF)

The SOF results from all the processes that cause HC emissions and their partial oxidation products. During the dilution and cooling down processes (temperatures below 500°C), the particles become coated with absorbed and condensed high molecular weight organic compounds as specified in table 1.

Unburned hydrocarbons including ketones, esters, ethers and organic acids, and Polynuclear aromatic hydrocarbons. The condensed material also includes inorganic species such as sulphur dioxide, nitrogen dioxide and sulphuric acid (sulphates) (Heywood, 1984). In addition some species originating from the lubrication oil are found

in the PM, the concentration of which depends on the oil consumption of the engine (Ferguson, 1986).

9.3 UNBURNED HYDROCARBON EMISSIONS

Fuel HC emissions originate from a small fraction of the injected fuel, which remains comparatively cold throughout the combustion process. There are five primary paths that exist by which the fuel can escape this normal combustion process in a direct injection diesel engine unburned and result in HC emissions:

1. Firstly the fuel/air mixture can become too lean to auto-ignite or to support a propagating flame at the conditions prevailing inside the combustion chamber. (Heywood, 1984).
2. Secondly, during the primary combustion process, the fuel/air mixture may be too rich to ignite or support a flame. This fuel can then be consumed only by slower thermal oxidation reactions later in the expansion process after mixing with additional air (Heywood, 1984).
3. The third source is due to the fuel emptying from the nozzle sac volume. (Greeves, et al, 1993)
4. Liquid fuel impingement on the combustion chamber wall is responsible for the fourth source. (Greeves, et al, 1993)

9.3.1 Overmixing or overleaning

As soon as fuel injection into the cylinder commences, a distribution in the fuel/air equivalence ratio across the fuel spray develops. This is illustrated in Figure 5:

In swirl flow ignition occurs in the slightly lean-of-stoichiometric region down-stream of the spray core. However, the fuel close to the spray boundary has already mixed beyond the lean limit of combustion ($\Phi < 0.3$) and will not auto-ignite or sustain a fast reaction front. This mixture can only oxidise by relatively slow thermal-oxidation reactions, which will be incomplete. Within this region unburned fuel, fuel decomposition products, and partial oxidation products (aldehydes and other oxygenates) will exist; and some of

these products will leave the cylinder without being burned. The magnitude of the unburned HC from these over-lean regions will depend on the:

- Amount of fuel injected during ignition delay;
- The mixing rate with air during this period; and
- The extent to which prevailing cylinder conditions are conducive to auto-ignition.

Thus, overleaning of fuel injected during ignition delay is a significant source of HC emissions, especially under conditions where the ignition delay is long (Heywood, 1984).

Figure 5: Schematic of diesel engine fuel spray showing equivalence ratio (ϕ) contours at the time of ignition. ϕ_L = equivalence at the lean combustion limit ($\approx$0.3) (Heywood, 1984: Fig 11.34)

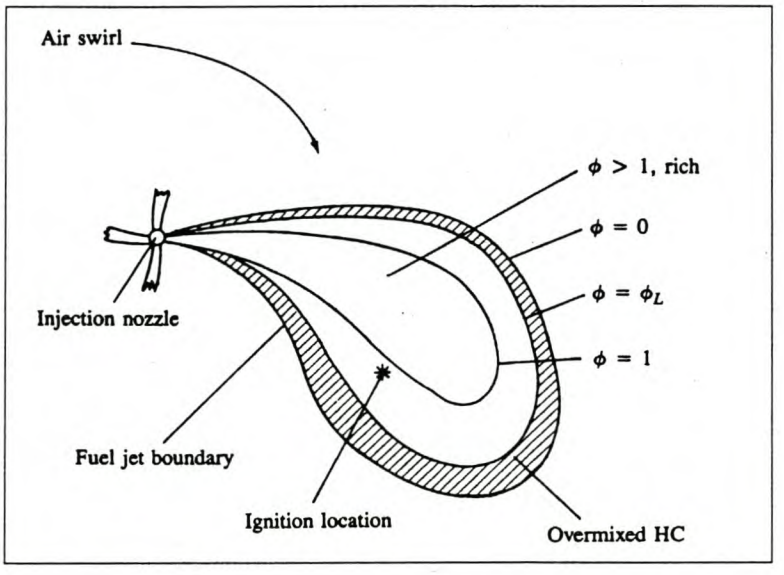

9.3.2 Under-mixing

There are two sources of fuel, which result in HC emissions due to slow and under-mixing of the fuel. In this case the most important source is the nozzle sac volume, although secondary injections can increase HC emissions if the problem is severe. The second source is the excess fuel that enters the cylinder under over-fuelling conditions.

At the end of the fuel injection process, the injector sac volume (the small volume left in the tip of the injector below the needle seat) is left filled with fuel. This fuel is heated during combustion and vaporised, and enters the cylinder at low velocity through the

nozzle holes. The fuel vapour mixes relatively slowly with air and may escape the primary combustion process.

In DI engines, exhaust smoke limits the full load equivalence ratio to about 0.7. Even though the overall equivalence ratio may remain lean, locally over-rich conditions may exist through the expansion stroke and into the exhaust process. HC emission concentrations show little variance with an increase in overall equivalence ratios until the critical value of about 0.9 is reached, when levels increase dramatically, mostly under acceleration conditions (Heywood, 1984).

9.3.3 Quenching and misfire

HC emissions show sensitivity to oil and coolant temperature, as emissions decrease as the temperatures increase. Since ignition delay has remained constant, over-mixing phenomena should remain approximately constant. Therefore wall quenching of the flame may also be a significant source of HC, depending on the amount of spray impingement on the combustion chamber walls.

In diesel engines, under adverse conditions such as low compression temperature and pressure and retarded injection timing, misfire may occur in a fraction of the operating cycle time, which causes HC emissions to increase as the percentage of misfire increases (Heywood, 1984).

9.4 CARBON MONOXIDE

Carbon monoxide (CO) emissions from internal combustion engines are controlled primary by the fuel/air equivalence ratio. In lean operating engines there appears to be an additional source of CO caused by the flame-fuel interaction with the walls, the oil films and the deposits. In theses circumstances the exhaust CO concentration is so low that it is not yet considered a practical problem.

As diesel engines operate well on the lean side of stoichiometric, CO emissions are low enough to be unimportant. It appears that Indirect Diesel Injection (IDI) engines emit less CO emissions than DI engines as the result of the higher mixing rates (Ferguson, 1986).

9.5 CARBON DIOXIDE

The formation of carbon dioxide is directly proportional to the amount of fuel burned and inversely proportional to the incompleteness of combustion. Improved efficiency is the only way to reduce CO_2 emissions, as it is an inescapable product of combustion. Diesel engines already produce lower CO_2 emissions than any other engine because of their high thermal efficiency, as combustion is associated with high compression ratios and high combustion temperatures (Hansen, et al, 1989).

9.6 THE EFFECT OF ENGINE PARAMETERS ON EMISSIONS FORMATION

9.6.1 Lubrication oil consumption and particulate emissions

It was found that lubrication oil consumption needs to be controlled not only at high speed and load, but also at low speed and load (Zelenka, et al, 1990). The reason for this is that at the high load conditions the heavy oil fractions are able to combust completely during the normal diesel combustion process, which is not the case at the low load conditions.

To achieve these objectives, activities in three different areas are necessary:

1. Minimisation of oil consumption from the cylinder wall, which is seen as the main source of lubrication oil particulates. Parameters that influence lubrication oil consumption from the wall are (Zelenka, et al, 1990), (Aufinger, et al, 1998):
   - Cylinder bore distortion.
   - Piston design and running characteristics.
   - Piston ring design and function.
   - Cylinder surface profile.
   - Cylinder surface temperature level.
2. Minimisation of all possible oil entrances into the intake system, such as valve stem seals, turbo-charger shaft seals and blow-by return (Zelenka, et al, 1990).
3. Lubrication oil formulation:

Development of lubrication oils which meet the requirements for very low lubrication oil consumption and for oxidation catalyst durability (Zelenka, et al, 1990). These oils must have the ability to affect the in-cylinder-oxidation efficiency and/or the particulate formation process (Needham, et al, 1991).

Piston oil ring unit pressure and reduced skirt clearances have a significant effect on oil consumption and PM emissions (Needham, et al, 1991). Results of a test done by Kawatani, et al show oil consumption as a function of speed and load in steady state operation.

Figure 6: The effect of piston unit pressure on steady state oil consumption and particulate emissions (Kawatani, et al, 1993: Fig 13)

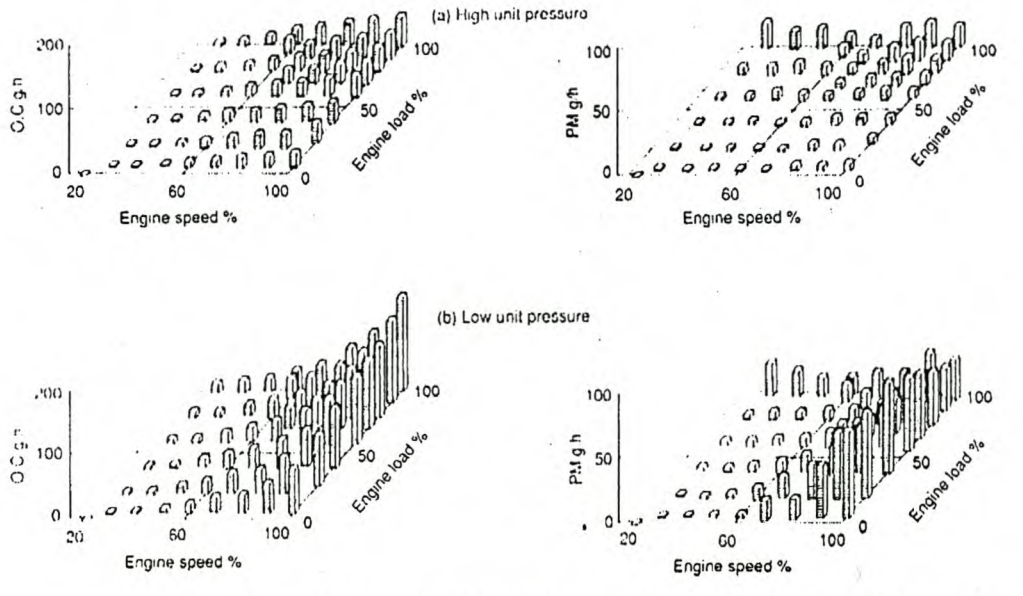

Fig. 13 Effect of piston oil ring unit pressure on steady state oil consumption and particulate (Engine B)

It is evident that oil consumption greatly increases with speed and load, as previously mentioned. Increased oil consumption contributes to an increase in PM. From this it is evident that the conversion rate for the oil consumed to PM is lower at low load. At high load, when combustion temperature is high, most of the consumed oil is burned out and does not leave the engine as PM. This is however not the case at low load conditions (Shore, 1988, Needham, et al, 1991, Kawatani, et al, 1993). What was also evident in the research done by Shore is that there is a strong speed dependency in the oil contribution to PM (the fraction of the PM mass that can be contributed to lubricant oil), being greater

at high speed. This may be due to more time available at low speed condition for the combustion of heavy lubricant oil fractions.

Figure 7: Typical oil consumption and particulate formation characteristics for a heavy-duty diesel engine (Needham, 1989: Fig 11)

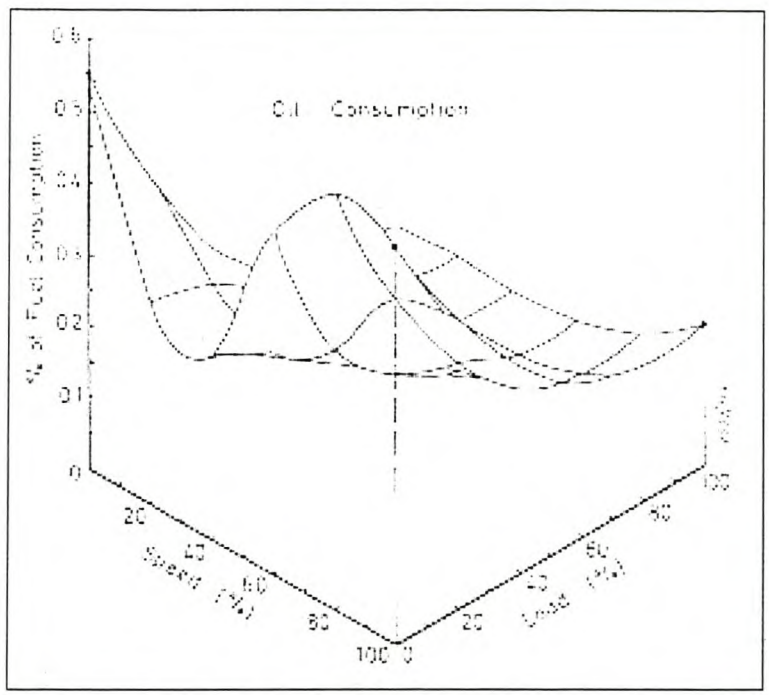

Tests done by Kawatani, et al on a 1991 model year base engine has shown that SOF account for approximately 40% of PM. Thereof as much as 90% are lubrication oil components, as shown in the figure 7 (Kawatani, et al, 1993).

9.6.2 Fuel quality

Emission sensitivity to fuel quality may vary from one engine technology to the next. Fuel injection equipment plays a very dominant role in the engine's dependency on fuel formulation to reduce exhaust gas emissions. The main diesel fuel parameters influencing the formation of NO_X and PM emissions are the cetane number, aromatic content and the sulphur content.

9.6.2.1 Cetane Number

The cetane number of a fuel has been identified as a strong influence on fuel-generated NO_X emissions (Herzog, et al, 1992 and Virk, et al, 1995).

The ignition quality of a fuel has a direct effect on the duration of ignition delay and subsequently has a direct influence on the premixed phase of diesel combustion. The longer ignition delay of a low cetane number fuel causes more fuel to be injected during the ignition delay period. This in turn results in more fuel being burned in the premixed combustion phase with attendant higher combustion temperatures and pressures, resulting in higher NO_X emissions (Virk, et al, 1995). To increase cetane number is an easy way to maintain the engine's fuel economy at reduced NO_X emissions levels (Aufinger, et al, 1998).

Reynolds has shown that a higher rated engine with electronically controlled fuel delivery proves to be insensitive to ignition quality over a high load cycle in terms of NO_X emissions. It was even found in certain specific cases that with an increase in cetane quality of the fuel the NO_X emissions increased. This is probably due to the high injection pressure and/or the engine management system responding differently to changes in fuel quality than would be expected. One of the reasons for this is that although the ignition delay time is short as the result of the high cetane quality, a great deal of fuel is physically prepared for combustion due to the high injection pressure. This results in a high rate of heat release during premixed combustion, which causes high combustion temperature during this phase and produces high NO_X emission.

For this reason Reynolds is of the opinion that a change in fuel quality does not greatly affect diesel engine emissions. Engine design changes however, provide greater benefits, especially where HC and CO emissions are concerned (Reynolds, 1995).

Cetane number is the only fuel parameter that influences CO and HC emission generation in a diesel engine (Martin, et al, 1997). HC emissions are reduced with higher cetane number, especially at light load/high-speed operation. Under heavy load conditions there are no significant differences between fuels of high and low natural cetane number. The natural cetane quality of the fuel has a significant effect on the levels of cold-start HC emissions on engines optimised for low NO_X emissions (Ullman, et al, 1994).

Cetane number has little effect on PM emissions under light and medium load conditions. However, under heavy load conditions at all speeds, PM emissions are significantly higher with the high cetane number fuel. Under increased load conditions and better

ignition quality fuel, a larger fraction of the injected fuel is burned during the diffusion phase. Unless an engine's air/fuel ratio is optimised for the diffusion combustion phase, relatively incomplete combustion can occur, resulting in increased PM and HC emissions (Virk, et al, 1995).

It was found that there is in general no difference in exhaust gas emissions (NO_X or PM) if the fuel has a natural cetane quality or when a cetane improver is used. (Virk, et al, 1995)

9.6.2.2 Aromatic Content

Probably a more important parameter for pure hydrocarbon fuels where reduction of NO_X formation is concerned is the total aromatic content, as NO_X emissions reduce with lower aromatic content (Rantanen, et al, 1993).

Hydro-treated diesel fuel with ultra low aromatic content displays significant emissions reduction performance on CO, HC, PAH and PM. ((Martin, et al, 1997). As can be expected the aromatic content of the fuel and the fuel's final boiling point tend to have the same correlation to the generation of PM. The heavier aromatics such as Tri- and Di-aromatics with higher final boiling points produce more PM emissions than Mono-aromatics (Tsurutani, et al, 1995).

9.6.2.3 Sulphur Content

The influence of fuel sulphur content on particulate formation has been studied in detail and all these studies correlate well with the study done by Zelenka (AVL) that indicates a mean gradient of (Zelenka, et al, 1990):

0.02 ± 0.004g/Hp.h total particulates per 0.1 wt. % sulphur, as indicated in figure 8.

Figure 8: Particulate emissions as function of sulphur content of the fuel. (Zelenka, 1990: Fig 11)

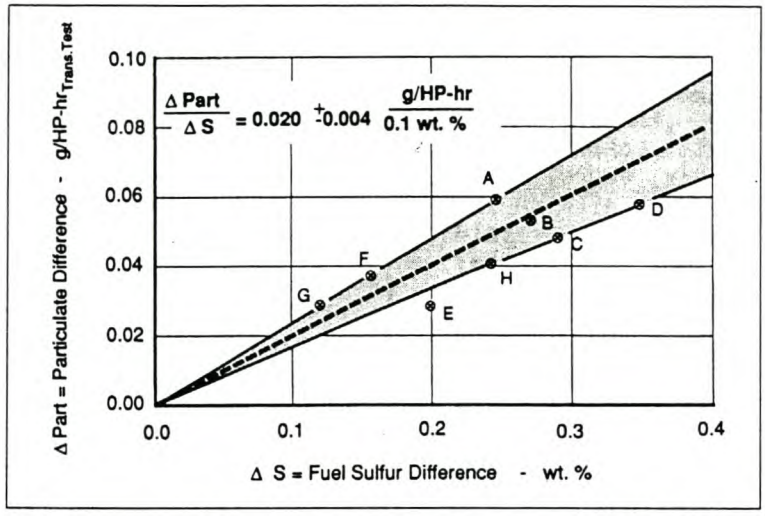

This PM formulation equation does not only apply to the differences in sulphates and bound water, but also to differences in lubricant oil particulates. This means that about a third of the total particulate sulphur gradient is due to the property of sulphates to attract HC from the gas phase, primarily attributed to the attraction of lubricant oil HCs.

Reducing the sulphur content of the fuel is advantageous in three ways:

1. Less particulate sulphates and bound water are formed (Zelenka, et al, 1990).
2. Less soluble organic PM from the lubrication oil is collected (Zelenka, et al, 1990).
3. The removal of sulphur from diesel fuel opens the door to the use of oxidation catalysts, since it virtually eliminates the formation of sulphates and acid in the catalytic system (Zelenka, et al, 1990, Walsh, 1993).

9.6.2.4 Fuel Density

Fuel density was found to have a significant effect on particulate emissions measured according to the ECE R49 test procedure. PM emissions were reduced by approximately 14% from one fuel to the other, with the density of the two fuels 849 kg/m^3 and 819 kg/m^3 respectively (Rantanen, et al, 1993 and Forti, 1994).

9.6.2.5 Fuel oxygen content

Oxygen content in diesel fuel was studied in detail by Ullman (Ullman, et al, 1994) at the Southwest Research Institute and indicated that oxygen content influenced transient CO

emissions more than any other fuel parameter studied by using statistical evaluation methods. On the engine used in the evaluation the variation in CO emissions were from 0.9 to 1.8 g/hp.h with a decrease in oxygen content, of which 70% of the variation was due to oxygen content alone. To increase the oxygen content in the fuel, glyme materials (monoglyme and diglyme) were added to the base fuel. Monoglyme is ethylene glycol dimethyl ether and diglyme is diethylene glycol dimethyl ether.

9.6.2.6 Synthetic derived fuels

- Synthetic fuel derived from the Fischer-Tropsch process showed very low levels of pollutants. The reason for this is that it contains only paraffins (mainly linear) with a very high cetane number (82.8), low viscosity (2.56 mm^2/s at 20°C) and density (0.761 kg/m^3 at 15°C) and a sulphur content of 0.0012% (Martin, et al, 1997).
- Oligomerisation fuel mainly containing iso-paraffins induces an increase in CO, HC and aldehyde emissions due to its very low cetane number (35.4) (Martin, et al, 1997).

9.6.3 The influence of low heat rejection engines on emissions

According to the second law of thermodynamics, higher combustion temperature is more efficient, as irreversibilities decrease with increasing temperature. The higher in-cylinder temperature causes shorter ignition delay, thus leading to a decrease in premixed combustion and a corresponding increase in the amount of fuel burned during the diffusion phase. This may affect the formation of NO_X and the amount of useful work extracted from the cycle. High temperature combustion should have a decreasing effect on incomplete combustion products such as CO, PM and HC (Assanis, et al, 1991).

9.6.4 Exhaust gas re-circulation (EGR)

Most of today's European IDI and DI light-duty diesel vehicles use exhaust gas re-circulation (EGR) very effectively to reduce NO_X in order to comply with the stringent light-duty diesel NO_X standards. EGR can be in the form of a relatively simple on-off EGR control system, or a sophisticated closed-loop system, in conjunction with electronic fuel injection control (Herzog, et al, 1992).

EGR basically leads to lower local maximum temperatures and lower oxygen concentrations within the combustion chamber, which inhibit NOx formation, as the NO formation velocity strongly depends on these (Bazari, et al, 1992, Dürnholz, et al, 1992). EGR mainly influences ignition delay and the resulting initial premixed combustion, due to the change in chemical kinetics caused by the reduced oxygen, by increased specific heat of the gases in the cylinder and by the increase in intake temperature. The fact that the specific heat of the recycled exhaust gas is predominantly higher than that of fresh air has a significant influence on flame temperature and NO_X formation (Needham, et al, 1991, Dürnholz, et al, 1992, Mikulic, et al, 1993). Ignition delay is also influenced by the mixture oxygen/inert gas concentration, with the result that, at constant air temperature, ignition delay decreases with an increase in oxygen concentration (Dürnholz, et al, 1992).

EGR can be utilising as hot or cooled re-circulated exhaust gas. Hot EGR increases intake charge temperature which results in an air/fuel ratio decrease. This increases the PM formation, or more precisely, the soot fraction of the particulate. The increase in PM can be mitigated by applying EGR cooling, though this will have little effect on NO_X emissions. At light load EGR is most effective in NO_X reduction with no effect on particulate matter. The latter is due to the fact that at light load; PM consists to a very high percentage (up to 90%) of soluble organic fractions (lubrication oil and fuel components) and very little soot. Both are hardly affected by EGR. Due to the vast availability of air at low loads, smoke is generally low and hardly affected even at high EGR rates. Therefore EGR proves to be beneficial at light loads, with regard to NO_X and particulate emissions (Herzog, et al, 1992). At high load, more commonly associated with heavy-duty diesel engines, EGR causes, percentage-wise, a sharp increase in particulate, which is more dramatic the higher the load. Due to this a very precise metering system is needed if EGR is to be used at high load to control NO_X without excessive particulate generation. Furthermore, the EGR rate has to be metered as a function of speed and load in order to ensure the correct balance between NO_X reduction and particulate increase (Herzog, et al, 1992).

Figure 9: The effect of oxygen concentration on ignition delay (Noboru, et al, 1993: Fig 6)

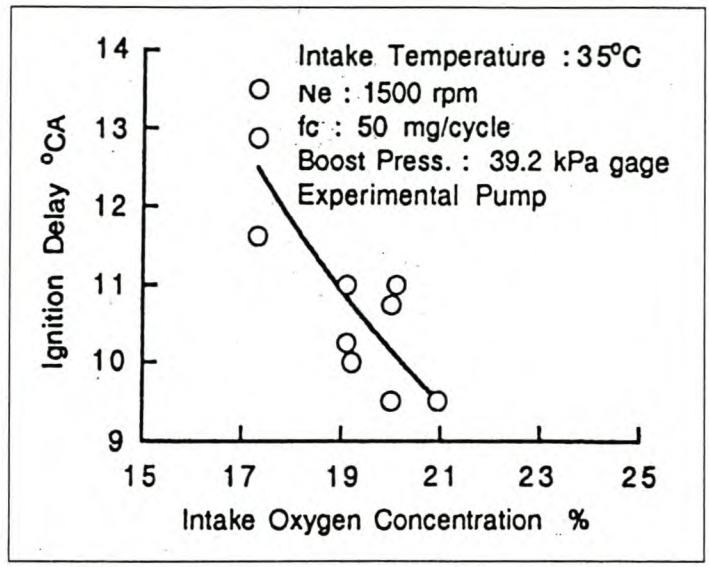

The specific fuel consumption increases with an increased EGR rate. This is probably due to the fact that the duration of ignition delay increases, as combustion shifts to later in the cycle (Mikulic, et al, 1993).

Serious concern exists about reduced engine durability due to the increased wear rates when introducing EGR:

Firstly, the wear rate increases approximately proportional to the soot mass flow rate through the engine and the re-circulating sulphuric acid arising from the fuel sulphur (Zelenka, et al, 1990, Needham, et al, 1991). An increased soot concentration in the lubricant exacerbates wear by reducing the effectiveness of the anti-wear additives in a degradation of the quality of the oil surface film. Valve train components, together with the top ring, are particularly susceptible to wear (Needham, et al, 1991). A possible solution for this problem is to use high quality lubrication oil, as used in existing light-duty diesel engines with EGR. It was found that cylinder wear of diesel engines equipped with EGR excessively increased under low coolant temperature conditions. The mechanism of abnormal wear was identified as corrosive wear rather than abrasive wear of cast iron, attributable to the formation of sulphuric acid through the reaction of water condensed on the surface of the cylinder with the combustion product SO_X, the latter being quantitatively increased with EGR operation. By increasing both the quantity

of metal detergent and the detergent's sulphuric aid neutralisation speed, cylinder wear could be remarkably reduced (Herzog, et al). Therefore it is essential to use EGR in combination with a low sulphur fuel and low soot emissions combustion systems, in order to reduce wear (Aufinger, et al, 1998).

Secondly, in many heavy-duty turbo-charged diesel engines the intake manifold pressure exceeds the exhaust manifold pressure over much of the engine operating range where EGR is to be applied. This excludes a simple EGR system being used and requires the additional complexity of an EGR pump or intake throttle, or possibly a reed valve system using the exhaust pulse energy. Alternatively, the EGR can be fed into the compressor intake but this causes major problems with compressor and inter-cooler fouling (Needham, et al, 1991).

9.6.5 Injection Equipment

9.6.5.1 Injection rate control

NO_X emissions will be reduced through reducing the amount of fuel injected during ignition delay. To achieve the initial rate control of the following measures must be implemented (Herzog, et al, 1992):

1. Lengthening of duration of injection by means of reducing spray hole diameter
2. Reduction of initial fuelling through adapted FIE (fuel injection equipment) by means of double plunger helicons and needle seat throttling interruption of the injection pressure event.
3. Initial pressure control at the pump.

As can be expected of combustion, NO_X formation is not solely dependent upon the initial rate of fuelling but also on the local mixture formation processes around the spray.

Tests done by AVL indicated that NO_X formation remained unaffected although fuelling during ignition delay has been reduced. This phenomenon can be explained by the fact that with reduction in spray hole diameter a higher degree of flame propagation toward the nozzle is caused, thereby increasing both air utilisation and spray combustion regions. This mechanism increases NO_X formation and thereby reduces the effect of lower rate of

fuel injected during ignition delay. These two counter current NO_X formation effects are generally valid. However, their relative significance on NO_X emissions is related to the duration of ignition delay. Reducing ignition delay yields ignition zones closer to the nozzle, and consequently the differences in the combustion regions of different nozzle hole sizes are diminished. As a consequence the NO_X reducing effect of reduced fuelling during ignition delay becomes more dominant with smaller ignition delay (Herzog, et al, 1992).

Another possibility of increasing the duration of injection (DOI) is the reduction of the geometric pumping rate (volume per degree cam angle), which reduces NO_X significantly, but exacerbates soot and PM emissions.

These results clearly indicate the challenge concerning the ideal pumping rate and consequently, the ideal injection rate. The use of the ideal rate of injection should reduce NO_X without any increase in soot and PM emissions. Furthermore, the injection rate-shaping techniques must also be aimed at the optimum mixing between fuel and charge. The initial spray not only has to provide the desired amount of fuel, but its distribution in the combustion chamber must be matched to yield optimum ignition and flame propagation (Herzog, et al, 1992).

Injection rate control can be used to limit both NO_X and particulates:
The former can be limited by shaping the start of injection to limit the amount of fuel injected during ignition delay (Racine, et al, 1991 and Bazari, et al, 1992). Particulates and HC emissions can be limited by a sharp injection cut at the end of injection to avoid all post injection, thus avoiding a poorly controlled and atomised end of injection (Racine, et al, 1991 and Bazari, et al, 1992). Rapid injector spill is also required to minimise the formation of smoke emissions. Rapid spill increases the mean effective injection pressure (MEIP) of the overall injection and improves fuel atomisation at the end of injection. It has a reducing effect on PM emissions, especially at high speed/light load operating points (Needham, et al, 1999).

The optimum rate of injection is as summarised below: (Zelenka, et al, 1990)

- During ignition delay the rate of injection (ROI) has to be small, followed by the main injection that requires a steeply enlarged ROI.

- As speed and load increase, the fullness of the ROI of the "main injection" should be raised, thus leading from a triangular-shaped ROI to a square shape at rated power.

Figure 10: Shape of ideal rate of injection for the optimum mixture formation for a swirl-supported combustion chamber (Zelenka, et al, 1990: Fig 7)

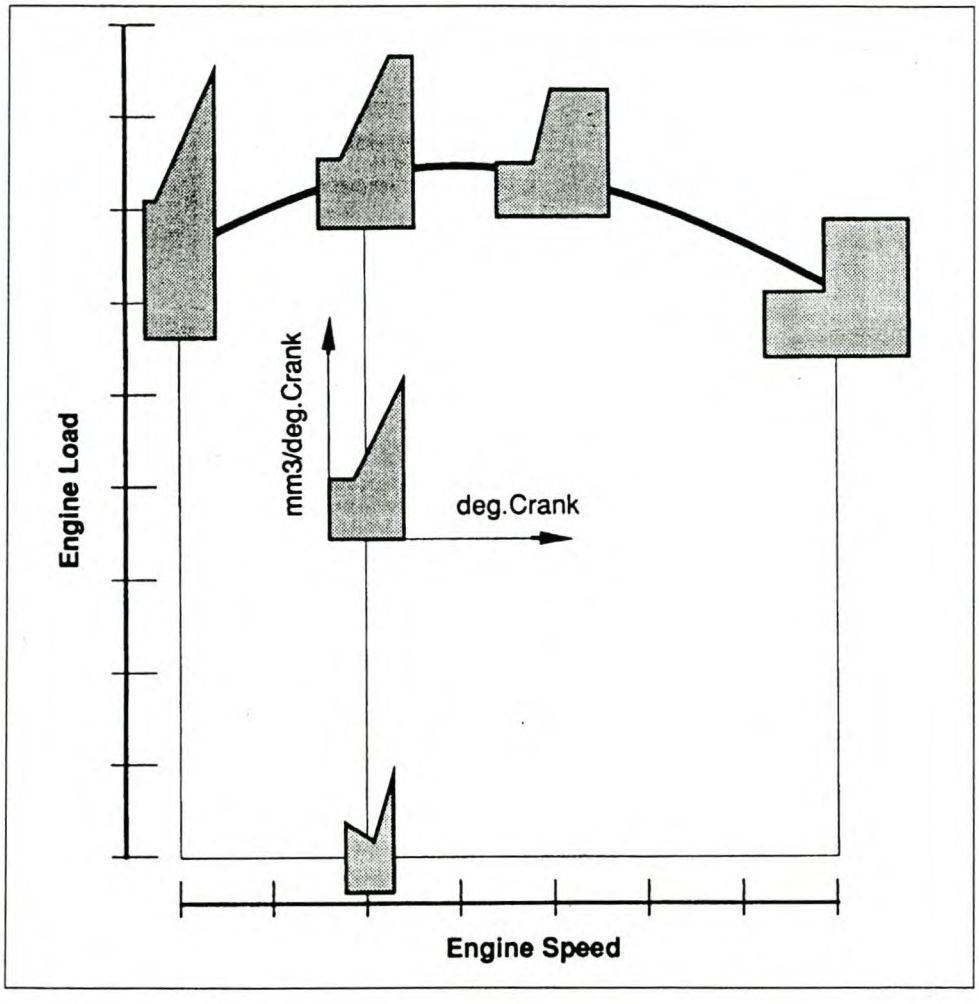

9.6.5.2 Pilot injection

By injection rate shaping the smoke level will be increased, because a larger amount of fuel is injected in the already burned flame. Therefore a way must be found to preheat the combustion chamber by means of a small amount of fuel burned, and the main combustion may only start after this pre-combustion. This requires a pilot injection quantity as a function of load and engine speed and an adapted main injection following the pilot injection after a pre-determined time. Unit injectors are the best option for the task (Mikulic, et al, 1993). The amount of fuel injected during the pilot injection is of the utmost importance:

- If too great an amount of fuel is injected, the quantity of mixture prepared during ignition delay is too large. This causes excessive premixed combustion, which results in NO_X formation and combustion noise.
- When too little fuel is injected, the combustion chamber is not heated enough to shorten ignition delay for the main injection.

More or less 50% of the total fuel charge should be injected during the first injection. The two injections should be very close together in order to minimise soot formation and enhance oxidation (Bower and Foster, 1993). Preferably the ignition delay between the pilot and main injection must be non-existent (Needham, et al, 1998).

Careful optimisation of the quantity of pilot injection and the interval between injections should be done in order to get maximum advantage out of pilot injection so as to improve the NO_X-PM trade-off. An advantage of pilot injection is that NO_X formation depends much less on the start of the main injection (engine operating with pilot injection) than it does on start of injection without pilot injection (Mikulic, et al, 1993 and Bower, 1993). Thus start of injection must be set much more accurately with an engine operation without pilot injection, in order to obtain the same NO_X scatter as for an engine operating with pilot injection.

9.6.5.3 High injection pressure

With high-pressure injection, ignition delay decreases and the rate of heat release during premixed combustion and the early part of diffusion combustion increases due to the higher injection rates. As fuel injection pressure rises, the air/fuel mixing process increases and rapid heat release takes place. This effectively reduces smoke and PM emissions because of the high-efficiency fuel atomisation, but on the other hand increases NO_X formation (Uyehara, 1992, Uchida, et al, 1993 and Kawatani, et al, 1993,).

The higher the injection pressure the lower the requirement for ignition quality of the fuel. The reason for this is that with better atomisation of the fuel the physical preparation of the fuel is shorter and therefore ignition delay is decreased. But the amount of fuel prepared during the ignition period remains the same, therefore higher cetane is still required to reduce NO_X emissions.

Particularly in the high speed/low load engine operating ranges, combustion tends to be relatively slower than the piston speed, which makes it necessary to shorten the injection period by higher injection pressure so that all the injected fuel is burned in the combustion bowl chamber.

9.6.5.4 Injector geometry

Any variation in nozzle hole diameter will influence both injection pressure and duration of injection. Therefore, when changing nozzle hole diameter either the injection pressure or the injection duration must be changed. As nozzle hole diameter decreases and injection pressure is compensated to keep injection duration constant, NO_X formation as well as BSFC (Brake Specific Fuel Consumption) are reduced. Particulates, HC and CO are influenced by load: at low load emissions decrease with an increase in hole diameter (Yan, et al, 1993) and at high load they increase, due to over mixing (Bazari, et al, 1992).

The amount of fuelling during ignition delay, achieved by varying the nozzle hole diameter, affects NO_X emissions. Decreasing fuelling results in a reduction in NO_X emissions, especially at full load. At part load NO_X initially increases, before diminishing later, as shown in the figure 11.

Figure 11: Effect of the amount of fuel injected during ignition delay on NO_X-emissions (Zeleka, et al, 1990)

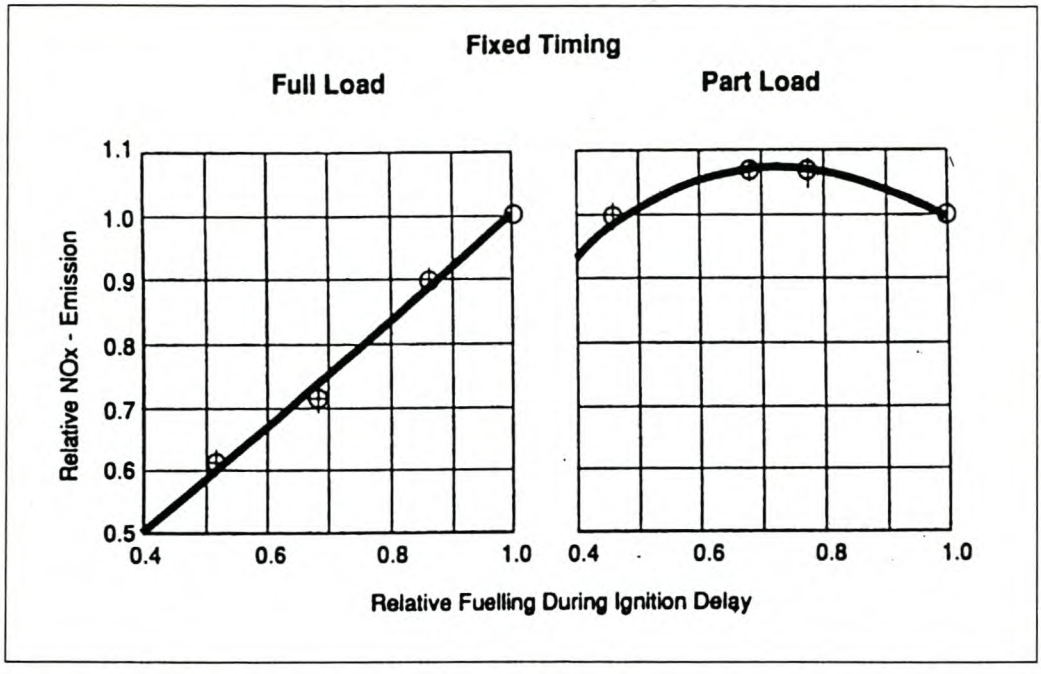

The effect of injector nozzle hole length on pollutant levels is very important. An increase in length/diameter ratio reduces the spray cone angle, but increases the penetration of the injector into the combustion chamber. Thus smoke and CO levels are reduced, but HC emissions increase as a result of wall impingement (Racine, et al, 1991).

9.6.5.5 Injection timing

Retarding injection timing has been up to now the most widely used method to reduce NO_X emissions (Yan, et al, 1993). This method however, has a negative effect on fuel efficiency and PM emissions.

As temperature and pressure increase as injection comes closer to TDC, ignition delay becomes shorter, with the result that NO_X emissions decrease (Uyehara, 1992). Delayed injection timing shortens ignition delay, as injection takes place closer to TDC where compression temperatures and pressures are higher. Therefore the greater part of combustion takes place in the expansion stroke, which causes combustion temperatures to be lower and less NO_X to be formed.

Over-delay causes an increase in specific fuel consumption (SFC). Delayed combustion causes a shorter effective expansion stroke which leads to lower efficiency. Delayed fuel

injection time has a greater effect on SFC at higher speed, as the time for combustion is limited (Corcione, et al, 1991, Bazari, et al, 1992).

9.6.5.6 Electronic fuel injection timing

Electronic fuel system control offers well-known freedom to optimise the various trade-offs (HC- NO_X -PM-BSFC) as a function of speed, load and ambient conditions in steady state and transient tests. This provides flexibility to adapt the engine for different environmental requirements (Zelenka, et al, 1990).

Electronic control enables the realisation of the highest dynamic engine requirements; such as good load response with minimised acceleration smoke puffs and dynamic injection timing advance for quick and clean cold start and warm-up.

When electronic fuel injection controls are introduced, NO_X reduction using EGR can be implemented, electronically controlled by the ECU to optimise exhaust gas emissions and reduce engine wear rates. Implementation can be introduced instead of or in addition to timing retardation, with the benefit of improved fuel economy at a given NO_X limit (Aufinger, et al, 1998).

9.6.6 Air swirl optimisation

Combustion in diesel engines is mixing-controlled, and the swirl imparted to the inlet air assists in faster air/fuel mixing and better combustion. This, combined with high injection pressure further increases the combustion efficiency, but as injection pressure increases the sensitivity of the smoke emissions to the swirl ratio diminishes (Racine, et al, 1991). However, high gas velocities are associated with the disadvantages of reduced thermal efficiency and increased thermal loading (Rao, et al, 1993).

With a high swirl ratio, (The swirl intensity level is set by swirl ratio H. It is the relation between rotational velocity of air swirl and crankshaft) especially at low speed, the amount of fuel prepared during ignition delay is considerably higher than at low swirl, and when combined with high-pressure injection the amount of premixed combustion is excessive and causes high NO_X emissions (Shundoh, et al, 1992 and Rao, et al, 1993). To keep NO_X formation within bounds, the swirl ratio must be reduced when injection

pressure is increased to avoid excessive air/fuel mixing during ignition delay (Needham, et al, 1999). Reduction of intake charge rotation inhibits both the transport of fuel into the charge during ignition delay and the supply of unburned charge into the burning spray. As a consequence NO_X will be reduced. Soot for the same reason will increase (Herzog, et al, 1992).

According to Bazari, et al (Bazari, et al, 1992), PM and HC emissions decrease with a higher swirl level, except at high load where swirl causes these emissions to increase due to overmixing. At high load the high injection pressure already provides a favourable air/fuel mixing at moderate swirl; at high swirl this operating point will be more prone to overmixing. With increased injection pressure and lower swirl ratio, the spray penetration increases and the combustion bowl diameter therefore needs to be enlarged to avoid impingement of fuel on the combustion bowl wall. As a consequence HC emissions increase (Racine, et al, 1991 and Needham, et al, 1999).

9.6.7 Turbo-charging

The characteristics of a reciprocating machine such as an internal combustion engine typically does not match up well with rotating machinery such as a turbo-charger over an entire operating range. Therefore a turbo-charged engine exhibits two distinctive features:

- Poor boosting capability, which results in insufficient engine torque over the low speed range; and
- Over-boosting, which results in excessive cylinder pressure and over-speed of the turbo-charger over the high-speed ranges (Endo, et al, 1993).

Careful turbo-charger matching is required to avoid low air/fuel ratios around peak torque without compromising fuel consumption at rated power due to excessive pumping work (Needham, et al, 1991). Changing charge pressures but keeping charge temperatures constant shows that with an increase in charge pressures the NO_X first increases and subsequently decreases again, whereas the soot shows the opposite behaviour (Herzog, et al, 1992).

Figure 12: The effect of inlet manifold pressure on BSFC, Excess air ratio and Emissions at Constant Absolute Inlet Manifold Pressure of 300K (Herzog, et al, 1992: Fig 3)

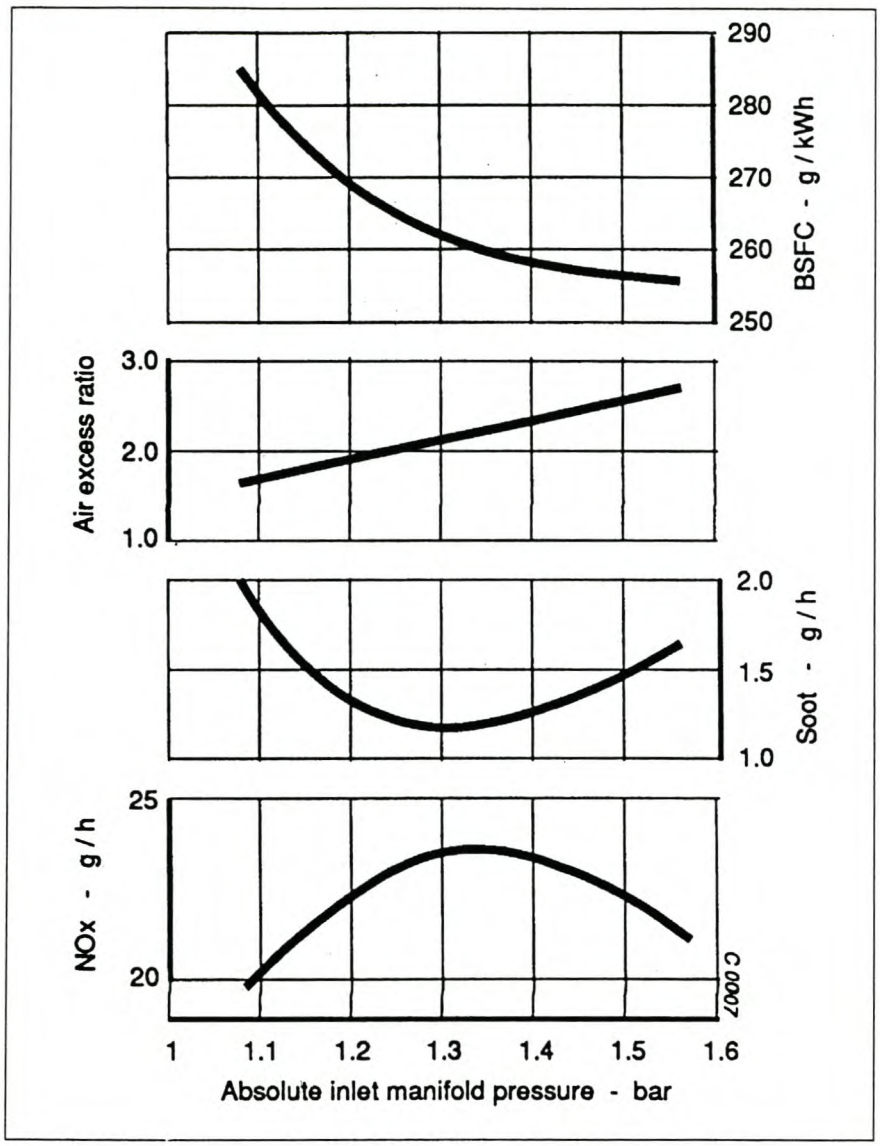

This tendency shifts to higher boosts as the load increases. There are a variety of counter current conditions contributing to this behaviour. Factors that increase NO_X formation with increasing boost pressures are higher oxygen availability and increased disruption of the fuel spray on its boundaries. On the other hand, with an increase in boost pressure, a slight decrease in cylinder flame temperature is observed. This is a result of increased excess air and reduced spray penetration at higher air density, leading to less expanded spray plumes, which results in reduced local air/fuel ratios across the spray. The latter is obviously dominating beyond the NO_X-maximum in the above figure. An increase in

boost pressure reduces ignition delay and premixed combustion, and enhances diffusion combustion (Uchida, et al, 1993). For this reason it can be stated that NO_X will increase as intake charge pressure increases and become practically constant, whereas soot behaves inversely (Herzog, et al, 1993). Higher boost levels may also induce higher swirl, squish and turbulence levels, which influence mixing rates and enhance NO_X formation. Boost pressure influences the degree of wall impingement, with the effect that the latter is reduced with an increase in boost pressure (Bazari, et al, 1992).

The primary control mechanism of turbo-charging is the change in the pressure and temperature of the air in the cylinder before compression. An additional factor, especially when emissions are expressed on a specific power basis rather than as a concentration, is that the IMEP (indicated mean effective pressure) in a turbo engine increases without the corresponding increase in friction losses. The brake power output will therefore, proportionally, increase more than the IMEP. The brake specific emission level will be lower at the same/concurring emission concentration (Watson and Janota, 1982).

A turbo-charged engine without inter-cooling will increase the inlet air temperature, which shortens ignition delay, especially at high speed and high load. At the same time premixed combustion will decrease, as less fuel was prepared during ignition delay. On the other hand the higher inlet temperatures improve the oxidation of HC emissions. The most important contributor in the formation of NO is temperature; therefore NO formation will increase as inlet pressure increases, although cylinder pressure and the air/fuel ratio are also conducive.

By increasing inlet pressure and keeping the air temperature constant NO concentration is increased, whereas the power output increases as the fuel supply is raised so as to keep the air/fuel ratio constant. The specific NO emissions remain basically constant. However, if the inlet air temperature is raised at a constant pressure air/fuel ratio, NO concentrations and brake specific emissions will increase as the power output decreases. An increased air/fuel ratio has two results, namely an increase in the O_2 concentration and a decrease in the combustion temperature as the excess air absorbs the energy. The low combustion temperature is, however, predominant because the local air/fuel ratio

changes little in the spray. NO formation decreases with the increase in the air/fuel ratio (Watson and Janota, 1982).

An increase in fuel consumption as well as an increase in smoke and particulate emissions with injection time delay is counteracted by turbo-charging because of the presence of a greater amount of excess air (Watson and Janota, 1982). Turbo-charging also improves the air/fuel mixing and diffusion combustion in order to limit soot and HC emissions.

At low speed and full load conditions, higher volumetric efficiency (ηv) is required because of the need for air to achieve acceptable torque, which results in better fuel consumption due to the better combustion. On the other hand, at higher speed and other load conditions, better boost pressure and less pumping losses are necessary to improve fuel economy (Endo, et al, 1993).

9.6.7.1 The effect of turbo-charger lag on emissions

Turbo-charger lag is the turbo-charger's inability to respond rapidly to the change in load simply due to its inertia. When a sudden load is applied to the engine, its speed drops. The governor responds quickly and provides more fuel, but due to the slow response of the turbo-charger, the drop in engine speed and the increase in exhaust temperature, the airflow rate drops still further. At this stage the engine is operating on a very rich air/fuel mixture, which results in poor combustion and black smoke. This reduces the turbo-charger response and further exacerbates the system's poor transient response (Pattas, et al, 1992). During this turbo-charger lag, high concentrations of PM (especially soot) and HC emissions are generated as the result of the over-rich mixture.

9.6.7.2 Variable geometry turbo-charger (VGT)

A VGT can be used to control exhaust emissions, as a higher degree of control over boost pressure and air/fuel ratio can be achieved over the complete operating range of the engine.

At high load conditions smoke and PM emissions may be reduced by employing higher air/fuel ratios. Similarly HC emissions can be reduced during cold starting by increasing exhaust back pressure (the increased exhaust back pressure will increase the pumping

work of the engine, therefore increasing engine load), and at high speed/low load conditions by increasing boost pressure and temperature to reduce ignition delay (Pilley, et al, 1989).

9.6.7.3 Waste gate valve

A waste gate valve allows one to select a smaller turbine housing to achieve higher boost at lower engine speed in order to improve low speed torque. On the other hand it allows one to reduce turbo over-speed and over-boosting at high engine speed. At these conditions the waste gate reduces the turbine backpressure, which causes less power to be available from the turbine, resulting in lower turbo speed and less boost to the intake manifold. As a result of the lower exhaust backpressure, pumping work is reduced. Therefore a turbo-charge system with a waste gate valve and a small turbine housing is able to make the turbo-machine characteristic match the reciprocating engine more closely (Endo, et al, 1993).

9.6.8 Inter-cooling or charge air cooling

Inter-cooling is the cooling of compressed air from the turbo-charger in order to increase the density of the intake air to enhance volumetric efficiency. Lower intake air temperatures are accompanied by lower combustion temperatures, which result in a decrease in NO_X emissions. Especially on turbo-charged engines, cooling the compressed air charge represents an effective means of inhibiting the formation of NO_X as well as soot emissions (Herzog, et al, 1992, Bosch Automotive Handbook).

Figure 13: The effect of inlet manifold temperature on BSFC, Excess air ratio and Emissions at Constant Absolute Inlet Manifold Pressure of 1.25 bar (Herzog, et al, 1992: Fig 2)

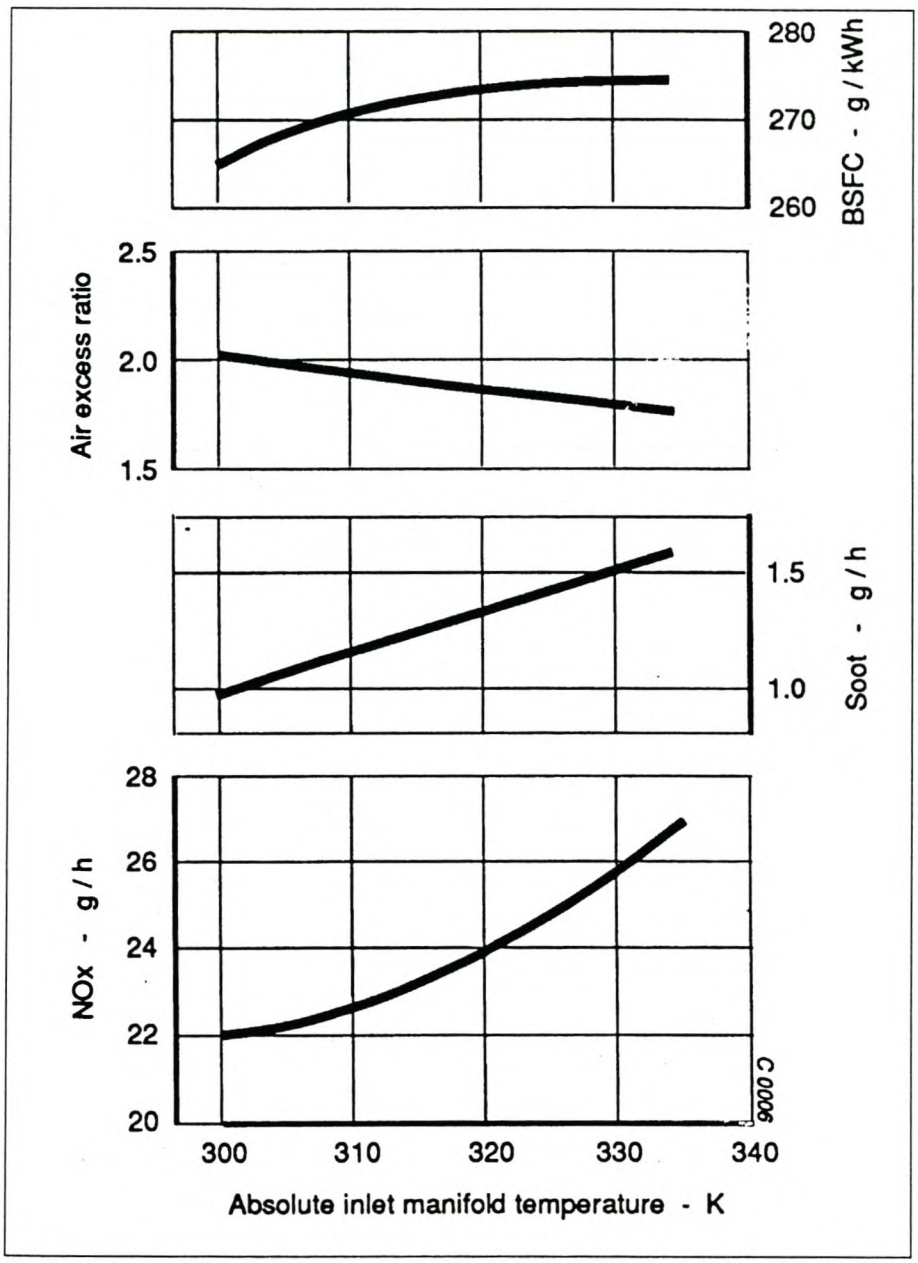

Charge cooling is most significant in its reducing effect on emissions at high load. BSFC, HC and PM are reduced at high load, with little or no change at low load (Bazari, et al, 1993). PM reduction is caused by a larger amount of excess air, which causes the air/fuel ratio to decrease (Watson and Janota, 1982).

9.7 MECHANISMS THAT DECREASE EMISSIONS FORMATION

9.7.1 Factors that influence ignition delay and the effect it has on emission generation

9.7.1.1 Injection timing

At normal operating conditions the minimum ignition timing is between 10° and 15° BTDC (Before Top Dead Centre). An increase in ignition delay with earlier or later injection timing occurs because the air temperature and pressure change significantly closer to TDC. If injection starts earlier, temperature and pressure are lower, therefore the delay will increase. If injection starts later the temperature and pressure are initially high, but decrease after TDC, as ignition delay proceeds.

9.7.1.2 Injection quantity or load

As load increases the residual gas temperature and wall temperature rise, and as a result the ignition delay decreases. The main influence at this point is the temperature and not the amount of fuel that is injected (Heywood, 1984).

9.7.1.3 Drop size, injection velocity and rate

These quantities are determined by injection pressure, injector nozzle hole size, nozzle type and geometry. An increase in injection pressure and a decrease in nozzle hole size shorten ignition delay, and a decrease in nozzle hole diameter increases fuel atomisation. Nozzle type and geometry have little or no effect on ignition delay.

9.7.1.4 Intake air temperature and pressure

This factor is of the utmost importance in the study as the duration of ignition delay has a direct effect on NO_X formation and indirectly affects soot and durability aspects. The intake air temperature and pressure will affect the delay via their effect on charge conditions during the delay period. Ignition delay decreases as charge temperature and pressure increase. Owing to this an increase in intake pressure will reduce delay and lower intake temperature will increase the delay period.

9.7.1.5 Engine speed

As speed increases the injection pressure increases and peak combustion temperature rises due to less heat transfer through the walls. These two effects cause the ignition delay to remain almost constant in crank angle degrees as speed increases, which implies a shorter duration in terms of real time.

9.7.1.6 Combustion chamber wall effects

The impingement of the spray on the combustion chamber wall obviously affects the fuel evaporation and mixing process. Impingement of fuel almost always occurs in small, high-speed diesel engine. This impingement of fuel on the walls does not reflect so much in a significant change in delay, but in the initial rate of burning that results from the higher rate of fuel evaporation and fuel mixing in these areas of the combustion chamber (Heywood, 1984).

9.7.1.7 Oxygen concentration

When the oxygen concentration is changed, for example when the exhaust gas is recycled through the intake system for the control of NO_X, the ignition delay increases with a decrease in oxygen concentration.

The duration of ignition delay influences the amount of premixed combustion that is summarised in the following mechanisms:

1. Higher engine speed enhances fuel/air mixing, which causes more mixture to be prepared during ignition delay, and thus premixed combustion is increased (Assanis, et al, 1991).
2. By increasing the compression ratio, the pressure and temperature are higher when the fuel is injected, thus mixture preparation takes place faster, resulting in shorter ignition delay and less premixed combustion (Mikulic, et al, 1993).
3. The reduction of the mixture quantity prepared during ignition delay by means of injection rate shaping or pilot injection (Mikulic, et al, 1993).

Combustion excitation is one of the dominating sources of engine noise (Aufinger, et al, 1998). High-pressure fuel injection is very effective and essential for the reduction of soot from DI diesel engines. On the other hand, using high-pressure fuel injection

increases the combustion noise attributable to in-cylinder pressure fluctuations during the combustion period.

The following engine parameters contribute to a reduction in premixed combustion and the resulting decrease in noise reduction:

1. An effective way to control premixed combustion is to suppress the initial fuel injection quantity and thus reduce combustion noise (Kawatani, et al, 1993).
2. Two-stage injection, achieved through the use of a two-spring nozzle holder (Aufinger, et al, 1998).
3. Reduced injection rate through a smaller injector plunger diameter (Aufinger, et al, 1998).
4. Revised injection nozzle tip design (Aufinger, et al, 1998).
5. Revised valve timing (Aufinger, et al, 1998).
6. An increase in boost pressure reduces combustion noise under high load conditions, particularly in medium speed ranges. As boost pressure is increased, ignition delay is shortened because in-cylinder temperature increases, thus premixed combustion decreases (Kawatani, et al, 1993).

9.7.2 The reduction of soot components

The air/fuel ratio plays a fundamental role in soot formation and emission levels in the exhaust gases of diesel engines (Corcione, et al, 1991). In-cylinder soot concentration measurements by means of optical methods have proven that during combustion, in-cylinder soot concentrations are considerably higher than those eventually found in the exhaust. Thus it can be concluded that most of the soot initially formed during combustion subsequently oxidises. The best soot reduction strategy would be to give highest priority to all those measures, which are conducive to the diminishing of the initial soot formation rather than to those enhancing the soot oxidation (Zelenka, et al, 1990).

In pursuing this guideline the following fuel/air mixing principles for low smoke formation have been developed:

1. Strive for good fuel atomisation by means of high fuel injection pressure and small injector nozzle hole diameter (Zelenka, et al, 1990).
2. Achieve mainly air-distributed fuel in the combustion chamber; with the amount of wall wetting being swirl dependent (Zelenka, et al, 1990).
3. Provide a high degree of air/fuel mixture potential throughout the entire duration of injection (Zelenka, et al, 1990).
4. Optimise the in-cylinder airflow by redesigning the combustion chamber (Kawatani, et al, 1993).

Achievement of the above in engine development practice results in the following:

9.7.2.1 Fuel system:

1. Use high injection pressure system with peak injection pressures of up to 1400 bar at rated power for a swirl supported combustion chamber (Zelenka, et al, 1990 Corcione, et al, 1991).
2. Increase the fuel injection pressure by increasing the pumping rate of the fuel injection pump (Kawatani, et al, 1993).
3. Vertical and bowl-axis-symmetric installation of the injector (Zelenka, et al, 1990).
4. Use an electronically controlled fuel system to provide flexible timing and fuelling capability (Zelenka, et al, 1990, Kawatani, et al, 1993).

9.7.2.2 Combustion bowl:

1. Cylinder axis-symmetric arrangement (Zelenka, et al, 1990).
2. Use of a re-entrant combustion chamber independent of the swirl level (Zelenka, et al, 1990).

9.7.3 Factors that affect particulate matter

For PM reduction essential countermeasures have to be taken to improve oil consumption for the reduction of oil-originated PM and to reduce the sulphur content in the fuel for the reduction of sulphate. Other approaches from the perspective of combustion

improvement are those such as the reduction of soot and the reduction of HC emissions (Kawatani, et al, 1993).

9.7.3.1 Reduction of the sulphate component in the INSOL by reducing sulphur content of the fuel:

A slightly higher sulphur content in the fuel causes PM to be considerably increased (Kawatani, et al, 1993).

9.7.3.2 Reduction of SOF originating from unburned fuel:

1. Improve the spill rate (the rate at which the injector closes) at the end of fuel injection. However, too rapid spill causes bouncing of the injection nozzle needle on the seat because of the increase in valve closing speed. The injection nozzle life is considerably shortened, due to wear of the valve seat (Kawatani, et al, 1993).
2. Wall impingement of the fuel spray on a cold wall should be suppressed to the utmost, as it results in unburned fuel in the SOF. Thus attention should be paid to spray hole centre position, spray hole directions of a fuel injection nozzle and the fuel injection timing, to make the fuel spray impinge against the same position over the entire engine operating range (Kawatani, et al, 1993).
3. Reduction of the sac and hole volumes of the injection nozzles to reduce the amount of fuel evaporating from the volumes usually not burned (Kawatani, et al, 1993 Racine, et al, 1991).

9.7.3.3 Reduction of the SOF originating from the lubrication oil:

The main areas where oil is consumed are in the cylinder or on the exhaust side rather than on the intake side involving valve stem seals. Oil in the cylinder is mainly consumed at the clearance between the piston and piston rings or between the cylinder liner and piston rings. An oxidation catalyst is effective for reducing SOF as a whole. On the other hand it has the risk of the PM being increased because SO_2 originating in the fuel sulphur is oxidised at the same time if the exhaust gas temperature is high enough (over 400-450°C), thereby resulting in sulphates being produced.

9.7.4 Factors that influence NO_X emissions

NO_X originates mainly at high temperatures where the oxygen concentration is high (Meyer, et al, 1991). Because of this the traditional way of controlling NO_X has been the application of turbo-charging with inter-cooling as well as retardation of injection timing, although retarding the injection timing influences fuel consumption and CO_2 emission formation.

The indirect injection diesel engine (IDI) combusts the fuel in a rich mixture (a very low supply of oxygen) in the pre-chamber. Since it is a rich mixture the flame temperature is lower than when it is a stoichiometric mixture, therefore the theoretical NO_X emission formation is lower (Uyehara, 1992). Not only temperature, but also equivalence ratio has an effect on NO_X formation, as it reduces the concentration of oxygen in the combustion zone. This means the lower the equivalence ratio, the less the NO_X formation (Heywood, 1984, Konno, et al, 1992).

The mixture formation dependent parameters that mainly influence NO_X formation are: (Zelenka, et al, 1990)

1. The amount of fuel injected during ignition delay.
2. The duration of ignition delay.
3. Preparation of the mixture in the combustion chamber.
4. Air/fuel mixing which is influenced by turbulence, swirl and squish levels in the combustion chamber.

9.7.5 Factors that influence HC emissions

1. Wall wetting as a result of high injection pressure with low swirl ratio, especially at low speed (Racine, et al, 1991).
2. Overmixing as a result of high injection pressure and high swirl ratio at high engine speed and low load conditions.
3. Lean air/fuel mixture at low part-load conditions (Dürnholz, et al, 1992).

9.8 LOW EMISSIONS ENGINE OF THE FUTURE

The following section stipulate the characteristics of the diesel engine in the future as foreseen by the top researchers in the diesel engine emission field:

1. Fully controllable variable geometry turbo-charger (Pilley, et al, 1989).
2. Effective charge cooling with charge cooler bypass option.
3. High injection pressure with rapid spill coupled with small nozzle hole diameter and medium or low swirl levels (Needham, et al, 1991, Corcione, et al, 1991).
4. Flexible fuel injection rate control to reduce the amount of fuel injected during ignition delay (Zelenka, et al, 1990).
5. Moderate EGR as a function of speed, load, temperature (Zelenka, et al, 1990).
6. Four-valve cylinder head (Needham, et al, 1991).
7. Variable inlet valve timing.
8. Low oil consumption (Needham, et al, 1991).
9. Low sulphur (0.05%/vol) diesel fuel (Needham, et al, 1991).
10. Exhaust oxidation catalyst to reduce the combustible emissions, perhaps with NO_X reducing capabilities (Zelenka, et al, 1990).
11. Glow plug-assisted part load operation, for minimising the ignition delay period (minimising the amount of premixed fuel burned) (Zelenka, et al, 1990).
12. Increase air utilisation by using axis-symmetric layout of both the injection nozzle and combustion bowl (Corcione, et al, 1991).

9.9 EMISSIONS LEGISLATION

Information Reference, Chapter 9.11: (Dieselnet, 2001)

9.9.1 United States

9.9.1.1 Applicability and Test Cycles

The following emission standards apply to new diesel engines used in heavy-duty highway vehicles. The current federal definition of a compression-ignition (diesel) engine is based on the engine cycle rather than the ignition mechanism, with the presence of a throttle as an indicator to distinguish between diesel-cycle and otto-cycle operation.

Heavy-duty vehicles are defined as vehicles of GVWR (gross vehicle weight rating) of above 8,500 lbs in the federal jurisdiction and above 14,000 lbs in California (model year 1995 and later). Diesel engines used in heavy-duty vehicles are further divided into service classes by GVWR, as follows.

- Light heavy-duty diesel engines: $8{,}500 < \text{LHDDE} < 19{,}500$ ($14{,}000 < \text{LHDDE} < 19{,}500$ in California, 1995+)
- Medium heavy-duty diesel engines: $19{,}500 \leq \text{MHDDE} \leq 33{,}000$
- Heavy heavy-duty diesel engines (including urban buses): $\text{HHDDE} > 33{,}000$

Current federal regulations do not require that complete heavy-duty diesel vehicles be chassis-certified, instead requiring certification of their engines (as an option, complete heavy-duty diesel vehicles under 14,000 lbs can be chassis-certified). Consequently, the basic standards are expressed in g/bhp.hr and require emission testing over the Transient FTP engine dynamometer cycle (however, chassis certification may be required for complete heavy-duty gasoline vehicles with pertinent emission standards expressed in g/mile).

Additional emission testing requirements, first introduced in 1998, include the following:

- Supplemental Emission Test (**SET**)
- Not-to-Exceed (**NTE**) limits

These tests were introduced for most signees of the 1998 Consent Decrees between the Environmental Protection Agency (**EPA**) and engine manufacturers for the period 1998 to 2004. Federal regulations require supplemental testing from all engine manufacturers effective from 2007. In California, the tests are required for all engines with the effective model year 2005.

The **SET** is a steady state test that was introduced to help to ensure that heavy-duty engine emissions are controlled during steady state type driving, such as a line-haul truck operating on a freeway. The test is identical to the EU 13-mode **ESC** (European Stationary Cycle) schedule (in the US commonly referred to as the "Euro III" cycle).

The **NTE** limits have been introduced as an additional instrument to make sure that heavy-duty engine emissions are controlled over the full range of speed and load combinations commonly experienced in use. The NTE approach establishes an area (the "NTE zone") under the torque curve of an engine where emissions must not exceed a specified value for any of the regulated pollutants.

The NTE test procedure does not involve a specific driving cycle of any specific length (mileage or time). Rather, it involves driving of any type that could occur within the bounds of the NTE control area, including operation under steady state or transient conditions and under varying ambient conditions. Emissions are averaged over a minimum time of thirty seconds and then compared to the applicable NTE emission limits.

9.9.1.2 Model Year 1987-2003

Model year 1987-2003 US federal (EPA) and California Air Resources Board (**ARB**) emission standards for heavy-duty diesel truck and bus engines are summarised in the following tables. Applicable to the 1994 and following year standards, sulphur content in the certification fuel has been reduced to 500 ppm wt.

Table 2: EPA Emission Standards for Heavy-Duty Diesel Engines, g/bhp.hr

Year	HC	CO	NO_X	PM
Heavy-Duty Diesel Truck Engines				
1990	1.3	15.5	6.0	0.60
1991	1.3	15.5	5.0	0.25
1994	1.3	15.5	5.0	0.10
1994	1.3	15.5	5.0	0.10
1998	1.3	15.5	4.0	0.10
Urban Bus Engines				
1991	1.3	15.5	5.0	0.25
1993	1.3	15.5	5.0	0.10
1994	1.3	15.5	5.0	0.07
1996	1.3	15.5	5.0	0.05*
1998	1.3	15.5	4.0	0.05*
* - In-use PM standard 0.07				

Table 3: California Emission Standards for Heavy-Duty Diesel Engines

Year	NMHC	THC	CO	NO_X	PM
Heavy-Duty Diesel Truck Engines					
1987	-	1.3	15.5	6.0	0.60
1991	1.2	1.3	15.5	5.0	0.25
1994	1.2	1.3	15.5	5.0	0.10
Urban Bus Engines					
1991	1.2	1.3	15.5	5.0	0.10
1994	1.2	1.3	15.5	5.0	0.07
1996	1.2	1.3	15.5	4.0	0.05

9.9.1.3 Useful Life and Warranty Periods

Compliance with emission standards has to be demonstrated over the useful life of the engine, which was adopted as follows (federal & California):

- LHDDE - 8 years/110,000 miles (whichever occurs first)
- MHDDE - 8 years/185,000 miles
- HHDDE - 8 years/290,000 miles

Federal useful life requirements were later increased to 10 years, with no change to the above mileage numbers, for the urban bus PM standard (1994+) and for the NO_X standard (1998+).

The emission warranty period is 5 years/100,000 miles (5 years/100,000 miles/3,000 hours in California), but no less than the basic mechanical warranty for the engine family.

9.9.1.4 Clean Fuel Fleet Programme

Table 4 shows a voluntary Clean Fuel Fleet (CFF) emission standard. It is a federal standard that applies to 1998-2003 model year engines, both compression ignition (CI) and spark ignition (SI), over 8,500 lbs GVWR. In addition to the CFF standard, vehicles must meet applicable conventional standards for other pollutants.

Table 4: Clean Fuel Fleet Programme for Heavy-Duty SI and CI Engines

Category*	CO	NMHC+NO_X	PM	HCHO
LEV (Federal Fuel)		3.8		
LEV (California Fuel)		3.5		
ILEV	14.4	2.5		0.050
ULEV	7.2	2.5	0.05	0.025
ZLEV	0	0	0	0
* LEV - low emission vehicle; ILEV - inherently low emission vehicle; ULEV - ultra low emission vehicle; ZEV - zero emission vehicle				

9.9.1.5 Model Year 2004 and Later

In October 1997, EPA adopted new emission standards for model year 2004 and later heavy-duty diesel truck and bus engines. These standards reflect the provisions of the Statement of Principles (SOP) signed in 1995 by the EPA, California ARB and the manufacturers of heavy-duty diesel engines. The goal was to reduce NO_X emissions from highway heavy-duty engines to levels approximately 2.0 g/bhp.hr, beginning in 2004. Manufacturers have the flexibility to certify their engines to one of the two options shown in Table 5.

Table 5: EPA Emission Standards for MY 2004 and Later HD Diesel Engines

Option	NMHC + NO_X	NMHC
1	2.4	n/a
2	2.5	0.5

All emission standards other than NMHC and NO_X applying to 1998 and later model year heavy-duty engines (Table 2) will continue at their 1998 levels.

EPA established a revised useful engine life, with significantly extended requirements for the heavy heavy-duty diesel engine service class, as follows:

- LHDDE - 110,000 miles/10 years
- MHDDE - 185,000 miles/10 years
- HHDDE - 435,000 miles/13 years/13,000 hours (but not less than 290,000 miles)

The emission warranty remains at 5 years/100,000 miles.

The federal 2004 standards for highway trucks are harmonised with California standards, with the intent that manufacturers can use a single engine or machine design for both markets. However, California certifications for model years 2005-2007 additionally require the Supplemental Emission Test and NTE limits of 1.25 times the FTP standards. California also adopted a different standard for urban bus engines.

9.9.1.6 Consent Decree

In October 1998, a court settlement was reached between the EPA, the Department of Justice, California ARB and engine manufacturers (Caterpillar, Cummins, Detroit Diesel,

Volvo, Mack Trucks/Renault and Navistar) over the issue of high NO_X emissions from heavy-duty diesel engines during certain driving modes. Since the early 1990s, the manufacturers used engine control software that caused engines to switch to a more fuel-efficient (but higher NO_X) driving mode during steady highway cruising. The EPA considered this engine control strategy an illegal "emission defeat device".

Provisions of the Consent Decree included the following:

- Civil penalties for engine manufacturers and requirements to allocate funds for pollution research;
- Upgrading existing engines to lower NO_X emissions;
- Supplemental Emission Test (steady state) with a limit equal to the FTP standard and NTE limits of 1.25 × FTP (with the exception of Navistar); and
- Meeting the 2004 emission standards by October 2002, 15 months ahead of time.

9.9.1.7 California Urban Bus Standard (2002)

In February 2000, the California ARB adopted a new regulation to reduce emissions of NO_X and PM from urban transit buses. The rule includes a number of components that affect both engine manufacturers and bus fleet operators. Fleet operators have to choose between a "diesel path" and an "alternative fuel path" for their future bus procurements. The alternative fuel path requires that 85% of buses purchased or leased each year through model year 2015 are fuelled by alternative fuels. Transit operators who stay on the diesel path can purchase diesel-fuelled buses, but are required to follow a more aggressive emission reduction schedule. When the regulation is fully implemented, buses on both paths will produce the same near-zero emission levels.

The regulation provides numerous detailed provisions and schedules, which can be summarised as follows:

- A NO_X fleet average of 4.8 g/bhp.hr begins in 2002 for both diesel and alternative fuel paths, which will require some transit agencies to retire their oldest, highest polluting buses.
- Ultra-low sulphur diesel fuel (15 ppm wt.) is required beginning July 1, 2002.

- All pre-2004 diesel buses have to be retrofitted with ARB-certified, 85% efficient diesel particulate filters. The retrofit begins in 2003 and will be completed through 2007.
- New bus engines have to be certified to increasingly more stringent emission standards (Table 6).
- Ultimately, 15% of new purchases have to be zero emission buses (**ZEB**s) (Table 6).

The urban transit bus fleet rule requirements and emission standards are summarised in Table 6.

Table 6: California Urban Transit Bus Fleet Rule

Date	Diesel Path		Alternative Fuel Path	
	NO_X, g/bhp.hr	**PM, g/bhp.hr**	**NO_X, g/bhp.hr**	**PM, g/bhp.hr**
2000	4.0	0.05	2.5*	0.05
7/2002	Ultra low sulphur diesel fuel		Ultra low sulphur diesel fuel	
10/2002	2.5 NO_X+NMHC	0.01	1.8 NO_X+NMHC*	0.03
10/2002	4.8 NO_X fleet average		4.8 NO_X fleet average	
2003-07	Diesel particulate filter retrofit		Diesel particulate filter retrofit	
7/2003	3 ZEBs for large fleets (>200)			
2004	0.5	0.01		
2007	0.2	0.01	0.2	0.01
2008	15% of ZEBs for large fleets (>200)			
2010			15% of ZEBs for large fleets (>200)	

Notes:

* - Optional standards. Although transit agencies on the alternative-fuel path are not required to purchase engines certified to these optional standards, it is expected that they will do so to qualify for incentive funding.

9.9.1.8 Model Year 2007 and Later

On December 21, 2000 the EPA signed emission standards for model year 2007 and later heavy-duty highway engines. The rule includes two components: (1) emission standards, and (2) diesel fuel regulation.

The first component of the regulation introduces new, very stringent emission standards as follows:

- PM - 0.01 g/bhp.hr
- NO_X - 0.20 g/bhp.hr
- NMHC - 0.14 g/bhp.hr

The PM emission standard will take full effect in the 2007 heavy-duty engine model year. The NO_X and NMHC standards will be phased in for diesel engines between 2007 and 2010. The phase-in would be on a percent-of-sales basis: 50% from 2007 to 2009 and 100% in 2010 (gasoline engines are subject to these standards based on a phase-in requiring 50% compliance in 2008 and 100% compliance in 2009).

Emission certification requirements also include the SET test, with limits equal to the FTP standards, and NTE limits of 1.5 times the FTP standards.

Effective from the 2007 model year, the regulation also eliminates the earlier crankcase emission control exception for turbocharged heavy-duty diesel engines. Crankcase emissions from these engines are treated the same as other exhaust emissions. Manufacturers are expected to control crankcase emissions by routing them back to the engine intake or to the exhaust stream upstream of the exhaust emission control devices.

The diesel fuel regulation limits the sulphur content in on-highway diesel fuel to 15 ppm (wt.), down from the previous 500 ppm. Refiners will be required to start producing the 15 ppm sulphur fuel beginning June 1, 2006. At the terminal level, highway diesel fuel sold as low sulphur fuel must meet the 15 ppm sulphur standard as of July 15, 2006. For retail stations and wholesale purchasers, highway diesel fuel sold as low sulphur fuel must meet the 15 ppm sulphur standard by September 1, 2006.

Refiners can also take advantage of a temporary compliance option that will allow them to continue producing 500 ppm fuel in 20% of the volume of diesel fuel they produce until December 31, 2009. In addition, refiners can participate in an averaging, banking and trading programme with other refiners in their geographic area.

Ultra low sulphur diesel fuel has been introduced as a "technology enabler" to pave the way for advanced, sulphur-intolerant exhaust emission control technologies, such as

catalytic diesel particulate filters and NO_X catalysts, which will be necessary to meet the 2007 emission standards.

The EPA estimates the cost of reducing the sulphur content of diesel fuel will result in a fuel price increase of approximately 4.5 cents to 5 cents per gallon. The EPA also estimates that the new emission standards will cause an increase in vehicle costs of between $1,200 and $1,900 (new heavy-duty trucks typically cost up to $150,000 and buses up to $250,000).

9.9.1.9 Test Cycles

Table 7: US Federal Test Cycles

Test Cycle	Description	Data Files
Heavy-Duty Engines		
FTP Transient	A transient engine dynamometer cycle for heavy-duty truck and bus engines. Includes segments designed to simulate both urban and freeway driving. Used for emission certification testing of heavy-duty diesel engines in the U.S.	Torque/speed points
AVL 8-Mode Heavy-Duty Cycle	A steady state test designed by AVL to produce emission results closely correlating with those measured over the U.S. FTP Transient test.	
CTA	Chicago Transit Authority engine cycle.	Torque/speed points
Heavy-Duty Vehicles (Chassis Cycles)		
Urban Dynamometer Driving Schedule (UDDS)	EPA transient chassis dynamometer test cycle for heavy-duty vehicles.	Speed points
Central Business District (CBD)	Transient chassis dynamometer test cycle for heavy-duty vehicles.	Speed points
Business-Arterial-Commuter (BAC)	A composite heavy-duty vehicle's fuel economy cycle, also known as the Transit Coach Operating Duty Cycle.	Speed points: CBD, Arterial, Commuter
WVU 5-Peak	5-speed chassis dynamometer test cycle for heavy-duty trucks developed by the West Virginia University.	Speed points

9.9.1.10 Heavy-Duty FTP Transient Cycle

The FTP (Federal Test Procedure) heavy-duty transient cycle is currently used for emission testing of heavy-duty on-road engines in the USA *(CFR Title 40, Part 86.1333)*. The transient test was developed to take into account the variety of heavy-duty trucks and buses in American cities, including traffic in and around the cities on roads and expressways. The cycle includes "motoring" segments and therefore requires a DC or AC electric dynamometer capable of both absorbing and supplying power.

The transient cycle consists of four phases: the first is a NYNF (New York Non Freeway) phase typical of light urban traffic with frequent stops and starts, the second is a LANF (Los Angeles Non Freeway) phase typical of crowded urban traffic with few stops, the third is a LAFY (Los Angeles Freeway) phase simulating crowded expressway traffic in Los Angeles, and the fourth phase repeats the first NYNF phase. It comprises a cold start after parking overnight, followed by idling, acceleration and deceleration phases, and a wide variety of different speeds and loads sequenced to simulate the running of the vehicle that corresponds to the engine being tested. There are a few stabilised running conditions, and the average load factor is about 20% to 25% of the maximum horsepower available at a given speed.

The cycle is carried out twice and the second repetition is made with a warm start after a stop of 1,200 seconds (20 minutes) on completion of the first cycle. The equivalent average speed is about 30 km/h and the equivalent distance travelled is 10.3 km for a running time of 1200 seconds. The variation of normalised speed and torque with time is shown in Figure 14.

Figure 14: Heavy-Duty FTP Transient Cycle

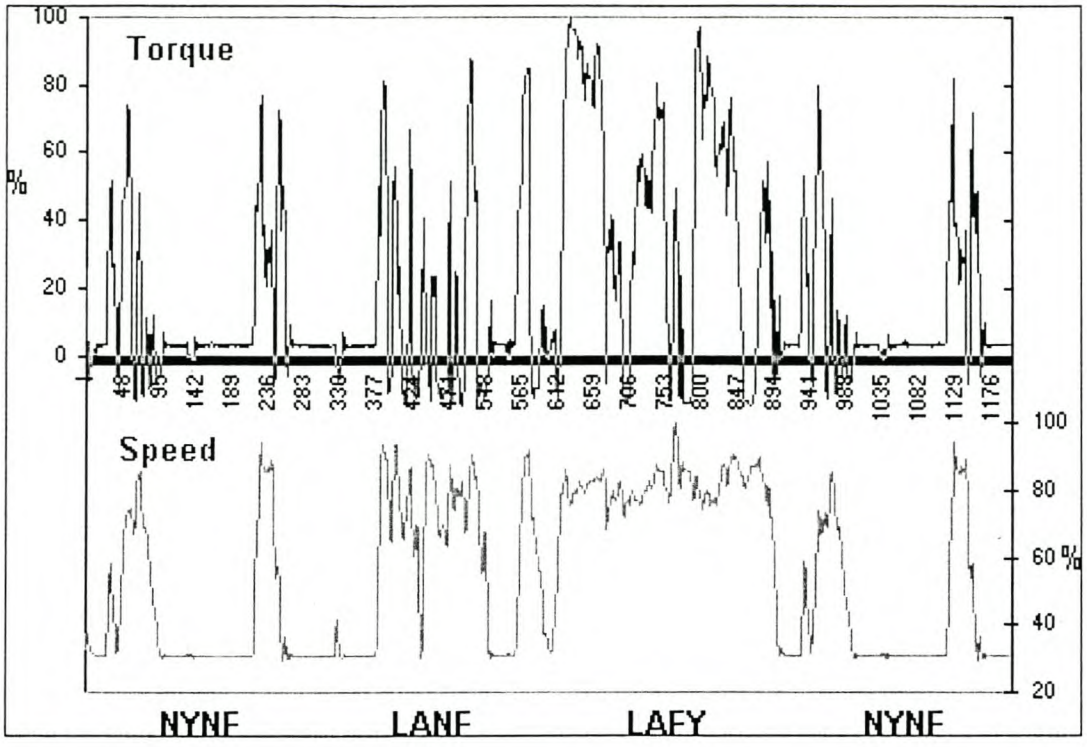

Heavy-duty diesel engines tested on the FTP cycle produce medium to high exhaust gas temperatures. Generally, the temperature is at a medium level between 250°C and 350°C, but there are some hot sections with temperatures reaching as high as 450°C.

9.9.2 Europe

9.9.2.1 Regulatory Framework

The European regulations for new heavy-duty diesel engines are commonly referred to as Euro I to Euro V. The Euro I standards for medium- and heavy-duty engines were introduced in 1992. The Euro II regulations came to power in 1996. These standards applied to both heavy-duty highway diesel engines and urban buses. The urban bus standards, however, were voluntary.

In 1999, the European Parliament and the Council of Environment Ministers adopted the final Euro III standard *(Directive 1999/96/EC of December 13, 1999, amending the Heavy Duty Diesel emissions Directive 88/77/EEC)* and also adopted Euro IV and V standards for the years 2005 and 2008 respectively. The standards also set specific,

stricter values for extra low emission vehicles (also known as "enhanced environmentally friendly vehicles" or EEVs) in view of their contribution to reducing atmospheric pollution in cities.

In April 2001, the European Commission adopted *Directive 2001/27/EC*, which introduced further amendments to Directive 88/77/EEC. The new Directive prohibits the use of emission "defeat devices" and "irrational" emission control strategies which would be reducing the efficiency of emission control systems when vehicles operate under normal driving conditions to levels below those determined during the emission testing procedure.

It is expected that the emission limit values set for 2005 and 2008 will require all new diesel-powered heavy-duty vehicles to be fitted with exhaust gas after treatment devices such as particulate traps and DeNOx catalysts. The 2008 NO_X standard will be reviewed by December 31, 2002 and either confirmed or modified, depending on the available emission control technology.

9.9.2.2 Emission Standards

Table 8 contains a summary of the emission standards and their implementation dates.

Table 8: EU Emission Standards for HD Diesel Engines

Tier	Date & Category	Test Cycle	CO	HC	NO_X	PM	Smoke
Euro I	1992, <85 kW	ECE R-49 4.5	4.5	1.1	8.0	0.612	
	1992, >85 kW		1.1	8.0	0.36		
Euro II	1996.10		4.0	1.1	7.0	0.25	
	1998.10		4.0	1.1	7.0	0.15	
Euro III	*1999.10, EEVs only*	*ESC & ELR*	*1.5*	*0.25*	*2.0*	*0.02*	*0.15*
	2000.10	ESC & ELR	2.1	0.66	5.0	0.10,0.13*	0.8
Euro IV	2005.10		1.5	0.46	3.5	0.02	0.5
Euro V	2008.10		1.5	0.46	2.0	0.02	0.5
* - For engines of less than 0.75 dm^3 swept volume per cylinder and a rated power speed of more than 3000 min^{-1}							

Changes in the engine test cycles have been introduced in the Euro III standard (year 2000). The old steady state engine test cycle ECE R-49 will be replaced by two cycles: a stationary cycle ESC (European Stationary Cycle) and a transient cycle ETC (European Transient Cycle). Smoke opacity is measured on the ELR (European Load Response) test.

For type approval of new vehicles with diesel engines according to the Euro III standard (year 2000), manufacturers have a choice of either of these tests. For type approval according to the Euro IV (year 2005) limit values and for EEVs, the emissions have to be determined on both the ETC and the ESC/ELR tests.

Emission standards for diesel engines that are tested on the ETC test cycle, as well as for heavy-duty gas engines are summarised in Table 9.

Table 9: Emission Standards for Diesel and Gas

Tier	Date & Category	Test Cycle	CO	NMHC	CH_4[a]	NO_X	PM[b]
Euro III	*1999.10, EEVs only*	*ETC*	*3.0*	*0.40*	*0.65*	*2.0*	*0.02*
	2000.10	ETC	5.45	0.78	1.6	5.0	0.16, 0.21[c]
Euro IV	2005.10		4.0	0.55	1.1	3.5	0.03
Euro V	2008.10		4.0	0.55	1.1	2.0	0.03

a - for natural gas engines only

b - not applicable for gas-fuelled engines at the year 2000 and 2005 stages

c - for engines of less than 0.75 dm^3 swept volume per cylinder and a rated power speed of more than 3000 min^{-1}

EU Member States will be allowed to use tax incentives to speed up the marketing of vehicles meeting the new standards. Such incentives have to comply with the following conditions:

- They apply to all new vehicles offered for sale on the market of a Member State which comply in advance with the mandatory limit values set out by the Directive;
- They cease when the new limit values come into effect (i.e. in 2000, 2005 or 2008); and
- For each type of vehicle they do not exceed the additional cost of the technical solutions introduced to ensure compliance with the limit values.

A new proposal that was submitted by the European Commission by December 2000 includes:

- Rules pertaining to the introduction of an on-board diagnostic system (OBD) for heavy-duty vehicles from October 1, 2005 (similarly as provided for in Directive 98/69/EC on the reduction of exhaust emissions from passenger cars and light commercial vehicles);

- Provisions on the durability of emission control devices with effect from October 1, 2005 (to ensure that they operate correctly during the normal life of a vehicle);
- Provisions to ensure the conformity of in-service vehicles which are properly maintained and used; and
- Appropriate limits for pollutants currently non-regulated as a consequence of the widespread introduction of new alternative fuels.

9.9.2.3 European Test Cycles

Table 10: European Union Test Cycles

Test Cycle	Description	Data Files
Heavy-Duty Engines		
ECE+EUDC	A combined chassis dynamometer test used for emission testing and certification in Europe. It is composed of four ECE Urban Driving Cycles simulating city driving and one Extra Urban Driving Cycle (EUDC), simulating highway driving conditions.	Speed points: ECE, EUDC, EUDC-lowP
ECE R-49	Steady state cycle for heavy-duty truck engines. Consists of a sequence of 13 engine dynamometer test modes. Used for heavy-duty engine emission certification before the year 2000.	
ESC (OICA)	New steady state cycle for truck and bus engines. Effective year 2000 the ESC test is used for emission certification of heavy-duty diesel engines.	
ELR	Effective year 2000, the ELR test is used for smoke opacity determination during emission certification of heavy-duty diesel engines.	
ETC (FIGE Transient)	New transient cycle for truck and bus engines. It is used, together with the ESC, for heavy-duty engine emission certification.	Torque/speed points
Braunschweig Cycle	Transient chassis dynamometer test cycle simulating an urban bus route.	Speed points

9.9.2.4 ECE R49

The R49 is a 13-mode steady state diesel engine test cycle introduced by ECE Regulation No.49 and then adopted by the EEC *(EEC Directive 88/77, EEC Journal Official L36, 8 Feb. 1988)*. It had been used for certification of heavy-duty highway engines through the Euro II emission standard. Effective October 2000 (Euro III), the R-49 cycle is replaced by the ESC schedule.

The R49 test is performed on an engine dynamometer operated through a sequence of 13 speed and load conditions. Exhaust emissions measured at each mode are expressed in g/kWh. The final test result is a weighted average of the 13 modes. The test conditions and weighting factors of the R49 cycle are shown in Figure 15 and Table 11. The areas of circles in Figure 15 are proportional to the weighting factors for the respective modes.

The running conditions of the R49 test cycle are identical to those of the US 13-mode cycle. The weighting factors, however, are different. Due to high weighting factors for modes 6 and 8 (high engine load), the European cycle is characterised by high average exhaust gas temperatures.

Figure 15: ECE R49

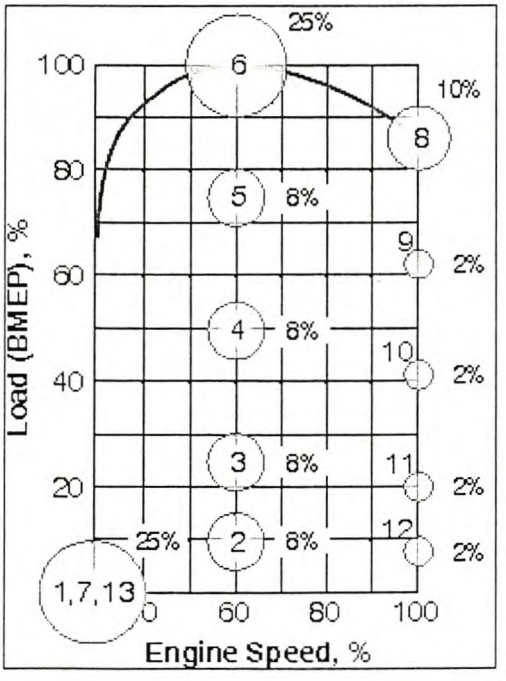

Table 11: ECE R49 and US 13-mode Cycles

Mode No.	Speed	Load, %	Weighting Factors	
			R49	US
1	idle	-	0.25/3	0.20/3
2	maximum	10	0.08	0.08
3	torque	25	0.08	0.08
4	speed	50	0.08	0.08
5		75	0.08	0.08
6		100	0.25	0.08
7	idle	-	0.25/3	0.20/3
8	rated	100	0.10	0.08
9	power	75	0.02	0.08
10	speed	50	0.02	0.08
11		25	0.02	0.08
12		10	0.02	0.08
13	idle	-	0.25/3	0.20/3

9.9.2.5 European Stationary Cycle (ESC)

The ESC test cycle (also known as OICA/ACEA cycle) has been introduced, together with the ETC (European Transient Cycle) and the ELR (European Load Response) tests, for emission certification of heavy-duty diesel engines in Europe starting in the year 2000 *(Directive 1999/96/EC of December 13, 1999)*. The ESC is a 13-mode, steady state procedure that replaces the ECE R49 test.

The engine is tested on an engine dynamometer over a sequence of steady state modes (Table 12, Figure 16). The engine must be operated for the prescribed time in each mode, completing engine speed and load changes in the first 20 seconds. The specified speed shall be held to within ±50 rpm and the specified torque shall be held to within ±2% of the maximum torque at the test speed. Emissions are measured during each mode and averaged over the cycle using a set of weighting factors. Particulate matter emissions are

sampled on one filter over the 13 modes. The final emission results are expressed in g/kWh.

During emission certification testing, the certification personnel may request additional random testing modes within the cycle control area (Figure 16). Maximum emissions at these extra modes are determined by interpolation between results from the neighbouring regular test modes.

Table 12: ESC Test Modes

Mode	Engine Speed	% Load	Weight factor, %	Duration
1	Low idle	0	15	4 minutes
2	A	100	8	2 minutes
3	B	50	10	2 minutes
4	B	75	10	2 minutes
5	A	50	5	2 minutes
6	A	75	5	2 minutes
7	A	25	5	2 minutes
8	B	100	9	2 minutes
9	B	25	10	2 minutes
10	C	100	8	2 minutes
11	C	25	5	2 minutes
12	C	75	5	2 minutes
13	C	50	5	2 minutes

Figure 16: European Stationary Cycle (ESC)

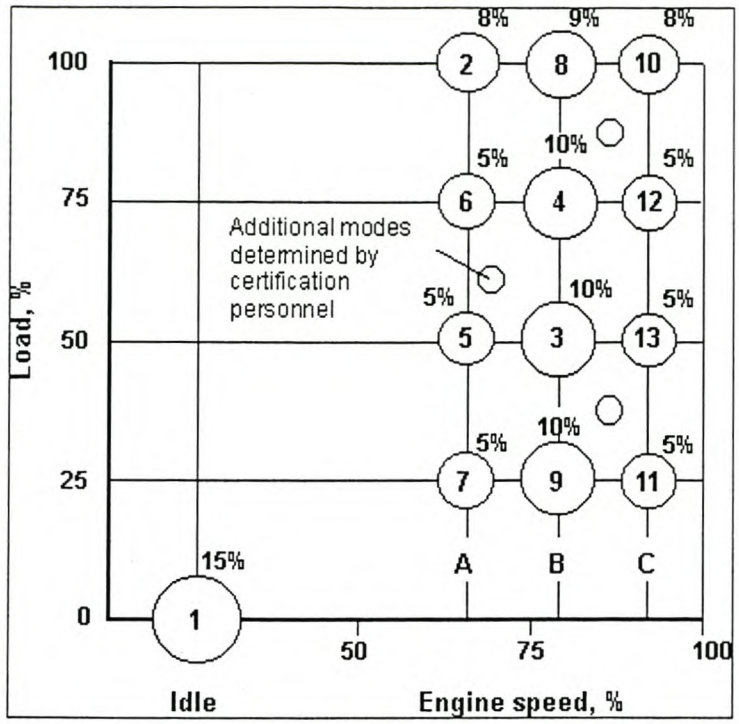

The engine speeds are defined as follows:

- The high speed n_{hi} is determined by calculating 70% of the declared maximum net power. The highest engine speed where this power value occurs (that is above the rated speed) on the power curve is defined as n_{hi}.
- The low speed n_{lo} is determined by calculating 50% of the declared maximum net power. The lowest engine speed where this power value occurs (that is below the rated speed) on the power curve is defined as n_{lo}.
- The engine speeds A, B, and C to be used during the test are then calculated from the following formulas:

$$A = n_{lo} + 0.25(n_{hi} - n_{lo})$$

$$B = n_{lo} + 0.50(n_{hi} - n_{lo})$$

$$C = n_{lo} + 0.75(n_{hi} - n_{lo})$$

The ESC test is characterised by high average load factors and very high exhaust gas temperatures.

9.9.2.6 European Load Response (ELR)

The ELR engine test has been introduced by the Euro III emission regulation, effective year 2000, for the purpose of smoke opacity measurement from heavy-duty diesel engines *(Directive 1999/96/EC of December 13, 1999).*

The test consists of a sequence of three load steps at each of the three engine speeds A (cycle 1), B (cycle 2) and C (cycle 3), followed by cycle 4 at a speed between speed A and speed C and a load between 10% and 100%, selected by the certification personnel. Speeds A, B, and C are defined in the ESC cycle. The sequence of dynamometer operation on the test engine is shown in Figure 17.

Figure 17: European Load Response (ELR)

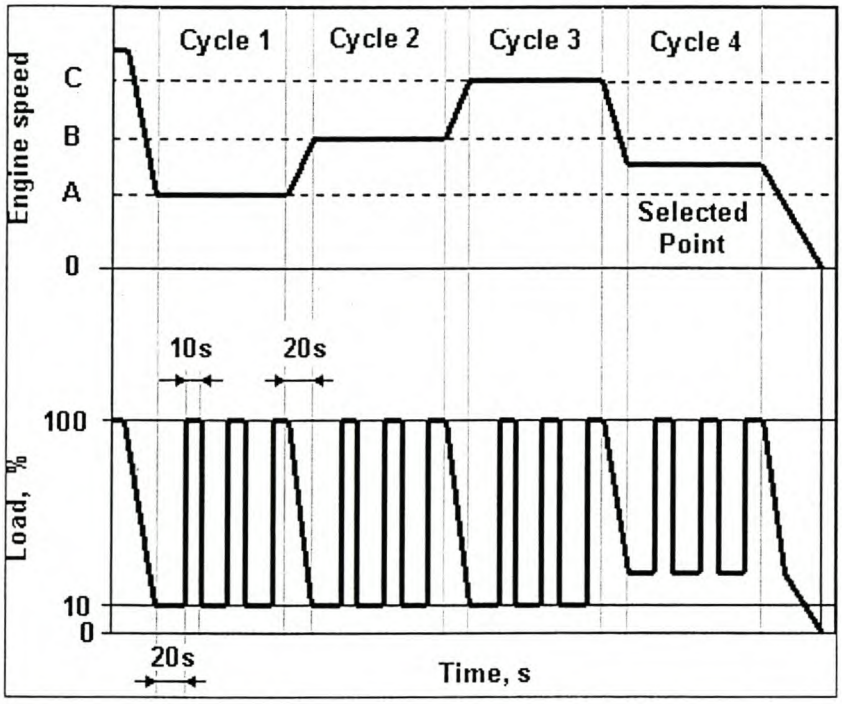

Smoke measurement values are continuously sampled during the ELR test with a frequency of at least 20 Hz. The smoke traces are then analysed to determine the final smoke values by calculation. Firstly, smoke values are averaged over 1 second time intervals using a special averaging algorithm. Secondly, load step smoke values are determined as the highest 1 sec average value at each of the three load steps for each of the test speeds. Thirdly, mean smoke values for each cycle (test speed) are calculated as arithmetic averages from the cycle's three-load step smoke values. The final smoke

value is determined as a weighted average from the mean values at speeds A (weighting factor 0.43), B (0.56), and C (0.01).

9.9.2.7 European Transient Cycle (ETC)

The ETC test cycle (also known as FIGE transient cycle) has been introduced, together with the ESC (European Stationary Cycle), for emission certification of heavy-duty diesel engines in Europe starting in the year 2000 *(Directive 1999/96/EC of December 13, 1999)*. The ESC and ETC cycles replace the earlier R49 test.

The ETC cycle has been developed by the FIGE Institute, Aachen, Germany, based on real road cycle measurements of heavy-duty vehicles *(FIGE Report 104 05 316, January 1994)*. The final ETC cycle is a shortened and slightly modified version of the original FIGE proposal.

Different driving conditions are represented by three parts of the ETC cycle, including urban, rural and motorway driving. The duration of the entire cycle is 1,800 seconds. The duration of each part is 600 seconds.

- Part one represents city driving with a maximum speed of 50 km/h, frequent starts, stops and idling.
- Part two is rural driving, starting with a steep acceleration segment. The average speed is about 72 km/h.
- Part three is motorway driving with an average speed of about 88 km/h.

The FIGE Institute developed the cycle in two variants: as a chassis and an engine dynamometer test. Vehicle speed versus time over the duration of the cycle is shown in Figure 17. For the purpose of engine certification, the ETC cycle is performed on an engine dynamometer. The pertinent engine speed and torque curves are shown in Figure 18 and Figure 19.

Figure 1: European Transient Cycle (ETC), Engine Speed

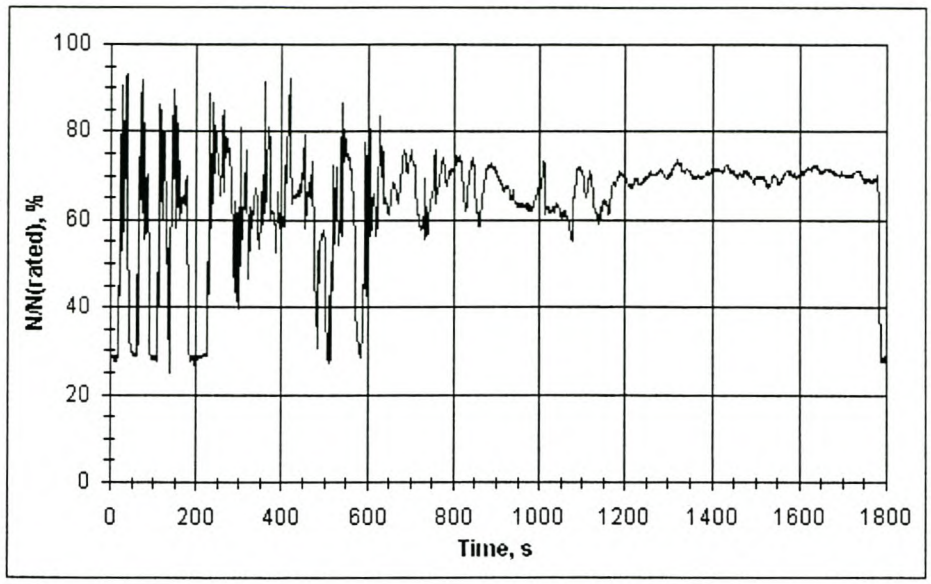

Figure 2: European Transient Cycle (ETC), Engine Load

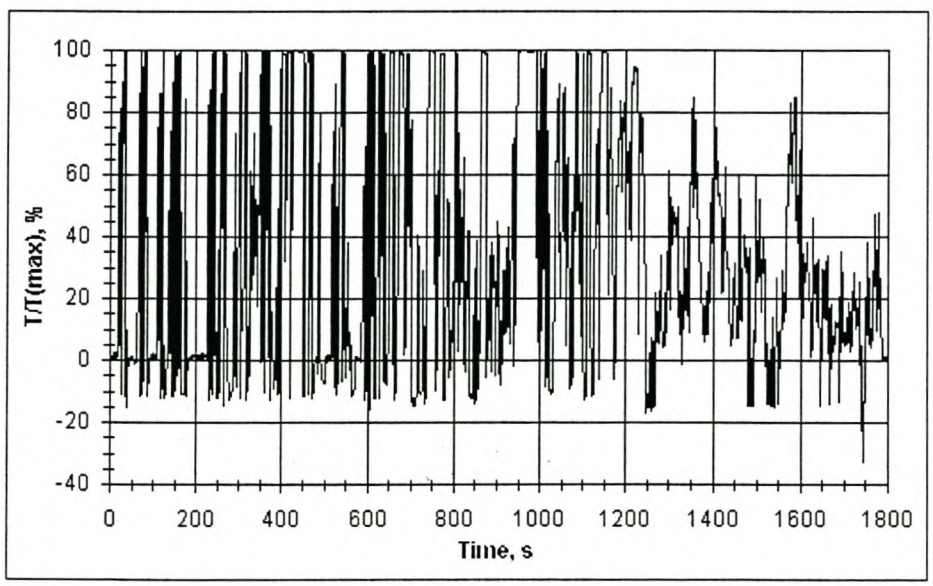

9.9.3 Japan

9.9.3.1 Regulatory Authorities

Japanese emission standards for on-road vehicles and engines are adopted by the Ministry of Transport (MOT). The MOT sets the emission targets and reduction rates based on recommendations by the Central Council for Environmental Pollution Control (CCEPC), an advisory body of the Environment Agency.

9.9.3.2 Commercial Vehicles

Emission standards for new diesel-fuelled commercial vehicles are summarised in Table 2. Light-duty trucks are tested on the 10-15 mode cycle. The test procedure for heavy-duty vehicles is the 13-mode cycle, which replaced the earlier 6-mode cycle. The test procedures and units of measurement are indicated in Table 13.

Table 13: Japanese Emission Standards for Diesel Commercial Vehicles

Vehicle Weight*	Date	Test	Unit	CO		HC		NO_X		PM	
				max	mean	max	mean	max	mean	max	mean
< 1700 kg	1988	10-15 mode	g/km	2.7	2.1	0.62	0.40	1.26	0.90		
	1993			2.7	2.1	0.62	0.40	0.84	0.60	0.34	0.20
	1997			2.7	2.1	0.62	0.40	0.55	0.40	0.14	0.08
	2002[a]				0.63		0.12		0.28		0.052
1700 - 2500 kg	1988	6 mode	ppm	980	790	670	510	500(DI) 350(IDI)	380(DI) 260 (IDI)		
	1993	10-15 mode	g/km	2.7	2.1	0.62	0.40	1.82	1.30	0.43	0.25
	1997/ 98			2.7	2.1	0.62	0.40	0.97	0.70	0.18	0.09
	2003[a]				0.63		0.12		0.49		0.06
> 2500 kg	1988/ 89	6 mode	ppm	980	790	670	510	520(DI) 350(IDI)	400(DI) 260 (IDI)		
	1994	13 mode	g/kWh	9.20	7.40	3.80	2.90	7.80(DI) 6.80 (IDI)	6.00(DI) 5.00 (IDI)	0.96	0.70
	1997-99[b]			9.20	7.40	3.80	2.90	5.80	4.50	0.49	0.25
	2004[a]				2.22		0.87		3.38		0.18

9.9.3.3 Japanese Test Cycles

Table 14: Japanese Test Cycles

Test Cycle	Description	Data Files
Heavy-Duty Engines		
10-Mode Cycle	Urban driving cycle used for emission testing from light-duty vehicles, later replaced by the 10-15 mode cycle.	Speed points
10-15 Mode Cycle	Urban driving cycle that is currently used in Japan for emission certification of light-duty vehicles.	Speed points
6-Mode Cycle	Two 6-mode cycles were used in Japan for heavy-duty vehicles weighting more than 2.5t or transporting more than ten passengers: one cycle for diesel vehicles and one cycle for gasoline/LPG vehicles. Total emissions were expressed in ppm as a weighted average from the 6 test modes.	
13-Mode Cycle	A newer cycle for heavy-duty vehicles that replaces the 6-mode cycles. The cycle includes 13 stabilized engine modes. The test modes are identical for diesel and gasoline vehicles, the weighting factors, however, are different. Emissions are expressed in g/kWh.	

9.9.3.4 Japanese 6-Mode Cycle

The 6-mode cycle was used in Japan for heavy-duty engines. It has been replaced by the newer 13-mode cycle and has only historical significance today.

The engine was tested over 6 different speed and load conditions. The modes were run in sequence and the duration of each mode was 3 minutes. Emissions were measured at each mode and averaged over the cycle using a set of weighting factors. The final test result was expressed as volumetric concentration in ppm.

There were two definitions of the test modes and weighting factors: one for diesel engines and another for gasoline and LPG engines. The diesel cycle parameters are listed in Table 15.

Table 15: Japanese Diesel 6-Mode Cycle

Mode	Speed (% of nominal)	Load (%)	Weighting factor
1	idle	-	0.355
2	40	100	0.071
3	40	25	0.059
4	60	100	0.107
5	60	25	0.122
6	80	75	0.286

9.9.3.5 Japanese 13-Mode Cycle

The 13-mode cycle replaced the older 6-mode cycle for the testing of heavy-duty engines in Japan.

The test includes a sequence of 13 steady state modes. The emissions are averaged over the entire cycle using a set of weighting factors and expressed in g/kWh. The test emphasises low-speed driving conditions and is characterised by low average engine loads and low exhaust temperatures.

There are differences in some test modes for diesel and gasoline engines and the weighting factors are different. The test parameters of the diesel cycle are listed in Table 16.

Table 16: Japanese Diesel 13-Mode Cycle

Mode	Speed (% of nominal)	Load (%)	Weighting factor
1	idle	-	0.410/2
2	40	20	0.037
3	40	40	0.027
4	idle	-	0.410/2
5	60	20	0.029
6	60	40	0.064
7	80	40	0.041
8	80	60	0.032
9	60	60	0.077
10	60	80	0.055
11	60	95	0.049
12	80	80	0.037
13	60	5	0.142

10 DURABILITY

It is a well-known fact that gas pressure and temperature result in mechanical and thermal stresses in combustion chamber components, but there are no rigid rules on the effects which combustion variables have on component life. What is known is that failure often occurs in conditions associated with rapid pressure rise (Taylor, 1989). Pressure and temperature result in two forms of loading, and components are exposed to the combined effect of these stresses: gas pressure, which causes mechanical forces within the components, and heat transfer from the hot gases, which produces temperature gradients in the components which lead to thermal stresses. High combustion pressures and high rates of pressure rise can result in engine failure due to piston cracking and erosion. Finite element analysis conducted by Taylor proved that the rate of pressure application did not have a significant effect on the levels of mechanical stress in the piston therefore peak pressures play the dominant role (Taylor, 1989). These failures normally occur in applications which frequently involve rapid load variations. In most cases of cracking, stresses have not exceeded the yield point of the material, indicating that the failure is fatigue-related.

For highly boosted diesel engines, one of the most important parameters to take into consideration concerning reliability is the thermal load of the engine parts, such as the cylinder head and the pistons. Charge air-cooling reduces the combustion temperatures to reduce the thermal load on the engine, but causes the maximum cylinder pressure to increase, owing to an increase in ignition delay (Bazari, et al, 1993). A factor that should also be taken into consideration is the heat transfer from the combustion gas to the combustion chamber. Heat transfer to the combustion chamber walls is dependent on intensity of swirl, squish and turbulence. In-cylinder flow processes enhance the air/fuel-mixing rate to maximise combustion efficiency and minimise PM emissions. On the other hand these flow processes increase the thermal loading on pistons, piston rings, the cylinder head and the exhaust valve.

Both the pressure forces and the thermal loading are of cyclic nature. The frequency of the pressure loading and gas temperature variation is equal to half the engine speed and is

referred to as high cycle loading. Thermal loading varies at the rate at which the load is changed on the engine and is considered as low cycle loading (Blech, 1982).

10.1 HIGH CYCLE LOADING

High cycle loading is the result of fluctuations in the cylinder pressure and surface temperature during the combustion cycle of the four-stroke engine. These fluctuations are the result of rapidly changing gas temperatures and heat transfer in the combustion chamber.

Any increase in peak cylinder pressure, caused by too high a compression ratio or too high an intake boost pressure, will lead to increased stresses in components such as pistons, cylinder liners, the cylinder head, connecting rods and the crank shaft. Cyclic pressure-induced stress is superimposed on thermal stress and contributes significantly to failure in areas such as the piston ring groove (Taylor, 1989). However, Blech stated that neither of these high cycle thermal stresses nor pressure forces contributed significantly to the failure of cylinder heads.

10.2 LOW CYCLE LOADING

Temperature gradients in the components surrounding the combustion chamber result from heat transfer from the hot combustion gases to the coolant. These temperature gradients result in thermal stresses due to differences in expansion. Component failure is most often witnessed in engines that undergo frequent and rapid load variations. The resulting variations in thermal stress lead to thermal fatigue due to step changes between low and high load. These transient stresses are far greater than the stresses that occur during normal steady state operation.

Blech developed a theory on the mechanism of thermal stress that indicates that prolonged operation under conditions of high temperature and compression stress results in plastic flow or compressive creep. Creep serves to relieve the compression stresses, but results in residual tensile stresses when the components cool, which finally leads to cracking (Taylor, 1989).

Failures that occur as a result of low cycle loading are as follows:

1. Piston cracking and erosion around the crown bowl lip. The piston bowl lip is clearly the region in the combustion chamber, which is the most sensitive to combustion behaviour (Taylor, 1989).
2. Cylinder head cracking occurs mainly in the flame plate between the valves, although not often (Blech, 1982).
3. Cylinder liner cracking is occasionally related to low cycle thermal loading conditions.
4. By raising the metal temperature the maximum thermal loading results in the components being far more sensitive to the high cycle forces. The thermal loading can thus have an effect on failures such as piston ring wear (Taylor, 1989).

10.3 EFFECT OF COMBUSTION BEHAVIOUR AND ENGINE STRESS ON ENGINE DURABILITY

It is clear that the nature of combustion and injection timing play a major role in the stress on engine components. Traditionally, researchers have attempted to maintain thermal loading within levels previously measured, by using criteria such as exhaust temperature, peak pressures, injection timing and rates of pressure rise in the hope that failure will not occur (Taylor, 1989).

In order to ascertain the influence of engine stress and combustion behaviour on durability, both these variables need to be determined. Neither of them can be measured directly and must be calculated from related information. A schematic layout can be seen in Figure 20.

Figure 20: Mechanism by means of which the nature of combustion of a fuel influences the durability of a compression–ignition engine (Taylor, 1989: Fig 2)

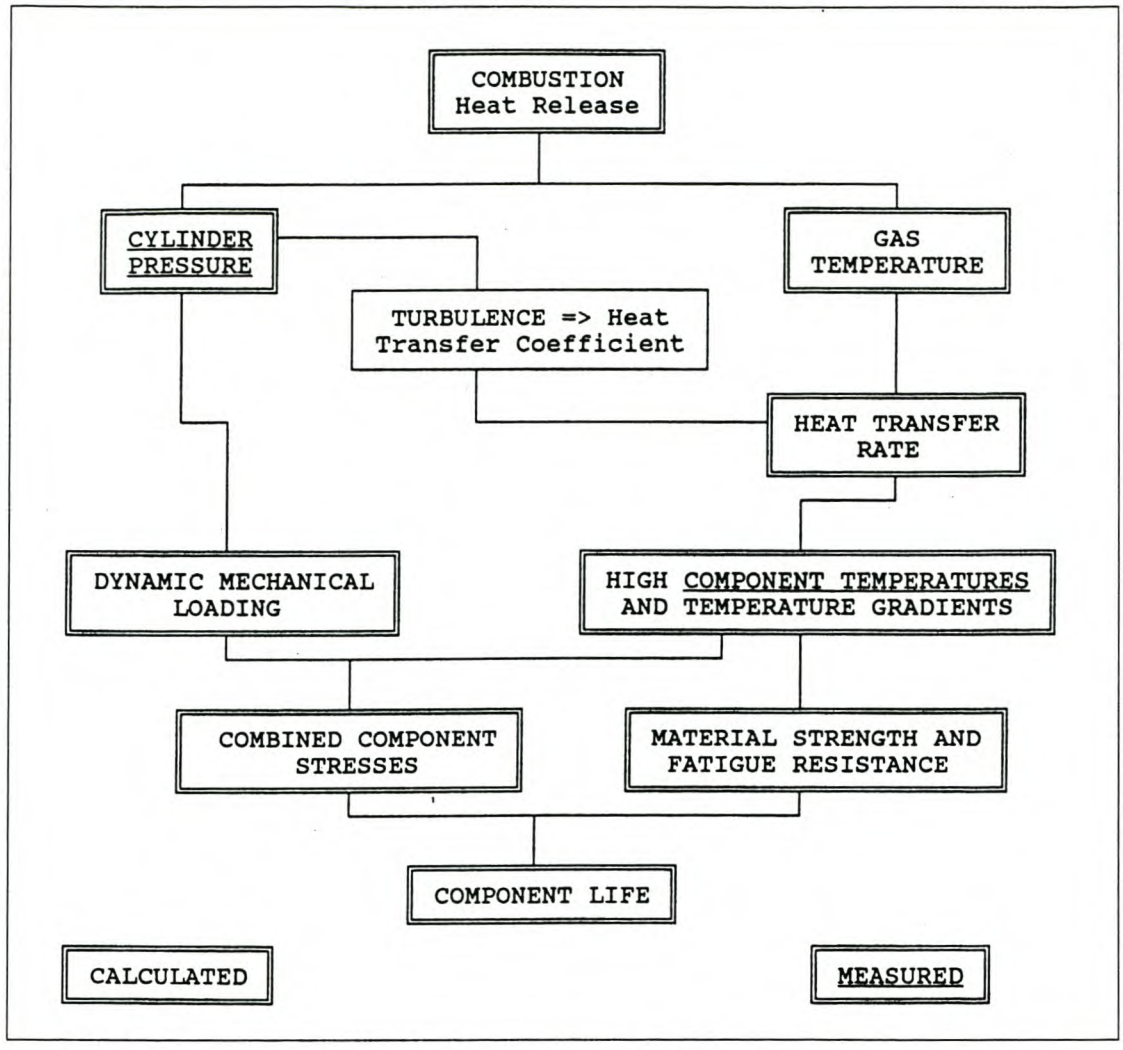

Combustion is quantified by variables determined from heat release analysis. Heat release analysis requires a number of engine variables such as an in-cylinder pressure trace, engine speed, torque, fuel consumption and combustion chamber geometry. The best way to display heat release data is graphically. It is clear that the nature of combustion plays a major role in the stress on engine components.

Engine stress is quantified from both thermal and mechanical data. Mechanical loading can be determined from cylinder pressure data and rates of pressure rise, whether or not they play a significant role. Thermal stresses are normally deduced from the surface heat transfer rates, which in this case have been measured as the amount of heat dissipated in

the cooling system. The heat transfer rate was also calculated from measured combustion chamber pressure (Taylor, 1987).

11 EXPERIMENTAL APPROACH

11.1 HEAT RELEASE ANALYSIS

The most important engine parameters under consideration in the study are torque, emissions, efficiency and reliability. One can achieve clearer insight into these measured parameters through reference to the rate of heat release. The heat release rate is defined by the energy released in the cylinder by the chemical reaction of fuel with oxidant. The rate of heat release can be calculated by using the cylinder pressure trace.

11.1.1 Measurement of pressure data using Piezo-electric Pressure Transducer

11.1.1.1 Piezo-electric pressure transducer

A typical piezo-electric transducer for in-cylinder pressure measurement comprises of the transducer, charge-voltage converter and amplifier, with a processor unit. The transducer does not provide a direct voltage signal output and in the case of the piezo-electric transducer the output signal is an electric charge. An AVL QH32C water-cooled pressure transducer was used to measure combustion chamber pressure. The pressure output signals are converted electrically in special circuits to provide a voltage signal. In this case the pressure signal conditioning was performed using an AVL 3057-AO1 charge amplifier.

The converted signals are then recorded by a high-speed data acquisition system. The signal conditioning flow diagram is shown in Figure 21.

Figure 21: The signal conditioning to obtain an in-cylinder pressure trace (AVL A to Z of vehicle testing)

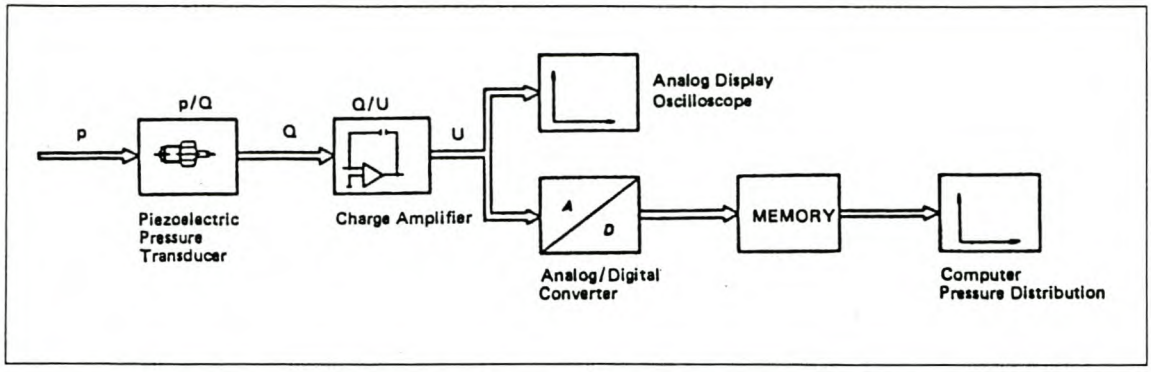

The advantage of a piezo-electric transducer over other systems is that, because of the high stiffness and the mechanical strength of the transducer element, practically no deformation occurs. Quartz crystal is used as the pressure sensitive element in modern precision pressure transducers. Further advantages of this type are:

- Outstanding linearity and stability;
- Small changes in sensitivity with temperature;
- No pyro-effect; and
- High signal to noise ratio of typically 10^5.

Because the electrical impedance of the insulation of the measurement system is finite, it is not possible to maintain reference zero point (e.g. atmospheric pressure) stability over a long period of time. For this reason, transducers of this type are used in preference for dynamic pressure measurement.

11.1.2 Capturing of pressure data using CAE developed RACER system

Capturing of in-cylinder pressure data was done using a computer software package developed at the Centre for Automotive Engineering (CAE) by Moran, Bell and Williams (Bell, 1998). The software package is called "Racer" or "Rapid Acquisition of Combustion and Engine Results", and the function of the package can be explained as the following:

Racer is an integrated data acquisition system that was designed to capture information on running automotive engines. The primary function of the Racer system is to capture and analyse engine combustion burn rate data. The pressure data is captured with respect to exact crankshaft position, but the system can also be used for many secondary functions, for example camshaft positioning measurement. Racer needs the following peripheral system to function:

- An IBM- compatible computer with at least 8Mb of RAM (16Mb or more recommended) operating under Windows, Windows95 or WindowsNT.
- A data capture card (PC30/DS4) and a BNC interface board.
- Crank-angle and Top Dead Centre (TDC) disk and magnetic sensors for crank angle position reference and for TDC reference, or any other system that can be used for the measurement of crank-angle and TDC position.

Unique features of this system enabled a crank-angle resolution of better than 0.1°, and combined with pressure data averaging (cycle-to-cycle), a high-resolution profile of pressure versus crank-angle is gained. This averaged profile was found to be highly repeatable for each test set of load, speed and fuel conditions. While being relatively smooth, the profile was sufficiently sensitive to exhibit high frequency engine events.

11.1.2.1 Data capturing method

The Racer software and data capture card are able to record vast magnitudes of information at a very high rate. The system is mostly used for the measurement of in-cylinder pressure data and this example will be used to explain the way the data is recorded and processed. Four incoming voltage signals are monitored, namely in-cylinder pressure, fuel injection pulse, TTL crank-angle signal and a TTL TDC signal. These signals are captured by the PC30-DS4 card, according to the capturing parameters such as sampling rate (or sampling frequency) and the duration (number of samples). During the sampling procedure Racer almost completely monopolises the computer until the computations are complete. The sampling procedure consists of the following operations:

11.1.2.1.1 Streaming the raw data to RAM

After the command is given to the system to start sampling, the PC30 card will capture all the data to high memory (Upper RAM in the computer extended memory). The amount of data captured depends on the RAM available in the system. The rate at which the data is transferred is faster than that which the CPU can handle; hence the CPU is bypassed during this stage of data sampling. The duration of sampling is dependent on sampling frequency and number of samples, as specified in the set-up of data sampling in Racer.

11.1.2.1.2 Deciphering raw data store in high memory

The data store in RAM is an array of voltages that need to be processed to decipher crank-angle and pressure signals. This process will place great demand on the computer's ECU and it is recommended that Racer dominate the computer system at this stage. The cycle-resolved data consists of voltage reading that indicates in-cylinder pressure and injection pulse at each angular degree for each cycle. An angular reference is allocated to the cylinder pressure value depending on the time fraction the sample was received within the crank angle time stamps captured by means of an magnetic proved on an 60 toothed reference connected to the crank shaft. Due to the nature of physical phenomena being sampled, the data will be very noisy, which makes it difficult (if not impossible) to perform defferential analysis required for calculating burn-rates. In order to minimise the cycle to cycle variations, the data of all the cycles are averaged to minimise noise and the end result is pressure and fuel injection pulse data versus crank-angle, correctly phased at TDC. The averaging technique has two advantages:

- To obtain an averaged pressure pulse, as there is cycle-to-cycle variation in combustion at steady state conditions in an engine.
- To minimise the effect of noise, such as electrical and data sampling high frequency noise, on any one signal.
- To raise the signal to noise ratio
- It incrementally increases the resolution of fine-scaled true repetitive engine events.

If further smoothing is required, the data is processed by means of a non-recursive digital filter. The digital filter limits the influence of electrical cross-talk and smooths out any

remaining random noise. With the filtering procedure caution must be taken not to smooth out high frequency pressure true events.

11.1.2.1.3 Pressure data manipulation

In order to do phase shifting of the TDC pulse the generation of Log (P) Log (V) diagrams is essential for the procedure that was used during these evaluations. The phase shifting procedure will be discussed in detail in the next section.

Racer will produce Pressure versus crank-angle data, calculate the rate of change of pressure to crank-angle and generate diagrams of pressure, rate of change in pressure versus crank-angle and Log (P) Log (V) diagrams.

11.1.3Errors in pressure data

As accurate and reliable pressure data is so important for the determination of rate of heat release, a way to check measured pressure data for possible errors should be implemented. The two common sources of error are pressure data phasing and thermal distortion. The errors induced as the result of pressure data phasing is limited by following procedures prescribed in literature. These procedure are discussed in detail in the " pressure data phasing "section below.

11.1.4Pressure Data Phasing Procedures (TDC setting)

The TDC reference position is determined while motoring the engine, but due to heat transfer and blow-by losses, the pressure curve is not symmetric with respect to TDC in motoring conditions (Ram Reddy, et al, 1993). When the logarithm of pressure is plotted against the logarithm of volume the compression and expansion stroke should almost form a straight line (Callahan, et al, 1985). A correct pressure data trace is illustrated in Figure 22 (Taylor, 1987).

Figure 22: Log Pressure / Log Volume Motoring (Taylor, 1987: Fig 13)

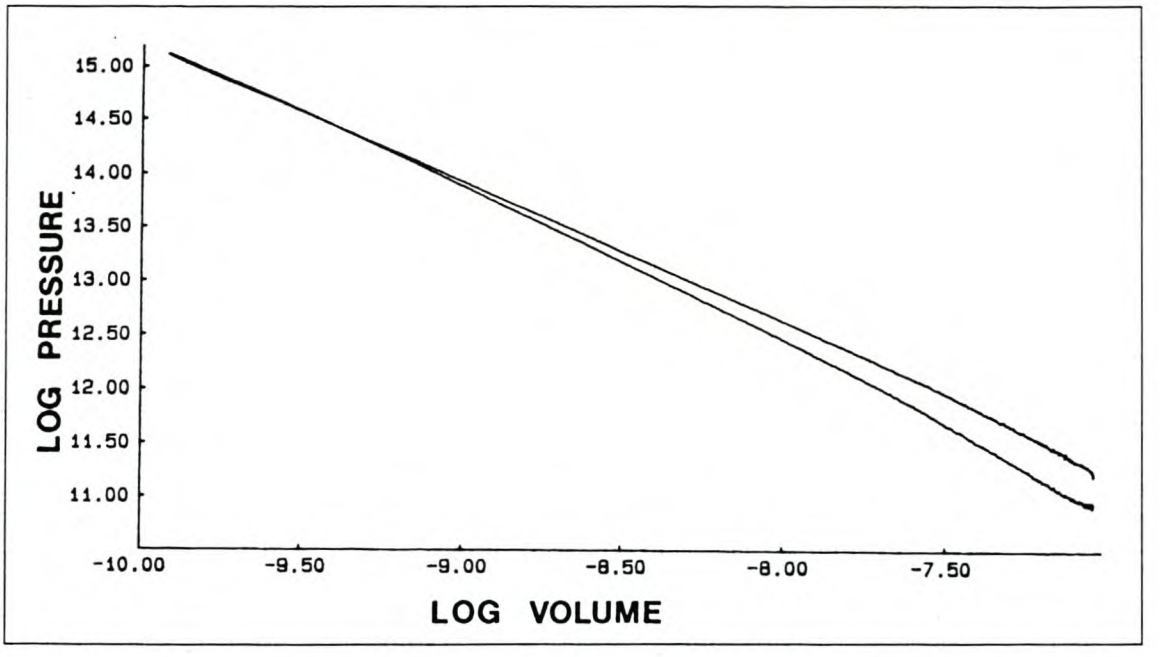

The gradient of this logarithm curve is equal to the polytropic constant at each instant. At any stage where the combustion chamber walls are hotter than the air inside, the polytropic constant is greater than 1.395, which is the value for compressed air. When the air temperature and the wall temperature are equal, the value is 1,395 momentarily and then decreases as combustion commences (Taylor, 1987).

When a hot motoring pressure trace is plotted on the logarithm of pressure / logarithm of volume axes it should yield a curve with the compression and expansion lines more or less on top of each other. The expansion line should initially return along the compression line without forming an acute angle or a loop (Callahan, et al, 1985). The relative position of the compression and expansion lines near peak pressure reflects on the change in the internal energy of the air in the combustion chamber. If the two lines form a loop, that portion of the cycle is incorrect as the work done on the piston is positive (Taylor, 1989). The point of peak pressure is where the polytropic constant becomes zero and should occur between 0.8 and 1° crank angle before TDC. This is as a result of heat transfer from the air to the combustion chamber walls. On this basis it can be deduced that the pressure is correctly phased with crank angle position, but no other errors can be detected by this method (Taylor, 1987).

A more accurate method of checking data is to calculate indicated mean effective pressure (IMEP) from cylinder pressure and subtract the break mean effective pressure (BMEP) to obtain friction mean effective pressure (FMEP). Repeat this procedure for a number of different loads at the same speed, and plot FMEP against BMEP. FMEP should not change significantly as BMEP increases, as some of the factors contributing to friction increase while others decrease (Hardenberg, et al, 1979, Taylor, 1989).

The final method is to compare calculated fuel consumption with measured fuel consumption. Owing to the fact that some fuel may still be burned after the crank angle at which the calculations are terminated, the calculated fuel consumption would be less than the measured, but only by a small margin. If the measured pressure data was checked by all these methods, then the conclusion can be reached that the data obtained from the equipment is accurate for combustion comparison purposes (Taylor, 1987).

11.1.5 Analysis of pressure data

In-cylinder pressure time history or pressure trace is measured in order to calculate both the indicated mean effective pressure, as a global engine performance index, as well as the rate of heat release, as quantitative information about the combustion process and the combustion parameters, ignition delay and combustion duration (Ram Reddy, et al, 1993).

Ignition delay is the time difference between the start of injection and the start of combustion. The start of injection is determined from the pulse received from the injection pulse sensor on the fuel line to the number one cylinder. This point corresponds with the first peak (the slope changes from positive to negative) on the rate of pressure rise curve as shown in Figure 23.

Figure 23: First derivative of pressure versus crank angle

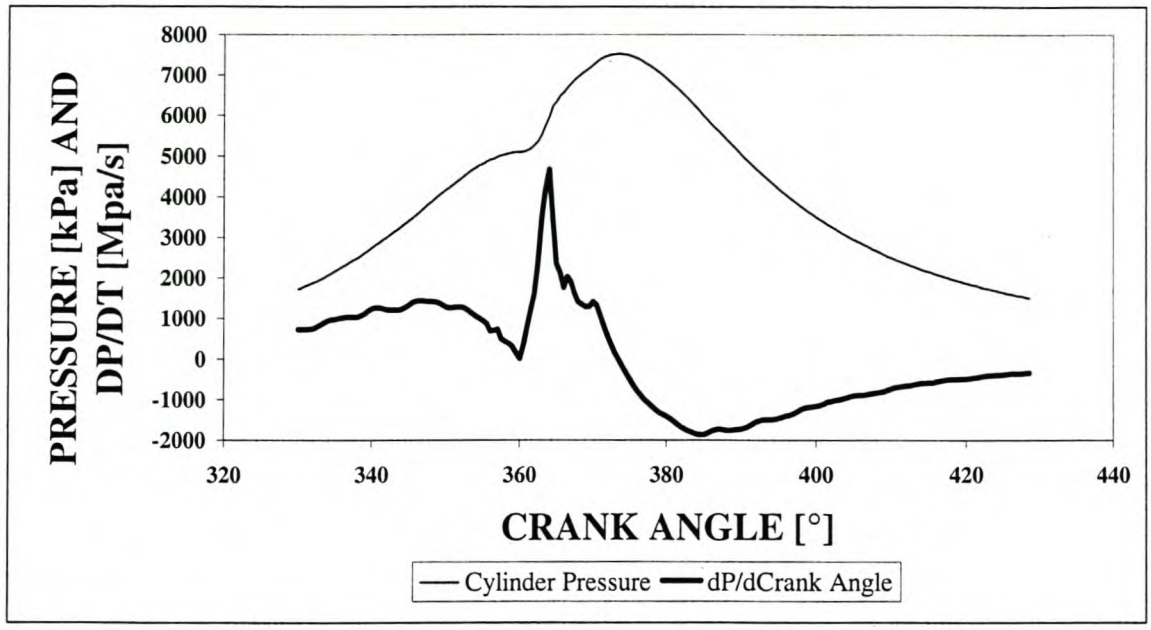

When the fuel is injected the rate of pressure rise decreases due to evaporation of the fuel, even though the pressure is rising due to compression. Once combustion starts the rate of pressure rise increases quite quickly and the derivative of Pressure (dP) curve indicates this clearly, as shown on the above curve.

Under certain operating conditions, such as low compression ratio, low speed and advanced fuel injection, when the fuel evaporation rate becomes slow, it is difficult to determine the point of start of injection on the dP-curve. In such instances the only alternative is to take the second derivative of pressure with time. This method gives a distinct point of change of sign in the slope.

The end of combustion is determined by evaluating the second change in slope from negative to positive of the dP-curve, as shown above (Ram Reddy, et al, 1993).

11.1.6 Heat-Release Analysis Programme

The single averaged pressure versus crank-angle profile was fed as input into a programme that would compute, inter alia, burn-rates. The workings of this programme are described below:

Cylinder pressure-temperature histories are affected by factors such as engine set-up geometry (compression ratios, surface area, valve timing, spark advance, connecting rod

length etc.) and heat-transfer considerations, which deal with how the conditions deviate from adiabatic system behaviour. The computer programme, therefore, is essentially a heat-balance model from which burn-rates (heat addition rates) can be ascertained from the following principle: any cylinder pressure-temperature behaviour that is not accounted for (by gas compression less heat losses) must have been generated by the fuel burning (Hansen, et al, 1994).

The workings of this model comprise a set of differential equations, which yield heat addition rates on a crank-angle basis. Due to the differential nature of the model, it is very sensitive to high-frequency noise, which is naturally amplified through differentiation. This necessitated the use of a non-recursive digital filter on the raw pressure data prior to the heat-release modelling. This type of software-based filter proved to be very useful for analytical removal of noise, without masking true high-frequency engine events.

The mathematical model used in the heat release model in this study was assembled by McLaren (1994), and was based on the one-zone heat release equation of Gatowski, Balles, Chun, Nelson, Ekchian and Heywood, (Hansen, et al, 1994).

$$\frac{dQ_{ch}}{d\theta} = \left(\frac{\gamma}{(\gamma-1)} \cdot \frac{p.dV}{d\theta}\right) + \left(\frac{1}{(\gamma-1)} \cdot V \cdot \frac{dP}{d\theta}\right)$$

$$+V_{cr} \cdot \left[\frac{T^{|}}{T_w} + \frac{T}{T_w \cdot (\gamma-1)} + \frac{1}{\phi \cdot T_w} \cdot \ln\left(\frac{\gamma-1}{\gamma^{|}-1}\right)\right] \cdot \frac{dP}{d\theta}$$

$$+\left(\frac{dQ_{ht}}{d\theta}\right)$$

where

$$\frac{dQ_{ht}}{d\theta} = \frac{h_c \times SA \times (T - T_w)}{\omega_{engine}}$$

where the term hc is a universally applicable expression of the in-cylinder convective heat transfer coefficient derived by Woschni (1967):

$$h_c = 131 \cdot c_1 \cdot B^{m-1} \cdot p^m \cdot T^{0.75-1.62\,m} \cdot \left(\omega_{charge}\right)^m$$

and where the charge velocity, ω_{charge}, is related to piston movement, swirl and combustion. Woschni used the following velocity:

$$\omega_{charge} = 2.28 \cdot \left(s_p + u_{swirl}\right) + 3.24 \cdot 10^{-3} \cdot c_2 \cdot T_{ivc} \cdot \frac{V_d}{V_{ivc}} \cdot \frac{\left(p - p_m\right)}{p_{ivc}}$$

The variables in the above equations are:

Q_{ch} [J] = chemical energy released,

θ [rad] = crank angle,

γ[-] = gas polytropic coefficient,

p [atm] = cylinder pressure,

V [m^3] = Volume,

V_{cr} [m^3] = crevice volume (est: 1% of TDC volume),

T [K] = charge gas temperature,

$T^{|}$ [K] = charge gas temperature,

T_w [K] = Gas temperature at inlet valve closure,

ϕ [-] = Equivalence ratio (differs for compression and expansion),

$\gamma^{|}$ [-] = crevice gas polytropic coefficient,

Q_{ht} [J] = heat transfer energy,

SA [m^2] = cylinder surface area,

ω_{engine} [rad/s] = engine speed,

c_1 [const] = calibration constant (=1 from Woschni),

B [m] = bore,

m [const] = Reynolds number exponent (= 0.8 from Woschni),

ω_{charge} [m/s] = charge velocity,

s_p [m/s] = mean piston speed,

u_{swirl} [m/s] = in-cylinder charge swirl velocity,

c_2 [const] = calibration constant (=1 from Woschni),

T_{ivc} [K] = gas temperature at inlet valve closure,

V_d [m^3] = displaced volume,

V_{ivc} [m^3] = volume at inlet valve closure,

p_m [Pa] = motoring pressure,

p_{ivc} [Pa] = chamber pressure at inlet valve closure.

Gatowski et al. (1984) confirmed that the final amount of heat release predicted was equal to the known amount of energy in the combustion chamber (mass of fuel multiplied by its lower heating value) less the chemical energy in the engine-out gases. Chun and Heywood (1987) noted, however, that the assumption of considering the ratio of specific heat as a linear function of temperature (as used by Gatowski) could be improved such that the model could match the more rigorous two-zone combustion models (Chun and Heywood, 1987).

Their improvement was three linear equations for the ratio of specific heat versus temperature for the three separate regimes of compression, combustion and expansion. Many coefficients for these linear equations are available, spanning different fuels and Air/Fuel ratios (Cheung and Heywood, 1993; Chun and Heywood, 1987; Gatowski et al., 1984; Mansouri and Heywood, 1980; Blizard and Keck, 1974). Listed below are the expressions used by the current model applied to Iso-Octane at a stoichiometric mixture concentration:

- $\gamma_{compression} = 1.40-(1.54/10000)*T[K]$
- $\gamma_{expansion} = 1.447-(1.262/10000)*T[K]$
- $\gamma_{combustion} = 1.255$

11.1.7 Formulation of the heat release analysis

In an engine, numerous dynamic processes occur, the combined effect whereof determines the performance and durability of the engine. Heat release analysis involves the calculation of the rate of combustion by measuring pressure and calculating the other processes. The models that are used in these calculations vary in complexity and accuracy and not all of them involve all the different processes. Combustion rate is calculated by solving the thermodynamic equations, which describe the interaction of the different processes in the engine (Taylor, 1989).

The heat release model used in this project is a zero-dimensional two-zone model, which was originally developed at the University of Illinois, Urbana, Illinois, USA. The model was upgraded to its two-zone status by Professor A.C. Hansen of the University of Natal, Pietermaritzburg, South Africa. The model is well documented in his PhD thesis (Hansen, 1989).

The complete model that is used in this study consists of a number of sub-models representing in-cylinder gas flow processes, heat transfer and combustion. For modelling the in-cylinder gas flow the combustion chamber volume was divided into an inner cylindrical volume and an outer annular volume and the total surface area of the combustion chamber was made up of six discrete surfaces shown schematically in Figure 24 (Hansen, 1989).

Figure 24: Division of the combustion chamber volume into an inner and outer volume and of the chamber surfaces area into six discrete elements. (Hansen, 1989: Fig 30)

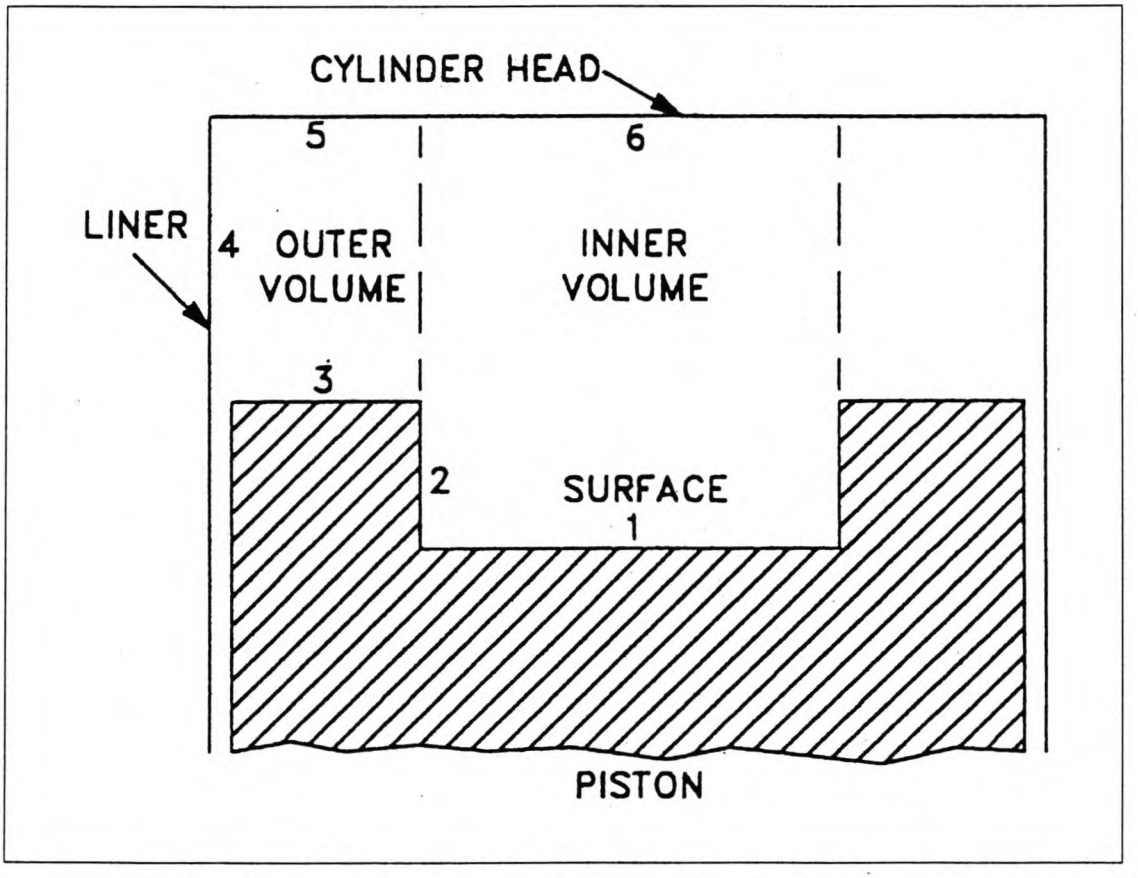

The mass of the cylinder contents at the inlet valve closing (IVC) is determined initially, and the measured cylinder pressure is used via the Ideal Gas Law to calculate the bulk gas temperature. With reference to the model structure shown in Figure 25, at each crank angle between IVC and exhaust valve opening (EVO), the in-cylinder gas flow components of squish, swirl and turbulence are employed in the calculation of the area-averaged resultant velocities at each of the designated surfaces in the combustion

chamber. These velocities, in conjunction with the gas properties of the boundary layer, as well as a convective temperature based on the combustion process, determine the convective heat transfer coefficients. (Hansen, et al, 1994)

Figure 25: Block diagram showing the structure of the two-zone combustion model. (Hansen, 1989: Figure 29)

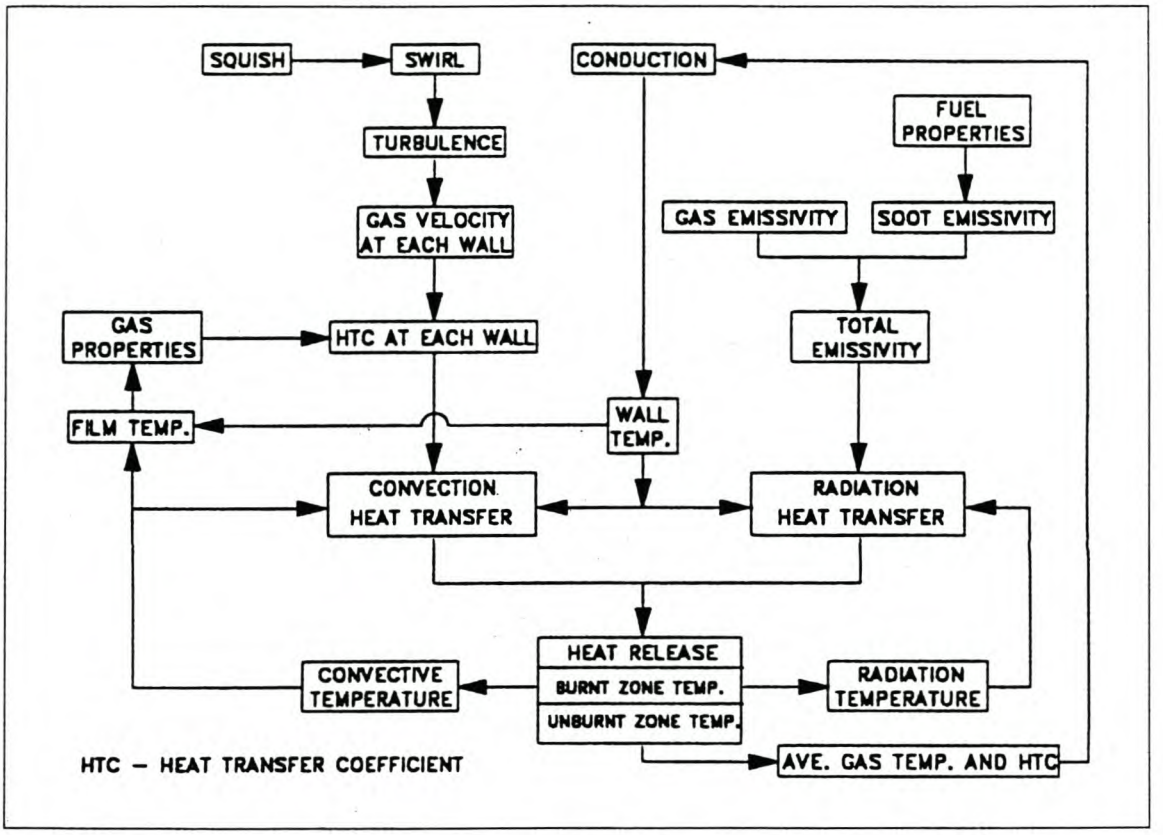

A sub-model of radiation heat transfer is included, which in turn requires the input of the total emissivity, wall temperature and a radiation temperature which are also based on the combustion process. The total emissivity is made up of two components resulting from gas radiation and soot radiation respectively. The calculation of the soot emissivity requires the input of the fuel properties. The computation of the wall temperature is performed with the aid of a conduction model (Hansen, 1989).

The heat release model into which the convective and radiation heat transfers were fed, was adapted from an existing heat release model so that the burnt products zone and the unburned zone were generated through the course of combustion. The temperature at each zone was then used in the calculation of the convective and radiation temperatures.

The measured pressure was required in the calculation of the bulk gas temperature and the rate of heat release (Hansen, 1989).

11.1.7.1 In-cylinder gas flow

The gas flow characteristics in the combustion chamber of a DI diesel engine during the compression and expansion strokes are governed primarily by piston velocity, squish, swirl and turbulence intensity. Variation in squish and swirl during the cycle is determined by the conservation of mass and angular momentum. Turbulence intensity was computed from a model of turbulence with its roots in the Navier-Stokes equations. The area-averaged resultant velocities at each of the six walls could therefore be calculated from the two orthogonal velocity components u_x and u_y, determined by piston motion, squish, swirl velocities and the turbulent kinetic energy of the volume adjoining the wall. These resultant velocities were then used in the calculation of the skin friction coefficient and the heat transfer coefficient, which was used to determine the convective heat transfer rates at each of the six walls (Hansen, 1989).

11.1.7.2 Heat transfer

An important component of the combustion process in a compression ignition engine is the heat transfer, which represents a loss of energy, reducing the amount of work done on the piston. Heat transfer has to be controlled so as to not only maximise efficiency but also to limit the temperature to engine components which are exposed. In engines heat loss from the combustion chamber gases are due to both convection and radiation with wall temperatures being governed by conduction (Hansen, 1989).

The convective heat transfer exchange between the gases in the combustion chamber and the chamber walls was determined through Reynolds' analogy (Hansen, 1989).

The model for radiation was selected so that it would be sufficiently complex to take into account fuel properties and equivalence ratio but not that sophisticated as to require substantial computations. This model was based on work done by Kunitomo (Hansen, 1989). The conduction model had to calculate temperatures at each of the six designated surfaces in the combustion chamber that were of the right order of magnitude and that were linked to the operating conditions. The combustion chamber was divided into the three main components of piston, liner and cylinder head. The heat transfers through

each of these three components were assumed to be one-dimensional and steady state and was represented by resistance networks. The resistance networks at each of the six surfaces consisted of two thermal resistances, the one representing the gas-to-wall convective resistance in the combustion chamber and the other a combined conduction and convection resistance from the wall to the water in the case of the liner, and the head or the oil in the case of the piston.

11.1.7.3 Two-Zone combustion model

A quasi-dimensional combustion model and an existing single zone model founded on the Krieger-Borman equation was modified to generate a burnt zone volume and to take into account flow-based convective and radiation heat transfer. The ideal gas law was applied to the burnt and unburned zones and to the total cylinder content. By assuming that the pressure and the gas constant were the same throughout the cylinder, the following equation can be derived:

$$P_b * V_b = m_b * R_b * T_b$$

$$P_u * V_u = m_u * R_u * T_u$$

$$P_t * V_t = m_t * R_t * T_t$$

Where	T:	Temperature [K]
	m:	mass [kg]
Subscripts	b:	Burned zone
	u:	Unburned zone
	t:	Total cylinder content

The thermodynamic cycle code in this model supplied the mass of burned gas and the bulk gas temperature T_t. The temperature of the unburned zone T_u was generated from a submodel relying on the First Law of Thermodynamics and taking into account heat transfer from the burnt zone to the unburned zone. The ratio of the instantaneous burnt mass of gas in the cylinder, m_b/m_t, was determined by tracking the production of CO_2, specified as one of the species in the gas mixture and comparing it to the total mass of CO_2 that would have been generated under stoichiometric conditions. The burned volume

V_b could then be determined from the ideal gas law for the burned zone (Hansen, et al, 1994).

The fixed geometry of the burned volume permitted the calculation of the surface area at the interface between the burned and the unburned zones. This surface area, the temperature difference between the two zones and an adjustable constant representing a gas-to-gas heat transfer coefficient were used to calculate the heat transfer between the two zones. The constant was adjusted so that the peak temperature of the burned zone did not exceed the adiabatic flame temperature (Hansen, 1989).

The temperatures and the masses of the burned and unburned zones, as well as the geometry of the burnt zone, were used in the calculation of the convective and radiation heat transfer components. A convective temperature, T_{cg} was calculated for each of the surface regions in the combustion chamber (Hansen, et al, 1994).

The radiation temperature, T_{rg} was calculated from an equation involving the maximum and instantaneous temperature of the burned zone, T_b and $T_{b,max}$ and a ratio varying from 0 to 1, based on the variation of crank-angle.

11.1.8 Application of the heat release model

The model requires the following information:

- An accurate description of the engine geometry for the calculation of the instantaneous combustion chamber volume and surface area is required.
- A description of the thermodynamic properties of the combustion chamber content.
- The experimental results such as the pressure trace and fuel consumption.

Measurement of engine specifications:

Table 17: Input parameters to the Heat Release Natal Two-Zone Combustion Model

Input parameters to the Heat Release Model	
1: Test Title (12 char max)	ADE364.LDE
2: Air Intake Temp °C	40
3: Manifold Pressure kPa	130
4: Residual Gas Fraction (0.05)	0.05
5: Duration of Calcs (80 °Crank Angle)	225
6: Crank Angle At Which Flow Calculation Start(330 °Crank Angle)	205
7: Crank Angle At Which Heat Release Calculation Start(330 °Crank Angle)	330
8: Carbon : Hydrogen : Oxygen Ratio (16 27.9 0)	16 27.9 1
9: fuel density (kg/l)	0.85
10: Higher Heat of Combust (44960 kJ/kg)	44960
11: Heat Transfer Model 1-Eichelberg 2-Woschnoi	2
12: Data filter from 2 °CA after peak Press. 1-on 0-off	1
13: Data Phasing shift (0 °CA)	-1
14: No of Cylinders (4)	4
15: Compression Ratio (16.4088)	16.5
16: Piston Bowl Diameter (0.0610)	0.0557
17: Piston Bowl Depth (0.0205)	0.022
18: Cylinder Bore (0.09835)	0.0975
19: Conrod Length (0.224)	0.23
20: Stroke (0.1271)	0.133
21: swirl ratio	0.6
22: Volumetric efficiency	0.69

The information in the above table is used to calculate the combustion chamber volume and surface area. The surface area is used to calculate the heat loss to the combustion chamber walls. The thermodynamic properties are necessary to calculate the amount and properties of the cylinder content. To determine the mass of air in the cylinder the volumetric efficiency is required.

The residual gas fraction is assumed to be 3.5% as it cannot be measured. The mass is increased by the amount of fuel injected. The equilibrium composition of the contents is calculated by using the Wienberg technique, which allows for the dissociation of the combustion products to be accounted for.

There are many sources of inaccuracy, therefore the researcher with knowledge of the relative effect of errors, estimates and assumptions in each of the inputs can direct more attention to those that have the greatest influence on model accuracy.

11.1.9 Reliability/Accuracy of the model

From a standard piezo-electric pressure transducer which produces a signal proportional to pressure one is unable to determine absolute pressure, as it has no fixed reference. The high-speed data acquisition system, RACER, developed by the CAE, equates the cylinder pressure (at crank angle degree just before close of inlet valve) with the inlet manifold boost pressure as fixed reference. Therefore the stored information is present in absolute form.

A sensitivity study of the model was conducted by Taylor (Taylor, 1987) who made use of the one zone model previously used at Department of Agricultural Engineering, University of Natal to gain an indication of the significance of various errors. Taylor used different data capturing software, but with the same output of pressure versus crank angle on which the crank angle reference was fixed.

Variables like engine load, mass of gas in the combustion chamber, residual gas fraction and heat transfer through the walls on their own did not cause large errors, except for the phasing of pressure data. It is evident that in the event of these errors becoming compounded a considerably large error could occur in the final result. In this research heat release analysis is applied as a diagnostic aid for comparing mainly combustion behaviour and emissions formation with varying intake charge pressure and temperature. Considerable effort was made to ensure consistency throughout the comparisons, while much attention was given to inputs such as pressure data, which can generate magnified errors in the heat release computations.

To ensure acceptable accuracy a number of techniques were applied for checking the final results (Taylor, 1987):

- The rate of heat release before and after combustion should be zero.
- A motoring pressure trace should yield zero heat release throughout.
- The relationship between the measured and calculated fuel consumption gives some indication of the overall accuracy. The calculated fuel consumption should be less than the measured fuel consumption, because not all the heat released in the expansion stroke is detected by the model.

The output of the existing model, developed by Hansen (Hansen, 1989), was verified and documented in his thesis. A number of assumptions were made, either to simplify the model or because at that stage there was insufficient knowledge to provide empirically based relationships for the different events occurring in the complex combustion process. In order to establish a model that generates reliable results it was critically examined and each of the sub-models were calibrated with experimental results (Hansen, 1989). The output from certain parts of the model, namely the gas flow sections, was compared to published data. However, the actual heat transfer calculations were compared with measured engine test data. To verify the complete model an energy balance between energy input computed for the heat released and energy input computed from the measured fuel delivery was applied (Hansen, 1989).

11.2 EXHAUST EMISSION MEASUREMENT

11.2.1 Exhaust Smoke Density

Exhaust smoke was measured according to the Bosch smoke scale, using the Bosch sampling system and a Bosch measuring unit. A specific volume of exhaust gas is drawn through a filter paper by a syringe type device, depositing any particulate matter contained in the exhaust onto the filter paper. The degree of blackening of the filter paper due to the particulate matter is then measured by the degree of light absorption by the calibrated Bosch measuring unit.

In order to obtain reproducibility of up to 0.5 Bosch units the sampling procedure should be executed consistently. The procedure involves that the sampling system is to be flushed with compressed air prior to the taking of each sample to ensure no carryover from test to test. A dummy sample follows flushing in order to ensure that the sampling line is filled with a representative sample.

The Bosch smoke scale is an arbitrary scale from 0 to 10 with 0 being calibrated with an unsoiled filter paper and the upper limit calibrated with a black, non-reflecting calibration paper.

A specially designed probe was inserted in the exhaust system which prevents solids contained in the exhaust gas to enter the sampling probe when sampling is not taking place, preventing build-up of particulate matter in the exhaust probe.

11.2.2 Gaseous emissions

A specially designed probe was inserted in the exhaust system, containing a heated particulate trap to prevent particulate matter from entering the sampling system used for measurement of exhaust emissions. The particulate trap consists of a heated container of which the temperature is controlled to above 192°C, and a filter container through which the sample flows. The filter container is filled with glass wool, which is very effective in removing PM from the sampled raw gas.
The sample was fed to a bank of gas analysers via a sampling line maintained at 190 °C. This is to ensure that the water content of the exhaust gas remained in its vapour state due to the solubility of hydrocarbons in water. In this way the hydrocarbon concentration of the exhaust sample is affected as little as possible.

A portion of the sample then passed through a Heated Flame Ionisation Detector measuring unburned hydrocarbons. The remainder of the sample is then dried by passing it through a chiller unit, whereafter it passes through the remaining analysers which are water sensitive. Nitrogen Oxide (NO), Carbon Dioxide (CO_2) and Carbon Monoxide (CO) were measured by using Siemens Ultramat 5E Non-Dispersive Infra Red (NDIR) analysers. Engine-out oxygen concentration was also measured using a Siemens Oxymat 5E analyser. The measurement of CO_2 and O_2, though not of direct interest, helps to give insight into the combustion process and are necessary for the determination of air/fuel ratio.

A catalytic converter using a carbon-based catalyst, placed inline before the NO analyser, converts Nitrogen Dioxide (NO_2) to NO, allowing the concentration of NO + NO_2 to be measured. The quantity NO + NO_2 is generally referred to as NO_X (total oxides of nitrogen) as the concentrations of higher oxides of nitrogen are known to be insignificant.

11.2.2.1 Hydrocarbon Analyser

Total hydrocarbon content was measured with a K M52044-D (Heated Flame Ionisation Detector), which gives a concentration in parts per million carbon ($ppmC_1$) on a methane scale in. The detector uses Hydrogen and bottled air for combustion of the pilot flame and high quality gases with certified concentration are used to reduce the possibility of contamination. The Fidamat can be fitted with a heated sample gas line to prevent condensation and absorption of the sample gas content in the line (Siemens Fidamat operational manual).

11.2.2.2 Oxygen Analyser

A Siemens Oxymat 5E Gas Analyser (model 7MB1020) was used for the measurement of oxygen, which utilises a paramagnetic alternating pressure principle, recording percentage volume. Because of its selectivity and corrosion resistance with respect to the sample gas, there are hardly any limitations to its applications (Siemens Oxymat operational manual).

The Oxymat 5E analyser has the following characteristic features:

- Short response time.
- Independent of instrument orientation.
- Results independent of thermal conductivity, specific heat, and viscosity of the sample gas.
- Negligible long-term drift.
- High corrosion resistance of parts in contact with the sample gas.
- High selectivity.

11.2.2.3 CO, CO_2, NO_X Analyser

The Ultramat 5E Gas Analyser (model 7MB1120) is a highly selective Non-Dispersive Infra-Red (NDIR) gas analyser operating on the infrared double-beam alternating light principle. The analyser is suitable for the measurement of gases with absorption bands in the wavelength range of 1 to 10 μm, for example CO, CO_2, NO, SO_2, NH_3, CH_4, and higher hydrocarbons (Siemens Ultramat operational manual).

The NO analyser recorded concentrations on the ppm scale and had an upper limit of 2000 ppm NO, which proved to be slightly restrictive, as concentrations exceeded this

level at some of the engine load points investigated. The CO and CO_2 analysers measured percentage concentration by volume (% vol.).

11.2.3 Calibration of the gas analysers

Calibration of the gas analysers was done before and after each test run, using certified standard gases having similar concentrations of the relevant compounds to that expected in the exhaust stream, owing to the long-term drift of the CO and CO_2 analyser. Calibrations were checked after engine testing was completed to ensure that no drift had occurred. Calibration gases were of a high quality: calibration certificates indicating the gas concentrations analysed as well as tolerances and maximum contamination levels were supplied. Nitrogen was used as a zero reference for all the analysers.
The calibration procedures were followed as prescribed in the analyser manuals.

For the calibration of the Fidamat K analyser zero gas is used. This is synthetic air with a hydrocarbon content of less than 2 ppm v/v. Calibration gas, a synthetic air with an oxygen and hydrocarbon concentration similar to the sample gas (an alkane - propane or butane - or substance similar to the sample gas is used as a hydrocarbon), is used for range calculation.

The Oxymat 5E is calibrated with O_2 and N_2 reference gases. The permissible oxygen content of the nitrogen reference gas is up to 3% of the particular measuring span for zero point calibration. Ultra-pure gas, 98 to 100% O_2, is used for span calibration.

The Ultramat 5E is calibrated by using zero gas for zero adjustment, and for sensitivity adjustment the test gas is used.

11.3 CONVERSION FROM CONCENTRATION TO BRAKE SPECIFIC EMISSION

In order to calculate brake specific emission from measured concentrations in the exhaust gas the following calculation procedures were followed. These procedures are documented in the Code of Federal Regulations (Code of Federal Regulations, 1997).

11.3.1 Hydrocarbon Emissions

$$BSHC = \frac{W_{HC}}{BHP}$$

$BSHC$ = Brake specific hydrocarbon emissions, [g/kWh].
W_{HC} = Mass rate of hydrocarbon in exhaust, [g/h].
BHP = Brake power, [kW].

$$W_{HC} = \frac{W_f\left(DHC/10^4\right)}{\left(DCO/10^4\right)+\left(DCO_2/10^4\right)+\left(DHC/10^4\right)}$$

DHC = HC volume concentration in the exhaust, [ppm] (dry).
W_f = Mass flow rate of fuel used in the engine, [g/h].
DCO = CO volume concentration in the exhaust, [ppm] (dry).
DCO_2 = CO_2 volume concentration in the exhaust, [ppm] (dry).

11.3.2 Carbon monoxide Emissions

$$BSCO = \frac{W_{CO}}{BHP}$$

$BSCO$ = Brake specific carbon monoxide emissions, [g/kWh].
W_{CO} = Mass rate of carbon monoxide in exhaust, [g/h].
BHP = Brake power, [kW].

$$W_{CO} = \frac{Mco * W_f\left(DCO/10^4\right)}{\left(M_C+\alpha M_H\right)\left[\left(DCO/10^4\right)+\left(DCO_2/10^4\right)+\left(DHC/10^4\right)\right]}$$

DHC = HC volume concentration in the exhaust, [ppm] (dry).
W_f = Mass flow rate of fuel used in the engine, [g/h].

DCO = CO volume concentration in the exhaust, [ppm] (dry).

DCO_2 = CO_2 volume concentration in the exhaust, [ppm] (dry).

M_{CO} = Molecular weight of CO.

M_C = Atomic weight of carbon.

α = Atomic hydrogen/carbon ratio of the fuel.

M_H = Atomic weight of hydrogen.

11.3.3 Oxides of nitrogen emissions

$$BSNOx = \frac{W_{NOx}}{BHP}$$

$BSNOx$ = Brake specific Oxides of nitrogen emissions [g/kWh].

W_{NOx} = Mass rate of Oxides of nitrogen in exhaust, [g/h].

BHP = Brake power, [kW].

$$W_{NOx} = \frac{M_{NOx} * W_f \left(DKNO/10^4\right)}{\left(M_C + \alpha M_H\right)\left[\left(DCO/10^4\right)+\left(DCO_2/10^4\right)+\left(DHC/10^4\right)\right]}$$

DHC = HC volume concentration in the exhaust, [ppm] (dry).

W_f = Mass flow rate of fuel used in the engine, [g/h].

DCO = CO volume concentration in the exhaust, [ppm] (dry).

DCO_2 = CO_2 volume concentration in the exhaust, [ppm] (dry).

M_C = Atomic weight of carbon.

α = Atomic hydrogen/carbon ratio of the fuel.

M_H = Atomic weight of hydrogen.

11.4 REGRESSION ANALYSIS

11.4.1 The Simple Linear Regression Model and Correlation

11.4.1.1 Determining the simple linear regression equation – Least-squares Method

The simple regression equation representing the straight-line regression model would be (Draper, 1981 and Berenson, 1989),

$$\Psi_i = b_0 + b_1 X_i$$

where Ψ_i is the predicted value of Y for observation i and X_i is the value of X for the observation i.

This equation requires the determination of two coefficients - b_0 (the Y intercept) and b_1 (the slope) in order to predict values of Y.

Simple linear regression analysis is concerned with finding the straight line that 'fits' the data best. This means that the difference between predicted value (Ψ_i) and the actual value (Y_I) are as small as possible. Because these differences will be both positive and negative for the different observations, mathematically we minimise

$$\sum_{i=1}^{n} (Y_i - \Psi_i)^2$$

Since $\Psi_I = b_0 + b_1 X_i$, we are minimising

$$\sum_{i=1}^{n} [Y_i - (b_0 + b_1 X_i)]^2$$

A mathematical technique which determines the two unknown's b_0 and b_1 that best fit the observed data, is known as the **Least-squares method**. In using the least-squares method, we obtain the following two equations, called the normal equations:

$$\sum_{i=1}^{n} Y_i = nb_0 + b_1 \sum_{i=1}^{n} X_i$$

$$\sum_{i=1}^{n} X_i Y_i = b_0 \sum_{i=1}^{n} X_i + b_1 \sum_{i=1}^{n} X_i^2$$

Solving

$$b_1 = \frac{n\sum_{i=1}^{n} X_i Y_i - \left(\sum_{i=1}^{n} X_i\right)\left(\sum_{i=1}^{n} Y_i\right)}{n\sum_{i=1}^{n} X_i^2 - \left(\sum_{i=1}^{n} X_i\right)^2}$$

$$b_0 = \frac{\sum_{i=1}^{n} Y_i - b_1 \sum_{i=1}^{n} X_i}{n}$$

11.4.1.2 Standard error of the estimation

Although the least-squares method results in a line that fits the data with the minimum amount of variation, the regression equation is not a perfect predictor. Therefore, we need to develop a statistic that measures the variability of the actual Y values, from the predicted Y values. The measure of variability around the line of regression is called the standard error of the estimate (Draper, 1981, Wonnacott, 1984)

The standard error of the estimate, given by the symbol S_{YX}, is defined as

$$S_{YX} = \sqrt{\frac{\sum_{i=1}^{n} (Y_i - \Psi_i)^2}{n-2}}$$

11.4.1.2.1 Measures of variation in regression and correlation

In order to examine how well the independent variable predicts the dependent variable in our statistical model, we need to develop several measures of variation. The first measure, **total sum of squares** (SST), is a measure of variation of the Y_I values around their mean, Y_{MEAN}. The SST can be divided into two components, the **explained**

variation or **sum of squares due to regression (SSR)** and **unexplained variation** or **error sum of squares (SSE)** (Wonnacott, 1984)

SSE = Error sum of squares

$$SSE = \sum_{i=!}^{n} (Y_i - \Psi_i)^2 = \sum_{i=1}^{n} Y_i^2 - b_0 \sum_{i=1}^{n} Y_i - b_1 \sum_{i=1}^{n} X_i Y_i$$

SSR = Regression sum of squares

$$SSR = \sum_{i=1}^{n} (\Psi_i - Y_{mean})^2 = b_0 \sum_{i=1}^{n} Y_i + b_1 \sum_{i=1}^{n} X_i Y_i - \frac{\left(\sum_{i=1}^{n} Y_i\right)}{n}$$

11.4.1.2.2 The Coefficient of Determination

The **coefficient of determination r^2** can be defined as:

$$r^2 = \frac{regression:\ sum\ of\ squares}{total\ sum\ of\ squares} = \frac{SSR}{SST}$$

The coefficient of determination measures the proportion of variation that is explained by the independent variable in the regression model.

To interpret the coefficient of determination, especially when dealing with multiple regression models, some researchers suggest that an **"adjusted" r^2** be computed to reflect both the numbers of predictor or explanatory variables in the model and the sample size.

$$r_{adj}^2 = 1 - \left[(1 - r^2) \frac{n-1}{n-2} \right]$$

The quantity r^2 is often used to judge the adequacy of the regression model. The statistic r^2 should be used with caution; it is always possible to make r^2 unity by simply adding enough terms to the model. For example, we can obtain a perfect fit to n data points with a polynomial of degree n-1. In addition, r^2 will always increase if an additional variable is added to the model, but this does not necessarily mean the new model is superior to the

old one. It can even be worse, but because of the loss of one degree of freedom, it is indicated as better (Hines, 1980).

11.4.1.3 Regression diagnostics: Residual Analysis

To evaluate the appropriateness of the regression model that has been fitted to the data we use a graphical approach called residual analysis (Berenson, 1989).

The residual or error values (ε_I) may be defined as the difference between the observed Y_I and the predicted (Ψ_i) values of the dependent variable for the given values X_I.

$$\varepsilon_i = Y_i - \Psi_i$$

Regression models are often fitted to data where the true functional relationship is unknown, thus we would like to know if the order of the model tentatively assumed is correct.

These residuals are plotted in different ways to test the adequacy of the model (Draper).

11.4.1.3.1 Overall Plots

When the residuals are plotted as a point scatter diagram or when the number of residuals are very large in a histogram form and if the model is correct, the residuals should conform to a normal distribution with zero mean. The mean must be zero as it is one of the assumptions of the least squares method (Berenson, 1989).

11.4.1.3.2 Time Sequence Plots

This entails plotting the residuals in the sequence that the data was gathered, which in most cases will be equally spaced in time. There must be no indication of a long-term time effect that is influencing the data or any trend with any independent variable other than time (Berenson, 1989).

The most common deviations from this is:

1. The variance is not constant but increases with time, implying that a weighted least squares analysis should have been used.
2. A linear term in time should have been included in the model.

3. Linear and quadratic terms in time should have been included in the model.

11.4.1.3.3 Plot Against Ψ_I

There should not be any abnormalities in the 'horizontal band' around zero when the residuals are plotted against Ψ. If this is the case the least squares model does not seem to be validated. If the plots are of the form as described in the previous section, the following steps can be taken (Berenson, 1989):

1. Variance is not constant, as assumed. There is a need for weighted least squares or a transformation on the observations Ψ_I before making the regression analysis.
2. An indication of an error in the analysis. The effect can also be caused by wrongly omitting a b_0 term in the model.
3. Indication of model inadequacy. An extra term is needed in the model (e.g. square or cross-product term), or the need for a transformation on the observations Y_I before analysis exists.

11.4.1.3.4 Plot Against the Predictor Variables X_{ji}

The form of these plots is the same as that against the Ψ_I, except that we use the values of the corresponding X_{ji}. Again, the overall impression of a horizontal band of residuals is regarded as satisfactory. Abnormalities in the figure above indicated the following:

1. The variance is not constant. There is a need for weighted least squares or a preliminary transformation on the Y's.
2. Error exists in the calculation. The linear effect of X is not removed.
3. A need for extra terms exists, for example, a quadratic term, in X_j in the model or a transformation on the Y's.

11.4.2Multiple Regression Models

The multiple regression models are expressed as

$$Y_i = \beta_0 + \beta_1 X_{1i} + \beta_2 X_{2i} + \varepsilon_i$$

In the case of a simple linear regression model the slope β_1 represents the unit change in Y per unit change in X_I. On the other hand, in multiple linear regression **β_1 represents the unit change in Y per unit change in X_1, taking into account the effect of X_2.**

The regression coefficients are calculated by means of three normal equations similar to the simple regression model (Draper, 1981 and Wonnacott, 1984).

11.4.2.1 Measures of variation in multiple regression

The variations can be expressed as both Error sum of squares (SSE) and Regression sum of squares (SSR).

SSE = Error sum of squares

$$SSE = \sum_{i=!}^{n} (Y_i - \Psi_i)^2 = \sum_{i=1}^{n} Y_i^2 - b_0 \sum_{i=1}^{n} Y_i - b_1 \sum_{i=1}^{n} X_{1i} Y_i - b_2 \sum_{i=1}^{n} X_{2i} Y_i$$

SSR = Regression sum of squares

$$SSR = \sum_{i=1}^{n} (\Psi_i - Y_{mean})^2 = b_0 \sum_{i=1}^{n} Y_i + b_1 \sum_{i=1}^{n} X_{1i} Y_i - b_2 \sum_{i=1}^{n} X_{2i} Y_i - \frac{\left(\sum_{i=1}^{n} Y_i\right)^2}{n}$$

11.4.2.2 Testing for the significance of the relationship between the dependent variable and the explanatory variables

Once a regression model has been fitted to the set of data, we can determine whether there is a significant relationship; since there is more than one explanatory variable, the null and alternative hypotheses can be set up as follows:

H_0:$\beta_1=\beta_2=0$ (There is no linear relationship between the dependent variable and the explanatory variables)

$H_1: \beta_1 \neq \beta_2 \neq 0$ (At least one regression coefficient is not equal to zero)

This null hypothesis may be tested by utilising an F-test, which is an indication of the ratio of two variances. When testing for the significance of the regression coefficients, the measure of the random error is called the **error variance**, so that the F-test is the ratio of the variance due to the regression, divided by the error variance:

$$F_{p,n-p-1} = \frac{MSR}{MSE}$$

where p is the number of explanatory variables in the regression model.

MSR = Mean square of regression

$$MSR = \frac{SSR}{p}$$

MSE = Mean square error

$$MSE = \frac{SSE}{n-p-1}$$

The data is given in the form of an anova table.

Source	df	Sums of Squares	Mean Squares (Variance)	F
Regression	p	SSR	MSR	F
Error	n-p-1	SSE	MSE	
Total	n-1	SST		

11.4.2.3 Measuring association in the multiple regression model

In multiple regression, since there is at least two explanatory variables, the coefficient of multiple determination represents the proportion of the variation in Y that is explained by the set of explanatory variables selected. The **coefficient of determination r^2** can be defined as:

$$r^2_{Y.12} = \frac{SSR}{SST}$$

Y: Dependent variable

12: Degrees of freedom

To reflect both the number of explanatory variables in the model and the sample size, the calculation of the "adjusted r^2" is suggested. It is especially necessary when one is comparing two or more regression models that predict the same dependent variable but have different numbers of explanatory or predictor values. The 'adjusted r^2'

$$r^2_{adj} = 1 - \left[\left(1 - r^2_{Y.12\ldots p}\right) \frac{n-1}{n-p-1} \right]$$

12 EXPERIMENTAL METHOD

The objective in this project was to determine the influence of intake charge conditions (intake air charge temperature and pressure) on combustion, exhaust emissions and engine durability. In order to limit the amount of testing required careful consideration was taken to decide on a maximum of two or three relevant test conditions on which to base all conclusions.

There were two basic types of data required. Firstly one needs the steady state measurements that include speed, torque, fuel consumption, air consumption and emissions measurements, which consist of HC, CO_2, CO and NO_X. Secondly, the high frequency measurement that consists of in-cylinder pressure trace and the fuel injection line pulse is required.

12.1 STEADY STATE MEASUREMENT

In order to investigate the effect of intake charge conditions on other engine test parameters such as power output, combustion efficiency and exhaust gas emissions, the effect of other parameters that will also influence these test parameters need to be accounted for. Ambient and atmospheric conditions should be taken into consideration when results are compared, as these conditions will influence engine output parameters, especially exhaust gas emissions like NO_X. Daimler Benz indicated in the Engine reference book (300 and 400 Series) that no power output correction for barometric pressure, humidity and temperature is required for turbo-charged engines. Other engine parameters should be kept constant in order to eliminate their effect on the test parameters. These engine parameters include diesel temperature control, dynamometer speed control, engine and fuel delivery or torque control, depending on the test that is required. Engine speed and fuel delivery were held constant, while other steady state parameters changed as intake conditions changed. The intake charge conditions have a large effect on volumetric efficiency, combustion efficiency and combustion temperature and pressure. To correlate these changes in combustion efficiency and exhaust gas

emissions as the result of change in inlet charge conditions the following steady state data were monitored, as illustrated in Table 18.

Table 18: Engine parameters measured.

PARAMETERS	MEASURED
Engine Speed	Froude EC38
Engine Torque	Froude EC38
Fuel Consumption	Mass Balance
Boost Pressure	Pressure Tranducer
Exhaust Back Pressure	Pressure Tranducer
Oil Pressure	Kent Cleareway Dile
Charge Air Temperature	Thermocouple Type J
Water Temperature In	Thermocouple Type J
Water Temperature Out	Thermocouple Type J
Oil Temperature	Thermocouple Type K
Diesel Temperature	Thermocouple Type K
Exhaust Temperature Before Turbo	Thermocouple Type K
Exhaust Temperature After Turbo	Thermocouple Type K
Bosch Smoke Emissions	Bosch Smoke Meter
Engine Air Flow Rate	D:D/2 Orifice Flow Meter
Water Flowrate through the Engine	D:D/2 Orifice Flow Meter

The engine test was done on an ADE 364T diesel engine and the specifications of the engine are documented later in this section. The design of the combustion chamber and fuel injection system, and the placing of the injector and valves are similar to a wide range of ADE-manufactured diesel engines. For this reason the engine is suitable for this research application as it covers the majority of engines in South Africa. The dynamometer used was a Froude Eddy Current dynamometer with a capability of 500 Nm up to 8000 revs/min. The engine and dynamometer were coupled with rubber couplings which are suitable for low speed applications as in a diesel engine. These rubber coupling absorb any crankshaft fluctuations which might have an effect on the stability of dynamometer control.

Test Parameters were measured as follows:

- Fuel measurement was done by means of a mass-based system designed and built for this purpose at the CAE. The fuel flow measurement device uses a precision

mass balance to determine the instantaneous mass of fuel in a container feeding fuel to the engine. The rate of mass loss of the container is measured, giving the mass consumption rate of the engine directly. Diesel engine performance is known to be sensitive to fuel temperature; therefore this was controlled at a predetermined value to ensure reproducibility of test results.

- All the temperature measurements were done by thermocouple. The air intake temperature and cooling water in and out temperatures were measured with type-J thermocouples and the rest by type-K thermocouples.
- The cooling water flow rate through the engine was measured with a D:D/2 orifice plate flow meter, which was designed by the author according to BS standards for this purpose and built at the University of Stellenbosch.
- Airflow measurement was measured with the aid of a flow nozzle, and the pressure difference over the nozzle was measured with a Betz manometer. The flow nozzle was fitted to a damping container (approximately 3 m^3 in volume) to damp any flow fluctuations caused by the engine
- Siemens gas analysers were used to determine the concentrations of exhaust emissions in the exhaust gas of the engine. Soot emissions were measured using a Bosch smoke meter.
- The engine was extensively instrumented to enable the measurement of all relevant engine parameters. Specialised instrumentation was used to monitor fuel flow and heat rejection to the engine coolant, amongst other parameters.

All these variables were linked with a personal computer and recorded. The above variables were given time to stabilise before they were recorded.

12.2 HIGH FREQUENCY MEASUREMENTS

As mentioned, the high-speed data that had been recorded includes an in-cylinder pressure trace and injection line pulse, as well as its reference to time (in this case crank angle).

The correctness of the reference to crank angle is of the utmost importance as heat release calculation is strongly dependent on the phasing of the pressure trace, as mentioned previously.

The start of injection was determined by means of an AVL injection line pulse sensor. The sensor is put on the injector line of the number one cylinder, as closely as possible to the injector. The increase in pressure in the injection line as the fuel pressure pulse moves down the line is detected by the sensor. The compression of the sensor causes a voltage output signal to be induced and this signal can be used to determine the start of injection for the purpose of determining rate of heat release.

The in-cylinder pressure trace is measured by an AVL piezo-electric pressure transducer (AVL QH32C water-cooled pressure transducer), which is mounted in the engine cylinder head to measure pressure in the number one cylinder. The number one cylinder is used in this case as it is nearest to the crankshaft pulley from where the crank angle and TDC pulse is generated to minimise error due to crankshaft elastic fluctuations. The pressure transducer was mounted in the engine head as specified by the manufacturer and illustrated in Figure 26.

Figure 26: Installation instruction for the AVL piezo-electric pressure transducer. (AVL brochure)

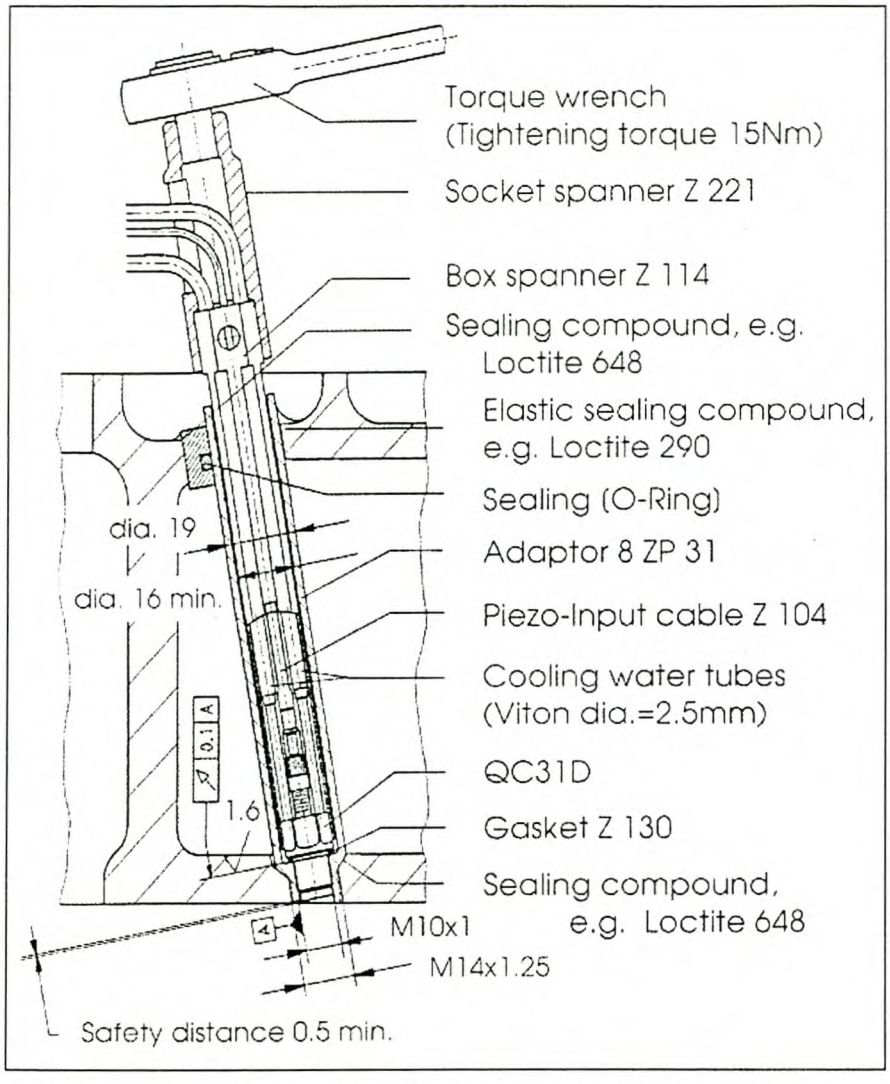

To avoid any interference with the piston, the pressure transducer was mounted one to two millimetres behind the interface of the cylinder with the cylinder volume.

12.3 DATA ACQUISITION SYSTEM

The data acquisition system used at the University of Stellenbosch called ETA (Engine Test Automation system), is an engine monitoring, control and data acquisition system designed to be versatile, reliable and easy to operate. The system is based around a modular, industrial, input/output processor unit interfaced to a personal computer. A separate unit monitors fuel consumption with the aid of a precision electronic mass

balance. A software programme provides a user-friendly and configurable interface and data storage package.

12.3.1 Input/Output processor unit

The heart of the system is an industrial quality input/output processor, the Action Instruments I/O PAKPLUS. This comprises a base unit with 16 mounting sockets, which together with numerous plug-in analogue and digital modules provide an interface between remote real-world signals and a computer. Communication between the computer and I/O PAK is via the common RS-232 system. The I/O PAK requires that valid start-up parameters be set before operation with the host computer is possible.

12.3.2 Temperature Measurement

Type K and type J thermocouple modules are connected to panel-mounted sockets. These thermocouples are fitted to the engine to monitor desired engine operating temperatures. The J-type thermocouples were used for the measuring of temperature in the range 0-150°C, that include charge air temperature, oil temperature and coolant temperature. A more accurate measurement is obtained with a type-J thermocouple, due to the smaller operating range of this type.

Type-K is used for the measurement of exhaust temp, where the large operating range of the thermocouple can be used.

12.3.3 Engine Speed and Torque

Two 0 to 10 V DC modules are installed for the measurement of engine speed and torque. Output signals are to be provided from the existing engine test bed sensors.

12.3.4 Pressure Measurement

There are industrial pressure transducers mounted in the I/O PAK enclosure for the monitoring of barometric pressure and certain engine parameters. All the transducers give 4 to 20 mA output signals and are powered by a regulated 24 V DC Power Supply.

12.3.5 Fuel Flow Measurement

Fuel consumption is monitored by a precision Mass Balance (Mettler Toledo PB 3002) on which a three-litre glass beaker sits. During fuel consumption monitoring fuel is drawn from and returned to the beaker. Therefore the fuel level and the instantaneous fuel mass in the beaker are constantly decreasing as fuel is consumed by the engine. After fuel consumption measurement has been completed the supply to the beaker is opened and it is filled to a certain level. The Mass Balance communicates via an RS-232 serial connection with the I/O PAK, which relays the information to the PC. The ETA software then calculates instantaneous Fuel Consumption.

12.3.6 Software

The software package forms the user interface with the ETA system and is a Microsoft Windows-based package that is designed to be both versatile and user friendly. Anyone familiar with Windows will find it easy to operate the package via the normal Windows menus. The software runs on any IBM Compatible PC (preferably a 486 DX or more powerful machine).

The software allows the configuring of 64 separate channels, 16 of which are configurable as 'real' channels that are responding directly to inputs from one of the 16 I/O PAK sites. The rest are configurable as 'virtual' or 'calculated' channels, that is to perform a mathematical operation on any number of channels to provide a specific response. For example, a power channel can be set up which can calculate instantaneous engine power from the outputs of the "real" channels of Speed and Torque (and the necessary constants).

12.4 ENGINE SPECIFICATIONS

The engine used for the research work is specified in terms of type, configuration and size. The specifications on maximum torque and maximum brake mean effective pressure are quoted from the original equipment manufacturer in Table 19.

The original maximum fuel delivery was not obeyed during the advanced research phase of this project, in order to evaluate combustion at different boost pressure and temperature at different load conditions at 1500 revs/min.

Table 19: Engine specification and description.

Engine	ADE 364T
Aspirated	Turbo-charged
Coolant	water, recirculating
Combustion process	4-stroke Diesel direct injection
Number of cylinders	4
Bore	97.5mm
Stroke	133mm
Total piston displacement	3972 cm^3
Compression ratio	16.5:1
Injection sequence	1-3-4-2
Maximum Torque	380 Nm
Maximum Mean effective pressure	12.1 Bar
Maximum Power output	87 kW

12.5 CHOICE OF TEST POINTS

In order to ensure that the influence of both intake charge temperature and boost pressure on combustion behaviour and exhaust emission formation is thoroughly evaluated, a variation of 5 different temperatures and 5 different boost pressures were used. This results in a matrix of 25 test points at one speed-torque point. Therefore careful selection of speed-torque points should be carried out when deciding at which points testing will take place.

The European ECE R13 test procedure was used as the basis for test point selection. The weighting factor of the test point determines the importance or the influence of the point on the final result. The points with the highest weighting are on medium speed (60% of rated speed) at 100% and 75% load and at rated speed at 100% load. This coincides well with the fact that engine parameters as well as emissions formation are far more dependent on load than on speed.

The decision was made to perform the engine tests at 1500 revs/min engine speed at 400 Nm at constant fuel delivery for all the test point and at 200 Nm at constant fuel delivery

for all the test point. At 300 Nm testing were performed at constant torque, therefore fuel delivery was controlled to maintain constant torque, while boost pressure and intake charge temperature were varied for the 25 test points. Therefore the test was performed at 100, 75 and 50% load conditions at a single speed. This will enable the researcher to evaluate the load dependency of emission formation as well as engine durability. Fuel delivery to the engine was kept constant as boost pressure and intake charge temperature were varied at the 100 and 50% load test points and torque was allowed to vary.

12.6 EXPERIMENTAL APPROACH AND TEST PROCEDURE

12.6.1 Standard engine tests

The standard engine was tested to get an indication of how the engine performs in terms of emission aspects and to measure the rate of heat release at standard operating conditions.

All steady state data, as well as high frequency measurements were measured at three speeds, 1500, 1900 and 2300 revs/min. At each speed the load was varied from 80 Nm to full load with 80 Nm intervals. This enabled the researcher to get an indication of how speed and load variation influence emission trends.

12.6.2 The intake charge variation matrix engine test procedure

In order to investigate the effects of varying turbo-charger pressure ratio and charge air inter-cooling the turbo-charger was removed from the engine and the engine was artificially boosted from an outside compressed air system to enable the simulation of various turbo-charger configurations. The objective was to create a situation in which only the intake air temperature and pressure were varied while all other parameters were held constant.

A typical experimental test matrix for the variation of boost pressure and intake charge temperature is shown in Figure 27.

Figure 27: The test point matrix for the 200Nm engine evaluation (50 % torque)

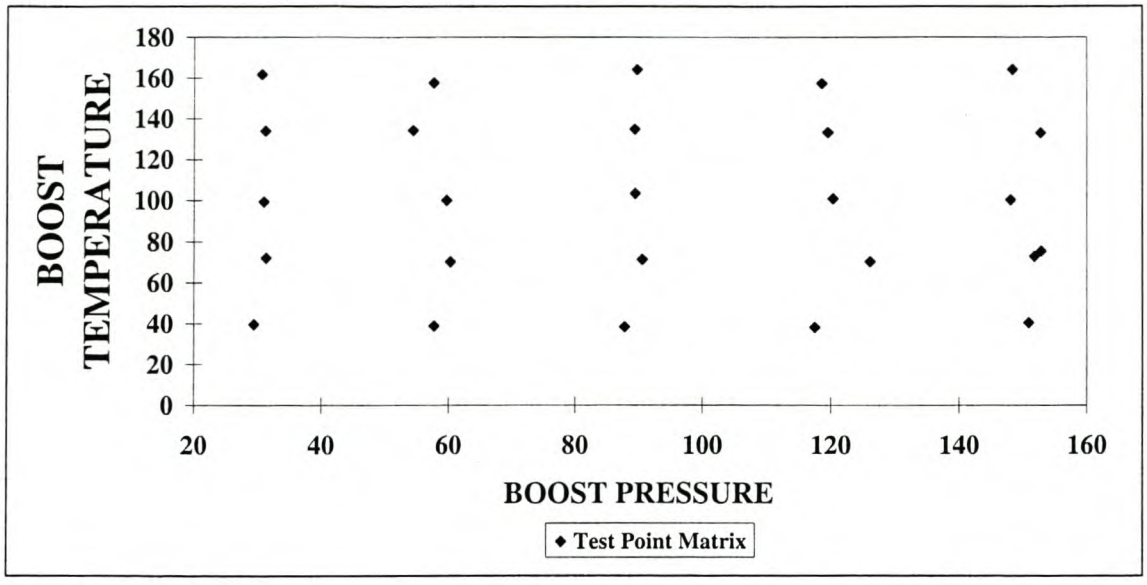

The compressed air was supplied from an existing system of the Aircraft Propulsion Laboratory at the University of Stellenbosch. The pressure control was done manually by means of a gate valve which made it possible to fix the manifold pressure at a predetermine value. The air consumption of the engine at the given intake charge pressure was measured with a flange tapping orifice flow meter. To minimise airflow fluctuations through the engine a large volume pressure vessel was used to act as a damping chamber. A Light Petroleum Gas (LPG) burner heated the charge air through the air-to-air heat exchanger in varying amounts. In this way the air charge temperature and pressure can be altered to a large extent at constant speed and fuelling of the engine.

At the different boost pressure setting the exhaust backpressure were set according to a calculated value. The calculation of the exhaust backpressure was based on energy balance in the turbine and compressor of the turbo-charger, according to the following equation (Lilly, 1984). The compressor power:

$$\dot{W} = \dot{m} CpTo_1 \left[\left(\frac{Po_2}{Po_1} \right)^{(\gamma-1)\gamma} - 1 \right] \Big/ \eta_{isTS}$$

$\dot{W}$ = Compressor Power

$\dot{m}$ = Mass flow rate

Cp = Specific heat capacity at constant pressure

To_1 = Inlet Air temperature

$\frac{Po_2}{Po_1}$ = Pressure Ratio

γ = Cp/Cv

η_{isTS} = Compressor efficiency

The turbine power:

$$\dot{W} = \dot{m} CpTo_3 \left[1 - \left(\frac{P_4}{Po_3} \right)^{(\gamma-1)\gamma} \right] \eta_{isTS}$$

$\dot{W}$ = Turbine Power

$\dot{m}$ = Mass flow rate

Cp = Specific heat capacity at constant pressure

To_1 = Inlet temperature (Exhaust temperature)

$\frac{P_4}{Po_3}$ = Pressure Ratio, P_4 was taken to be atmospheric pressure

γ = Cp/Cv

η_{isTS} = Turbine efficiency

The two equations were programmed into a Pascal computer program to calculate the exhaust backpressure, Po_3.

As discussed above, the engine tests were performed at 1500 revs/min engine speed at 100, 75 and 50% loading. The fuel delivery was kept constant while the boost pressure and intake charge temperature were varied at 1500 revs/min for the 100% and 50% load conditions. With the 100% load test point the test was started at 150 kPa boost pressure (gauge pressure) and 40°C intake air temperature, the load was set at 400 Nm torque and the test point was completed. The delivery at this point was kept constant for the rest of the test matrix (the other 24 test points). This test matrix will be referred to as the 400 Nm test matrix. The same procedure was followed at the 50% load test points, with the starting torque set at 200 Nm and will be referred to as the 200 Nm test matrix.

The test procedure at the 75% load condition differs from the procedure used in the other two test matrixes, as in this case the torque was held constant at 300 Nm. The boost

pressure and intake air temperature were varied, while fuel delivery was set to retain constant torque at all 25 test points.

12.7 OBJECTIVES OF THE ENGINE RESEARCH

12.7.1 Standard engine

The objectives of the testing that was done on the standard engine as configured by the original equipment manufacturer were as follows:

- To prove that the engine that is used in the evaluation is in acceptable condition and that it is performing to the specification of the OEM.
- To indicate the exhaust gas emissions levels of the engine at its standard operation conditions.
- To evaluate power output, fuel consumption, engine durability and exhaust gas emissions by referring to combustion analysis.

12.7.2 The intake charge variation matrix engine test procedure

The objectives of the testing done on the re-configured engine in order to evaluate the influence of boost pressure and intake charge temperature on the diesel engine combustion, emission generation and engine durability, were as follows:

- Evaluate and discuss the steady state engine parameters and the influence boost pressure and intake charge temperature have on them
- Evaluate and discuss the exhaust gas emissions
- To prove and explain the events in the steady state data and exhaust gas emissions data by referring to combustion analysis data.

13 RESULTS AND DISCUSSION

13.1 STANDARD ENGINE

13.1.1 Introduction

The engine variables were tabulated and the most relevant variables' dependency on speed and torque were plotted relevant to these engine parameters. The first objective as indicated is to show that the engine was operating within the OEM specifications to prove that the condition of the engine is acceptable.

13.1.2 Volume of fuel injected (Fuel delivery)

It was decided to do a 120% load point at 1500 revs/min because the intake charge variation matrix engine evaluations will be performed at different loads at 1500 revs/min. The reason for this is to evaluate lower than normal air/fuel ratios on the standard engine and its effect on exhaust gas emissions and durability of the engine.

The fuel delivery is higher than the OEM specification at 1500 revs/min for the 120 % test point, as expected. The 100% load point at all the test speeds is more or less within the maximum expected delivery level except for 1900 revs/min which is slightly above, as seen in Figure 28. The higher fuel delivery will result in higher power output, higher boost pressure and high Bosch smoke levels.

The combustion behaviour at 1500 revs/min, 120% load is typical of an over-fuelled condition, where the fuelling supplied to the engine exceeds the amount the engine and turbo-charger combination were designed for. At this operating condition the cylinder pressure will also exceed the maximum cylinder pressure for which the engine's bottom-end was designed.

The ABN HI label that is used in Figure 28 indicates the high tolerance level allowed by the original equipment manufacturer (OEM).

Figure 28: Fuel delivery as a function of speed for the standard ADE 364T engine

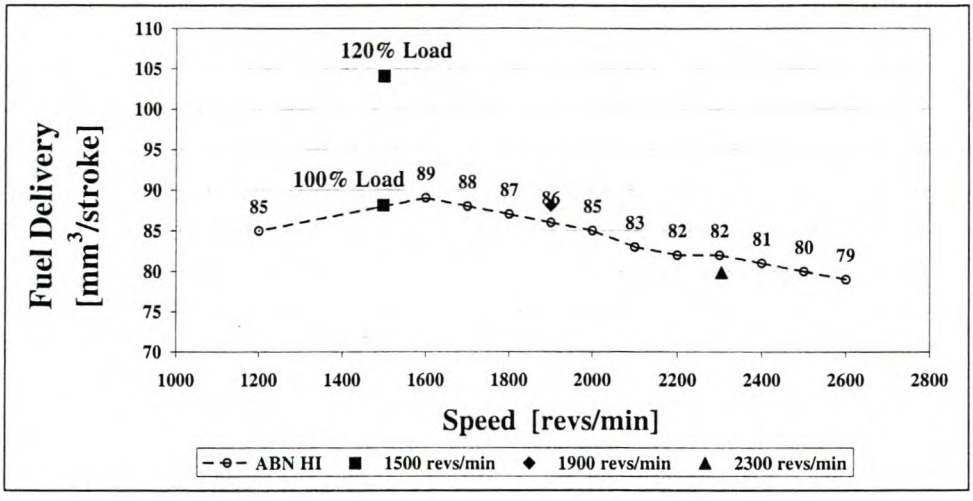

13.1.3 Turbo-charger boost pressure

At higher than the higher limit fuel delivery to the engine for the 1900 revs/min test point, it was expected that the boost pressure would also be higher. This is however not the case as the boost pressure is just above the lower limit in Figure 29. The only conclusion that can be made is that the turbo-charger does not perform as it should, with a resulting lower air/fuel ratio over the operating range of the engine. Air/fuel ratio has a direct influence on the fuel consumption and exhaust gas emissions of an engine. The less the air/fuel ratio the lower the excess air ratio, which decreases efficiency of combustion. The lack of oxygen decreases the oxidation rate of soot and unburned Hydrocarbon during the diffusion combustion phase, which results in an increase in the PM emission and a resulting increase in black smoke. More than the allowable fraction of the fuel is converted to PM emissions, which should have burned completely during the expansion stroke to provide useful work, causing combustion efficiency to be low. The reduced engine efficiency is evident in the Specific Fuel Consumption (SFC) figure that will be discussed later in the section.

Figure 29: Boost pressure as a function of speed for the standard ADE 364T engine

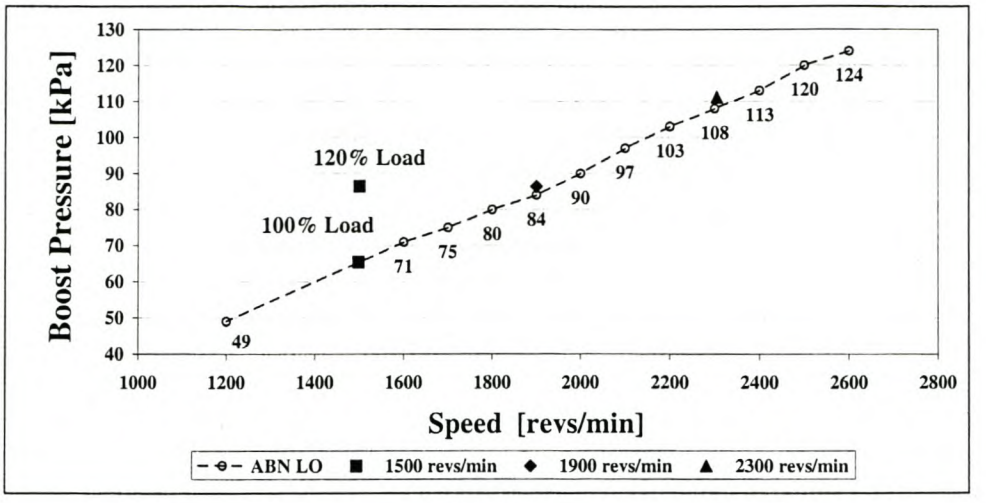

13.1.4 Torque delivered

The high fuel delivery resulted in the torque output of the engine to be higher than the specification for this engine. Torque output follows the delivery closely, as fuel delivery overshadows all the other factors that contribute to torque, as long as the engine is operated under acceptable air/fuel ratios (>18:1) for this engine. Below air/fuel ratios of 18 to 1 the engine burns the fuel so inefficiently that the proportional increase in fuelling does not result in the proportional increase in torque output. The test point at 1500 revs/min, 120% load at which the engine was operating at 17.2 air/fuel ratio is border-line as the Bosch smoke level is above 6, which is not acceptable for this engine as seen on Figure 31.

Figure 30: Engine Torque as a function of speed for the standard ADE 364T engine

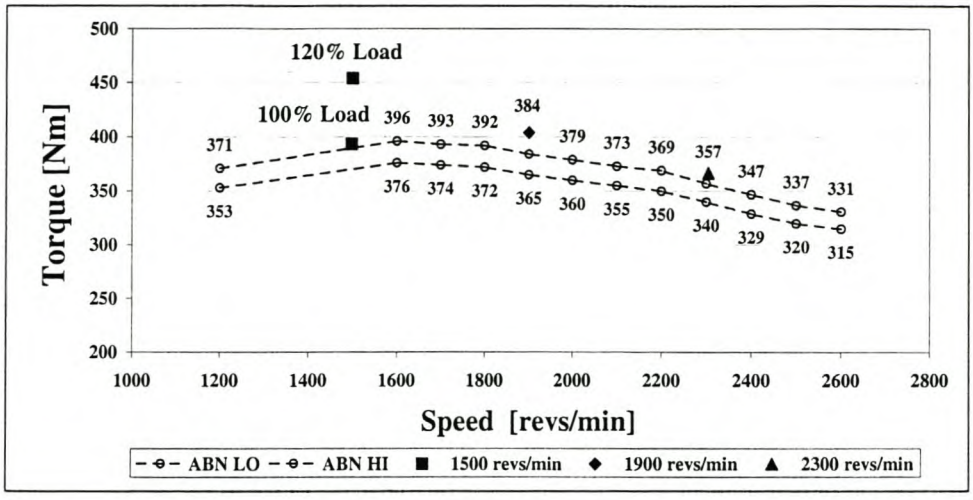

13.1.5 Exhaust smoke density

From Figure 31 below it is evident that, as discussed earlier, the turbo-charger does not operate to the level it should. At all the 100 % test points the delivery is more or less on the higher limit of the standard specification and the smoke level is far above the levels of acceptance. This indicates that the efficiency of combustion of the fuel is lower than one expects at the delivery rate. The reduced turbo-charger boost pressure that results in lower airflow rate causes high PM pollutant levels.

Figure 31: Bosch smoke as a function of speed for the standard ADE 364T engine

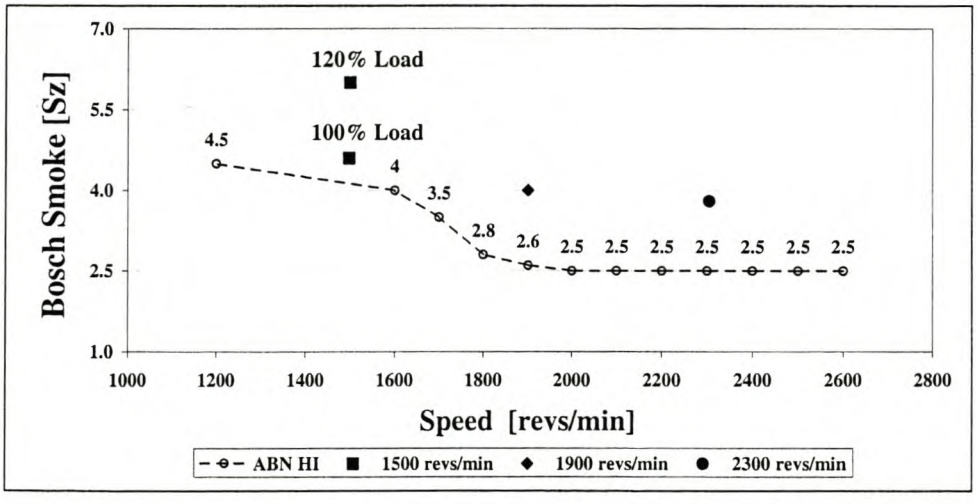

13.1.6 Fuel efficiency of the engine

The rest of the discussion on the standard engine test results will include the steady state and exhaust emission test results at part load for the different engine speeds, and combustion analysis will be referred to in both discussions.

Specific fuel consumption is one of the best engine parameters to evaluate engine efficiency. It takes into consideration the amount of fuel the engine uses and also how efficiently the fuel is combusted to generate shaft power output. When boost pressure was evaluated it was mentioned that a reduction in combustion efficiency is noted when the fuel delivery is increased to an over-fuelled situation. At 1500 revs/min at the highest load point (120% load) the fuel delivery is high enough to be considered over-fuelled when the delivery and Bosch smoke levels are compared to the OEM specifications. The SFC figure below proves that in an over-fuelled situation the overall combustion efficiency decreases. This is evident in the slight rise in SFC for the 1500 revs/min results between 393 and 453 Nm torque.

The SFC results data shows a distinct step in the 1900 and 2300 revs/min data. The first reason for the step is that the tests were done on consecutive days and the ambient temperature was considerably lower the second day, with negligible difference in atmospheric pressure. Higher ambient air density as the result of the lower air temperature increases the volumetric efficiency of the engine to increase the completeness of combustion. Secondly, the fuel inlet temperature was higher the second day, which caused the fuel mass flow to be lower, as seen in the fuel mass consumption data. Therefore the combination of the two effects results in lower engine efficiency on the second day.

Figure 32: Specific Fuel consumption for three different speeds at increasing load.

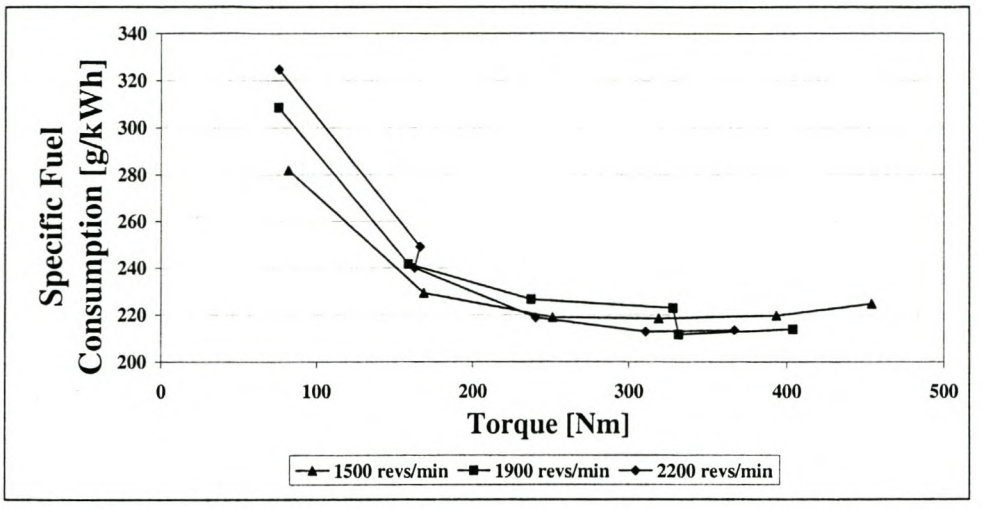

13.1.7 Air/fuel Ratio

The low air/fuel ratio (17.2) that is apparent for the 120% load point at 1500 revs/min was indicated in the previous section to result in an increase in SFC. Therefore the increase SFC at this point indicates that the engine combustion chamber design was not designed for air/fuel ratios lower than 18 at 1500 revs/min.

The step-change that was discussed in the previous section is also indicated as an increase in air/fuel ratio. From the data it is apparent that a slight increase in air/fuel ratio results in a considerable improvement in SFC.

Figure 33: Air Fuel Ratio for three different speeds at increasing load.

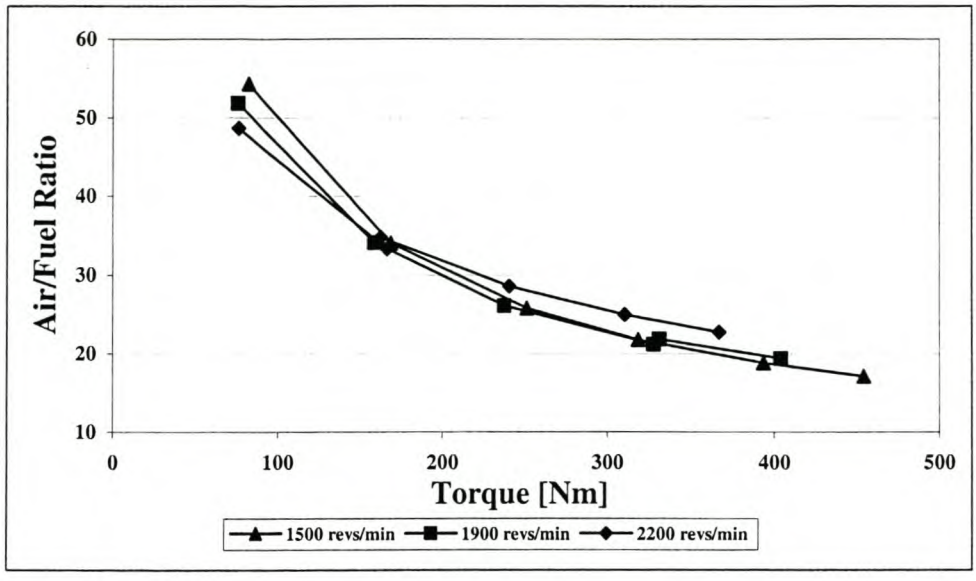

13.1.8 Carbon monoxide emission concentration

The carbon monoxide concentration remains extremely low and almost constant as load increases until a certain point is reached, in this case 240 Nm. This is due to the increase in equivalence ratio ($\phi < 1$, nearing 1). The turbo-charger has a positive effect on CO emissions as speed increases and turbo-charger efficiency subsequently increases. This results in a better equivalence ratio (lower value or higher air/fuel ratio) at high speed-high load than at low speed-high load conditions. This results in low CO emission concentration and is evident in the data even though concentrations are extremely low.

CO concentration is a good standard to measure the completeness of combustion in all engine types. In diesel combustion when air/fuel ratios reach a certain value (normally between 18 and 20 depending on the fuel injection pressure, swirl ratio and combustion chamber design) the CO concentration rises sharply and is followed by an increase in PM emissions. This is the case at the 120% load, 1500 revs/min test point. The excess air ratio at this test point is not sufficient or there is not enough time to allow complete combustion or oxidation of the partly burned Hydrocarbon compositions and the soot particles that were formed earlier in the combustion phase (Ferguson, 1986). Oxidation needs to complete before the temperature of the combustion gas drops below a certain

level (around 800°C) and the remaining soot particles and unburned HC freeze in composition and leave the engine as exhaust gas pollutants (Heywood, 1984).

Figure 34: Carbon Monoxide concentration for three different speeds at increasing load.

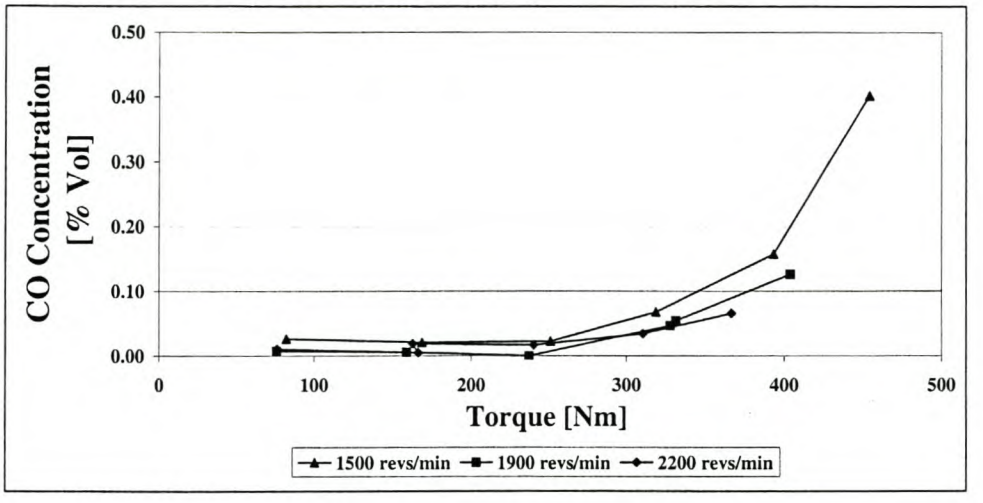

13.1.9 Hydrocarbon Emission Concentration

HC emissions formation is dependent on mixing controlled combustion phase temperature and equivalence ratio. As combustion temperature increases HC emissions decrease and the lower the equivalence ratio the lower HC's. From the results below it is evident that HC emissions have a stronger dependency on combustion temperature than on equivalence ratio. One of the objectives of the research is to determine statistically the relative dependencies on engine parameters such as temperature and equivalence ratio in the formulation of HC emissions. This will be detailed later in the thesis. Combustion temperature is strongly dependent on intake air temperature and boost pressure, therefore these two variables will have an influence on HC emissions.

Strangely, step changes occur in the data: the higher HC value is at a higher ambient intake charge and exhaust temperature, and for this reason equivalence ratio plays a definite role, although it is less pronounced.

Figure 35: Specific Hydrocarbon emissions for three different speeds at increasing load

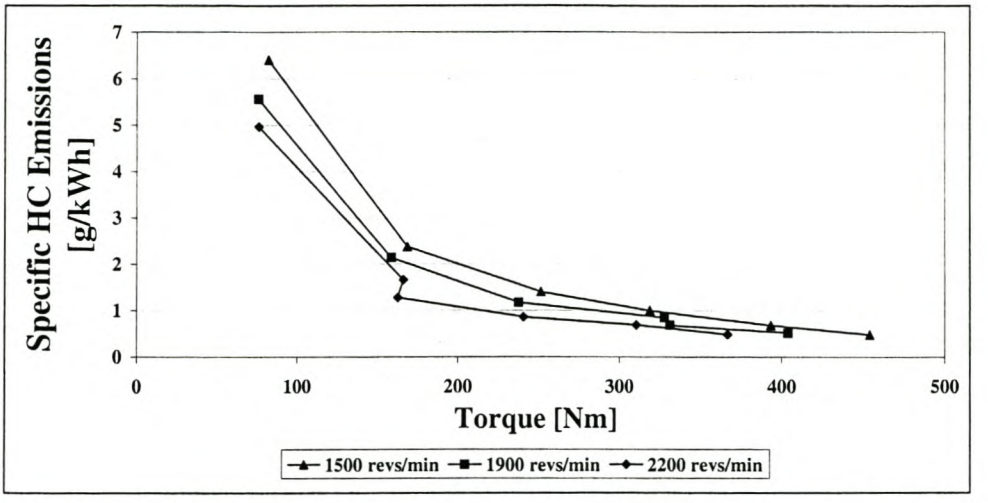

13.1.10 NOx Emission Concentration

NOx concentration increases with load as the larger quantity of fuel injected causes higher combustion temperatures, which increase NO formation. The slight decrease in NOx emissions as speed increases can possibly be attributed to a decrease in ignition delay.

Figure 36: Specific Nitric Oxide emissions for three different speeds at increasing load

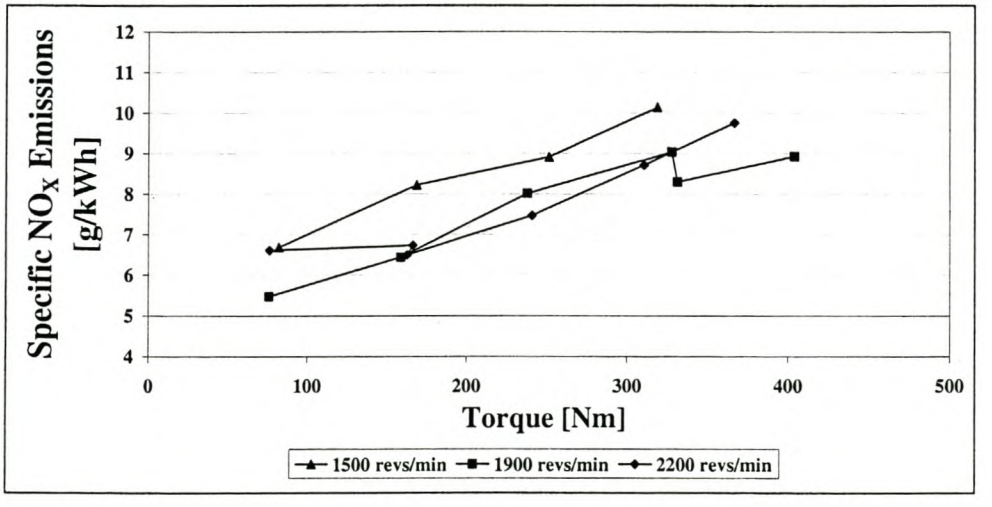

13.2 THE INTAKE CHARGE VARIATION MATRIX ENGINE TEST RESULTS

13.2.1 Introduction

The three test matrices that were done at 1500 revs/min on the test engine will be discussed to indicate what effect the change in boost pressure and in charge temperature has on performance, combustion efficiency, durability and exhaust gas emissions. The data from the 400 Nm test matrix will be discussed in detail, while the 200 Nm and 300 Nm tests will be compared to indicate what effect load variation has on the engine parameters in question. As the 300 Nm test varies slightly from the other two as it was performed at constant load, these variations will also be discussed.

13.2.2 Air Mass Flow through the Engine

One of the most important parameters in diesel engine optimisation is maximising air mass flow. The introduction of turbo-charging on automotive diesel engines in the late sixties was to achieve that objective. Turbo-charging increases air mass flow through the engine to improve the power density and efficiency of the engine. The introduction of inter-cooling was for exactly the same reason and more, and therefore the discussion of results will start off with air mass flow and the influence of turbo-charging and inter-cooling on this.

From the results below it is evident that an increase in boost pressure causes a dramatic increase in air mass flow rate through the engine. It must be stated that in simulating the operation of a turbo-charger to obtain a certain boost pressure, an exhaust backpressure must be applied to the exhaust side. The calculation of the exhaust backpressure was based on energy balance in the turbine and compressor of the turbo-charger as discussed in section 12.6.2 (Lilly, 1984). This is the perfectly matched situation for the turbo-charger at all test points, which will not be the case in a "real" situation. In other words the compressor and turbine will operate at a predetermined fitted efficiency, which is not the case in the real situation. Therefore the results might be more optimistic than when the engine is running with a turbo-charger, as the exhaust backpressure might be less in

these tests. Exhaust backpressure influences air flow rate and efficiency of the engine as an increase in back pressure increases pumping work. On the other hand is not possible to know compressor and turbine efficiency at all the engine operating conditions, as matching of the turbo-charger depends on engine utilisation.

Figure 37 below indicates than air mass flow rate has a strong dependency on boost pressure, but only a slight dependency on boost temperature as the result of an increase in volumetric efficiency. As the fuel delivery stays more or less constant for the 25-test points (400 and 200 Nm test), the air/fuel ratio increases as airflow rate increases. This results in an increase in the excess air ratio during combustion to increase combustion efficiency and reduce PM emissions. The same trends are seen in the 200 and 300 Nm data.

Figure 37: Air mass flow through the engine as a function of boost pressure and temperature for the 400 Nm test (1500revs/min, 100% load).

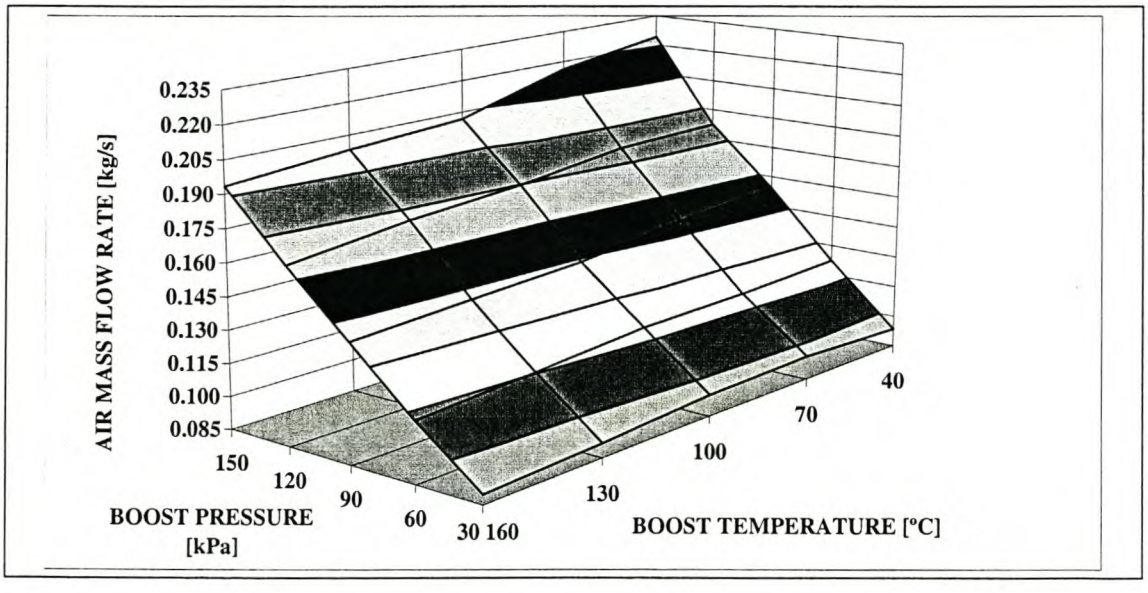

13.2.3 Engine Fuel Efficiency

With the increase in air/fuel ratio, the amount of air available for the combustion of the fuel quantity increases. This results in more complete combustion of the fuel and better oxidation of soot particles formed during premixed combustion and the beginning of diffusion combustion, as more oxygen is available during the late combustion phase. The extra energy that is released as a consequence of the increased excess air in the combustion chamber increases the power output and the fuel consumption of the engine. The combined effect of these two parameters can be seen in benefits in SFC as boost pressure is increased and boost temperature reduced.

Because SFC is an indicator of efficiency, the assumption can be dawn that the relationship between torque and efficiency is better at higher boost pressure and lower charge temperature. As boost pressure increases the margin in improved efficiency reduce as expected.

Figure 38: Torque vs Specific Fuel Consumption (SFC) with varying boost temperature and pressure for the 400 Nm test (1500revs/min, 100% load).

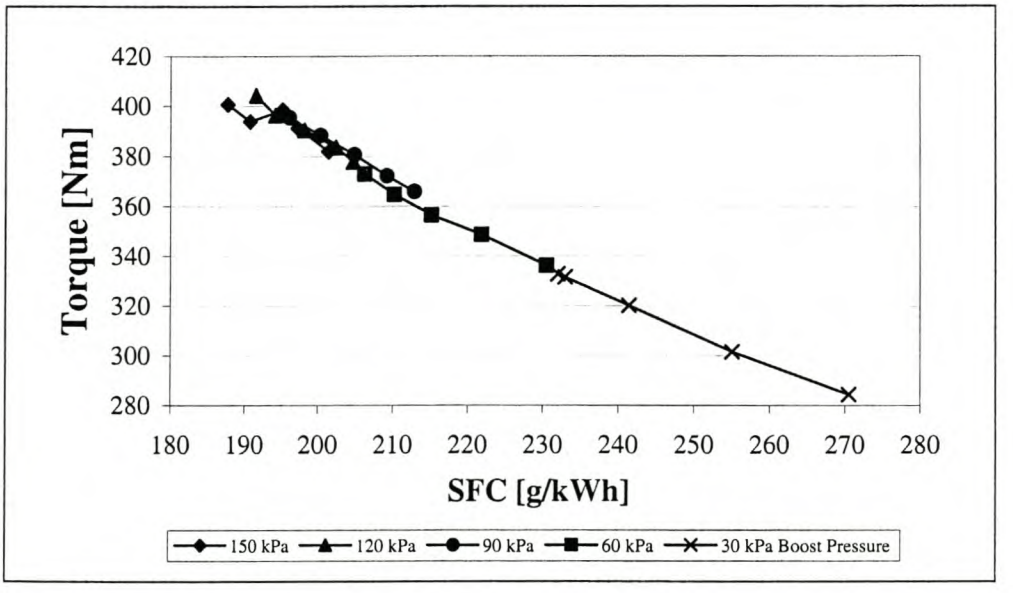

From the data below it is evident that inter-cooling plays a more pronounced role in the decrease in SFC than in the increase in airflow rate, although turbo-charging still is more predominant.

The 200 and 400 Nm tests were done at constant fuel delivery and if there is a difference in torque output of the engine it is because of a difference in combustion efficiency. From the data of the 400 Nm test as shown in Figure 38 it is clear that there is a dramatic variation in torque delivered by the engine as boost pressure and temperature varied. The varying thermodynamic cycle efficiency was evident in the SFC data, and the Bosch smoke data proved the fuel was burned more completely in the cases where the air/fuel ratio was higher

The reaction of SFC at the 200 and 300 Nm tests on boost pressure and temperature variation shows the same tendency as the 400 Nm test, with the exception that it seems that air inlet temperature has more of an influence on SFC at conditions of higher air/fuel ratios (part load). This phenomenon is apparent at both 200 and 300 Nm, even though fuel was kept constant at 200 Nm and varied at 300 Nm, therefore it must be a true event. The reason for this is not yet apparent, as the phenomenon has not been considered in literature. This issue will be raised when statistical analysis is performed. The SFC three-dimensional plots on the 200 Nm and 300 Nm data are shown in appendix A.

Figure 39: Specific Fuel Consumption (SFC) with varying boost temperature and pressure for the 400 Nm test (1500revs/min, 100% load).

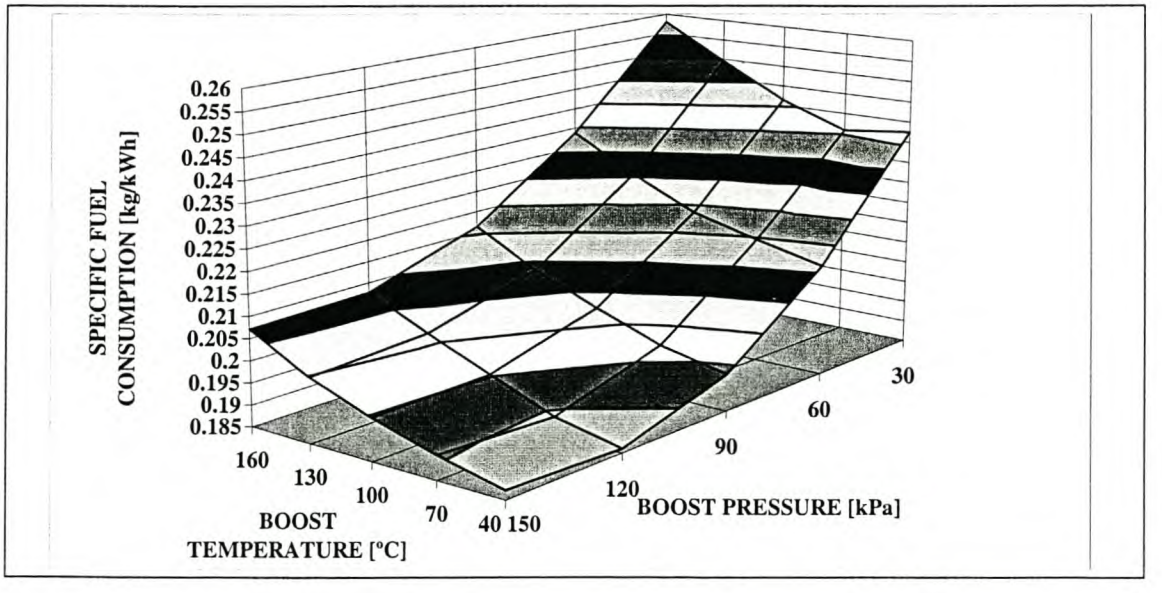

13.2.4 Exhaust Smoke Density

As the completeness of combustion increases with the increase in air/fuel ratio, the PM pollutants in the exhaust gas reduce. It is not only the oxidation of soot that is increased during the late combustion as mentioned before, but also the formation, as more oxygen is available in the flame zone where soot is first formed. With more oxygen available during combustion less partly burned fuel leaves the combustion chamber as either Unburned Hydrocarbons or as SOF absorbed in the soot particles. When the tests were done a particulate sampler was not available, therefore Particulate mass was never measured and only Bosch smoke levels can be compared. An increase in air/fuel ratio will not only reduce the number of soot particles in the diesel exhaust gas, but also the mass of the individual particles.

Smoke formation's dependency on boost pressure and temperature is very similar to air flow's dependency on these two variable engine parameters, except that it is less linear than air flow rate. Smoke concentration is very dependent on air/fuel ratio (the relationship will be statistically determined), as for air flow rate, Bosch smoke is predominately dependent on boost pressure and not intake charge temperature. The non-linearity of Bosch smoke as a function of increase in boost pressure (air/fuel ratio) can be explained through Bosch smoke levels in the exhaust gas which, as mentioned before, is dependent on the formation of soot particles in the beginning of combustion and then oxidation of these soot particles later in combustion. As the excess air ratio decreases, the formation of soot increases and the oxidation rate decreases, therefore a double effect occurs when airflow rate decreases through the engine, with the resulting non-linear relationship.

Figure 40: Smoke density with varying boost temperature and pressure for the 400 Nm test (1500revs/min, 100% load).

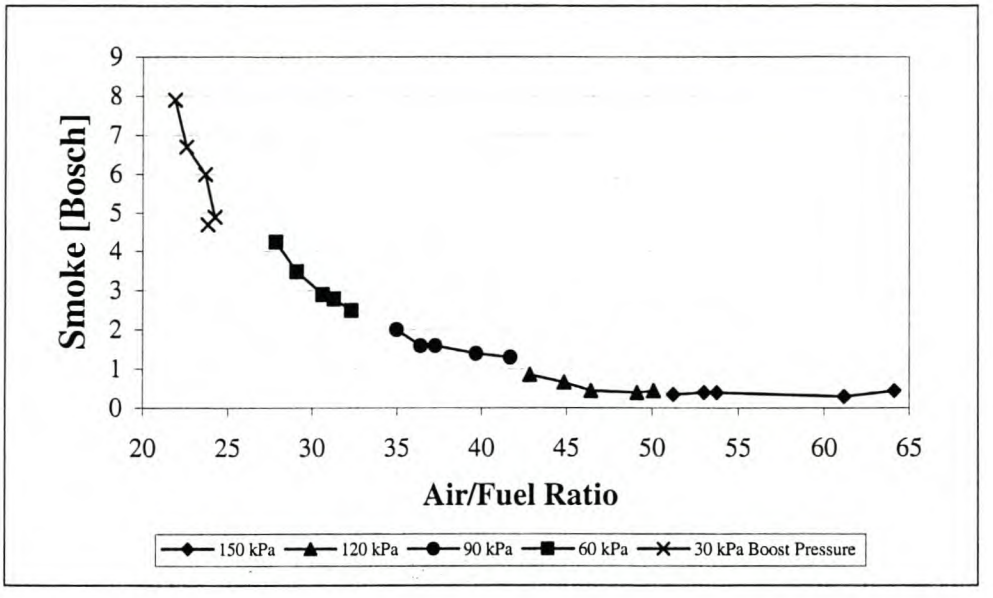

The Bosch smoke concentration shows a different trend at part load conditions and differs for the 200Nm (constant fuelling case) and 300 Nm (constant torque case) tests as well. The 200 Nm test shows that boost pressure and temperature have little or no effect on Bosch smoke: the reason for this is that air/fuel ratios are so high due to the low fuel delivery at the part load condition. It is only at two points where the Bosch number rises above 1 and these are the test points where boost pressure is at the lowest and boost temperature at the highest (air flow rate here is at the lowest).

In the 300 Nm case the air/fuel ratio becomes more critical, therefore Bosch smoke increases sharply when boost pressure drops below 60 kPa. The excess air is therefore not sufficient to sustain complete combustion when the air/fuel ratio drops below the critical value of less than 20 to 1. It seems that the air/fuel ratios in the 300 Nm case (the lowest boost pressure and highest boost temperature) are lower than in the 400 Nm case, as Bosch smoke levels are higher in this case. The only other parameter that has an influence on soot formation is mixing rate, which should not be different between the two cases as engine speed and boost pressure are the same, and swirl, squish and turbulence are more or less the same. The fuel consumption at the 300 Nm test case shows the same trend as Bosch smoke and therefore proves that air/fuel ratios are abnormal in the case where smoke is high. This condition can be regarded as an over-fuelled situation. The

Bosch smoke three-dimensional plots and the fuel consumption [k/g] of the 300 Nm test are shown in appendix A.

Figure 41: Bosch smoke plotted against boost pressure and temperature for the 400 Nm test (1500revs/min, 100% load).

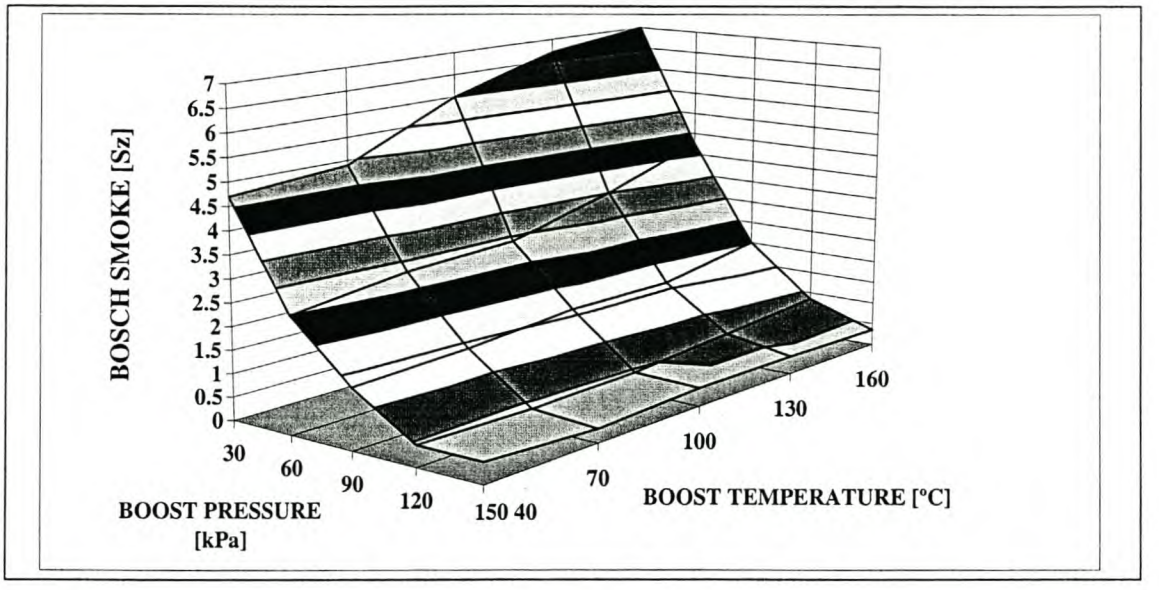

The 400 Nm data shows the same tendency as Bosch smoke where at higher air fuel ratios the efficiency gain is small (the gradient of the plot decreases at the higher boost pressure and lower intake charge temperature), but when the air/fuel ratios become more critical the efficiency loss is more pronounced (the gradient of the plot increases at the lower values of torque output). At these conditions more and more of the fuel leaves the engine unburned or in the form of soot and is not converted into shaft work.

13.2.5 Torque delivered by the engine

The gain in efficiency is more dramatic in these tests as the engine was operating at constant compression ratio. In reality the compression ratio should be adjusted when the boost pressure of an engine is increased. This results in the peak combustion pressure of 129 Bar in the most efficient case where the engine delivered 400 Nm torque and 72 Bar in the least efficient case at 284 Nm torque. This results in an Indicated Mean Effective Pressure (IMEP) of respectively 14.5 Bar and 11 Bar for the best and worst cases for the same fuel delivery. If it were possible to alter the compression ratio in order to equalise

the maximum pressure in the worst case and the best case, the IMEP would have been slightly more for the lower boost pressure cases if one refers to the indicator diagram, with a resulting higher respective Brake Mean Effective Pressure (BMEP) or torque delivery. Therefore data is more optimistic than for two turbo-charged engines operating at the two different conditions, but is still gives a good indication of what effect boost pressure and temperature have on engine torque output.

Figure 42: Indicated Mean Effective Pressure vs Torque plotted against boost pressure and temperature for the 400 Nm test (1500revs/min, 100% load).

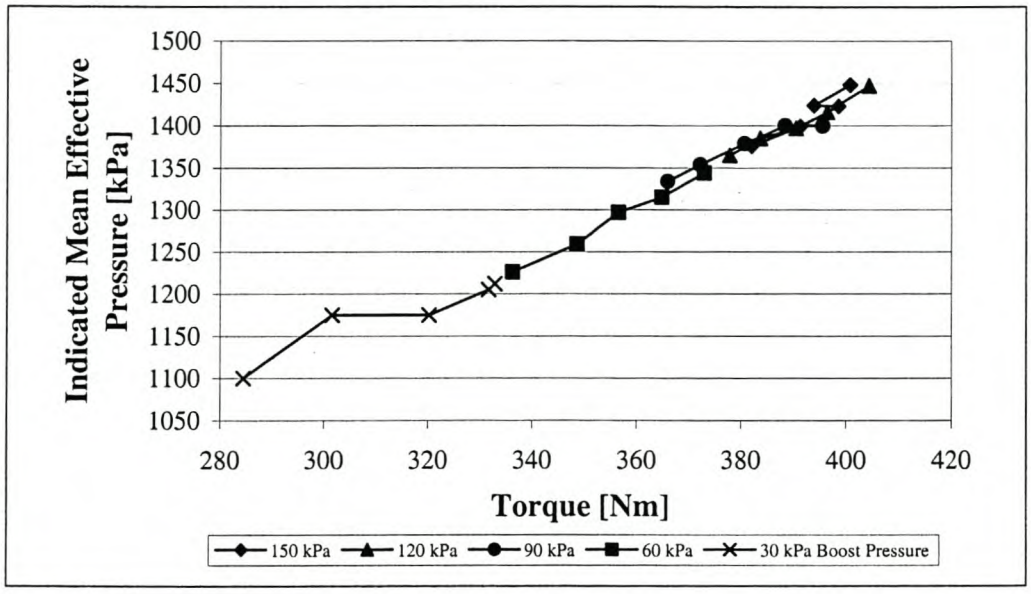

The difference in torque delivered for the 200 Nm case for the variation in boost pressure and temperature is what is expected for a high air/fuel ratio situation. The gain in efficiency is noticeable, but not as pronounced as in the 400 Nm case, as the difference in air/fuel ratio does not result in big changes in torque output. The torque three-dimensional plots on the 200 Nm data will be shown in appendix A. In the 300 Nm test case, torque was held constant.

Figure 43: Torque output with varying boost temperature and pressure for the 400 Nm test (1500revs/min, 100% load).

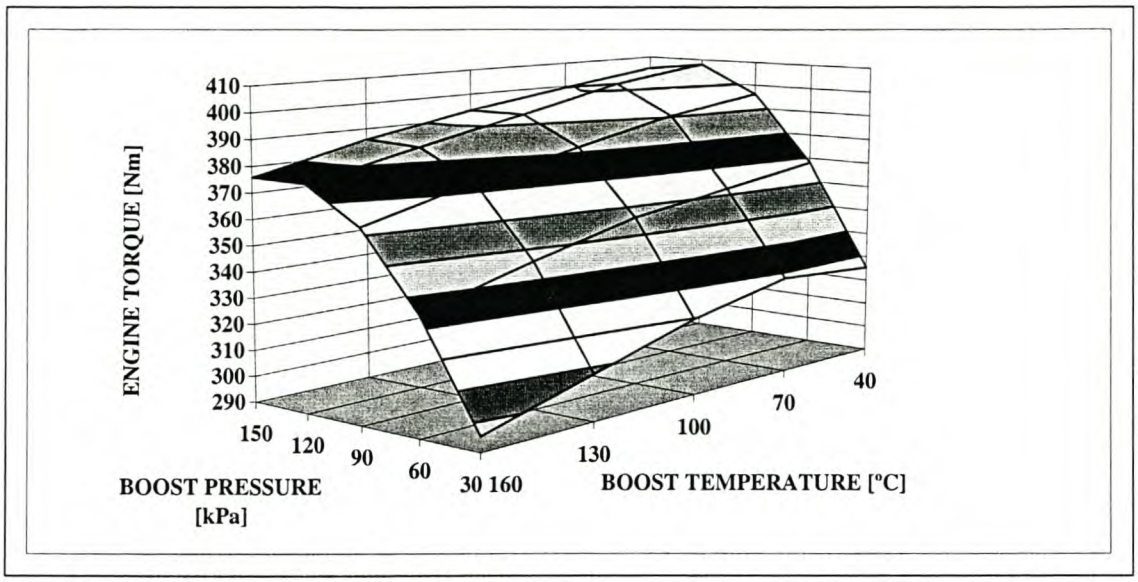

13.2.6 Heat Rejection to the Cooling System

Heat rejection to the cooling system is the amount of heat transferred from the combustion chamber directly to the water jackets in the cylinder head and around the cylinder liners. It is also the amount of heat transferred indirectly from the combustion chamber, through the piston to the lubricant oil, and exchanged to the cooling system in the oil cooler. Therefore almost all heat transferred from the combustion chamber is dissipated through the cooling system, except for the amount of heat that is transferred through the engine material and lost to the atmosphere through convection and radiation. This amount of heat is small compared to heat loss to the cooling system, and is therefore negligible. Therefore it is assumed that the heat rejected to the cooling system is a good indication of combustion gas and combustion chamber temperature. Coolant temperature in the water jackets does not vary much as the temperature of the coolant leaving the engine is controlled with the thermostat. Because heat transfer is governed by temperature differences, the heat rejection increases as component temperature, and the subsequent combustion gas temperature, increases. Heat transfer from the hot gases produces temperature gradients in the combustion chamber components which lead to thermal stresses. Therefore the higher the combustion gas temperature the higher the rate

of heat transfer, that results in higher component stress and temperature. Thermal stress normally results in fatigue failures, depending on the magnitude of the stress levels. Higher component temperature increases the mechanical wear rate of the components, especially the liner and rings.

By using heat rejection as a measure of thermal stress and component temperature (which were not measured during these tests), the assumption is made that the magnitude of heat rejection is a good indication of the life expectancy of the engine.

There is a dramatic decrease in heat rejection to the cooling system as boost pressure increases and intake air temperature decreases. The reason for this is twofold:

- With a reduction in intake air temperature, the temperature of the combustion chamber content at the start of the compression stroke is lower, therefore the gas temperature is lower as the start of combustion and subsequently the combustion gas temperature is also lower. With lower mean combustion gas temperature the heat transfer to the combustion chamber walls is lower and results in lower heat rejection to the cooling system.
- With the increase in boost pressure the air mass flow rate increases, as seen at the start of the discussion, which results in an increase in the excess air ratio during combustion. The higher the excess air ratio the greater the mass of air which needs to be heated during combustion and therefore the combustion gas temperature rise is less, due to the specific heat of the air. This mechanism plays a prominent role during the diffusion combustion phase.

It is shown in the 400 Nm test that the heat rejection varied from 25 kW to 37.2 kW at a constant fuel delivery. Therefore the energy that is not dissipated to the cooling system must have left the engine as exhaust gas energy or converted as shaft power. The exhaust energy increased, but not with the same margin, therefore the increase in power output as boost pressure increases and intake air temperature decreases is due to the decreased heat transfer to the cooling system.

The heat rejection data in the 200 Nm test shows a strong dependency on intake air temperature, but no change as a function of boost pressure. At 50 % load the air/fuel ratio is high and the additional increase in airflow rate does not have a big impact on

excess air ratio. It is therefore only the intake air temperature that causes a change in the heat transfer rate to the combustion chamber walls in low load conditions.

The heat rejection data in the 300 Nm test shows a similar trend as the 400 Nm test, except that the rate of increase in heat rejection as a function of boost pressure is higher for lower boost pressure. The reason for this is that axcess air ratio is lower in the low boost pressure test cases, because the delivery had to be increased to keep the torque constant. On the other hand the axcess air ratio is higher at high boost pressure compared to the same test conditions as in the 400 Nm test case. At the high boost pressure the rate of increase in heat rejection is lower. This proves that in over-fuelled situations, it is not only the combustion efficiency that decreases and results in an increase in the PM pollutant levels, but that the heat rejection increases as well.

Figure 44: Heat Rejection to the Cooling System with varying boost temperature and pressure for the 400 Nm test (1500revs/min, 100% load).

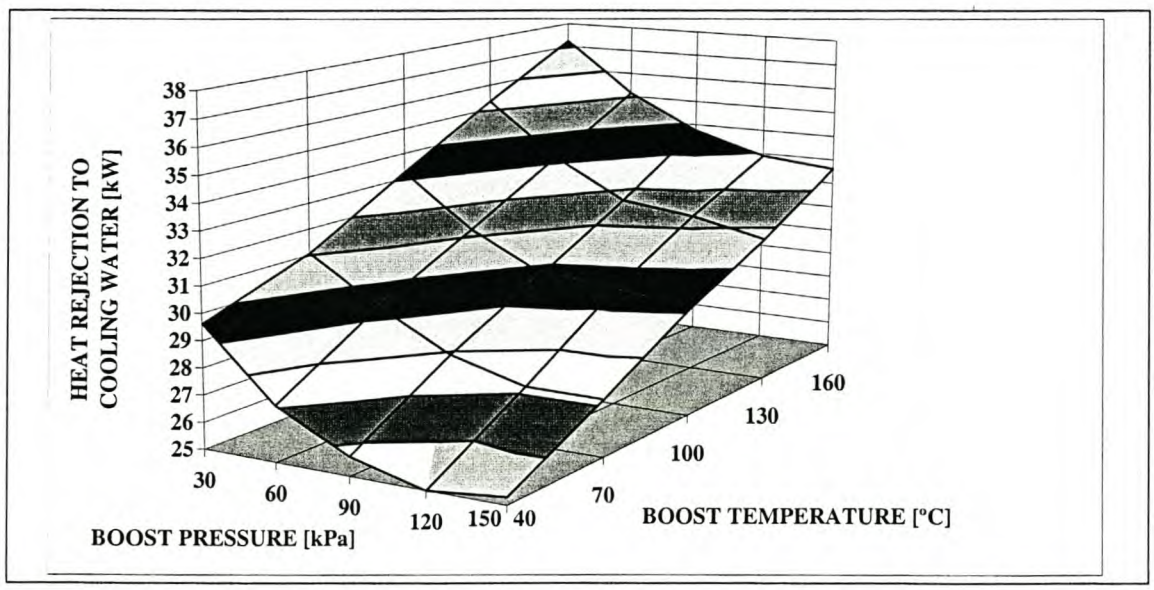

13.2.7 Combustion Chamber Temperature

The average combustion gas temperature data as indicated in Figure 45 confirms that the heat rejection increases in the same proportion as the combustion gas temperature increases, as the air flow rate through the engine decreases (as the result of lower boost pressure). At high boost pressure the combustion gas temperature does not decrease

much as boost pressure decreases; the same phenomenon is seen in the heat rejection data. But at low boost pressure (60 and 30 kPa gauge pressure) the combustion gas temperature increases much with a decrease in boost pressure; the same is seen with heat rejection. There is a strong link between all these parameters and the results can be seen as a chain reaction, because the one parameter influences the other. Higher boost pressure influences air mass flow; the higher air mass flow results in lower combustion temperature which in turn results in reduced heat transfer to the combustion chamber walls.

When the heat rejection data and the average combustion temperature (the average combustion temperature is calculated and is one of the outputs from the heat release analysis, refer to chapter 11.1.7) are compared it is evident that heat rejection is a stronger function of inlet temperature than combustion gas temperature. This is surprising as the one has a direct influence on the other, because heat transfer is governed by temperature differences. The reason for this is not obvious and will be investigated when the statistical analysis is performed.

Figure 45: Average Combustion gas temperature with varying boost temperature and pressure for the 400 Nm test (1500revs/min, 100% load).

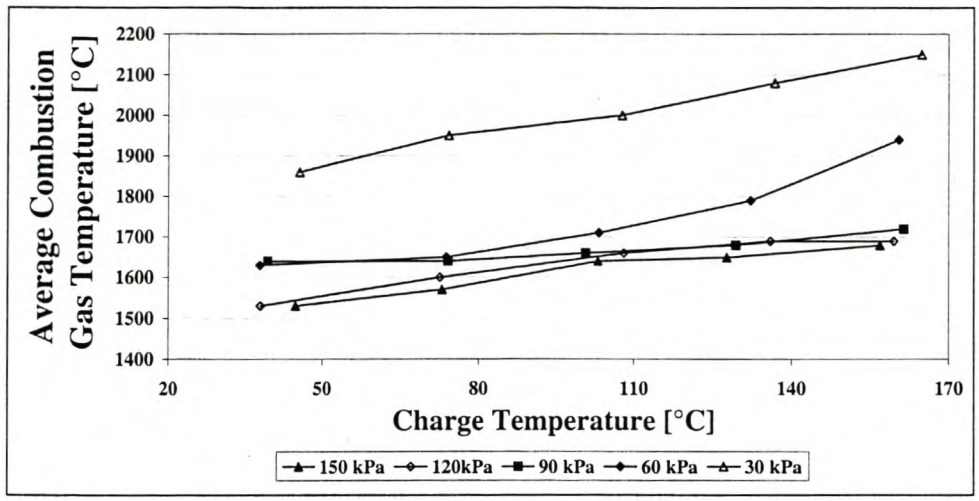

The exhaust gas temperature correlates well with the average combustion gas temperature, as it should (indicating that the combustion model provides accurate results). The results show a higher dependency on boost pressure than on intake air temperature, as in combustion gas temperature and for the same reason (the higher air flow rate results in more excess air).

Figure 46: Exhaust gas temperature with varying boost temperature and pressure (1500revs/min, 100% load).

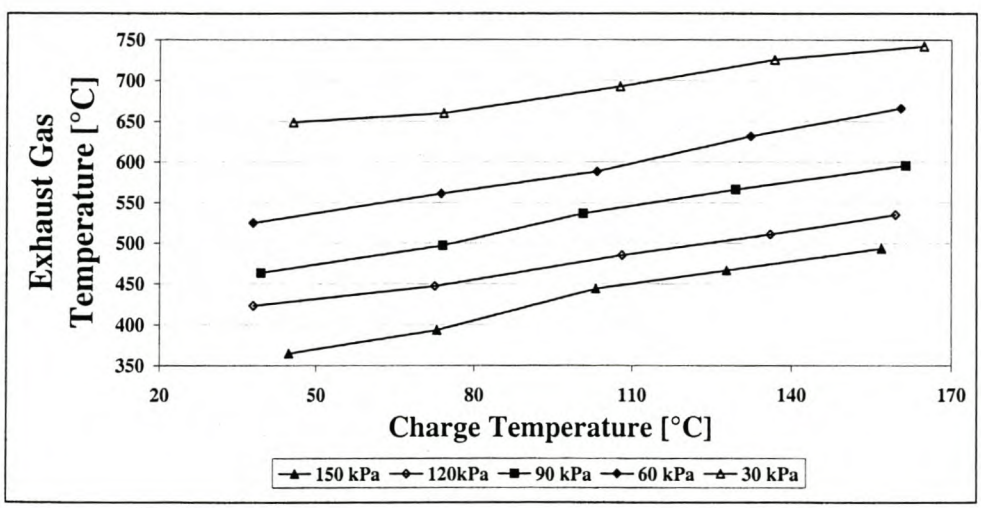

13.2.8 Hydrocarbon Emissions

Two factors influence HC emissions formation:

- The first condition is called overmixing (Heywood, 1984), where the air/fuel equivalence ratio drops below 0.3, and under these conditions, the mixture cannot sustain combustion. Only decomposition reactions occur, resulting in HC fractions to leave the engine unburned.
- The second source of HC emissions results from very rich air/fuel ratios, in the regions of equivalence ratios of 0.7 and higher. These conditions are not likely to occur in the tests that were performed; perhaps at isolated test points.

In the 400 Nm test the HC emissions concentration is very low, but it tends to increase as boost pressure (airflow rate) increases due to overmixing. The concentration is also extremely low at the 30 kPa boost pressure test points. The reason for this is that the high combustion gas temperature assists in the oxidation of the unburned HC fractions that exist in the combustion chamber to the end of diffusion combustion. The specific HC emissions show the same trends as the concentrations, with the maximum value at the 150 kPa boost pressure condition of close to 0.8 g/kWh.

At 50% load (the 200 Nm test) the function of HC concentration as a function of boost pressure and temperature is vastly different to the full load test point. The data, plotted three-dimensionally, can be seen in appendix A. The data shows negligible dependency on intake charge temperature variation, but even though the concentration is low, it is dependent on varying boost pressure. The HC concentration increases as boost pressure increases, as was seen with the 400 Nm data, as the result of over-mixing. But at 30 kPa boost pressure the concentration is higher than in the 60 kPa case, which is the opposite of what occurred in the 400Nm case. The only explanation for this phenomenon is that HC will decrease as boost pressure decreases due to less over-mixing, because the airflow rate decreases as boost pressure decreases. In both the 400 and 200 Nm tests the over-mixing seems not to play a role below 90 kPa boost pressure and the HC concentration levels off as a function of boost pressure. In the 400 Nm test, exhaust temperature at 30 kPa ranges between 650 and 750 °C, therefore the combustion chamber

temperature in the later combustion phase is higher than in the 200 Nm test where the exhaust temperature ranges between 325 and 410 °C. Conditions are more favourable in the 400 Nm case for oxidation of partly decomposed HC compounds to take place later during combustion than in the 200 Nm case, and therefore there is an increase in HC concentration in the lower load test and a decrease in HC concentration in the 100% load case. In the 200 Nm case freezing of the unburned compounds takes place earlier in the late combustion phase as the result of lower gas temperature, which causes higher HC concentration.

The specific HC emissions at 200 Nm show the same decreasing tendency as HC concentration as boost pressure decreases, and the same increase at 30kPa boost pressure. At 30kPa and high charge temperature conditions the Specific HC emissions show an increase, which is the result of higher HC concentration and a drop in power output.

Figure 47: Hydrocarbon emission concentration as a function of boost temperature and pressure for the 400 Nm test (1500revs/min, 100% load).

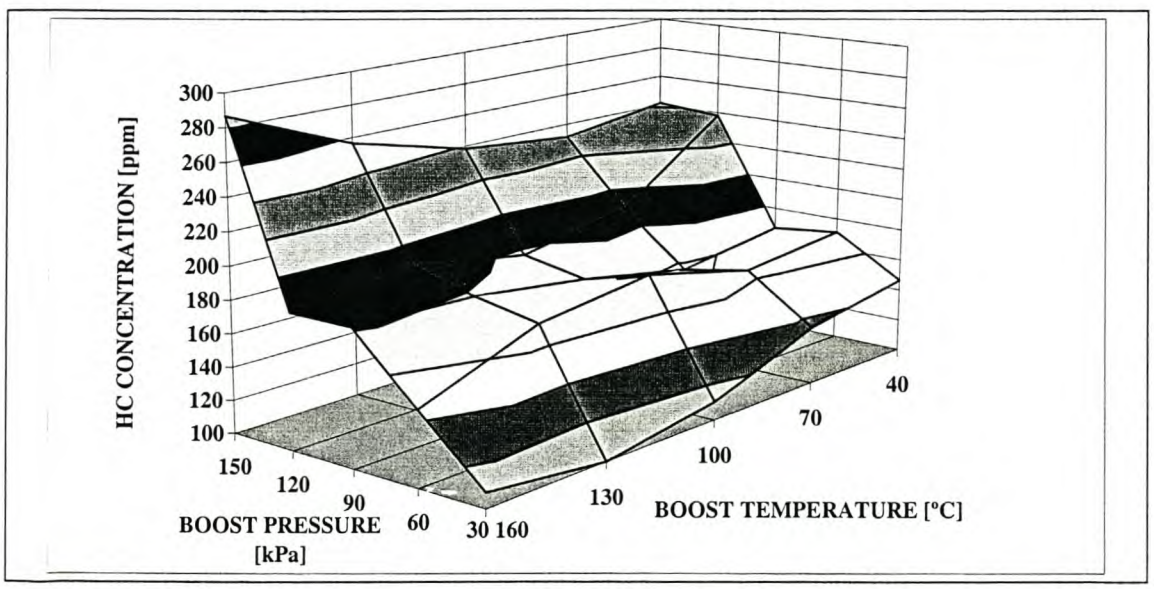

13.2.9 Oxides of Nitrogen Emissions

The gas analyser that was used for measuring the concentration of NO in the exhaust gas has a maximum limit of 2000 ppm, which was not adequate for the concentration that existed in the exhaust gas at some test points during these tests. From the data that is

shown below only half the test points are below the limit. From the limited data available at the 400 Nm data set it is evident that boost temperature plays the dominant role in the formation of NO. The role boost pressure plays is to increase pressure in the combustion chamber during ignition delay, resulting in shorter ignition delay (this will be discussed in detail later in the section). The increased oxygen concentration in the combustible mix does not seem to play a dominant role in NO formation as boost pressure increases and intake charge temperature decreases. It might play a role, but is dominated by the decrease in combustion gas temperature, and from the data recorded in the tests performed it might not be possible to see what effect the increased oxygen concentration has in NO formation. The statistical analysis might shed more light on the matter.

The Specific NO emission is not plotted, because most of the data is off the measuring scale of the analysers and therefore it is not worthwhile to discuss.

The NO emission concentration at the 50% load test point shows the same trend as at the 400 Nm test point, except that the values are lower due to the lower fuel delivery at lower load. The data, plotted three-dimensionally, can be seen in appendix A.

Figure 48: Nitric Oxide emission concentration as a function of boost temperature and pressure for the 400 Nm test (1500revs/min, 100% load).

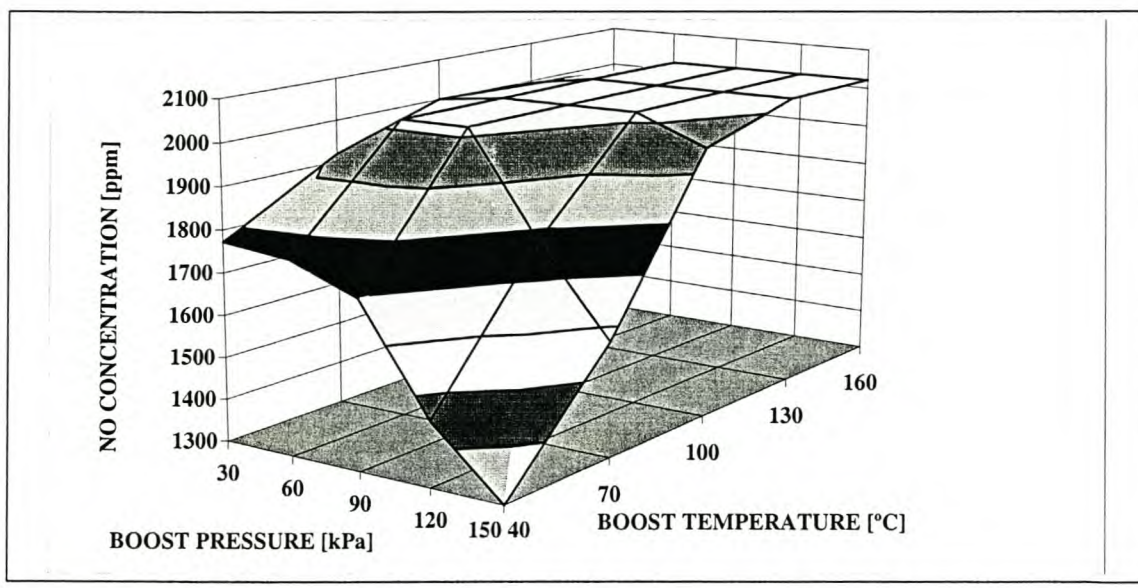

NO formation is dependent on the duration of ignition delay; the longer ignition delay, the higher the NO concentration in the exhaust gas. During ignition delay the fuel is

physically and chemically prepared for combustion. The chemical preparation is dependent on the chemical composition of the fuel that determines the cetane number. As the temperature and pressure increase the decomposition reaction will reach completion faster, to result in shorter chemical delay. The physical preparation, which is dependent on the combustion chamber conditions during ignition delay, will differ from test to test as pressure, temperature and gas dynamics differ depending on the test condition. The higher the boost pressure supplied to the engine the higher the pressure condition during ignition delay and this will result in higher gas temperature due to the compressibility of air. At higher temperature and pressure the rate of evaporation of the fuel increases and the rate of temperature of the combustible mixture increases, therefore the fuel that is prepared for combustion will ignite sooner to result in shorter physical delay. In the test performed all these factors resulted in shorter ignition delay as seen in Figure 49.

It is evident from the data in Figure 49 that boost pressure has a greater influence on ignition delay than intake charge temperature for the reason that was discussed in the previous paragraph. The data below proves the fact that ignition delay will be longer as boost pressure decreases, and will result in higher combustion rate during premixed combustion.

Figure 49: Ignition Delay as a function of Intake air temperature for different boost pressure for the 400 Nm test (1500revs/min, 100% load).

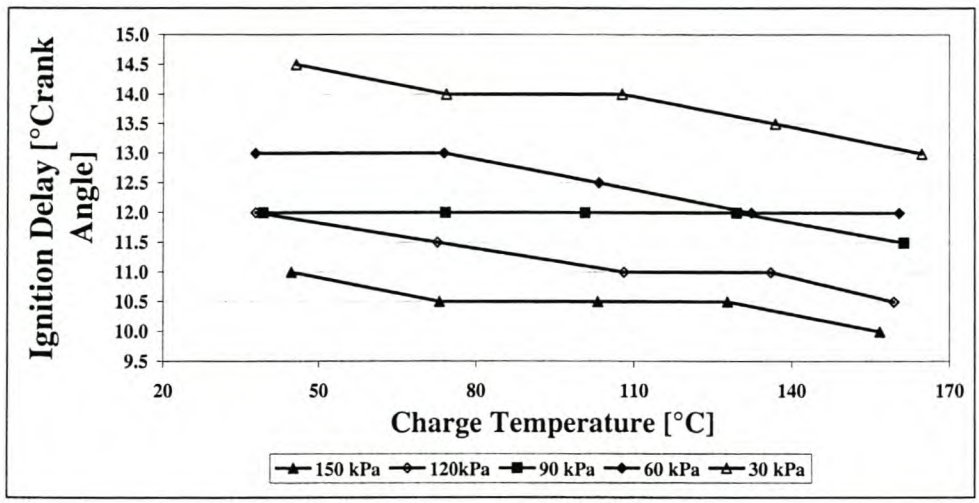

Higher cylinder pressure, as boost pressure increases, reduces ignition delay for the reasons discussed in the previous section. This reduction in ignition delay results in smoother combustion due to less premixed combustion. In the data below it is evident that with an increase in intake charge temperature the ignition delay is further reduced to cause lower cylinder pressure.

On the other hand the NO emission concentration is not significantly dependent on boost pressure. Boost pressure plays the dominant role in the amount of air mass flow through the engine. Therefore, with the increase in boost pressure an increase in excess air ratio is established and it is the excess air ratio that determines bulk combustion gas temperature (the higher the excess air ratio, the lower bulk gas temperature). The combustion model that is used in the processing of this data determines a burned zone gas temperature, but this temperature is not reflecting the maximum temperature that exists in localised regions in the flame or post-flame zone. It is in these localised regions in the post-flame zones that the combustion gas is compressed to very high temperature resulting, in thermal NO formation.

For this reason NO formation is high at high boost pressure and high intake charge temperature, even though the maximum bulk gas temperature and exhaust gas temperature are low due to the high excess air ratio. On the other hand the NO formation can still be moderately low (1800 ppm NO emission concentration) at lower boost

pressure (30 kPa) when the intake charge temperature is kept low (40 °C). The reason for this is that the bulk gas temperature, as combustion starts, is proportional to the temperature of the intake charge (Ideal gas law for the behaviour of an ideal gas at different pressure, temperature and volume) and the localised regions where combustion starts is at the same temperature. This ignition temperature seems to have the dominant effect on NO formation, and because the combustion rate is so high in the premixed flame zone the surrounding gas temperature (combustion chamber bulk gas temperature) does not have an influence on the localised flame zone temperature. This is because there is not enough time for heat transfer or for gas mixing to take place. Therefore, NO formation is dominated by intake air temperature and boost pressure plays a secondary role.

Figure 50: Maximum Cylinder Pressure as a function of Intake air temperature for different boost pressure for the 400 Nm test (1500revs/min, 100% load).

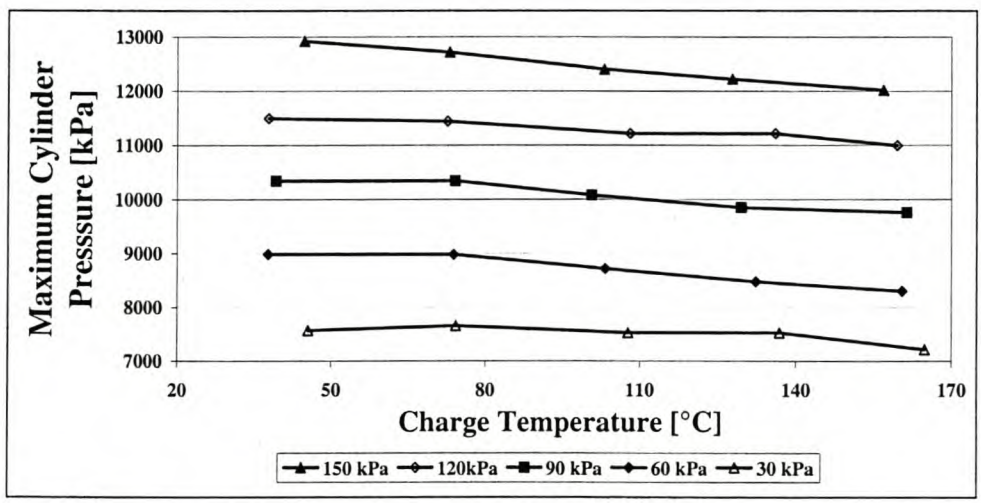

The data below on Rate of Heat release demonstrates the effects of boost temperature on ignition delay and rate of combustion during the premixed and diffusion combustion phases. It is clear from the data that, at constant boost pressure, ignition delay is longer in the cases where intake charge temperature is lower, and this results in more premixed combustion in the 70°C case and less diffusion combustion. At the opposite, the ignition delay is 1° crank angle shorter (160 °C intake air temperature), with reduced premixed combustion and increased diffusion combustion. As the ignition temperature dominates NO formation, even though combustion rate is higher in the 70°C test, the NO

concentration will still be lower in this case than the 160°C case. The shift of combustion from Premixed to Diffusion does not have a noticeable effect on Bosch smoke emissions (Figure 41) as air mass flow rate brought about by boost pressure is the dominant effect in smoke formation.

Figure 51: Rate of Heat Release results for the 400 Nm test (1500revs/min, 100% load) with varying intake charge temperature at 60kPa boost pressure

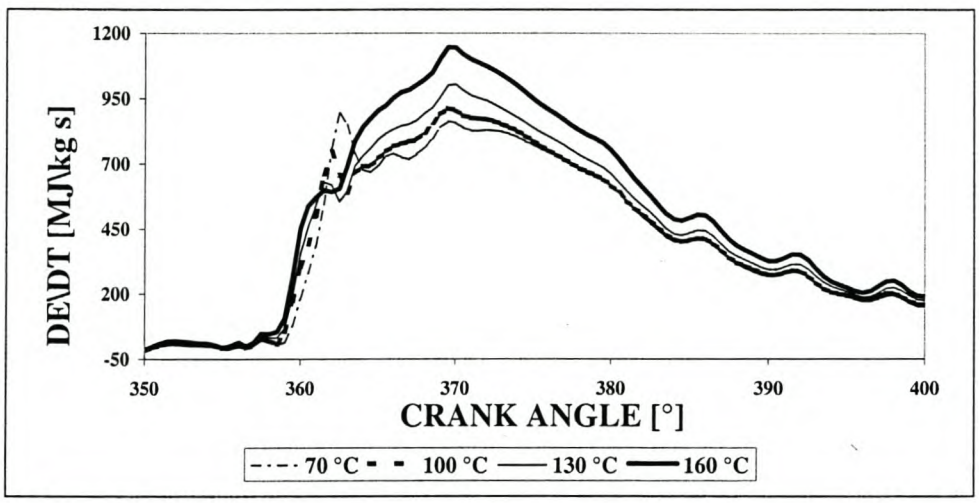

The rate of Heat release data for the different boost pressure settings was taken at the 160°C intake charge condition. The influence of cylinder pressure during ignition delay on the duration of ignition delay is demonstrated here. In the higher boost pressure case the ignition delay is 3.5 degrees crank angle shorter than in the low boost pressure case. The longer ignition delay and resulting higher rate of premixed combustion have an increasing effect on NO formation, while the increase in pressure seems to play an insignificant role.

Figure 52: Rate of Heat Release results with varying intake boost pressure for the 400 Nm test (1500revs/min, 100% load).

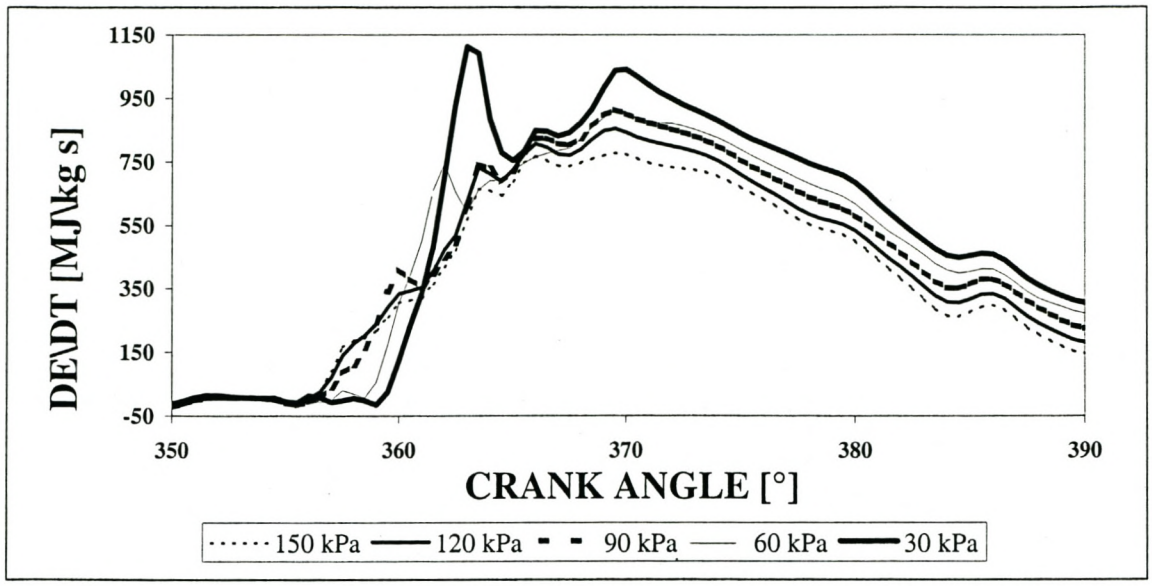

13.3 MULTIPLE LINEAR REGRESSION

The multiple regression models were built from both steady state data and combustion data to predict the formation of exhaust emission pollutant levels and determine statistically which parameters influence the formation significantly. All three data sets (200, 300 and 400 Nm test) were lumped together as one data set consisting of 75 points to construct the mathematical models.

The regression analysis package in Microsoft Excel was used for the statistical analysis and the evaluation procedure as described in chapter 11.4 were followed to ensure the significance of the regression analysis.

13.3.1 Nitric Oxide emissions

In building the model on NO emission all the parameters that were measured during the engine evaluation in the steady state and high speed data were tested in regression models to obtain the best set of independent or regressor variables to achieve a good model. The variables used after the initial evaluation were:

- Fuel mass flow
- Boost pressure
- Intake charge temperature
- Exhaust gas temperature
- Maximum Cylinder Pressure

The model was further refined and it was decided to leave maximum cylinder pressure out of the model as cylinder pressure has strong dependency on boost pressure. The final model that was formulated produced the best-adjusted R squared of 0.97.

$$NO\ [ppm] = -640.09 + 131.71\ (Fuel\ Mass\ Flow\ [kg/h]) - 1.47\ (Boost\ Pressure\ [kPa]) + 3.88\ (Intake\ Charge\ Temperature\ [°C]) + 1.21\ (Exhaust\ Temperature\ [°C])$$

The model shows a strong dependency on fuel consumption or engine load which was discussed in the NO emission section above. The order of magnitude of the fuel mass consumption is one unit lower than boost pressure and intake charge temperature, but the

fuel mass flow variable coefficient is two orders of magnitudes higher than the boost pressure coefficient. This indicates that engine fuel consumed plays a dominant role in the formation of NO emissions. The exhaust temperature influences NO emission concentration more or less in the same degree as boost pressure, while intake charge temperature influences it 2.6 times more than boost pressure.

13.3.2 Bosch Smoke emissions

The same procedure was followed in the smoke emission case as in the NO emission case. The variables used after the initial evaluation were:

- Fuel mass flow
- Boost pressure
- Intake charge temperature
- Exhaust gas temperature
- SFC
- Oxygen concentration in the exhaust gas

In refining the model the decision was made to not use Intake charge temperature as a regressor, because the influence of the variable seemed to be negligible. The final model that was formulated came up with the best-adjusted R squared of 0.965.

Bosch Smoke [Sz]= 37.78 – 0.012 (Engine Torque Output [Nm]) + 0.0288 (Boost Pressure [kPa]) – 1.70 (Oxygen Exhaust Gas Concentration [ppm]) – 0.032 (Exhaust Temperature [°C]) – 7.32 (Specific Fuel Consumption [g/kWh])

The model shows a strong dependency on SFC and O_2 concentration which was evident in the previous section. SFC is a measure of combustion efficiency, and as smoke is reduced the combustion efficiency increases. The more oxygen available in the combustion chamber during combustion the higher the rate of oxidation of soot and SOF during the diffusion combustion phase. The model rates engine boost pressure as a player in the formation of smoke emissions, because boost pressure increases airflow rate and therefore increases the oxygen availability during combustion.

According to the model there is an inverse relationship between exhaust smoke density and torque delivered from the engine. The reason for this is due to the way the experiments were set, the majority of the test case being done at constant fuelling and with the engine torque varying with changing boost pressure and temperature as seen on Figure 38. The increase in boost pressure results in an increase thermodynamic cycle efficiency to increase engine torque. This phenomenon will not be seen in a standard engine set-up, where boost pressure is dependent on turbo-charger operation.

13.3.3 Heat rejection to the cooling System

The variables that were used to establish an accurate model for the Heat transfer rate to the cooling system were:

- Boost pressure
- Intake charge temperature
- Exhaust gas temperature
- SFC
- Torque
- Bosch Smoke
- Oxygen concentration in the exhaust gas

In refining the model the decision was made to use Boost pressure, intake charge temperature, Bosch smoke and engine Torque delivered as regressor variables. The significance of the other parameters was not adequate and therefore excluded from the model. SFC is a strongly dependent on airflow rate through the engine, that are governed by boost pressure and a good correlation between SFC and smoke concentration were established in the previous section, oxygen concentration is dependent and boost pressure and temperature. Therefore the parameters excluded from the model had a secondary significance. The final model that was formulated came up with the best-adjusted R squared of 0.971.

Heat Rejection [kW]= 5.951 + 0.0357 (Engine Torque Output [Nm]) + 0.00964 (Exhaust temperature [°C]) – 0.0407 (Intake Charge Temperature [°C]) + 0.2876 (Bosch Smoke [Sz])

The model shows a strong dependency on intake charge temperature and torque output. It was mentioned in the previous section that the intake charge temperature, according to the three-dimensional plots, dominantly contribute to heat rejection to the cooling system. At higher engine torque, heat rejection was less due to the higher excess air rate during combustion, which resulted in lower combustion temperature.

14 CONCLUSIONS

On completion of the engine testing, data processing and data evaluation it is possible to evaluate a number of important conclusions on engine behaviour running under different intake charge and turbo-charger boost pressure conditions. By running the engine at different intake boost pressures and intake charge temperatures a 25-point matrix was formed at three different operating conditions. This enabled the researcher to form an opinion on how boost pressure and intake charge temperature influence engine power output, fuel consumption, engine durability and exhaust gas emissions. The opinion is proved when, in most cases, the 75 test points were used to build a multiple linear regression model of all the independent variables such as NO emissions concentration, Bosch smoke concentration and heat rejection as a function of all dependent variables. The dependent variables include, for example, boost pressure, intake charge temperature, fuel mass flow and engine torque delivered.

From the data it is evident that boost pressure has a positive influence on most engine parameters, as an increase in boost pressure results in an increase in air mass flow through the engine. An increase in air mass flow reduces combustion chamber gas temperature as the result of an increase in excess air ratio during combustion. Lower combustion gas temperature reduces the heat transfer through the combustion chamber walls to reduce the thermal stress as the result of temperature gradients in these components. Lower heat transfer also reduces material temperature to reduce the wear rate of these components. With a reduction in energy lost through heat transfer to the combustion chamber walls, less heat is dissipated to the water jackets directly to the cooling system and indirectly though lubricant oil to the oil cooler to the cooling system. Therefore more energy is available as shaft energy to increase the thermal efficiency of the engine or as exhaust gas energy of which part can be absorbed by the turbine of the turbo-charger.

A further result of the increase in excess air ratio is that less soot is formed during the first part of combustion and more soot and partly decomposed HC compounds are oxidised during the late combustion phase. Therefore, with an increase in boost pressure

Bosch smoke emissions reduces, but with a change in intake air temperature no difference in smoke concentration is seen except at the very low boost pressure and very high boost temperature test points where low air/fuel ratios exist and the slight increase in air-flow rate as a result of lower air inlet temperature has a big influence.

The HC emission level for the engine is low, but the emission levels showed some variation, as especially boost pressure changed. No noticeable changes as a function of boost temperature is seen, except at the very low boost pressure and very high boost temperature test points for the same reason as with Bosch smoke. At high boost pressure HC concentration is higher due to over-mixing; it reduces as boost pressure decreases, and at full load at lower boost pressure (30 kPa) it decreases further as combustion chamber gas temperature increases as the result of lower excess air ratio at low boost pressure. Therefore three mechanisms work together to determine HC concentration: on the one hand the mixture is not over-lean as in the high boost pressure test points, the mixture becomes richer as the air flow rate decreases with lower boost pressure, but under full load conditions combustion gas temperature is high enough at the low boost pressure test point to allow the partly decomposed HC compound to oxidise. At 50% load the opposite happens at low boost pressure (30 kPa) because combustion chamber gas temperature does not increase at the high rate as in the full load case, as air/fuel ratios are leaner.

At the high boost pressure and low intake charge temperature test point combustion efficiency is higher than in the opposite pressure and temperature intake condition. This is confirmed by Bosch smoke and the heat rejection to the cooling system data. The increased combustion efficiency results in higher engine torque at the high boost pressure and low boost temperature conditions, even though the fuel delivered to the engine was kept constant for the 100% and 50% tests. This results in an SFC increase of 58% from the high boost pressure and low boost temperature to the low boost pressure and high boost temperature conditions for the 50% load condition, and an SFC increase of 44% for the 100% load condition.

NO emission, on the other hand, is more dependent on intake air temperature than on boost pressure, which was proved in the multiple regression modelling performed on the test data. It was found that average burned gas temperature does not play a role in NO

formation, but it does play a role in decomposition of NO, if the gas temperature is high enough to allow these reactions to occur. The temperature that plays the dominant role in NO formation is the flame zone and the post flame zone temperature. As explained in the results discussion on NO formation, intake air temperature plays a role in the ignition mixture temperature and the subsequent flame zone temperature.

A lower intake air temperature condition results in longer ignition delay and increases the rate of combustion. The increased rate of combustion is far less dominant in the formation of NO emissions than intake air temperature, as seen in the results discussion. The combustion chamber pressure increases with an increase in boost pressure, but this results in lower NO emission because of lower combustion chamber temperature, as airflow increases as boost pressure increases.

The results generated from testing done during the project clearly show that intake charge temperature and boost pressure affect the performance parameters of the modern diesel engine. These performance parameters include engine output parameters such as power output and fuel consumption and also exhaust gas emission parameters. When these results were correlated by means of combustion analysis, it was possible to explain the trends in changes as boost pressure and intake temperature were varied. The variation in steady state performance parameters were correlated to changes in parameters like ignition delay, peak combustion pressure and temperature during premixed combustion and duration of combustion.

One of the main outputs from the project is that it will give readers insight into the performance characteristics of a modern diesel engine. This document explains both practical and theoretical aspects of diesel combustion and the main parameters as influenced by boost pressure and temperature. The report gives the basic information for diesel engine upgrade, as it discusses durability (thermal and pressure aspects) and combustion behaviour.

15 REFERENCES

1. Assanis D., Wiese K., Schwarz E., Bryzik W. "The Effect of Ceramic Coating on Diesel Engine Performance and Exhaust Emissions" University of Illinois and U.S. Army Tank Command. SAE 910460.
2. Aufinger H.P., Cichocki R. "Challenges To Meet Heavy Duty Diesel Engine Euro II And US 1998 Emission Regulations" AVL List GmbH (Austria). SAE 980156.
3. Bazari Z., French B.A. "Performance and Emissions Trade-Offs for a HSDI Diesel Engine - An Optimisation Study" Lloyd's Register and Ford Motor Co. SAE 930592.
4. Bell A.J. "Unpublished Thesis." Department of Mechanical Engineering, University of Stellenbosch, Stellenbosch, RSA, 2001.
5. Benson R.S., Whitehouse N.D. "Internal Combustion Engines" Pergamon Press, Oxford, U.K., 1983.
6. Berenson M.L., Levine D.M. "Basic Business Statistics" Fourth edition, Prentice-Hall International Editions, 1889.
7. Blech J.J. "Heat Transfer and Stress Analysis of Engine Heads and the Evaluation of Methods of Preventing Heat Cracks" SAE 820504.
8. Bower G.R., Foster D.E. "The Effect of Split Injection on Soot and NO_X Production in an Engine-Fed Combustion Chamber" SAE 932655.
9. Callahan T.J., Yost D.M., Ryan T.W. "Acquisition and Interpretation of Diesel Engine Heat Release Data" SAE 852068.
10. "Code of Federal Regulations" National Archive and Record Administration, 1997.
11. Corcione F.E., Prati M.V., Vagileco B.M., Valentino G. "Improvement of Combustion System of a Small DI Diesel Engine for Low Exhaust Emissions" SAE 910481, 1991.
12. Corcione F.E., Vagileco B.M., Valentino G. "In-Cylinder Fluid Motion and Emissions of a Conventional and Re-entrant Diesel Combustion System" SAE 911842.
13. Daimler Benz Engine reference book (300 and 400 Series).
14. Dieselnet, http://www.Dieselnet.com/Standards, 2001.

15. Draper N., Smith H. "Applied Regression Analysis-Second Edition" John Wiley and Sons, 1981.
16. Durnholz M., Eifler G., Endres H. "Exhaust-Gas Recirculation - A Measure to Reduce Exhaust Emissions of DI Diesel Engines" SAE 920725.
17. Edwards J.D. "Combustion: The Formation and Emissions of Trace Species" Ann Arbor Science Publishers Inc., Michigan, USA, 1977.
18. Endo S., Nakagawa H., Fujii T., Sato A. "State-of-the-Art: Hino High Boosted Diesel Engine" SAE 931867.
19. Engler B.H., Leyrer J., Lox E.S., Ostgathe K. "Catalytic Reduction of NOx with Hydrocarbons Under Lean Diesel Exhaust Gas Conditions" SAE 930735.
20. Ferguson C.R. "Internal combustion engines: Applied Thermo sciences", John Willey & Sons, Singapore, 1986.
21. Forti, L. "The Particulate Number: A Diesel Engine Test Method to Characterize a Fuel's Tendency to Form Particulates" SAE 942021.
22. Greeves G., Tullis S. "Contribution of EUI-200 and Quiescent Combustion System Toward US94 Emissions" SAE 930274.
23. Hansen A.C., De la Harpe E.R., Lyne P.W.L. "Development of Emissions Indices for SASOL Diesel Fuels with the Aid of Combustion Modelling" SASOL OIL (Research and development), 1994.
24. Hansen A.C. "A Diagnostic Quasi-Dimensional Model of Heat Transfer and Combustion in Compression Ignition Engines" Department of Agricultural Engineering, University of Natal, Pietermaritzburg, RSA, 1989.
25. Hardenberg H.O., Hase F.W. "An Empirical Formula for Computing the Pressure Rise Delay of a Fuel from its Cetane Number and from the Relevant Parameters of Direct Injection Diesel Engines" SAE 790493.
26. Herzog P.L., Burgler L., Winklhofer E., Zelenka P., Cartellieri W. "NO_X Reduction Strategies For DI Diesel Engines" AVL List GmbH., SAE 920470.
27. Heywood J.B. "Internal Combustion Engine Fundamentals" McGraw-Hill Publishers, New York, 1984.
28. Hines W.W., Montgomery D.C. "Probability and Statistics in the Engineering and Management Science" Second Edition, John Wiley and Sons, 1980.

29. Kawatani T, et al. "Technology for Meeting the 1994 USA Exhaust Emissions Regulations on Heavy-Duty Diesel Engines" SAE 932654.
30. Konno M., Chikahisa T., Murayama T., Iwamoto M. "Catalytic Reduction of NO_X in Actual Diesel Engine Exhaust" SAE 920091.
31. Konno M., Chikahisa T., Murayama T. "An Investigation on the Simultaneous Reduction of Particulate and NO_X By Controlling Both the Turbulence and the Mixture Formation in DI Diesel Engines" SAE 932797.
32. Konno M., Chikahisa T., Murayama T. "Reduction of Smoke and NO_X by Strong Turbulence Generation During the Combustion Process in D.I. Diesel Engines" SAE 920467.
33. Lilly L.R.C. 'Diesel Engine Reference Book" Butterworths, London, 1984.
34. Martin B., Aakko P., Beckman D., Del Giacomo N., Giavazzi F. "Influence on the future fuel Formulation on Diesel Engine Emissions – A Joint European Study" SAE 972966.
35. Meyer R.C., and Shahed S.M. "An Intake Charge Cooling System For Application to Diesel, Gasoline and Natural Gas Engine" Southwest Research Institute, SAE 910420.
36. Mikulic L., Kuhn M., Schommers J., Willig E. "Exhaust-Emissions Optimization of Di-Diesel Passenger Car Engine with High-Pressure Fuel Injection and EGR" Mercedes-Benz AG, SAE 931035.
37. Motagne X., Philippet A. "Oxidation Exhaust Catalyst of Diesel Engines and Diesel Fuel Sulphur Content" The Institution of Mechanical Engineers: Combustion Engine Group, London, 1993.
38. Nauss K. "Diesel Exhaust: A Critical Analysis of Emissions, Exposure, and Health Effects" Summary of a Health Effects Institute (HEI) Special Report, HEI Diesel Working Group, 1999.
39. Needham J.R., Bouthenet A. "Competitive Fuel Economy and Low Emissions Achieved Trough Flexible Injection Control" Ricardo Consulting Engineers Ltd, SAE 9931020.
40. Needham J.R., Doyle D.M., and Nicol A.J. "The Low NO_X Truck Engine" Ricardo Consulting Engineers Ltd, SAE 910731.

41. Noburu R.T. "Combustion Characteristics as influenced by Ignition Delay." SAE 930601.
42. Obert E.F. "Internal Combustion Engines and Air Pollution" University of Wisconsin, Harper and Row Publishers, Inc, 1973.
43. Pattas K.N., Stamatelos A.M. "Transient Behaviour of Turbocharged-Engine Vehicles Equipped with Diesel Particulate Traps" SAE 920361.
44. Pilley A.D., Noble A.D., Beaumont A.J., Needham J.R., Porter B.C. "Optimization of Heavy-Duty Diesel Engine Transient Emissions by Advanced Control of a Variable Geometry Turbocharger" SAE 890395.
45. Racine R., Miettaux M., Drutel Y., Heidt J. "Application of a High Flexible Electronic Injection System to a Heavy Duty Diesel Engine" SAE 910184.
46. Ram Reddy P. et al. "Evaluation of Combustion Parameters in Direct Injection Diesel Engines - An Easy and Reliable Method" Indian Institute of Technology, SAE 930605.
47. Rantanen L. et al. "Effect of Fuel on the Regulated, Unregulated and Mutagenic Emissions of DI Diesel Engines" SAE 932686.
48. Rao K.K., Winterbone D.E., Clough E. "Influence of Swirl on High Pressure Injection in Hydra Diesel Engine" SAE 930978.
49. Reynolds E.G. "The Effect of Fuel Processes on Heavy Duty Automotive Diesel Engine Emissions" SAE 952350.
50. Reynolds E.G. "The Effect of Fuel Processes on Heavy Duty Automotive Diesel Engine Emissions" SAE 952350.
51. Robert Bosch GmbH. "Bosch Automotive Handbook", 5th Edition, Bentley Publishers, 1999.
52. Saeed M.N., and Henein N.A. "Ignition Delay Correlations For Neat Ethanol and Ethanol-DF2 Blends in a DI Diesel Engine" SAE 841343, 1983.
53. Shore P.R. "Advances in the use of Tritium as a Radio Tracer for Oil Consumption Measurement" Ricardo Consulting Engineers Ltd, SAE 881583.
54. Shundoh S, et al. "NOx Reduction from Diesel Combustion Using Pilot Injection with High Pressure Fuel Injection" SAE 920461.
55. Siemens Fidamat operational manual

56. Siemens Oxymat operational manual
57. Siemens Ultramat operational manual
58. Taylor A.B. "Combustion Stresses in Compression Ignition Engines" Department of Agricultural Engineering, University of Natal, Pietermaritzburg, 1989.
59. Taylor A.B. "Combustion Quality of Selected Compression Ignition Fuels" Department of Agricultural Engineering, University of Natal, Pietermaritzburg, 1987.
60. Tsurutani K., Kumamoto M., Takei Y., Fujimoto Y., Matsudaira J. "The Effect of Fuel Properties and Oxygenates on Diesel Exhaust Emissions" SAE952349.
61. Uchida N, et al. "Combined Effect of EGR and Supercharging on Diesel Combustion and Emissions" SAE 930601.
62. Ullman T.L., Spreen K.B., Mason R.L. "Effect of Cetane Number, Cetane Improver, Aromatic, and Oxygenates on 1994 Heavy-Duty Diesel Engine Emissions" SAE941020.
63. Uyehara O. "A Method to Estimate Hydrocarbons in Engine Exhaust and Factors that Affect NO_X and Particulate in Diesel Engine Exhaust" SAE 910732.
64. Uyehara O. "Factors that Affect NO_X and Particulate in Diesel Engine Exhaust - Part II" University of Wisconsin, SAE 920695.
65. Virk K.S., Lachowicz D.R. "Testing of Diesel Fuels for their Effects on Exhaust Emissions and Engine Performance" SAE952362
66. Virk K.S., Lachowicz D.R. "Testing of Diesel Fuels for Their Effects on Exhaust Emissions and Engine Performance" SAE 952362.
67. Walsh M. "Global Trend in Diesel Particulate Control, 1993 Update" SAE 930126.
68. Watson N., Janota M.S. "Turbo charging the Internal Combustion Engine" Macmillan Publishers Ltd, 1982.
69. Wonnacott T.H., Wonnacott R.J. "Introductory Statistics for Business and Economics" Third Edition, John Wiley and Sons, 1984.
70. Yan J., Rogalla R., Kramer T. "Diesel Combustion and Transient Optimisation Using Taguchi Methods" SAE 930600.
71. Zelenka P., Kriegler W., Herzog P.L., Cartellieri W.P. "Ways Towards the Clean Heavy-Duty Diesel" SAE 900602.

APPENDIX A

Figure 1: Specific Fuel Consumption at 75 % Load (300 Nm, Constant Torque)

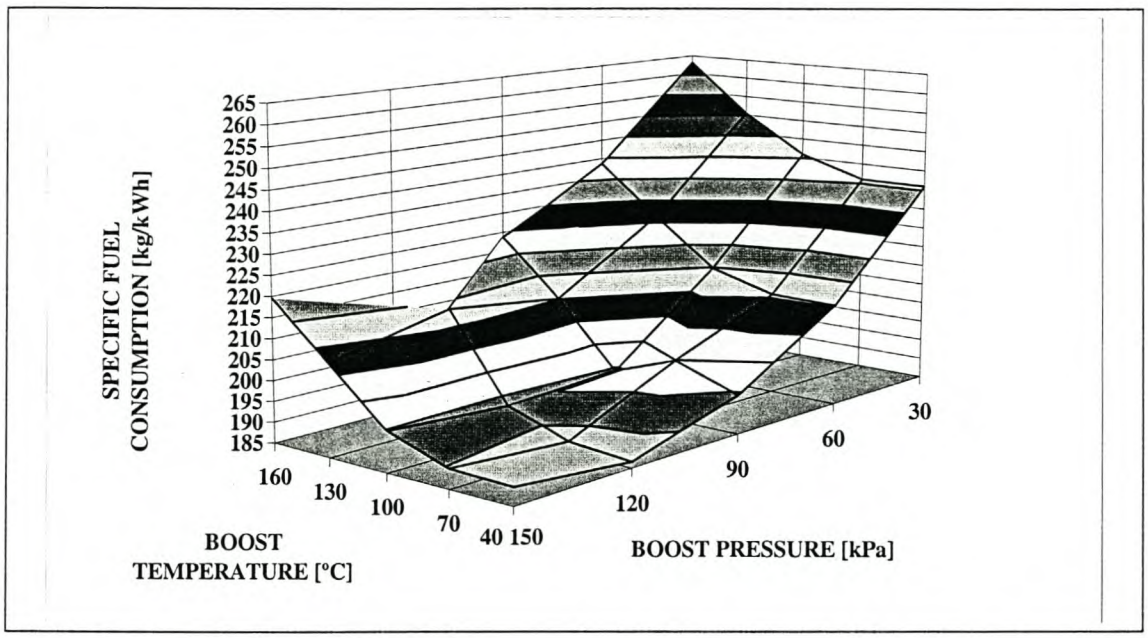

Figure 2: Specific Fuel Consumption at 50 % Load (200 Nm, Constant Fuelling)

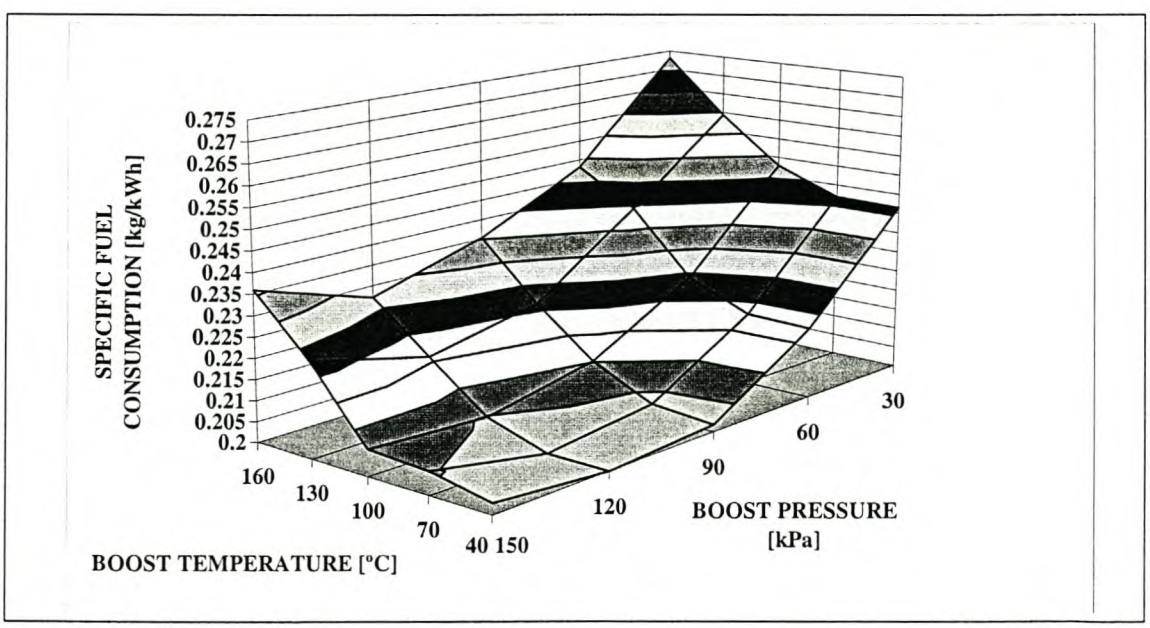

Figure 3: Bosch Smoke at 75 % Load (300 Nm, Constant Torque)

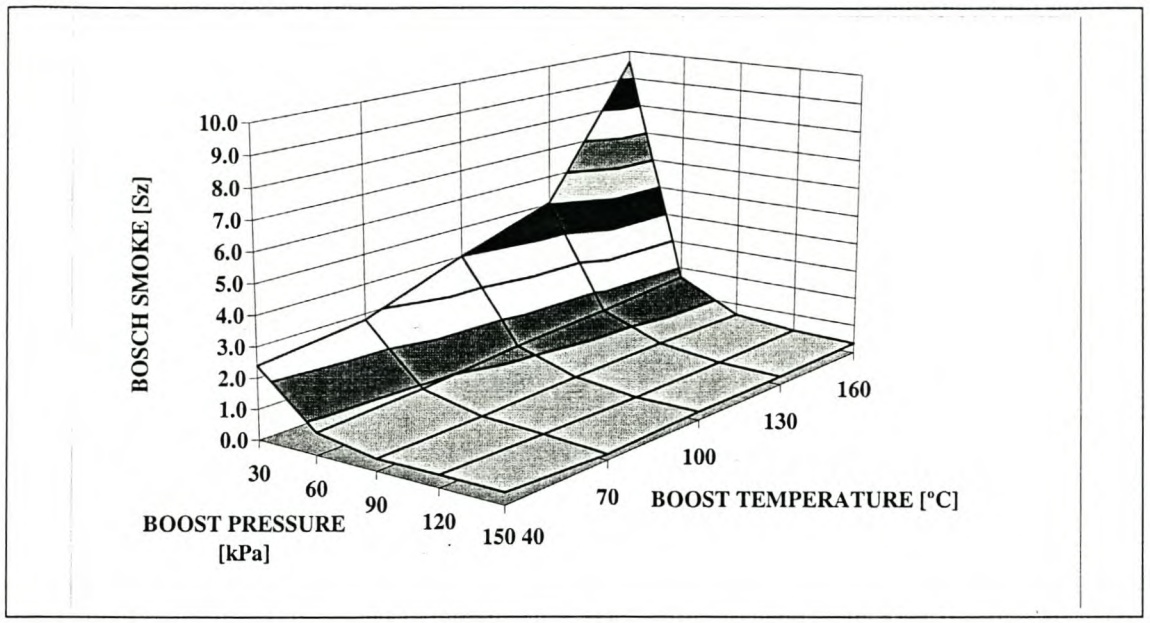

Figure 4: Fuel Mass Consumption at 75 % Load (300 Nm, Constant Torque)

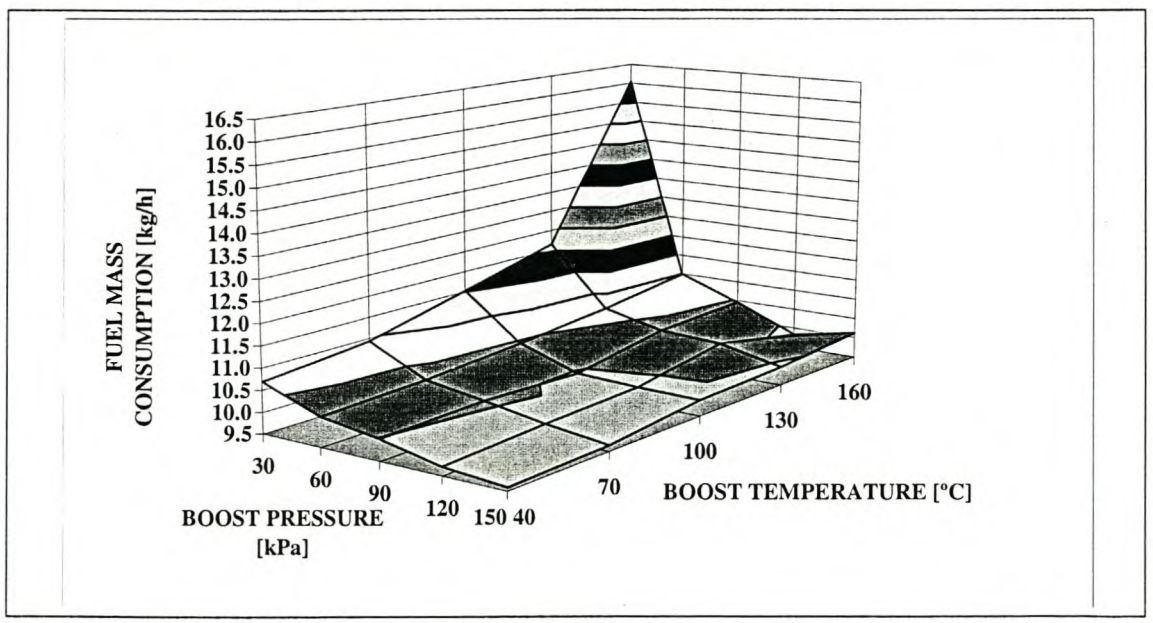

Figure 5: Torque Output at 50 % Load (200 Nm, Constant Fuelling)

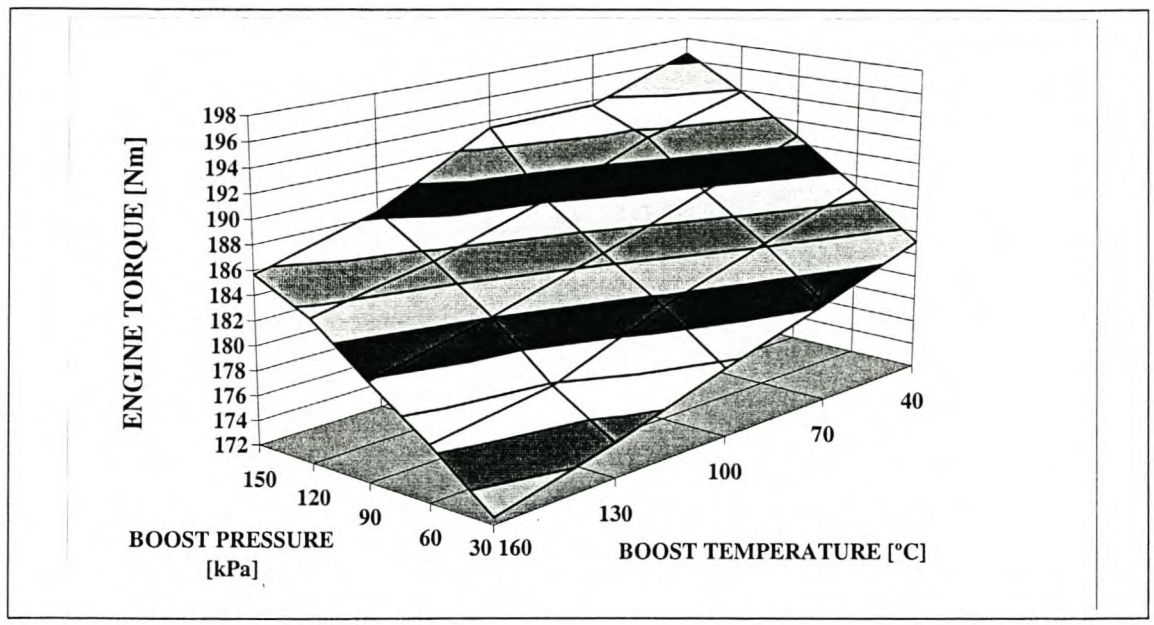

Figure 6: Heat Rejection to the Cooling System at 75 % Load (300 Nm, Constant Torque)

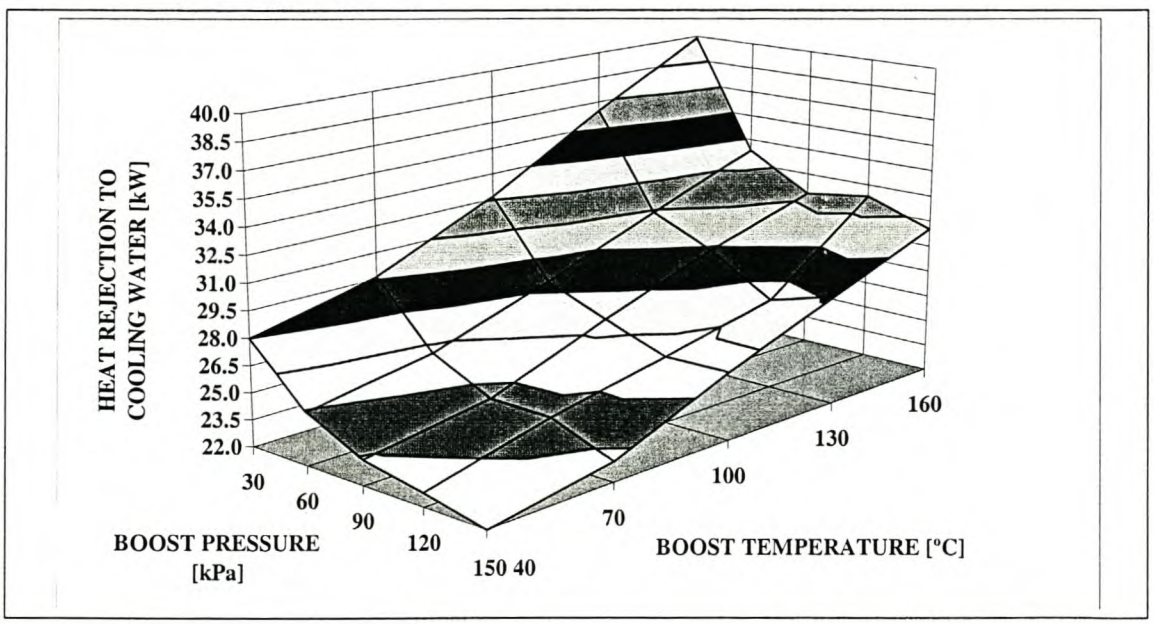

Figure 7: Heat Rejection to the Cooling System at 50 % Load (200 Nm, Constant Fuelling)

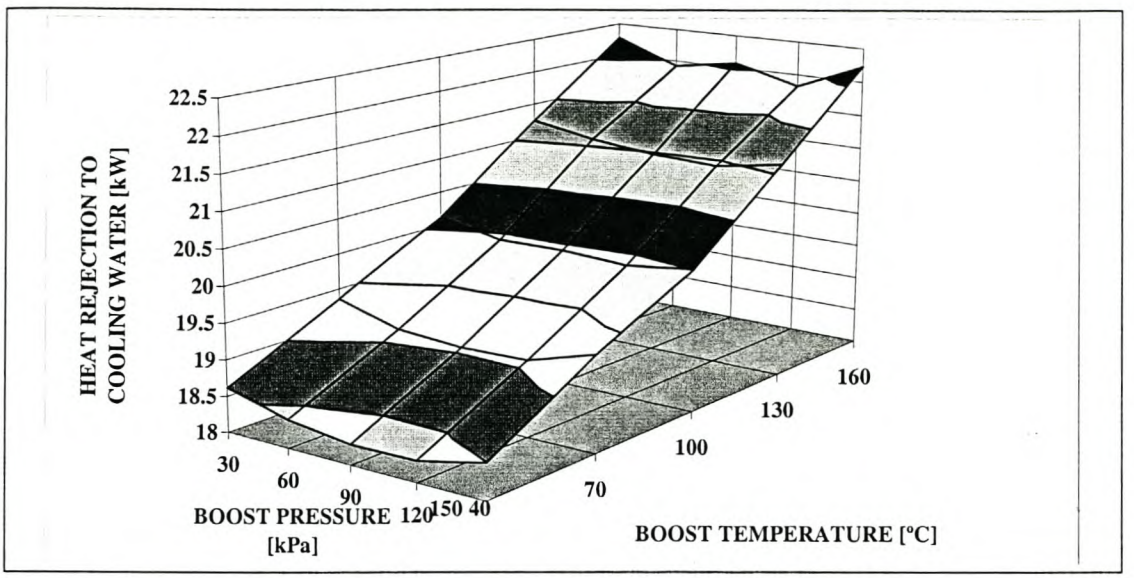

Figure 8: Exhaust Gas Temperature 100 % Load (400 Nm, Constant Fuelling)

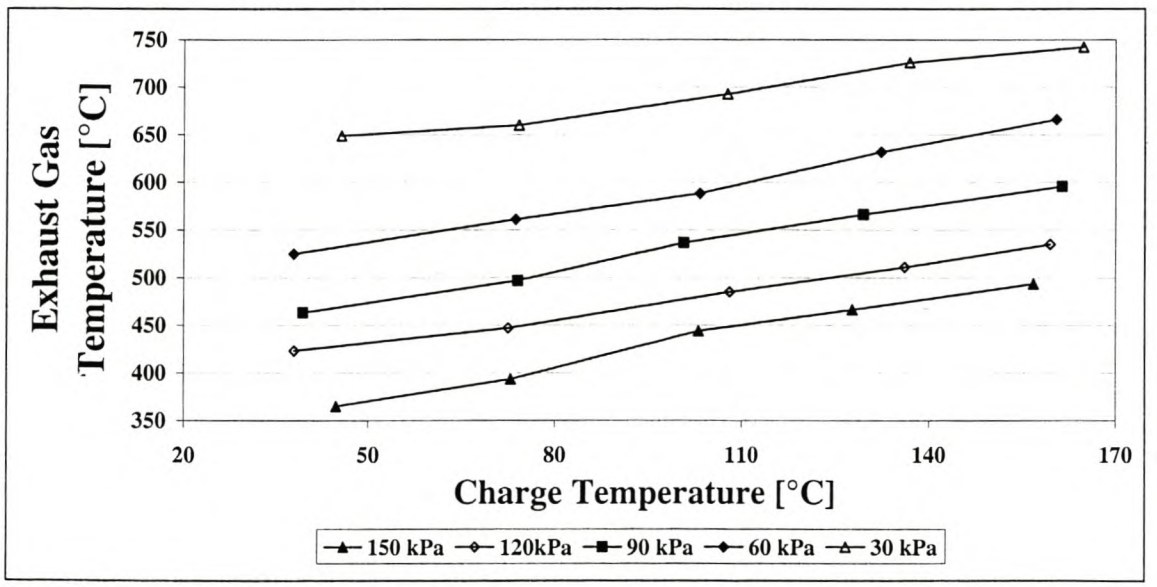

Figure 9: Exhaust Gas Temperature 75 % Load (300 Nm, Constant Torque)

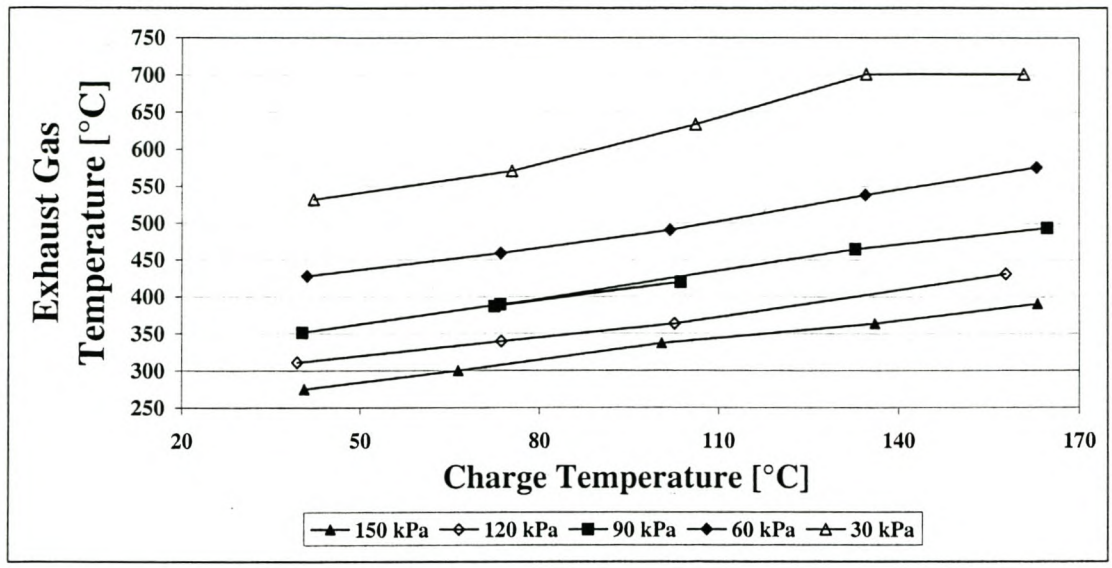

Figure 10: Exhaust Gas Temperature 50 % Load (200 Nm, Constant Fuelling)

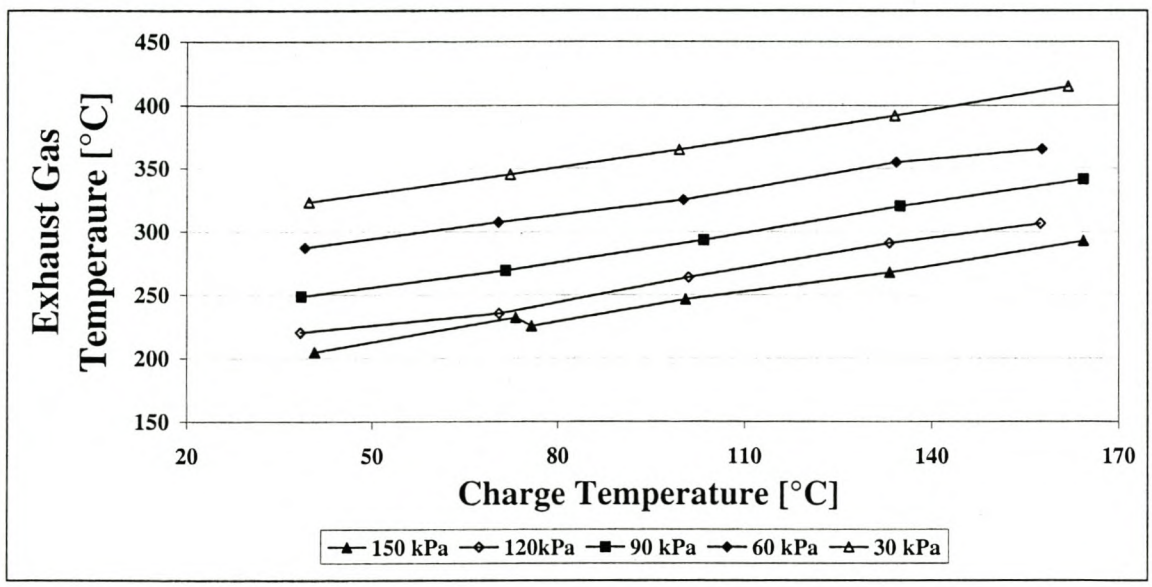

Figure 11: Specific HC emissions at 100 % Load (400 Nm, Constant Fuelling)

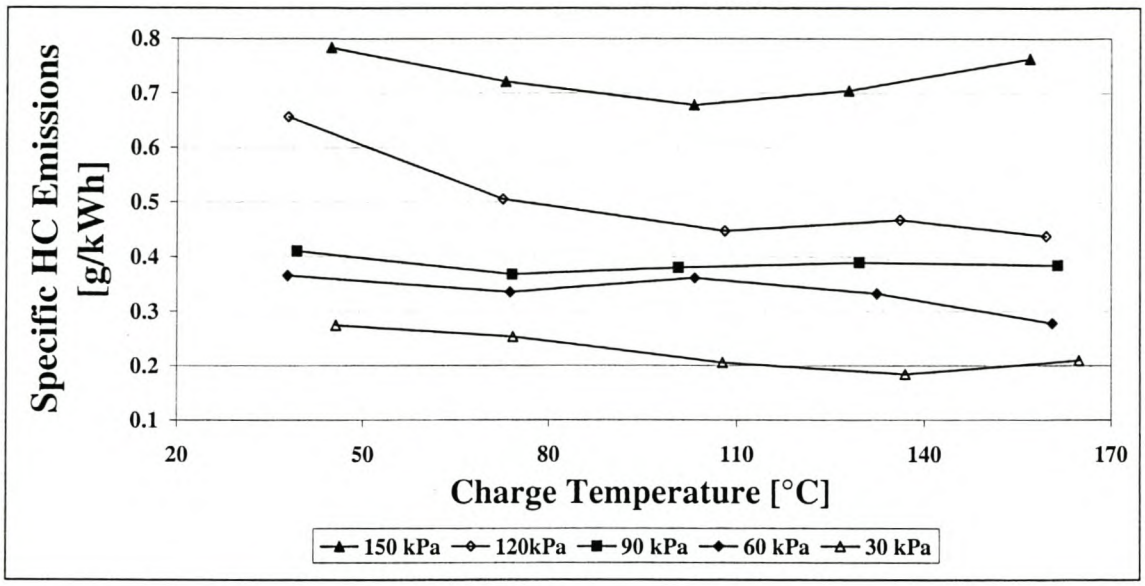

Figure 12: HC emissions concentration at 50 % Load (200 Nm, Constant Fuelling)

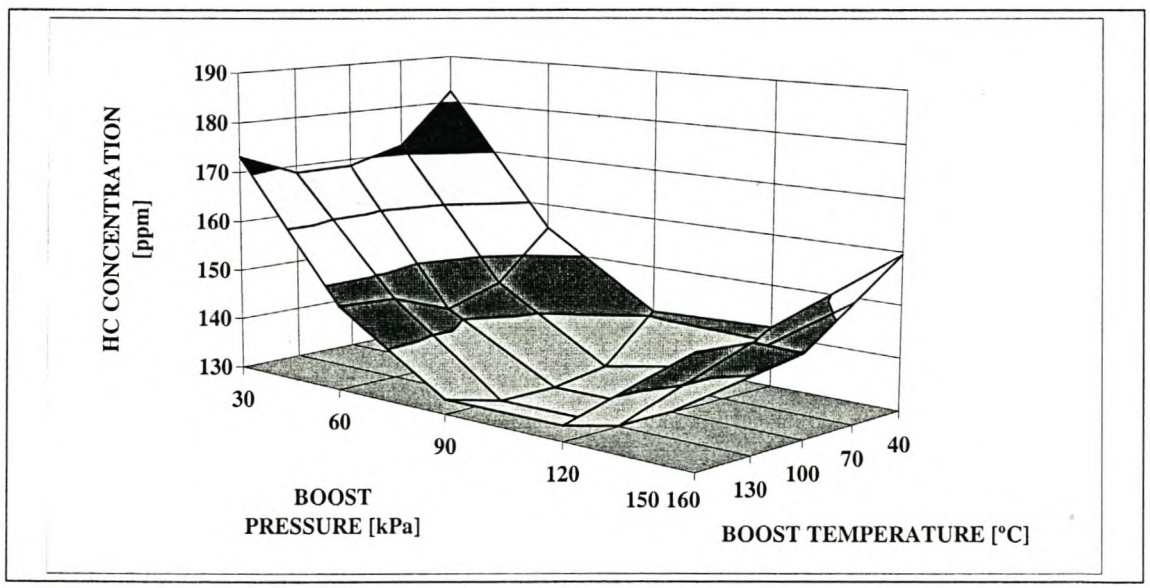

Figure 13: Specific HC emissions at 50 % Load (200 Nm, Constant Fuelling)

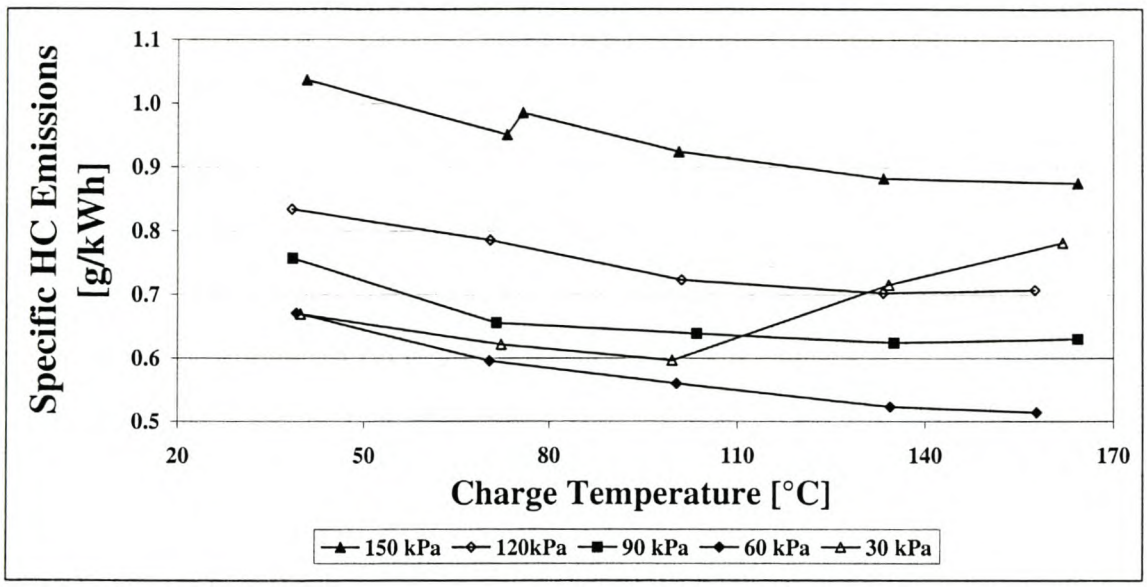

Figure 14: NO emission concentration at 50 % Load (200 Nm, Constant Fuelling)

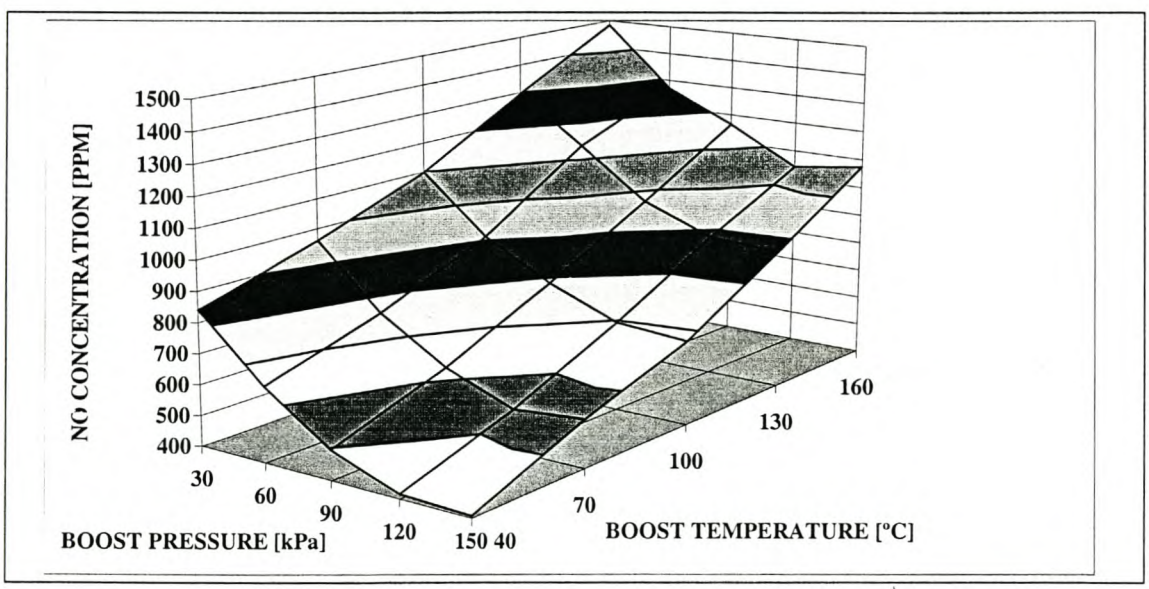

Figure 15: Specific NO emissions at 50 % Load (200 Nm, Constant Fuelling)

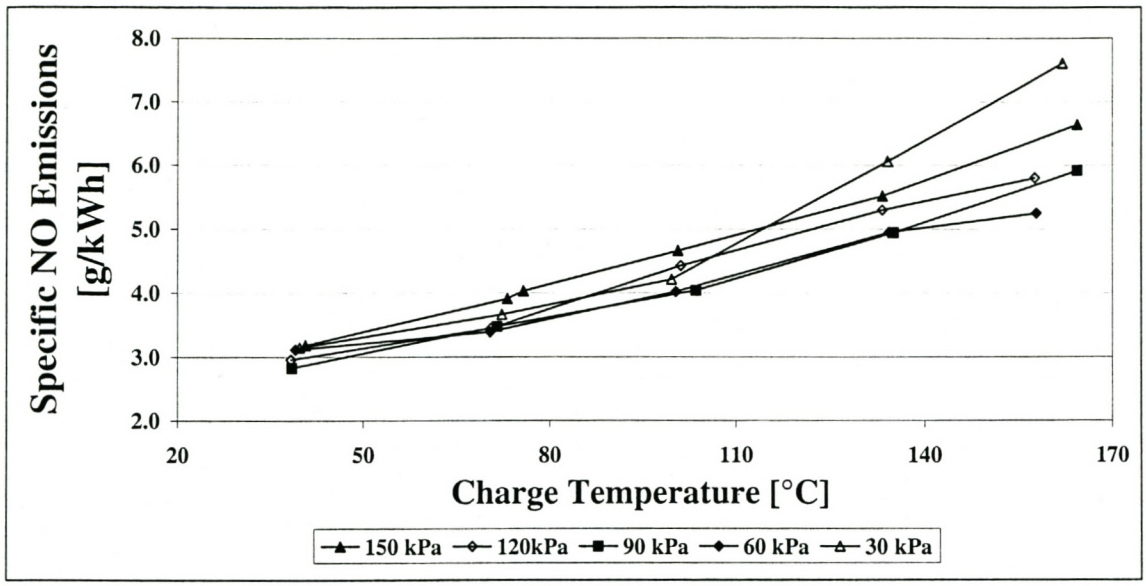

APPENDIX B

CENTRE FOR AUTOMOTIVE ENGINEERING — CAE

ENGINE TEST SHEET :

Standard Engine Test Results

Customer:

TEST BELL : EC 38	DATE 09/11/1995	TEST No.	
OPERATOR : LDE			
ENG TYPE : ADE 364T Disp : 3.97201	ENGINE RATING : 86@2600 Cylinders 4	INJ. PUMP TYPE/SERIAL No. :	GOVERNOR No. : RQV 300 1300MW68-2 (RV3952)
ENG No.: MC010795A075068W	TEST STANDARD : DIN 70020	SPECIAL COMPONENTS : Cylinder pressure transducer and shaft encoder disk	OIL TYPE : BP Vanellus FUEL TYPE : Cal Ref Diesel
TEST ORDER No. :	TEST DESCRIPTION :	FITTED :	SPILL TIMING : 16 °CA BTDC Batch:
ENGINE HOURS - START: Rebuilt (0)	BAROMETRIC PRESS : 757.0 mmHg	COMPRESSOR ■ NO	ETA File : Dyno Zero : After : Cool Orofice 60 15.0
ENGINE HOURS - END: -	FUEL DENSITY : 0.866 @ 20.0 °C	FAN ■ NO	Racer Files : Dyno Span : (403.6) After : (403.6) Bell Mouth 100.0

	Dynamometer			Engine			Fuel System					Lubrication	Cooling System					Air Induction System									Exhaust System										
										Temp			Temperature		Coolant		Temperature				Press	Flow		Emissions						Pressure	Temp					
Point	Speed	Torque	Power	Corr. Factor	Corr. Power	Corr. Torque	Flow	Del.	S.F.C.	Pump Inlet	Dens	Press	Temp.	In	Out	Flow Delta P	Heat Rejec-tion	Cell Temp	Manifold	Cell Wet B	Cell Dry B	Vol Eff	Boost Manifold In	Air/ Fuel	Air Flow	NO	CO_2	CO	HC	O_2		Ex Back Press	Before Turbine	After Turbine	Smoke		
	r/min	Nm	kW		kW	Nm	kg/hr	mm3/st	g/kWh	°C	kg/dm³	kPa	°C	°C	°C	kg/sec	kW	°C	°C	°C	°C		kPa		kg/s	ppm	%Vol	%Vol	ppm	%Vol		mmH2O	°C	°C	Bosch		
12	1498	82.1	12.9	1	13	82	3.6	23.6	282	46.1			97	51.7	79.7	0.06	5.3	31	46.3	29.2	31.2	0.94	6.9	54.28	0.0547	429.0	4.08	0.03	410.85	14.84		10.9	245.8	244.5095	0.4		
13	1498	168.4	26.4	1	26	168	6.1	39.4	229	44.4			102	52.5	81.8	0.08	7.9	32	57.4	29.5	31.5	0.93	18.0	34.08	0.0574	1022.2	6.62	0.02	295.56	11.46		17.1	351.2	354.6035	1.5		
4	1496.723	251.3	39.4	1	39	251	8.6	56.1	219	42.2			108	48.1	82.1	0.09	10.9	34	74.2	31	33.5	0.93	33.3	25.82	0.0619	1518.1	8.89	0.02	239.38	8.44		24.2	473.9	468.8885	1.8		
5	1494.151	318.7	49.9	1	50	319	10.9	71.0	219	42.9			112	54.2	83.6	0.14	13.9	34	89.7	31.8	34.2	0.94	47.2	21.85	0.0661	2031.2	10.60	0.07	199.37	6.14		29.6	561.8	545.3593	3		
14	1498	393.4	61.7	1	62	393	13.6	88.1	220	44.3			116	52.9	83.8	0.18	18.7	34	108.4	31.4	33.7	0.95	65.5	18.87	0.0711	2040.9	12.10	0.16	156.21	4.06		37.0	576.7	623.1475	4.6		
15	1500	453.9	71.3	1	71	454	16.0	104.1	225	45.2			121	55.9	85.2	0.20	20.6	34	131.5	32	34.3	0.96	86.5	17.18	0.0765	2041.4	13.31	0.40	118.13	2.22		44.5	710.2	707.4185	6		
6	1894.145	75.8	15.0	1	15	76	4.6	23.9	309	45.7			102	50.6	80.3	0.07	6.8	33	54.5	31	33.2	0.88	12.8	51.83	0.0668	335.7	4.31	0.01	341.29	14.53		17.0	289.2	277.2833	1.4		
7	1893.794	158.5	31.4	1	31	159	7.6	39.1	242	44.6			107	52.8	81.1	0.11	10.3	34	67.5	31.3	33.5	0.89	25.3	34.15	0.0721	757.5	6.54	0.01	252.32	11.57		23.6	407.7	391.567	1.6		
8	1891.632	237.5	47.1	1	47	238	10.7	54.9	227	45.3			112	50.7	82.2	0.12	13.4	34	83.0	32	34	0.90	40.1	26.18	0.0775	1302.0	8.72	0.00	190.49	8.68		31.2	515.7	488.058	2.2		
9	1889.761	327.8	64.9	1	65	328	14.5	74.5	223	46.8			120	50.4	82.9	0.16	18.1	37	108.0	33	36.5	0.91	63.6	21.25	0.0854	1822.5	10.52	0.05	170.35	6.25		42.8	633.9	594.6208	3.2		
i	1900	331.3	65.9	1	66	331	14.0	71.5	212	49.8			114	52.9	81.7	0.21	20.9	27	94.0	24	27	0.87	62.4	21.95	0.0851	1709.8	10.04	0.05	140.92	6.98		42.5	620.3	456.7257	3.2		
ii	1900	403.8	80.4	1	80	404	17.2	88.1	214	47.7			119	55.5	83.4	0.25	23.5	29	119.0	26	29	0.89	86.4	19.45	0.0929	2042.0	11.32	0.13	119.00	5.21		53.9	708.3	535.6858	4		
10	2282.45	76.1	18.2	1	18	76	5.9	25.2	325	51.2			110	47.5	80.2	0.08	9.1	34	65.5	32	34.2	0.85	21.1	48.67	0.0798	410.1	4.47	0.01	308.12	14.32		24.6	322.5	309.938	1.2		
11	2281.924	166.0	39.7	1	40	166	9.9	42.2	249	49.0			113	53.3	82.1	0.11	10.9	34	87.1	32	34.2	0.87	43.9	33.34	0.0915	787.4	6.74	0.01	194.35	11.30		37.9	447.0	426.016	1.6		
iii	2300	162.5	39.1	1	39	162	9.4	39.8	240	61.6			111	49.3	80.3	0.11	12.0	28	77.4	25.5	27.5	0.83	43.1	34.80	0.0908	755.8	6.44	0.02	148.98	11.91		37.7	447.1	328.601	2		
iv	2304	240.5	58.0	1	58	240	12.7	53.7	219	58.2			117	53.0	81.7	0.16	16.2	28	99.1	26.6	28.2	0.85	65.5	28.58	0.1008	1153.8	7.64	0.02	132.76	13.19		49.9	539.6	398.926	2		
v	2303.59	310.4	74.9	1	75	310	15.9	67.4	213	55.8			122	54.3	82.7	0.21	20.2	30	121.7	27.8	29.8	0.87	88.9	25.04	0.1109	1571.7	8.90	0.03	123.72	8.52		62.6	620.1	459.396	2.5		
vi	2304.775	366.7	88.5	1	89	367	18.9	79.8	213	54.0			127	55.9	83.4	0.25	23.9	31	142.5	29	31	0.88	111.2	22.82	0.1198	1919.7	10.17	0.07	95.70	6.79		75.1	681.6	513.9428	3.8		

REMARKS :

APPROVED BY

SIGNATURE

DATE

CENTRE FOR AUTOMOTIVE ENGINEERING — CAE

Customer:

ENGINE TEST SHEET :

Boost Pressure and Intake Charge Temperature Matrix for the 50% Load Condition

TEST BELL : EC 39 | DATE | TEST No.

OPERATOR : LDE | 13/03/1996

ENG TYPE : ADE 364T Disp : 3.972014	ENGINE RATING : 88@2600 Cylinders 4	INJ. PUMP TYPE/SERIAL No. :	GOVERNOR No. : RQV 300 1300MW68-2 (RV3952)
ENG No.: MC01079SA075068W	TEST STANDARD : DIN 70020	SPECIAL COMPONENTS : Cylinder pressure transducer and shaft encoder disk	OIL TYPE : BP Vanellus FUEL TYPE : Cal Ref Diesel
TEST ORDER No. :	TEST DESCRIPTION :	FITTED :	SPILL TIMING : 16 °CA BTDC Batch:
ENGINE HOURS - START: Rebuilt (0)	BAROMETRIC PRESS : 757.0 mmHg	COMPRESSOR NO	ETA File : Dyno Zero : After : Cool Orofice 50 40.0
ENGINE HOURS - END: -	FUEL DENSITY : 0.856 @ 20.0 °C	FAN NO	Racer Files : Dyno Span : (403.6) After : (403.6) Bell Mouth 100.0

	Dynamometer				Engine		Fuel System					Lubrication	Cooling System					Air Induction System										Exhaust System								
										Temp			Temperature		Coolant	Heat	Temperature					Press		Flow		Emissions					Pressure	Temp	Smoke
Point	Speed	Torque	Power	Corr. Factor	Corr. Power	Corr. Torque	Flow	Del.	S.F.C.	Pump Inlet	Dens	Press	Temp.	In	Out	Flow Delta P	Rejec-tion	Cell Temp	Manifold	Manifold	Delta T I.C.	Cell Wet B	Cell Dry B	Inlet Depress.	Boost I.C. In	Air/ Fuel	Air Flow	NO	CO_2	CO	HC	O_2	Ex Back Press	Out	
	r/min	Nm	kW		kW	Nm	kg/hr	mm3/st	g/kWh	°C	kg/dm³	kPa	°C	°C	°C	kg/sec	kW	°C	°C	°C	°C	°C	°C	mmH2O	kPa		kg/s	ppm	%Vol	ppm	ppm	%Vol	mmH2O	°C	Bosch
1	1554	197	32	1	32	198	6.6	41.4	205	44	0.856		103	27	77	2.4	406.3	19	41			16	23	210	151	58.77	0.108	440	3.11	0.040	157	17.8	76	204.9	3.1
2	1553	200	33	1	33	201	6.8	42.5	208	34	0.856		102	28	78	2.1	358.1	19	73			16	22	160	152	49.62	0.093	575	3.36	0.030	154	17.4	78	232.0	2.25
2a	1551	191	31	1	31	192	6.5	40.7	208	35	0.856		102	29	78	2.1	352.3	20	76			16	21	160	153	51.81	0.093	562	3.19	0.045	151	17.6	75	225.3	2.2
3	1549	187	30	1	31	188	6.5	40.7	212	36	0.856		102	29	78	1.8	304.3	21	101			16	21	115	148	44.41	0.080	674	3.39	0.028	147	17.3	74	246.6	1.35
4	1548	189	31	1	31	190	6.5	41.2	213	38	0.856		104	31	78	1.4	228.3	21	133			16	22	86	153	38.41	0.070	829	3.53	0.038	146	17.0	75	268.0	1.4
5	1547	186	30	1	30	187	6.5	41.2	215	40	0.856		106	33	79	1.1	176.1	23	164			16	22	55	148	33.75	0.061	1034	3.73	0.018	151	16.6	75	292.9	2.5
6	1546	192	31	1	31	194	6.5	40.8	206	44	0.856		101	27	77	2.1	361.6	23	38			16	22	160	118	51.93	0.093	453	3.49	0.035	141	17.2	59	220.4	2
7	1545	190	31	1	31	192	6.5	40.7	208	41	0.856		102	27	78	2.1	370.4	24	70			16	21	135	126	47.21	0.085	530	3.56	0.020	134	17.1	58	235.3	1.2
8	1545	187	30	1	31	189	6.5	40.8	212	41	0.856		103	29	78	2.2	367.5	24	101			16	20	110	120	43.66	0.078	722	3.84	0.028	130	16.6	59	263.8	0.3
9	1553	188	31	1	31	190	6.6	41.2	213	43	0.856		105	31	78	2.1	349.6	25	133			15	20	90.0	120	38.96	0.071	910	4.07	0.025	133	16.2	60	291.0	0.9
10	1551	183	30	1	30	186	6.5	41.0	216	42	0.856		106	32	79	2.0	316.2	26	157			15	20	75	119	34.27	0.062	1013	4.20	0.043	136	15.9	60	306.5	0.15
11	1551	188	31	1	31	191	6.5	40.7	209	44	0.856		102	28	77	1.4	237.3	26	38			16	21	86	88	38.82	0.070	488	4.02	0.028	144	16.4	47	248.9	1
12	1549	187	30	1	31	190	6.5	40.7	210	41	0.856		102	28	78	1.6	267.2	27	71			16	22	55	91	31.66	0.057	625	4.22	0.030	130	16.1	46	269.3	0.65
13	1550	183	30	1	30	186	6.4	40.5	213	41	0.856		103	29	78	1.5	246.9	27	103			16	21.0	50.0	89	30.80	0.055	760	4.46	0.058	132	15.7	46	293.4	0.5
14	1549	182	29	1	30	185	6.5	41.0	217	42	0.856		104	31	79	1.5	240.1	27	135			15	21	72	89	35.61	0.064	961	4.71	0.053	133	15.2	45	320.3	0.35
15	1548	179	29	1	29	182	6.5	41.0	221	41	0.856		106	32	79	1.5	248.4	28	164			15	21	65	90	32.14	0.058	1176	4.93	0.033	138	14.9	46	341.5	0.1
16	1548	190	31	1	31	193	6.6	41.3	209	41	0.856		103	29	78	2.4	410.1	28	39			16	20	210	58	57.94	0.106	650	4.89	0.050	154	15.1	29	287.5	3.45
17	1547	186	30	1	31	190	6.5	41.2	213	39	0.856		103	29	78	2.4	401.9	28	70			15	19	160	60	50.33	0.092	728	5.12	0.045	141	14.8	30	307.4	2.8
18	1549	184	30	1	30	188	6.5	41.1	215	39	0.856		104	30	78	1.8	301.0	28	100			16	20	115	60	42.89	0.078	900	5.38	0.060	138	14.3	30	325.3	1.05
19	1551	179	29	1	30	182	6.5	41.0	221	39	0.856		105	31	78	1.4	235.4	28	134			16	21	85	54	36.79	0.067	1174	5.87	0.058	137	13.6	28	355.0	1.15
20	1550	179	29	1	30	182	6.5	40.9	220	40	0.856		105	32	78	1.2	184.6	29	158			16	21	50	58	30.83	0.056	1261	5.93	0.053	136	13.5	28	365.3	1.65
21	1550	183	30	1	30	186	6.5	40.7	214	43	0.856		102	28	77	2.4	397.3	29	40			16	20	160	29	50.81	0.092	785	5.99	0.055	184	13.5	15	323.5	3
22	1550	178	29	1	30	182	6.5	40.7	219	40	0.856		102	28	77	2.2	364.8	29	72			16	20	135	31	47.71	0.086	938	6.28	0.075	175	13.1	15	345.3	2.7
23	1550	177	29	1	29	180	6.5	40.8	222	40	0.856		103	29	78	2.2	360.2	29	100			16	20	110	31	43.90	0.079	1113	6.57	0.060	174	12.6	15	364.8	1.6
24	1549	174	28	1	29	178	8.2	51.5	284	40	0.856		104	31	78	2.1	343.9	30	134			16	20	95	31	31.18	0.071	1315	6.92	0.063	171	12.0	15	391.8	1.1
25	1547	172	28	1	28	175	9.2	57.6	323	41	0.856		105	32	78	2.0	323.3	30	162			15	19.0	80	31	24.42	0.062	1535	7.29	0.080	174	11.4	14	414.9	0.3

REMARKS :

APPROVED BY :

SIGNATURE :

DATE :

CENTRE FOR AUTOMOTIVE ENGINEERING — CAE

Customer:

ENGINE TEST SHEET : Number 2

Boost Pressure and Intake Charge Temperature Matrix for the 50% Load Condition

TEST BELL : EC 38 | DATE : 13/03/1996 | TEST No. : 3.0

OPERATOR : LDE

ENG TYPE : ADE 364T	Disp : 3.972014	ENGINE RATING : 88@2600	Cylinders 4
ENG No. : MC01079SA075068W		TEST STANDARD : DIN 70020	
TEST ORDER No. :		TEST DESCRIPTION : 0.0	
ENGINE HOURS - START:	ReCuilt (0)	CAROMETRIC PRESS : 767.0	mmHg
ENGINE HOURS - END:	-	FUEL DENSITY : 0.856 @ 20.0 °C	

INJ. PUMP TYPE/SERIAL No. :			
SPECIAL COMPONENTS :	Cylinder pressure transducer and shaft encoder disk		
FITTED :			
COMPRESSOR	NO	ETA File :	
FAN	NO	RaCer Files :	

GOVERNOR No. :	RQV 300 1300MW68-2 (RV3952)		
OIL TYPE :	BP Vanellus	FUEL TYPE :	Cal Ref Diesel
SPILL TIMING :	15 °CA BTDC	Batch:	
Coolant Density :	1020.7 gravity : 9.8	Barometric Pressure :	100.5
Coolant Cp Value:	3.4		

Point	Speed	Torque	BMEP	Power	Fuel Flow	IMEP Gross	PMEP	FMEP	Ignition Delay	Ignition Point	Maximum Pressure	Maximum dP/dTh	Maximum dQ/dTh	Burn Gas Temp	Burn Angle	Cooling System Temp In	Cooling System Temp Out	Orifice Delta P	Heat Rejection	Air Induction System Temperature Air In	Air Induction System Temperature Air Flow (Betz)	Specific Emissions Fuel Flow	Air Flow	Power	M_C	M_H	M_{NO}	H/C Ratio	Specific NO	Specific HC	Specific CO	M_{CO}	Exhaust Emissions NO	CO_2	CO	HC	O_2
	r/min	Nm	[kPa]	kW	kg/hr	[kPa]	[kPa]	[kPa]	deg CA	deg CA	kPa	kPa/deg	kJ/deg	°C	deg CA	°C	°C	mm Cool	kW	°C	mm H2O	g/h	kg/h	kW					g/kWh	g/kWh	g/kWh		ppm	ppm	ppm	ppm	ppm
1	1554	197	624	32	6.61	897			12.0	357	11703	5333	936	3360	73.0	27	77	275	406	19	11.40	6605.0	388.15	32.10	12	1	30	0.5	3.184	1.024	5.82068	28	440.2	31075	400	157.4	178050
2	1553	200	634	33	6.78											28	78	215	358	19	8.60	6783.3	336.56	32.60	12	1	30	0.5	3.908	0.942	4.10577	28	574.6	33567	300	154.1	173833
2a	1551	191	604	31	6.49	847			12.0	357	11632	5095	642	3360	51.0	29	78	215	352	20	8.60	6485.0	335.98	30.99	12	1	30	0.5	4.027	0.972	6.49233	28	561.7	31850	450	150.7	176025
3	1549	187	593	30	6.48	795			11.5	356.5	11274	3768	516	2840	49.5	29	78	160	304	21	6.30	6475.0	287.57	30.38	12	1	30	0.5	4.661	0.917	3.82558	28	674.1	33850	275	147.5	172750
4	1548	189	596	31	6.55	778			11.4	356.4	11267	2731	531	2830	43.6	31	78	95	228	21	4.80	6546.0	251.44	30.56	12	1	30	0.5	5.519	0.874	5.08926	28	829.1	35260	380	145.9	169920
5	1547	186	588	30	6.54	779			11.4	356.4	10980	2275	542	2410	43.6	33	79	60	176	23	3.70	6540.0	220.75	30.12	12	1	30	0.5	6.639	0.872	2.26122	28	1033.7	37275	175	150.9	166300
6	1546	192	608	31	6.47				12.5	357.5	10579	5345	685	3000	50.5	27	77	215	362	23	8.60	6470.0	335.98	31.11	12	1	30	0.5	2.959	0.826	4.60101	28	452.8	34900	350	140.6	172400
7	1545	190	601	31	6.46	803			12.5	357.5	10579	5345	685	3250	50.5	27	78	225	370	24	7.10	6455.0	304.76	30.75	12	1	30	0.5	3.447	0.781	2.61550	28	530.3	35575	200	133.6	171125
8	1545	187	591	30	6.47	796			12.5	357.5	10184	4253	620	3080	50.5	29	78	230	367	24	6.10	6470.0	282.48	30.24	12	1	30	0.5	4.426	0.718	3.39436	28	721.5	38375	275	130.2	166425
9	1553	188	594	31	6.57	793			12.5	357.5	10053	3395	571	2720	50.5	31	78	225	350	25	5.00	6565.0	255.75	30.51	12	1	30	0.5	5.297	0.699	2.92806	28	910.0	40725	250	133.5	162075
10	1551	183	579	30	6.52	780			12.0	357	9875	2866	600	2580	49.0	32	79	190	316	26	4.10	6522.5	223.55	29.73	12	1	30	0.5	5.803	0.701	4.89934	28	1012.9	42025	425	136.0	159375
11	1551	188	596	31	6.48	804			14.0	359	9558	5489	945	2760	49.0	28	77	95	237	26	4.80	6477.5	251.44	30.58	12	1	30	0.5	2.829	0.752	3.20673	28	488.2	40225	275	144.3	163950
12	1549	187	592	30	6.47	814			13.5	358.5	9240	5150	763	3000	49.5	28	78	120	267	27	3.20	6472.5	204.95	30.36	12	1	30	0.5	3.475	0.651	3.35688	28	624.8	42200	300	130.1	161100
13	1550	183	580	30	6.44	792			13.0	358.0	9023	3968	737	2670	50.0	29	78	105	247	27	3.00	6442.5	198.44	29.74	12	1	30	0.5	4.040	0.631	6.14723	28	760.4	44625	575	132.0	156975
14	1549	182	575	29	6.52	779			13.0	358.0	8837	3548	636	2660	50	31	79	105	240	27	4.10	6515.0	231.99	29.48	12	1	30	0.5	4.943	0.618	5.43446	28	960.8	47100	525	133.5	152125
15	1548	179	565	29	6.52	774			13.0	358.0	8737	3178	639	2660	50	32	79	115	248	28	3.60	6517.5	209.47	28.96	12	1	30	0.5	5.915	0.626	3.28820	28	1176.3	49300	325	138.4	148900
16	1548	190	601	31	6.57	811			14.5	359.5	8268	7379	1513	2900	46.5	29	78	290	410	28	11.10	6565.0	380.41	30.78	12	1	30	0.5	3.113	0.664	4.81916	28	649.9	48850	500	154.2	151050
17	1547	186	590	30	6.55	806			14.0	359	8099	5129	1166	2670	46.0	29	78	275	402	28	8.30	6547.5	329.51	30.21	12	1	30	0.5	3.389	0.590	4.21524	28	728.0	51175	450	141.0	147875
18	1549	184	583	30	6.54	797			14.0	359	7915	4536	1018	2510	49.0	30	78	160	301	28	6.00	6542.5	280.64	29.89	12	1	30	0.5	4.023	0.554	5.39323	28	900.4	53750	600	137.8	143450
19	1551	179	565	29	6.53	775			14.0	359	7569	3895	921	2480	47.0	31	78	100	235	28	4.40	6532.5	240.32	29.00	12	1	30	0.5	4.949	0.518	4.87614	28	1174.3	58725	575	136.7	136000
20	1550	179	565	29	6.51	769			14.0	359	7570	3554	771	2470	47.0	32	78	65	185	29	3.30	6505.0	200.56	28.99	12	1	30	0.5	5.251	0.510	4.39713	28	1261.5	59275	525	136.1	134500
21	1550	183	578	30	6.49	788			15.5	360.5	7227	7124	1788	2590	45.5	28	77	275	397	29	8.30	6485.0	329.51	29.67	12	1	30	0.5	3.147	0.664	4.43459	28	785.3	59925	550	184.1	135025
22	1550	178	565	29	6.48	840			15.5	360.5	7013	7031	1434	2600	45.5	28	77	230	365	29	7.30	6477.5	309.02	28.96	12	1	30	0.5	3.665	0.614	5.89420	28	938.4	62750	750	174.8	130875
23	1550	177	559	29	6.49	841			15.2	360.2	6869	5469	1276	2340	45.8	29	78	230	360	29	6.20	6487.5	284.79	28.67	12	1	30	0.5	4.214	0.591	4.57164	28	1112.9	65675	600	173.6	126150
24	1549	174	550	28	8.19	824			15.0	360	6693	4588	1614	2340	48	31	78	220	344	30	5.00	8187.5	255.31	28.23	12	1	30	0.5	6.061	0.710	5.79777	28	1314.5	69150	625	171.1	120375
25	1547	172	543	28	9.16	753			14.0	359	6563	3897	1345	2270	49	32	78	200	323	30	4.10	9155.0	223.55	27.79	12	1	30	0.5	7.610	0.774	7.98775	28	1534.8	72925	800	173.5	114350

REMARKS :

APPROVED BY :

SIGNATURE :

DATE :

CENTRE FOR AUTOMOTIVE ENGINEERING — CAE

Customer:

ENGINE TEST SHEET :

Boost Pressure and Intake Charge Temperature Matrix for the 75% Load Condition

TEST BELL : EC 38 | DATE | TEST No.

OPERATOR : LDE | 15/05/1996

ENG TYPE : ADE 364T Disp : 3.97201 | ENGINE RATING : 88@2600 Cylinders 4 | INJ. PUMP TYPE/SERIAL No. : | GOVERNOR No. : RQV 300 1300MW68-2 (RV3952)

ENG No.: MC01079SA075068W | TEST STANDARD : DIN 70020 | SPECIAL COMPONENTS : Cylinder pressure transducer and shaft encoder disk | OIL TYPE : BP Vanellus | FUEL TYPE : Cal Ref Diesel

TEST ORDER No. : | TEST DESCRIPTION : | FITTED : | SPILL TIMING : 15 °CA BTDC | Batch:

ENGINE HOURS - START: Rebuilt (0) | BAROMETRIC PRESS : 755.75 mmHg | COMPRESSOR NO | ETA File : | Dyno Zero : After : Cool Orofice 50 40.0

ENGINE HOURS - END: - | FUEL DENSITY : 0.856 @ 20.0 °C | FAN NO | Racer Files : | Dyno Span : (403.6) After : (403.6) Bell Mouth 100.0

	Dynamometer				Engine		Fuel System					Lubrication		Cooling System				Air Induction System										Exhaust System						
										Temp				Temperature		Coolant	Heat	Temperature						Press		Flow		Emissions					Pressure	Temp	
Point	Speed	Torque	Power	Corr. Factor	Corr. Power	Corr. Torque	Flow	Del.	S.F.C.	Pump Inlet	Dens	Press	Temp.	In	Out	Flow Delta P	Rejection	Cell Temp	Manifold	Manifold	Delta T I.C.	Cell Wet B	Cell Dry B	Inlet Depress.	Boost I.C. In	Air/ Fuel	Air Flow	NO	CO_2	CO	HC	NO	Ex Back Press	Out	Smoke
	r/min	Nm	kW		kW	Nm	kg/hr	mm3/st	g/kWh	°C	kg/dm^3	kPa	°C	°C	°C	kg/sec	kW	°C	°C	°C	°C	°C	°C	mmH2O	kPa		kg/s	ppm	%Vol	ppm	ppm	g/kWh	mmH2O	°C	Bosch
1	1560	304	50		50	304	9.58	59.8	193	32	0.856		106	25	78	0.099	22.0	18	41			16	23		152		0.224						75.6	274.9	0.4
2	1558	304	50		50	304	9.64	60.3	195	34	0.856		111	27	78	0.108	23.1	19	66			16	21		151		0.204						74.9	300.1	0.2
3	1556	306	50		50	306	9.89	61.9	198	37	0.856		113	29	80	0.122	25.8	20	101			16	21		149		0.192						73.6	337.0	0.3
4	1555	304	49		49	304	9.95	62.3	201	39	0.856		115	31	80	0.136	28.2	20	136			16	22		154		0.189						74.5	364.1	0.3
5	1554	306	50		50	306	10.12	63.4	203	40	0.856		118	33	81	0.152	30.5	21	163			16	22		154		0.182						75.0	390.9	0.35
6	1553	306	50		50	306	9.70	60.8	195	39	0.856		114	29	78	0.110	22.8	22	39			16	21		123		0.180						67.6	311.1	0.425
7	1553	306	50		50	306	9.82	61.6	197	38	0.856		113	29	80	0.115	24.5	22	74			16	21		123		0.188						62.8	339.7	0.35
8	1553	305	50		50	305	9.91	62.1	200	39	0.856		114	30	80	0.123	25.8	22	103			16	20		125		0.166						59.8	363.7	0.3
9	1552	304	49		49	304	10.26	64.4	207	44	0.856		118	34	81	0.137	27.2	24	158			15	20		122		0.154						60.7	431.4	0.35
10	1550	306	50		50	306	9.84	61.8	198	39	0.856		113	29	78	0.153	31.8	25	40			15	20		92		0.130						45.9	351.5	0.4
11	1550	304	49		49	304	9.99	62.8	203	40	0.856		114	30	80	0.111	23.4	25	73			16	21		91		0.144						47.1	389.8	0.4
12	1551	303	49		49	303	10.05	63.1	205	40	0.856		115	31	81	0.118	24.5	26	104			16	21		91		0.136						44.2	419.9	0.45
13	1550	304	49		49	304	9.96	62.6	202	40	0.856		114	30	80	0.130	27.0	25	72			16	22		91		0.130						45.7	387.1	0.55
14	1551	305	50		50	305	10.34	65.0	209	42	0.856		117	33	81	0.146	29.4	26	133			16	21.0		89		0.124						44.6	464.8	0.6
15	1550	304	49		49	304	10.45	65.7	212	41	0.856		119	35	82	0.160	31.3	26	165			15	21		91		0.122						46.0	493.8	0.6
16	1550	307	50		50	307	10.19	64.0	204	40	0.856		116	31	79	0.122	24.9	26	41			15	21		59		0.110						32.2	428.0	0.725
17	1549	305	49		49	305	10.27	64.6	208	38	0.856		116	31	80	0.126	26.1	26	73			16	21		60.8		0.1						30.7	459.3	0.9
18	1550	304	49		49	304	10.44	65.6	212	39	0.856		117	32	81	0.139	28.4	26	102			16	21		62		0.104						29.1	490.6	1.2
19	1549	303	49		49	303	10.67	67.1	217	40	0.856		119	35	82	0.157	30.9	27	134			16	20		60		0.099						29.5	538.3	1.4
20	1548	304	49		49	304	10.98	69.1	223	40	0.856		120	36	82	0.173	33.3	27	163			15	19		61		0.097						29.0	576.1	1.65
21	1547	304	49		49	304	10.70	67.3	217	34	0.856		118	33	80	0.142	28.0	27	42			16	20		29		0.080						14.0	532.1	2.4
22	1547	303	49		49	303	10.93	68.9	223	37	0.856		118	34	82	0.147	29.6	27	75			16	21		31		0.080						13.5	570.5	2.8
23	1547	308	50		50	308	11.52	72.5	231	37	0.856		119	35	82	0.166	32.7	27	106			16	21		32		0.079						15.9	633.5	4
24	1546	304	49		49	304	12.14	76.5	247	39	0.856		121	38	83	0.194	36.5	27	135			16	20		31		0.076						15.7	700.9	5.05
25	1545	305	49		49	305	16.06	101.2	326	41	0.856		123	41	84	0.221	39.9	27	161			16	20		31		0.074						14.9	701.5	9.6

REMARKS :

APPROVED BY :

SIGNATURE :

DATE :

CENTRE FOR AUTOMOTIVE ENGINEERING — CAE

Customer:

ENGINE TEST SHEET :

Boost Pressure and Intake Charge Temperature Matrix for the 100% Load Condition

TEST BELL : EC 39 | DATE | TEST No.

OPERATOR : LDE | 12/03/1996

ENG TYPE : ADE 364T | Disp : 3.972014 | ENGINE RATING : 66@2600 | Cylinders 4 | INJ. PUMP TYPE/SERIAL No. : | GOVERNOR No. : RQV 300 1300MW66-2 (RV3962)

ENG No.: MC01079SA076066W | TEST STANDARD : DIN 70020 | SPECIAL COMPONENTS : Cylinder pressure transducer and shaft encoder disk | OIL TYPE : BP Vanellus | FUEL TYPE : Cal Ref Diesel

TEST ORDER No. : | TEST DESCRIPTION : | FITTED : | SPILL TIMING : 15 °CA BTDC | Batch:

ENGINE HOURS - START: Rebuilt (0) | BAROMETRIC PRESS : 757.0 mmHg | COMPRESSOR | NO | ETA File : | Dyno Zero : After : Cool Orofice 50 40.0

ENGINE HOURS - END: - | FUEL DENSITY : 0.832 @ 20.0 °C | FAN | NO | Racer Files : | Dyno Span : (403.6) After : (403.6) Bell Mouth 100.0

	Dynamometer			Engine			Fuel System					Lubrication	Cooling System				Air Induction System										Exhaust System									
										Temp			Temperature		Coolant	Heat	Temperature					Press	Flow		Emissions					Pressure	Temp	Energy		
Point	Speed	Torque	Power	Corr Factor	Corr. Power	Corr. Torque	Flow	Del.	S.F.C.	Pump Inlet	Dens	Press	Temp	In	Out	Flow Delta P	Reject-tion	Cell Temp	Manifold	Manifold	Delta T I.C.	Cell Wet B	Cell Dry B	Inlet Depress	Boost I.C In	Air/ Fuel	Air Flow	NO	CO_2	CO	HC	O_2	Ex Back Press	Out	Out	Smoke
	r/min	Nm	kW		kW	Nm	kg/hr	mm3/st	g/kWh	°C	kg/dm³	kPa	°C	°C	°C	kg/sec	kW	°C	°C	°C	°C	°C	°C	mmH2O	kPa		kg/s	ppm	%Vol	ppm	ppm	%Vol	kPa	°C	kW	Bosch
1	1552.604	400.73	65	1	65	401	12.23	78.9	188	50	0.832		111	30.7	79	0.117	23.8	14	44.702						153	64.09	0.218	1276	5.75	0.014	241	13.92	72	364.9	66.0	0.5
2	1550.375	393.9125	64	1	64	394	12.2	78.8	191	50	0.832		113	32.2	80	0.130	26.0	15	72.95						153	61.17	0.207	1571	6.09	0.018	231	13.43	74	393.4	87.6	0.3
3	1547.77	398.54	65	1	65	399	12.61	81.6	195	52	0.832		117	35.0	80	0.158	29.4	17	103.0925						148	53.75	0.188	1954	6.83	0.013	238	12.23	75	444.1	90.1	0.4
4	1547.012	391.304	63	1	63	391	12.505	81.0	197	52	0.832		118	37.7	81	0.171	31.1	19	127.8						148	52.99	0.184	2021	7.15	0.028	257	11.78	75	466.7	92.4	0.4
5	1545.878	382.005	62	1	62	382	12.455	80.7	201	53	0.832		120	39.5	82	0.191	33.8	19	156.7725						148	51.22	0.177	2021	7.54	0.033	287	11.16	75	493.7	94.4	0.4
6	1546.588	404.275	65	1	65	404	12.545	81.2	192	53	0.832		117	34.3	80	0.136	26.0	18	37.8725						116	50.05	0.174	1450	6.92	0.018	238	12.21	61	423.3	79.3	0.5
7	1548.128	396.42	64	1	64	396	12.4825	80.8	194	53	0.832		117	35	81	0.142	27.5	18	72.56						121	49.10	0.170	1777	7.25	0.020	189	11.77	58	447	82.1	0.4
8	1546.113	390.4933	63	1	63	390	12.53	81.2	198	53	0.832		118	37.6	82	0.165	30.5	20	108.0917						121	46.42	0.162	2020	7.83	0.025	177	10.88	60	485.2	84.5	0.5
9	1545.306	383.65	62	1	62	384	12.564	81.4	202	42	0.832		116	38.5	82	0.173	31.4	21	136.068						122	44.86	0.157	2021	8.12	0.014	188	10.25	59	511.1	86.2	0.7
10	1545.185	377.8525	61	1	61	378	12.515	81.1	205	45	0.832		116	39.9	82	0.185	32.9	24	159.4325						119	42.85	0.149	2021	8.44	0.038	181	9.63	60	535.3	85.7	0.9
11	1544.69	395.53	64	1	64	396	12.55	81.4	196	43	0.832		112	34.3	80	0.131	25.3	22	39.3025						91	41.66	0.145	1695	7.94	0.020	166	10.75	46	463.6	72.3	1.3
12	1545.045	388.4025	63	1	63	388	12.59	81.6	200	43	0.832		112	35.1	82	0.138	26.8	23	74.0575						92	39.68	0.139	2020	8.52	0.043	157	9.93	45	497.0	74.2	1.4
13	1544.04	380.675	62	1	62	381	12.6075	81.8	205	43	0.832		114	38	82	0.160	29.8	22	100.705						90	37.24	0.130	2020	9.12	0.035	170	8.92	45	537	75.7	1.6
14	1543.565	372.2475	60	1	60	372	12.5875	81.7	209	44	0.832		115	39.0	83	0.174	31.9	24	129.525						90	36.38	0.127	2020	9.58	0.053	179	8.17	45	566.2	77.9	1.6
15	1543.213	365.945	59	1	59	366	12.5875	81.7	213	44	0.832		116	41.0	82	0.194	33.5	24	161.32						91	34.97	0.122	2020	10.02	0.063	181	7.44	45	595.8	79.0	2.0
16	1548.483	373.005	60	1	60	373	12.4725	80.7	206	44	0.832		113	36.3	81	0.146	27.1	22	37.78						60	32.28	0.112	1757	9.62	0.073	171	8.38	31	525.2	63.8	2.5
17	1548.838	364.8325	59	1	59	365	12.4375	80.4	210	43	0.832		114	37.2	82	0.154	28.9	22	73.755						61	31.26	0.108	2019	10.26	0.093	164	7.41	30	560.9	66.1	2.8
18	1549.015	356.5325	58	1	58	357	12.4425	80.5	215	44	0.832		115	38.5	82	0.168	30.8	21	103.31						61.9	30.58	0.1	2020	10.72	0.105	180	6.66	30.1	588.2	68.0	2.9
19	1547.178	348.675	56	1	56	349	12.5325	81.1	222	44	0.832		117	41.2	82	0.193	33.1	25	132.345						61	29.06	0.101	2021	11.40	0.170	171	5.47	30	632.0	69.9	3.5
20	1547.003	336.1925	54	1	54	336	12.555	81.3	231	46	0.832		117	42.5	83	0.208	35.0	26	160.415						60	27.83	0.097	2020	11.98	0.233	145	4.48	30	666.0	70.8	4.3
21	1546.872	332.81	54	1	54	333	12.508	81.0	232	46	0.832		115	39.4	82	0.173	30.9	27	45.542						30	23.79	0.083	1772	12.35	0.346	146	4.21	29	649.0	58.9	4.7
22	1547	331.6025	54	1	54	332	12.515	81.0	233	47	0.832		115	40.3	83	0.181	32.2	27	74.21						35	24.21	0.084	1919	12.47	0.358	136	4.01	29	660.0	61.0	4.9
23	1546.585	320.1975	52	1	52	320	12.52	81.1	241	46	0.832		116	41.0	83	0.189	33.0	27	107.7375						36	23.66	0.082	2000	13.04	0.430	111	3.07	28	692.8	62.8	6.0
24	1547.535	301.5725	49	1	49	302	12.465	80.7	255	45	0.832		117	42.2	83	0.205	34.8	29	136.8875						34	22.53	0.078	1994	13.77	0.503	100	1.83	28	725.8	62.5	6.7
25	1546.587	284.4333	46	1	46	284	12.46	80.7	270	47	0.832		117	43	83	0.216	36.3	29	164.7633						33	21.87	0.076	1927	14.09	0.843	109	0.97	27	742	62.1	7.9

REMARKS :

APPROVED BY

SIGNATURE

DATE

CENTRE FOR AUTOMOTIVE ENGINEERING — CAE

Customer:

ENGINE TEST SHEET : Number 2

Boost Pressure and Intake Charge Temperature Matrix for the 100% Load Condition

TEST BELL : 2 (D400) | DATE | TEST No.

OPERATOR : LDE | 12/03/1996 | 3.0

ENG TYPE : ADE 364T Disp : 3.972014	ENGINE RATING : 88@2600 Cylinders 4	INJ. PUMP TYPE/SERIAL No. :	GOVERNOR No. : RQV 300 1300MW88-2 (RV3952)
ENG No.: MC01079SA076088W	TEST STANDARD : DIN 70020	SPECIAL COMPONENTS : Cylinder pressure transducer and shaft encoder disk	OIL TYPE : BP Vanellus FUEL TYPE : Cal Ref Diesel
TEST ORDER No. :	TEST DESCRIPTION : 0.0	FITTED :	SPILL TIMING : 15 °CA BTDC Batch:
ENGINE HOURS - START: ReCuilt (0)	CAROMETRIC PRESS : 767.0 mmHg	COMPRESSOR NO ETA File :	Coolant Density : 1020.7 gravity : 9.8 Barometric Pressure : 100.5
ENGINE HOURS - END: -	FUEL DENSITY : 0.832 @ 20.0 °C	FAN NO RaCer Files :	Coolant Cp Value: 3.4

Point	Dynamometer: Speed	Torque	BMEP	Power	Fuel Flow	IMEP Gross	PMEP	FMEP	Combustion Analysis Results: Ignition Delay	Ignition Point	Maximum Pressure	Maximum dP/dTh	Maximum dQ/dTh	Burn: Burn Gas Temp	Burn Angle	Max Combustion Gas	Average Combustion Gas	Cooling System: Coolant Orifice Delta P	Heat Rejection	Air Induction System: Temperature Air In	Air Flow (Betz)	Specific Emissions: Fuel Flow	Air Flow	Power	M_C	M_H	M_{NO}	H/C Ratio	Specific NO	Specific HC	Specific CO	M_{CO}	Exhaust Emissions: NO	CO_2	CO	HC	O_2
	r/min	Nm	[kPa]	kW	kg/hr	[kPa]	[kPa]	[kPa]	deg CA	deg CA	kPa	kPa/deg	kJ/deg	°C	deg CA	°C	°C	mm Cool	kW	°C	mm H2O	g/h	kg/h	kW					g/kWh	g/kWh	g/kWh		ppm	ppm	ppm	ppm	ppm
1	1553	401	1268	65	12.23	1448			11.0	357	12922	4778	681	2120	49.0	1990	1530	255	24	14	280	12230.0	783.82	65.15	12	1	30	0.5	4.602	0.782	1.016	28	1276.3	57500	140	241.2	139220
2	1550	394	1246	64	12.20	1424			10.5	356.5	12719	3561	718	2180	49.5	2040	1570	330	26	15	253	12200.0	746.29	63.95	12	1	30	0.5	5.434	0.719	1.218	28	1570.5	60900	175	231.2	134250
3	1548	399	1261	65	12.61	1423			10.5	356.5	12405	3408	770	2200	49.5	2130	1640	505	29	17	210	12610.0	677.80	64.60	12	1	30	0.5	6.174	0.677	0.795	28	1953.5	68325	125	238.4	122300
4	1547	391	1238	63	12.51	1399			10.5	356.5	12222	3430	778	2200	49.5	2140	1650	590	31	19	202	12505.0	662.67	63.39	12	1	30	0.5	6.151	0.702	1.715	28	2021.0	71540	280	256.6	117800
5	1546	382	1209	62	12.46	1376			10.0	356	12021	3383	794	2220	50.0	2160	1680	725	34	19	183	12455.0	637.94	61.84	12	1	30	0.5	5.959	0.760	1.928	28	2021.1	75350	325	286.8	111625
																									12	1	30										
6	1547	404	1279	65	12.55	1447			12.0	358	11496	4542	704	2070	48.0	2000	1530	370	26	18	248	12545.0	627.85	65.48	12	1	30	0.5	4.442	0.655	1.078	28	1450.2	69150	175	237.9	122050
7	1548	396	1254	64	12.48	1416			11.5	357.5	11440	3727	767	2210	48.5	2100	1600	405	27	18	220	12482.5	612.83	64.27	12	1	30	0.5	5.265	0.504	1.192	28	1776.9	72500	200	189.3	117650
8	1546	390	1235	63	12.53	1397			11.0	357	11218	3443	816	2210	49.0	2160	1660	545	30	20	195	12530.0	581.70	63.22	12	1	30	0.5	5.658	0.446	1.409	28	2020.1	78250	250	176.9	108800
9	1545	384	1214	62	12.56	1385			11.0	357	11216	3568	844	2240	49.0	2190	1690	600	31	21	180	12564.0	563.57	62.08	12	1	30	0.5	5.581	0.467	0.778	28	2020.8	81160	140	188.2	102480
10	1545	378	1195	61	12.52	1365			10.5	356.5	10997	3478	855	2240	49.5	2190	1690	685	33	24	165	12515.0	536.24	61.14	12	1	30	0.5	5.412	0.436	2.021	28	2020.5	84425	375	181.2	96300
11	1545	396	1251	64	12.55	1400			12.0	358	10343	3879	828	2190	50.0	2160	1640	338	25	22	220	12550.0	522.89	63.98	12	1	30	0.5	4.636	0.409	1.101	28	1695.0	79375	200	166.4	107525
12	1545	388	1229	63	12.59	1400			12.0	358	10343	3881	828	2190	50.0	2160	1640	380	27	23	193	12590.0	499.63	62.84	12	1	30	0.5	5.249	0.366	2.221	28	2020.4	85175	425	156.7	99300
13	1544	381	1204	62	12.61	1379			12.0	358	10077	3595	897	2210	50.0	2180	1660	515	30	22	168	12607.5	469.52	61.55	12	1	30	0.5	5.015	0.379	1.748	28	2020.3	91225	350	169.6	89175
14	1544	372	1178	60	12.59	1354			12.0	358	9849	3236	876	2230	50.0	2200	1680	610	32	24	159	12587.5	457.95	60.17	12	1	30	0.5	4.868	0.388	2.546	28	2020.0	95825	525	178.8	81650
15	1543	366	1158	59	12.59	1334			11.5	357.5	9759	3263	913	2260	50.5	2240	1720	745	34	24	138	12587.5	440.13	59.14	12	1	30	0.5	4.736	0.383	2.948	28	2020.2	100150	625	181.4	74350
16	1548	373	1180	60	12.47	1344			13.0	359	8988	7187	1269	2180	51.0	2160	1630	425	27	22	175	12472.5	402.62	60.49	12	1	30	0.5	4.150	0.363	3.446	28	1756.8	96175	725	171.0	83750
17	1549	365	1154	59	12.44	1315			13.0	359	8982	4594	894	2210	51.0	2180	1650	480	29	22	155	12437.5	388.80	59.17	12	1	30	0.5	4.552	0.332	4.195	28	2019.2	102600	925	164.0	74075
18	1549	357	1128	58	12.44	1297			12.5	358.5	8723	3778	885	2270	51.5	2240	1710	564	31	21	140	12442.5	380.49	57.83	12	1	30	0.5	4.458	0.358	4.662	28	2020.0	107175	1050	180.3	66575
19	1547	349	1103	56	12.53	1259			12.0	358	8479	2957	867	2350	52.0	2340	1790	735	33	25	128	12532.5	364.22	56.49	12	1	30	0.5	4.303	0.328	7.284	28	2020.7	113975	1700	171.4	54650
20	1547	336	1064	54	12.56	1226			12.0	358	8303	2472	1147	2540	52.0	2530	1940	850	35	26	115	12555.0	349.39	54.46	12	1	30	0.5	4.237	0.273	9.811	28	2020.2	119750	2325	144.7	44825
21	1547	333	1053	54	12.51	1212			14.5	360.5	7575	6507	1855	2490	51.5	2480	1860	600	31	27	134	12508.0	297.54	53.91	12	1	30	0.5	3.597	0.267	14.130	28	1772.1	123500	3460	146.4	42080
22	1547	332	1049	54	12.52	1205			14.0	360	7658	6212	1678	2590	52.0	2580	1950	655	32	27	125	12515.0	303.03	53.72	12	1	30	0.5	3.872	0.246	14.514	28	1919.0	124675	3575	135.7	40075
23	1547	320	1013	52	12.52	1175			14.0	360	7527	4670	1392	2700	52.0	2700	2000	710	33	27	115	12520.0	296.17	51.86	12	1	30	0.5	3.982	0.199	17.226	28	2000.0	130425	4300	111.2	30850
24	1548	302	954	49	12.47	1175			13.5	359.5	7527	4673	1113	2750	52.5	2750	2080	825	35	29	100	12465.0	280.89	48.87	12	1	30	0.5	3.959	0.178	20.073	28	1994.2	137725	5025	99.7	18325
25	1547	284	900	46	12.46	1100			13.0	359	7217	3780	1100	2830	53.0	2830	2150	915	36	29	92	12460.0	272.55	46.07	12	1	30	0.5	3.880	0.198	34.157	28	1927.4	140867	8433	109.2	9667

REMARKS :

APPROVED BY :

SIGNATURE :

DATE :